E77-10051
NASA-CR-149258
III

(E77-10051) EVALUATION OF ERTS
MULTISPECTRAL SIGNATURES IN RELATION TO
GROUND CONTROL SIGNATURES USING A
NESTED-SAMPLING APPROACH Final Report
(Stanford Univ.) 275 p HC A12/MF A01

N77-14550

Unclas
G3/43 00051

EVALUATION OF ERTS MULTISPECTRAL SIGNATURES IN RELATION TO GROUND CONTROL SIGNATURES USING A NESTED-SAMPLING APPROACH

Ronald J. P. Lyon

Principal Investigator
Remote Sensing Laboratories
School of Earth Sciences
Stanford University
Stanford, California

OCTOBER 1977

FINAL REPORT (TYPE III)

RESEARCH CONTRACT NAS 5-21884 (UN-142)

PREPARED FOR:

The National Aeronautics and Space Administration
Goddard Space Flight Center
Greenbelt, Maryland 20771

1637A

REMOTE SENSING LABORATORY
SCHOOL OF EARTH SCIENCES

STANFORD UNIVERSITY • STANFORD, CALIFORNIA

EVALUATION OF ERTS MULTISPECTRAL SIGNATURES IN RELATION TO GROUND CONTROL SIGNATURES USING A NESTED-SAMPLING APPROACH

Ronald J. P. Lyon
Department of Applied Earth Sciences
Stanford University
Stanford, California 94305

FEBRUARY 1975 (REVISED AND CONDENSED OCTOBER 1976)

FINAL REPORT (TYPE III)

RESEARCH CONTRACT NAS 5-21884 (UN-142)

Original photography may be purchased from:
EROS Data Center
10th and Dakota Avenue
Sioux Falls, SD 57198

PREPARED FOR:

The National Aeronautics and Space Administration
Goddard Space Flight Center
Greenbelt, Maryland 20771

1. Report No.	2. Government Accession No.	3. Recipient's Catalog No.
4. Title and Subtitle Evaluation of ERTS Multispectral Signatures in Relation to Ground Control Signatures Using a Nested-Sampling Approach		5. Report Date April 1975 6. Performing Organization Code
7. Author(s) R.J.P. Lyon		8. Performing Organization Report No.
9. Performing Organization Name and Address School of Earth Sciences Stanford University Stanford, California 94305		10. Work Unit No. 11. Contract or Grant No. NAS 5-21884 13. Type of Report and Period Covered Type III Final Report
12. Sponsoring Agency Name and Address NASA Goddard Space Flight Center Greenbelt, Maryland 20771		14. Sponsoring Agency Code
15. Supplementary Notes		

16. Abstract

Ground-measured spectral signatures of wavelength bands matching ERTS MSS were collected using a radiometer at several Californian and Nevadan sites, and directly compared with similar data from ERTS CCTs. The comparison was tested at the highest possible spatial resolution (approximately that of one acre, or 0.4 hectare) for ERTS, using deconvoluted MSS data, and contrasted with that of ground-measured spectra, originally from 1 meter squares. In the mobile traverses of the Stanford grassland sites these 1 meter fields of view were integrated into eighty-meter transects along the 5 km track across four major rock/soil types. Suitable software was developed to read the MSS CCT tapes, to shadeprint individual bands (and ratios of bands) with user-determined greyscale stretching. Four new algorithms for unsupervised and supervised, normalized and unnormalized clustering were developed, into a program termed STANSORT. Parallel software allowed the field data to be calibrated, and by using concurrently continuously collected, upward-and downward-viewing, 4-band radiometers, bidirectional (or directional) reflectances could be calculated. Rapid sampling logic in the field A-D conversion hardware, gave (Continued)

17. Key Words (Selected by Author(s))	18. Distribution Statement
Spectral signatures biogeochemical, mining, reflectance, California, Nevada, grassland	

19. Security Classif. (of this report)	20. Security Classif. (of this page)	21. No. of Pages	22. Price*
Unclassified	Unclassified		

*For sale by the Clearinghouse for Federal Scientific and Technical Information, Springfield, Virginia 22151.

1. Report No.	2. Government Accession No.	3. Recipient's Catalog No.
4. Title and Subtitle		5. Report Date
		6. Performing Organization Code
7. Author(s)		8. Performing Organization Report No.
9. Performing Organization Name and Address		10. Work Unit No.
		11. Contract or Grant No.
		13. Type of Report and Period Covered
12. Sponsoring Agency Name and Address		
		14. Sponsoring Agency Code
15. Supplementary Notes		

16. Abstract

(ABSTRACT CONTINUED)

these answers at 200 m sec intervals or multiples. Atmospheric calibrations, and hence correction of ERTS data, was made possible for the Stanford area, by the sequential observation from space by ERTS of a 45-pixel area of carbon black (refinery refuse). By also using a comparably sized area of concrete (NASA/ARC hardstands) each set of zero-reflectance and standard-target observations enable local ERTS CCT data to be translated into bidirectional reflectance. Application of these methods to ground studies of mineralized areas in California and Nevada, as well as to geological maps of New Guinea, showed the direct application of the ERTS system to mineral exploration.

Four published papers are included as Appendices.

17. Key Words (Selected by Author(s))	18. Distribution Statement		
19. Security Classif. (of this report)	20. Security Classif. (of this page)	21. No. of Pages	22. Price*
Unclassified	Unclassified		

*For sale by the Clearinghouse for Federal Scientific and Technical Information, Springfield, Virginia 22151.

PREFACE

ERTS digital data have been compared with ground-measured bi-directional reflectances in 12 separate test node areas. The basic philosophy direction of the studies has been

1. How do ERTS Spectra for any given pixel vary with Season?
2. How does seasonal vegetation (grass, etc.) respond with time of the year, when seen both on ERTS and in comparable ground measurements?
3. How does vegetation growing on known mineralization, with measured anomolous metal content in its leaves, appear in ERTS type spectra during its growing cycle?
4. Can ERTS spectra be used to differentiate rock and soil materials of economic interest in mineralized areas?

To do these experiments we have had to develop software to do the following tasks.

5 Read, unpack and handle ERTS CCT tapes on both IBM and PDP-10 computers.

6 Develop fully interactive programs for use by geologists (both in undergraduate and graduate classes, as well as by professional research workers, all of whom have had little or no programming experience. Data displays on CRT's were developed to have a map-like format for these purposes.

7 Develop programs to reduce field radiance measurements to bi-directional reflectances, in turn to be correlated with ERTS data.

1.1 SUMMARY

1.1.1 Software (STANSORT) has been developed to read and process ERTS CCT tapes to produce the following products.

1.1.1.1 Location prints ("shade prints") of approximate scale 1:24,000, aspect ratio 0.9, on a conventional lineprint. Such prints can be made from original data, ratios, etc.

1.1.1.2 Algorithms written to do unsupervised clustering, edge detection, reflectance, and atmospheric corrections. Debanding and deconvolution functions were also programmed.

1.1.1.3 Images, correctly scaled, skewed and with a 1.0 aspect ratio, of either raw data, as Black/White prints, or color composites of any three sets forming CIR or other hybrid imagery (eg. Ch 5 + R54 + (Ch. 7-Ch.5)).

1.1.2 Applications to a variety of terrain classification problems were completed, with special emphasis directed to the effect of varying percentages of vegetated cover on the responses of soils and rock.

1.1.2.1 Biomass studies; relating the ground-measured reflectances to the ERTS reflectances, and both to the biomass (dead weight/m^2 of vegetation). Detailed studies of soil types, vegetation species, etc. were made to find correlations. Soil types could be clearly differentiated either year in May by the relative vigor of grasses in the spring "dieback" period each year. Grassland species were too evenly mixed by the feeding cattle to give any differentiation of soil type.

1.1.2.2 A detailed study of the effect of heavy metal (Mo) poisoning on a mixed Pinon Pine and Juniper "forest" in western Nevada, showed a positive correlation of plant growth with Mo content in ashed leaves for Juniper. With Pinon Pine, the correlation was negative, and the trees showed morphological changes in proportion to Mo content.

Since the conclusion of this contract effort, considerable work has been performed in this and other U.S. mining districts (Yerington, Coldfield, Nevada) and overseas (Almeria, Malaga and Rio Tinto, Spain; Karasjok, Norway etc.). These works are already appearing in publications.

Hardware was procured, integrated, and experimental techniques perfected to produce meaningful data on reflectance of certain materials for comparison with ERTS.

Significantly in all these projects the efforts have been directed to the spot-locality "ground truth" in an effort to derive 1:1 correlations with ERTS data.

TABLE OF CONTENTS

* See published paper – Appendix A.

TABLE OF CONTENTS PAGE

TABLE OF CONTENTS

PAGE

TABLE OF CONTENTS

PAGE

LIST OF ILLUSTRATIONS

LIST OF ILLUSTRATIONS CONTINUED -2

Page

LIST OF ILLUSTRATIONS CONTINUED -3 Page

LIST OF ILLUSTRATIONS CONTINUED -4

LIST OF ILLUSTRATIONS -4 | Page

LIST OF ILLUSTRATIONS -5

Page

LIST OF TABLES

12

1.0 INTRODUCTION

This project was proposed in early 1971 at which time ERTS was only a possibility which might produce a few images of reasonable quality for analysis. The prime instrument on board clearly was the RBV camera, and only a few research groups were interested (more than casually) in the MSS scanner and its concomitant digital tape processing. In no way could anyone have foretold the incredible success of ERTS-1, still running now in 1976 four years after its launch. ERTS-2 (now LANDSAT-2) is performing even better than ERTS-1.

To write an introduction now seems difficult. Almost all of what we hoped to achieve has been surpassed manyfold. In the original statement of work we hoped to locate and measure seasonal responses from a five square kilometer target of grasses and soil on the Stanford Grassland site. Today we argue about spectral response from individual 0.4 hectare pixels, and whether we have their location fixed to ± 50 m. We have established a 0.95 correlation between ground-based ERTS-type measurements, and the biomass ratio (gm/m^2 wet weight/dead weight of cover) of the site. We have a 0.70 correlation with biomass ratio with several ERTS overpasses from comparable seasons.

In our other area of primary research, that of exploration for mineral deposits, we have progressed from wondering if we could find a "mineral district" of several square kilometers, to again debating the spectral reflectance of soil and rock areas to the nearest 50 m in position. Now we define the mineralogy and chemical composition of the iron-oxide stainings using R54 ratio--the ratio of the ERTS-derived bidirectional reflectances of Channels 5 and 4.

Finally, concepts as "stretched- and enhanced-images," sampling, shade- and dot-prints (to either 1:62,500, 1:50,000 or even 1:24,000 scales) have become practical realities in everyday use--not only by "high-powered computer experts", but at Stanford, by graduate and undergraduate students in various academic majors. Therein lies the most significant aspect of this study effort, the transfer of technology, from concept, to classroom with practical use in field work, performed by growing groups of students.

2.0 BODY OF THE REPORT

This report covers a funded period from May 1973 through middle 1974, with access to LANDSAT-1 (ERTS) data retroactive to July 1972. The research efforts initiated under this contract (NAS 5-21884) are still continuing with various levels of funding from a wide variety of sources. Today the project is called STANSEARCH -- the application of LANDSAT data directly to mineral exploration.

Several papers have been published, others are in press. Four of these are included here as Appendices.

2.0.1 ORGANIZATION

The report is divided into three main sections;

2.1 Direct Image Interpretation

2.2 Reduction and Processing of LANDSAT (CCT) Tapes

2.3 Interpretation of Tapes

By far the greater effort has been directed into tape analysis, with excellent results well beyond our original objectives. In fact today (in 1976), it is difficult to write about the primitive beginnings in 1972/73.

Section 2.1 deals mainly with efforts at transmission densitometry using the 4 spectral images, and met with only moderate success.

Section 2.2 covers the following themes;

2.2.1 Unpacking CCT tapes and data manipulation

2.2.2 Spectral Image production - Enhanced B/W and Color images.

Section 2.3 Interpretation of Taped Data

2.3.1 Atmospheric Effects

2.3.2 Stanford Grassland - Soils

2.3.3 Stanford Grassland - Vegetation

2.3.4 Stanford Grassland - Biomass

2.3.5 Californian Grassland - Biomass/Soils

2.3.6 Biogeochemistry - Molybdenum poisoning as guide to a Mineral Deposit

2.3.7 Snow mapping

References, Results and New Technology appear at the rear followed by reprints of the four published papers.

2.1 DIRECT IMAGE INTERPRETATION

2.1.0 Feasibility of Using ERTS MSS Imagery for Spot Transmission Measurements

2.1.1 Image Densitometry and CCT-Generated Shade Prints

The effort reported here concerns the density/transmission measurements on selected ERTS frames, designed to be related to the MSS tape output (CCT) and shade prints.

The Stanford Grassland test area was examined initially and conventional photo interpretation techniques used to obtain relative information over the total time period available in our tape collection.

2.1.1.1 Image Densitometry-Positive Imagery - 70 mm

Two approaches have been used. Firstly conventional photo interpretational descriptions of features of local geological interest were made, in particular noting tone-contrasts and changes. Secondly the 70 mm positives were measured (a) using a McBeth Quantalog TD102 densitometer with a specially prepared, smaller (0.7mm) diameter aperture, and (b) with an ISCO SR spectroradiometer, using a fiber optics probe used to observe the image-plane brightness of the transparency when projected with a lantern-slide projector. These measurements can be made up to 6 meters away from the projector, by which time the fiber optics subtend only 0.5 mrad, equal to a circle containing above 15 ERTS resolution cells (magnification 35.3x). See Figure 1. A wavelength of 0.625 micrometers was used for maximum sensitivity of the ISCO and all 4 ERTS MSS images were measured, using the grey scale wedges for calibration.

All these sets of data have been tabulated and the spectral radiance (at the center of each MSS filter) plotted (mwatts $cm^{-2} ster^{-1} 0.1\mu m^{-1}$), in Figure 2.

2.1.2 Discussion

An experiment was conducted to evaluate the feasibility of using ERTS-1 MSS imagery for spot transmission measurements on selected sites. Using the

15-unit linear gray scale on the 70 mm positive imagery as the base of comparison, a correlation was made between the transmittance measured at each site on the imagery and the radiance values (counts) recorded on CCT tape by the spacecraft over the same sites.

The imagery (1075-18170-6) was enlarged (35.3 diameters) by a 750-watt projector and focused on a white cardboard screen 6 meters from the lens. The end of a 3 mm fiber optic, set flush with and normal to the face of the screen, was aimed directly (critical) at the projector lens. An ISCO SR spectroradiometer recorded the light intensities at a wave length of 0.625 micrometers (selected for maximum scale readings). See Figure 1.

Observations were made on 30 sub-sites (Wiltren test site 58, east of Travis A.F.B.) which were pre-selected for their differing image "brightness" and total area; all are dried salt lakes. Observations were also made on "average" gray backgrounds and on small lakes. The site observations were preceded and followed by a series of similar readings on the 15-unit gray scale beside the image. Transmission values (ranging from 1 to 15) for each site were established from curves (essentially straight lines) of the gray scale values (ISCO readings vs 15-unit gray scale). Unfortunately, during the 3-hour experiment, there was a significant decrease in light intensity of the lamp between the two series of gray-scale readings, thus producing a time-range of transmission values for each site. This range of values was compared with the radiance values (counts) obtained from the tapes over the same sites (Figure 2). The values from the tapes had to be averaged because at 6 meters the 3mm diameter fiber optic covers an area of about 15 pixels.

There is very good correlation between the density values obtained from projected imagery and radiance values received by the detector on the spacecraft. A shorter experiment time and closer integration of gray scale and site readings would avoid the variation in lamp intensities. See Figure 2. Detailed data outputs from the tapes are shown in Figures 4, 5 and 6.

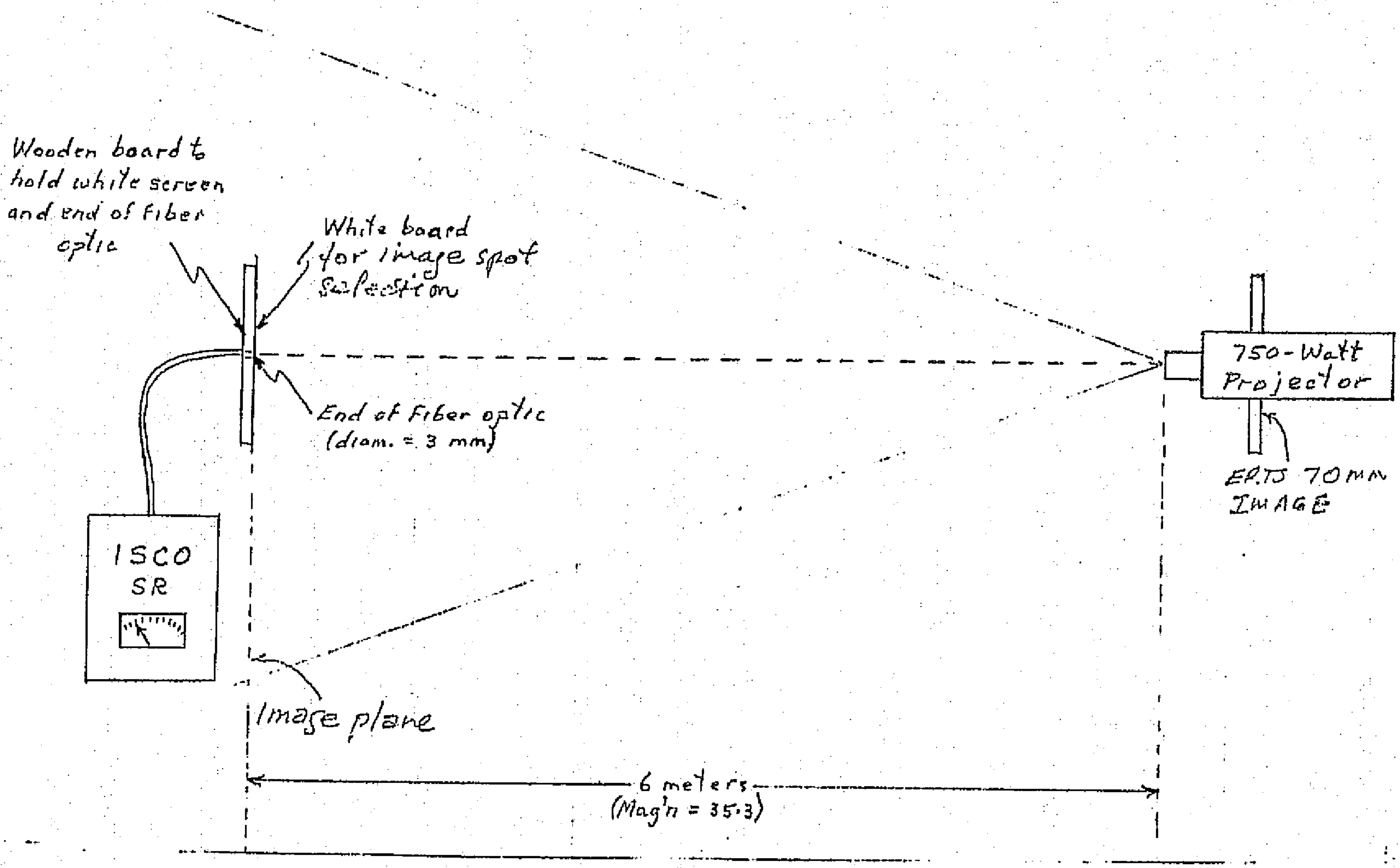

Figure 2.1.1.1. Schematic Diagram Illustrating the Arrangement of the Equipment.

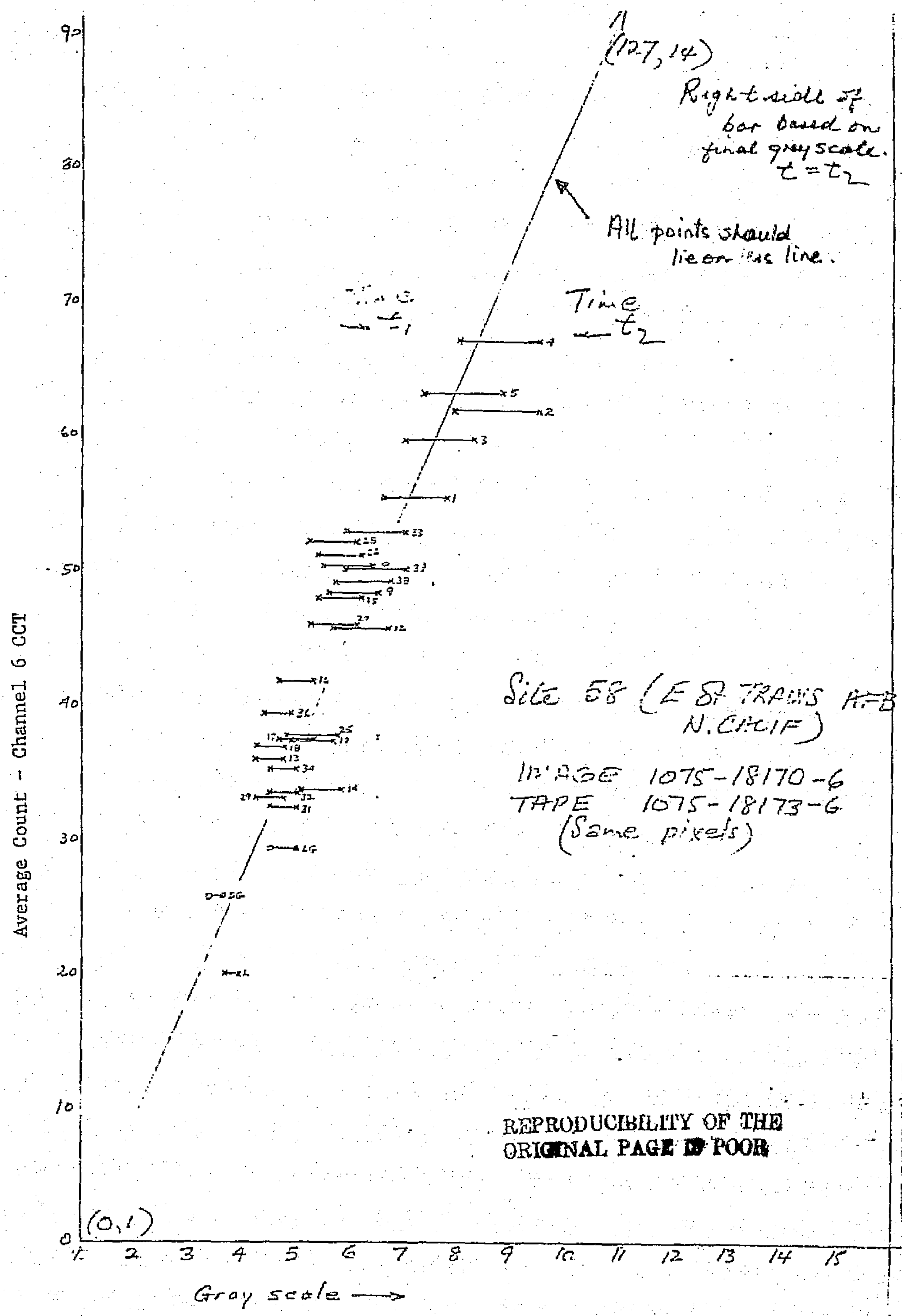

Figure 2.1.1.2. Correlation of Spot Transmission Measurements with Average Count from Original Tapes.

2.13 CONVENTIONAL PHOTOINTERPRETATIONS OF ERTS CHANNEL 7 - STANFORD

The Stanford Grassland test site is about 5000 acres of rolling grassland at about 450 feet elevation situated due east of NASA/ARC (Moffett Field) on the west shores of San Francisco Bay. The area is now bisected by Interstate 280 which runs approximately NW-SE along the "grain" of the country. Both the grassland and the freeway are clearly visible on channel 5 imagery contrasting strongly with the enclosing cities. The site includes 4 Lakes-Felt, Lagunita, Searsville and Bear.

(a) ERTS 1075-18173 (October 6, 1972) Sun El 41°/azimuth 146°

Freeway slightly darker than the fields. Felt Lake, black with white rim (drying up). Menlo Country Club Golf Course (CCGC) white, Stanford University Golf Course (SUGC) white. Santa Clara gravels (Qsc) = Monterey shales (Tm), about equally bright with Page Mill basalt (Tpb.) Butano sandstone (Tbu) darker. Stanford Linear Accelerator (SLAC) dark. Searsville Lake dark, Portola Road white, Jasper Ridge serpentine (Ksp) = sediments enclosing. Lake Lagunita dry.

$$Qsc = Tm = Tpb > Tbu$$

(b) 1111-18181 (November 11) 60% clouds no use

(c) 1112-18181 (November 29) Sun El 27°/azimuth 155°

All transparencies badly "cracked", need new prints

General fields white, no contrast with Menlo CCGS, Stanford GC lighter tone. SLAC dark, freeway darker, Searsville Lake dark. Portola Road grey. POOR IMAGE.

(d) 1147-18181 (December 17) 90% clouds, no use

(e) 1165-18175 (January 4) Sun 24°/ azimuth 151°

Good contrast. Qsc light-grey peaked on hills/valleys, contrasting with Tm. Freeway darker, SLAC darker, West end of SLAC patchy topography. Tm > Tpb. Where Tbu without trees approximately equal to Tm. Serpentine on Jasper Ridge (Ksp) lighter than sediments, both darker than Qsc.

$$Tm > Tpb$$

$$Tbu \text{ w/o trees} = Tm$$

$$Ksp < Tbu, \text{ both} > Qsc$$

(f) 1183-18175 (January 22) Sun 26°/azimuth 148°

Excellent contrast. Qsc light speckled (but different to 1165) contrasting with Tm. Freeway darker, Tm lightest, Tbu little lighter than Tpb, above equal to SUGC, SLAC dark. Serprentine (Ksp) lighter than seds, darker than Qsc.

(g) 1201-18181 (February 9) 80% clouds, no use

(h) 1219-18182 (February 27) 100% clouds, no use

(i) 1237-18183 (March 17) 40% clouds, ground obscured

(j) 1255-18183 (April 4) Sun 49°/azimuth 134°

Good grey scale, overall tone light. Searsville Lake now very dark (full of water). Freeway and SLAC dark-medium grey, trees along creek same grey. Topographic relief effect now lost. Field at south end of Felt Lake darker tone than that around the lake. Tpb = Tm and only slightly brighter, Lake Lagunita now full (black). Qsc even toned (not speckled). Menlo CCGC equals Stanford's UGC in light tone. Alpine Road Quarry Lake and Foothill Park Lake clear, black surroundings brighter. Golf courses now more clear with fairways appearing relative to trees.

(k) 1273-18183 (April 22) Sun 55° El/azimuth 129°

Golf courses now the brightest areas with patterns of fairways showing clearly. Qsc - Tm = Tpb + Tbu. Campus trees a little more grey. Topography not clearly shown. Jasper Ridge about equal to Ladera. Tbu on ridges a little darker than Ksp.

(l) 1291-18182 (May 10) Sun 60 El/Azimuth 123°

Image transparency hazy, paper print better.

Golf courses clearly brightest areas with Menlo CCGC being brightest. Freeway-SLAC darker area, Lagunita Lake medium black. Field to south of Felt Lake not so dark in contrast with those around lake. General fields around SLAC more bright across creek towards Ladera (Webb Ranch) (Tus) boundary.

Natural open grass patches on skyline almost as bright as golf courses.

2.1.4 MEASUREMENTS ON SPECIFIC IMAGE SETS (ALL 4 CHANNELS)

2.1.4.1 Densitometry using McBeth Quantalog (0.7 mm aperture)

Conventional D log E curves for each channel of Frame 1075-18173 were

prepared using special graphs developed by the Principal Investigator while in Australia. These show the 15 step, linear-wedge values on a logarithmitic abscissa in radiance ($x10^{-3}$ watts. Cm^{-2}.$ster^{-1}$), see Figure 3.

In the normal manner the density on each step of the wedge was measured to create the "characteristic curve" for that channel. Subsequently then the density of selected target areas was read, plotted, and from the curve the radiance read out.

Because it was not possible to make the aperture disc less than 0.7mm the spot size on a 70mm formal transparency was very large (2.5km, or 70 pixels) and only major terrain elements could be measured.

The resultant spectral radiance through MSS bandpasses appear in Table I (watts.Cm^{-2}.$ster^{-1}$. .01µm x 10^{-3}).

2.1.4.2 Transmission Measurements using the Stanford 6-Meter System

1. <u>Stanford Grasslands Test Site</u>

Methods used have been explained above. Spectral radiance data are listed in Table II. (Watt. Cm^{-2}.$ster^{-1}$.01µm.$x10^{-3}$) for the Stanford locality.

2. <u>Site 58, Area East of Travis AFB, California</u>

An area of small dry salt lakes was located and measured using the system. The data from these measurements have been used to create Figure 2. In detail Figures 4, 5 and 6 show sequentially on a USGS Topographic map of the area, a shadeprint of the area from CCT tapes and the actual raw numerics from a tape-dump (NUMBER); indicating the method of data extraction.

2.1.5 CONCLUSIONS

1. A reasonable agreementwas found between the two densitometer systems.
2. The large area subtended even by the 6 m projection system makes the system not very useful for our work. In addition diffraction effects from using such a small aperture (0.7mm) worry us with the McBeth unit.
3. We have decided to leave this optical method and concentrate on the taped data output, which gives us the ultimate in ERTS resolution (0.4 hectare or 1 acre).

TABLE 2.1.1.1

SPECTRAL RADIANCE OF ERTS TRANSPARENCIES USING McBETH QUANTALOG

(MEASUREMENT AREA = 70 PIXELS)

IMAGE 1075-18173	IMAGE A ($W.Cm^{-2}.ster^{-1}.0.01\mu m.x10^{-3}$) OCT 6, 1972				IMAGE B 1183-18175 JAN 22, 1973
LOCALITY	CH.4	CH.5	CH.6	CH.7	CH.7
JASPER RIDGE (total)	0.51	0.34	0.42	0.65	0.44
BEAR GULCH RESERVOIR (W. MENLO PARK)	0.64	0.38	0.50	0.71	0.57
LAKE LAGUNITA (DRY)	–	0.44	0.52	0.74	0.57
SAND HILL ROAD (TUS)	0.62	0.43	0.51	0.76	0.62
FELT LAKE AREA (QSC)	0.61	0.42	0.44	0.70	0.63
SALT PONDS ON BAY MARSH ROAD REDWOOD CITY	0.79	0.75	0.58	0.51	––

NOTE: AREAS COVER 70 PIXELS (2.5 KM WIDTH)

TABLE 2.1.1.2

SPECTRAL RADIANCE OF ERTS TRANSPARENCIES USING STANFORD 6 METER PROJECTION SYSTEM

(MEASUREMENT AREA = 15 PIXELS)

LOCATION - SEE MAP ATTACHED

IMAGE 1075 - 18173 ($W. Cm^{-2}.ster^{-1}.0.01\mu m \times 10^{-3}$)

(OCTOBER 6, 1972)

LOCALITY	Ch. 4	Ch. 5	Ch. 6	Ch. 7
A. San Francisco Bay Salt Ponds				
Pond A (Western most)	0.60	0.74	0.48	-
Pond B (Striped)	1.17	1.06	0.76	0.80
B = B_1	1.12	1.25	0.96	0.89
B = B_2	1.32	1.16	0.96	0.88
Pond C	0.63	0.66	0.41	-
B. Stanford Test Area				
Grass cover over: -				
Monterey Shale (Tm)	0.63	0.55	0.46	0.70
Santa Clara gravel (QSc)	0.65	0.58	0.51	0.76
Unnamed sandstone - Webb Ranch (Tus)	0.62	0.52	0.54	0.83
Serpentine Jasper Ridge (Total)	n.d.*	n.d.	0.45	0.50
Grass over Serpentine	0.49	0.35	n.d.	n.d.
Trees over Franciscan	0.42	0.21	n.d.	n.d.
Felt Lake area (Lake + Qsc)	0.57	0.33	0.33	0.44
C. Golf Courses				
Stanford Driving Range	0.59	0.46	0.60	0.95
Palo Alto Hills Golf Course	n.d.	n.d.	0.56	0.88
Sharon Heights Golf Course	n.d.	n.d.	0.60	0.89
Menlo Country Club Golf Course	n.d.	n.d.	0.62	1.08

*n.d. = not determined, usually not specifically locatable.

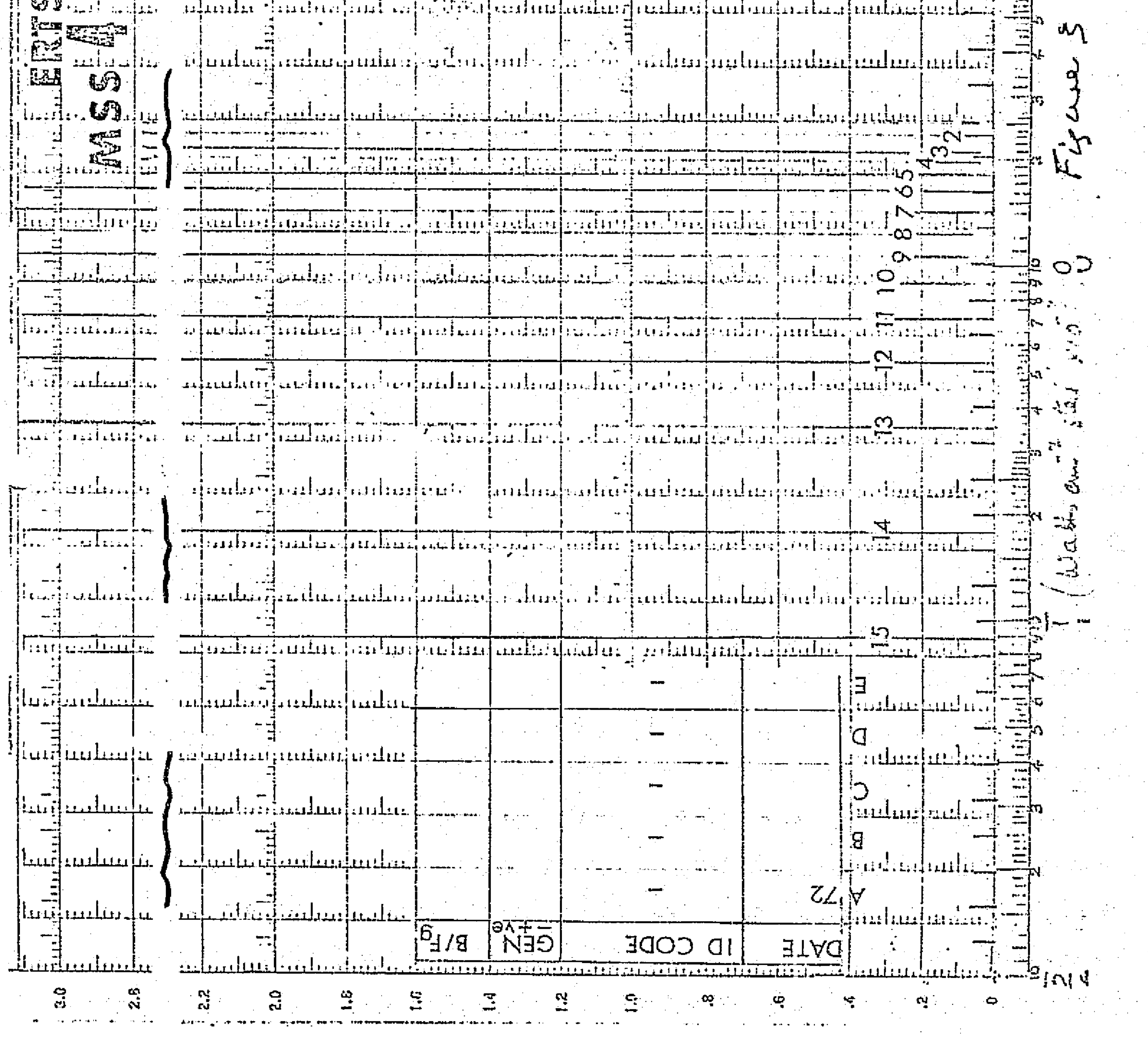

Figure 2.1.1.3 D log E plot paper prepared for ERTS linear density steps.

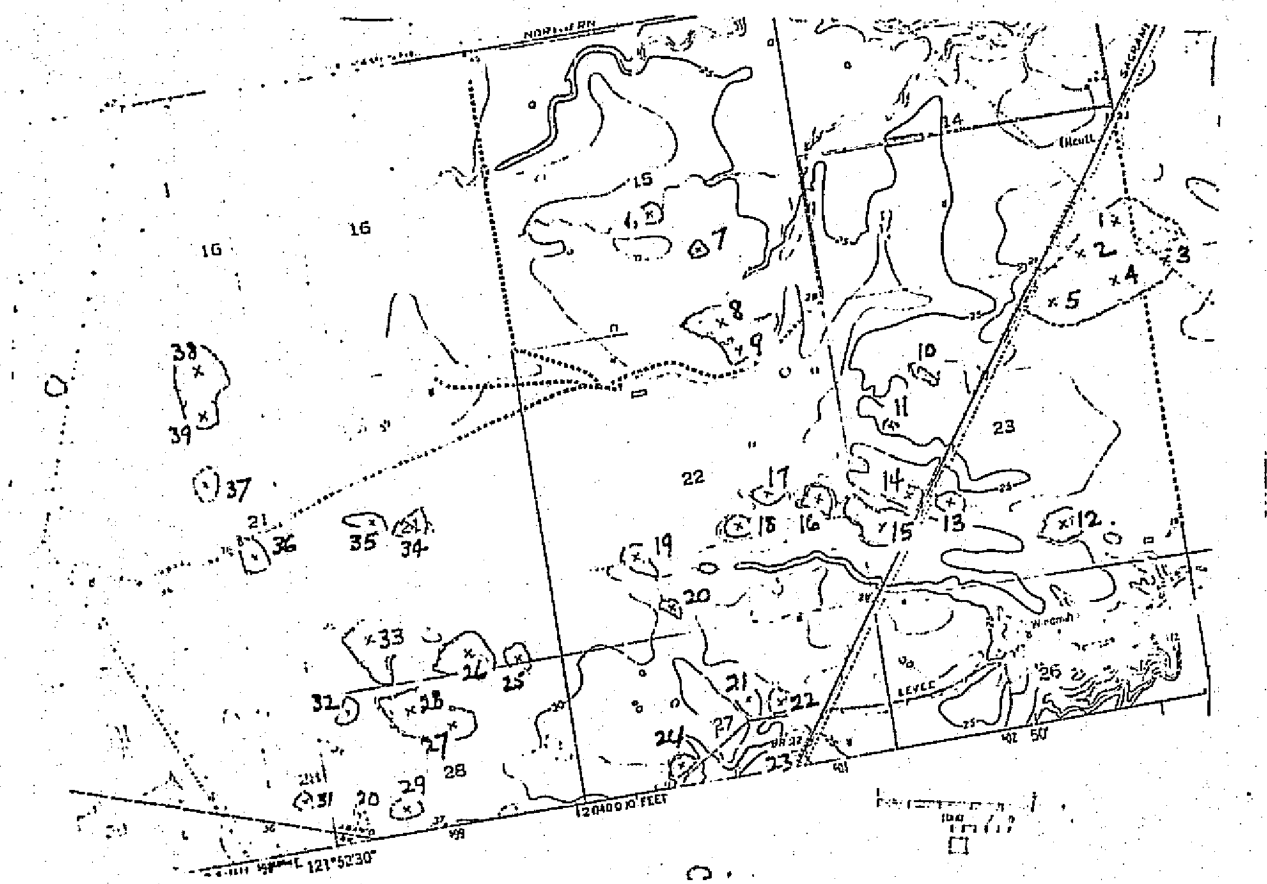

Figure 2.1.1.4 Map of Site 58 - East of Travis AFB, California
Scale Approximately 0.5 mile = 1 inch.

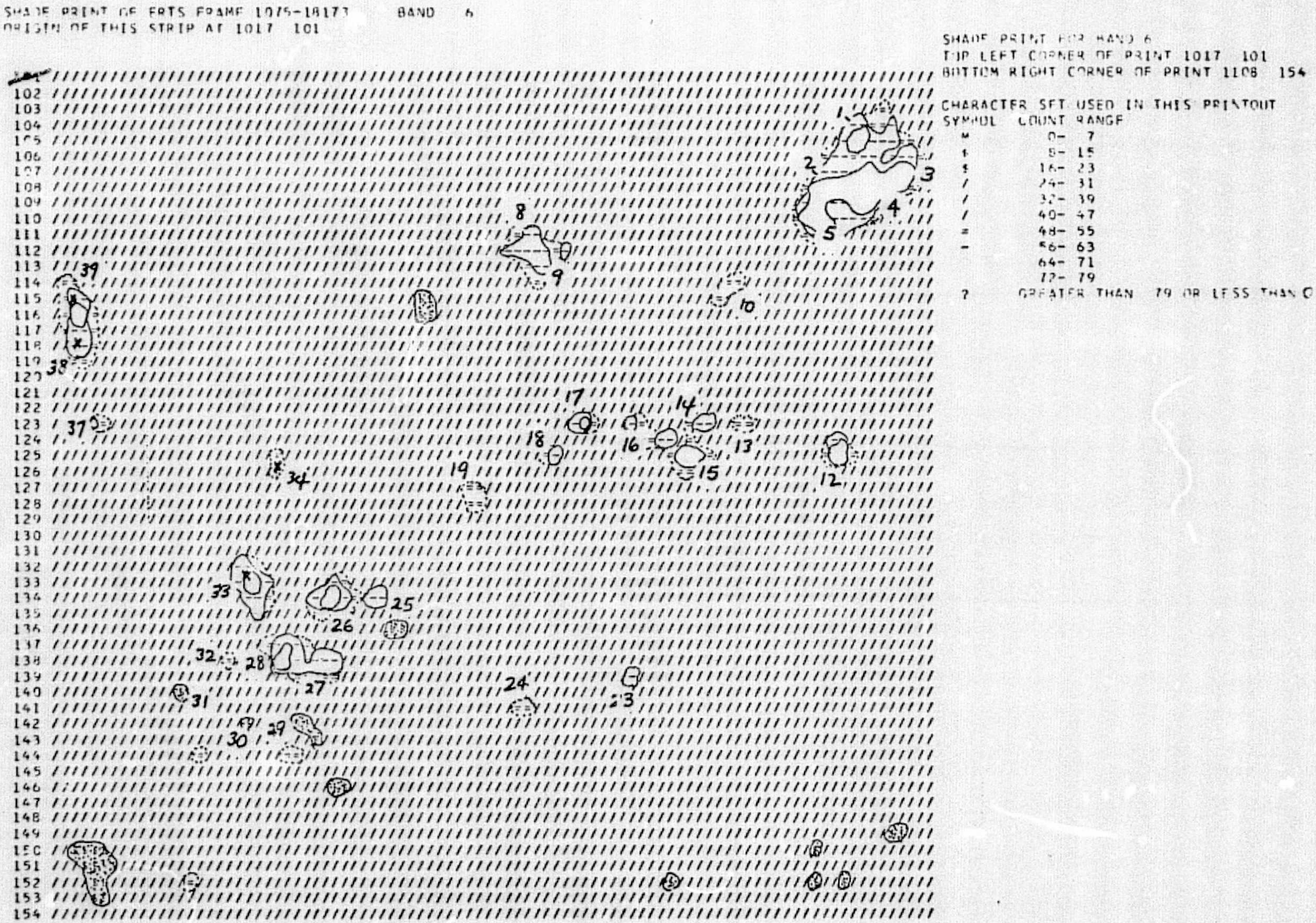

Figure 2.1.1.5 Shade Print of Site 58 Numbered Sub-Sites May Be Found in Numerical Data Sets, Figure 6.

25

SITE 58 E. OF TRAVIS AFB

NUMERICAL OUTPUT FOR ERTS FRAME 1075-18173

DRY PONDS #7-5

DIAGONAL POINTS OF AREA 1093 101 . 1108 110

BAND 4

32 34 32 29 31 29 23 25 29 27 27 29 28 29 29 32
34 32 32 32 31 28 29 31 31 28 25 25 27 28 28 28
36 37 36 33 32 32 32 [illegible] 37 44 45 37 29 29 26 25
32 35 35 32 31 31 33 [illegible] 61 54 56 59 46 35 32 32
34 34 34 34 33 35 57 63 61 58 58 63 52 47 40 31
37 39 37 [illegible] 64 62 59 55 60 46 43 57 57 52 34
34 34 36 [illegible] 56 55 56 57 63 59 63 65 63 47 32
32 34 47 [illegible] 58 53 58 63 69 55 57 [illegible] 31 28
33 37 57 69 64 64 66 69 63 52 40 [illegible] 32 32
36 44 [illegible] 56 61 64 64 61 59 42 36 31 31 32 31

BAND 5

32 33 32 32 30 27 26 26 30 23 22 25 27 27 30 30
32 32 31 31 27 26 24 26 27 26 24 24 22 27 26 26
35 38 35 32 32 29 27 29 39 42 51 38 27 25 21 22
35 35 35 29 28 28 41 63 70 61 61 66 49 35 32 28
33 34 34 28 23 36 72 72 72 65 72 73 54 57 44 30
36 41 36 33 72 70 73 59 61 65 52 55 62 64 56 33
32 35 33 48 61 61 57 63 77 69 63 74 73 69 52 30
31 37 57 59 60 69 53 76 76 76 67 61 69 59 29 27
32 40 61 75 72 69 72 75 79 73 69 55 45 38 32 29
39 61 [illegible] 75 70 70 68 68 58 46 35 28 28 29 29

BAND 6

33 31 30 30 30 28 25 25 29 29 26 26 26 30 31 30
32 32 30 32 27 25 25 27 28 30 28 28 23 28 27 28
33 33 33 29 28 26 26 28 36 41 49 36 28 29 26 26
30 31 31 30 28 25 39 58 55 55 55 55 45 31 28 30
31 31 31 28 27 37 67 69 66 61 61 61 51 49 39 29
34 36 32 31 41 62 63 53 57 62 66 59 57 57 52 31
31 31 31 45 57 60 59 60 69 66 60 63 69 68 53 28
30 36 52 [illegible] 59 64 76 76 76 73 64 69 68 68 30 27
31 34 59 55 56 63 63 66 72 [illegible] 67 33 33 28 26
34 55 72 72 65 63 63 63 60 51 42 31 28 26 26 26

BAND 7

17 16 15 15 14 12 12 13 16 16 15 14 14 14 15 15
15 16 14 14 13 12 12 12 15 15 15 14 14 14 13 13
17 17 17 15 14 13 13 14 17 21 22 19 16 16 15 16
16 16 15 15 13 13 15 27 [illegible] 20 15 15 16
15 15 15 14 13 17 29 [illegible] 28 27 27 26 23 15 13
17 17 15 16 23 29 23 24 25 26 21 23 26 25 24 14
16 17 17 22 27 27 27 28 32 33 29 33 32 30 21 13
14 16 24 29 29 29 33 31 32 31 28 27 [illegible] 12 12
15 19 27 30 29 29 23 30 31 30 29 [illegible] 13 19 13 13
16 26 33 31 30 29 29 28 29 24 17 15 14 13 13 13

DRY PONDS #13-18

DIAGONAL POINTS OF AREA 1067 120 1090 125

BAND 4

31 32 34 32 31 32 32 31 31 31 31 31 31 31 31 31 28 28 29 [illegible] [illegible] 31 32 31
33 32 32 33 31 33 33 32 32 32 32 29 29 32 29 32 33 33 32 [illegible] 29 33 33 32
32 31 41 31 [illegible] [illegible] 46 32 32 29 36 41 42 31 35 39 49 43 30 [illegible] 32 32 32 31
30 30 31 35 [illegible] 54 35 35 41 [illegible] 35 [illegible] 31 47 [illegible] 41 44 [illegible] 41
29 30 33 30 [illegible] 30 30 34 [illegible] 57 54 [illegible] 51 [illegible] 34 39 41 39
32 43 61 47 29 29 29 29 29 32 29 29 29 33 50 66 68 66 50 35 34 34 29 32

BAND 5

29 31 31 31 31 31 31 29 29 27 27 26 27 29 31 29 27 26 26 26 27 29 29 27
32 32 29 32 32 33 32 32 32 29 29 27 27 27 27 29 33 29 32 29 29 32 33 29
29 29 29 29 [illegible] 41 46 29 29 29 32 44 39 27 35 41 53 46 39 35 32 29 29 32
28 28 26 41 [illegible] 57 33 33 40 [illegible] 34 34 33 34 57 [illegible] 44 57 59 41
30 [illegible] 40 32 33 30 27 27 33 [illegible] 55 64 [illegible] 56 [illegible] 32 32 41 46 38
32 53 61 68 27 27 29 29 29 27 27 26 29 35 54 [illegible] 69 52 33 32 32 27 29

BAND 6

28 32 32 30 30 30 32 32 32 30 27 27 28 28 28 30 28 25 27 25 25 30 30 30
29 29 29 31 [illegible] 29 28 29 29 28 [illegible] 28 28 26 28 28 31 [illegible] 28 25 28 [illegible] 31 29
28 28 25 26 [illegible] 42 28 28 26 [illegible] 42 36 [illegible] 31 40 47 [illegible] 31 31 31 [illegible] 28 28
29 [illegible] 41 [illegible] 49 29 29 42 [illegible] 31 33 [illegible] 29 35 51 [illegible] 47 39 51 59 37
27 [illegible] 31 31 31 29 27 27 31 46 53 51 [illegible] 41 51 45 32 29 27 39 45 34
30 [illegible] 45 23 28 26 28 28 26 28 26 30 39 [illegible] 49 35 31 28 28 26

17 16 18 14 13 15

BAND 7

15 15 16 15 15 15 15 15 15 13 14 13 14 14 14 14 13 [illegible] 12 12 12 14 15 14
13 14 14 15 15 15 14 14 14 14 14 13 14 14 14 14 15 13 14 13 14 14 15 15
14 13 12 13 [illegible] 19 13 13 13 17 21 17 14 16 19 22 20 16 15 14 15 14 14
13 13 13 13 [illegible] 23 14 14 [illegible] 22 15 15 14 17 25 31 [illegible] 13 23 24 17
13 14 14 14 15 15 13 13 13 16 22 25 25 29 26 [illegible] 23 22 16 14 15 [illegible] 20 17
16 25 [illegible] 19 13 14 14 14 14 14 [illegible] 23 26 [illegible] 29 19 15 15 15 14 14

DRY PONDS # 25-28; 32,33

DIAGONAL POINTS OF AREA 1034 129 1052 138

BAND 4

31 30 31 34 34 34 34 31 31 34 31 31 31 31 31 31 31 34 34
33 33 33 30 33 34 33 33 33 30 30 30 30 30 30 33 33 34 33
32 32 29 32 32 32 34 32 32 32 29 27 28 29 29 29 29 32 32
32 37 52 59 47 32 29 32 32 32 31 31 31 31 31 31 31 32 32
32 42 54 64 65 62 44 32 33 36 36 46 61 57 49 32 36 40 36
31 32 39 59 41 51 36 31 36 39 59 [illegible] 56 53 59 43 59 [illegible] 49
31 31 31 38 54 49 34 30 35 40 49 49 47 44 42 31 31 35 31
33 33 30 33 37 39 34 41 44 33 30 30 33 30 29 29 27 29 29
32 33 43 32 41 53 61 63 [illegible] 59 43 36 36 32 29 29 29 29 29
34 47 42 34 32 38 56 63 55 53 53 53 52 34 28 28 31 31 31

BAND 5

30 28 30 30 30 30 30 30 30 33 33 30 30 33 33 33 30 33 33
30 30 30 30 33 32 30 32 30 30 30 27 27 30 30 30 32 32 33
29 29 29 29 33 32 32 32 32 29 27 26 27 27 27 29 27 29 29
31 37 57 41 47 31 31 29 31 31 27 29 31 29 29 29 27 29 31
29 40 51 69 [illegible] 59 46 29 32 33 38 51 54 61 49 32 33 40 33
30 32 44 61 56 53 39 30 36 39 63 [illegible] 70 63 46 63 [illegible] 49
33 30 33 61 59 50 34 30 34 44 59 57 59 52 47 30 33 36 33
30 33 32 32 33 38 33 41 43 32 30 30 32 30 27 26 26 26 26
27 42 44 29 40 [illegible] 62 67 62 59 44 33 33 27 27 27 27 26 27
35 52 42 31 31 42 61 67 61 56 59 61 54 32 27 27 27 27 27

BAND 6

28 29 28 29 31 31 28 29 31 31 31 28 29 31 29 29 28 31 29
31 27 29 27 31 31 29 29 31 29 29 27 29 29 27 31 31 31 29
31 30 30 30 [illegible] 31 31 31 31 30 26 26 28 25 26 30 28 30 31
32 40 57 58 [illegible] 42 30 30 33 30 30 [illegible] 30 28 30 28 [illegible] 28 28
31 36 56 [illegible] 45 28 31 31 35 [illegible] 54 35 29 [illegible] 37 31
28 30 44 [illegible] 36 28 33 36 [illegible] 55 44 58 [illegible] 44
29 29 31 41 55 47 31 [illegible] 35 44 54 51 47 47 42 28 31 37 29
29 [illegible] 29 29 35 35 31 [illegible] 32 31 29 27 31 29 27 26 26 26 23
28 [illegible] 43 28 41 [illegible] 53 37 33 30 [illegible] 28 30 26 26 28
36 54 42 30 30 42 [illegible] 59 54 57 [illegible] 27 28 27 28 30

33 26 25 28 32 27

BAND 7

15 13 14 14 15 15 15 15 16 16 15 15 16 15 15 14 15 16 15
15 14 14 14 15 15 15 15 16 15 13 13 13 14 14 15 16 16 15
16 15 15 14 15 15 16 15 15 15 15 14 14 14 14 14 14 16 16
15 13 [illegible] 15 15 15 16 14 16 14 14 14 14 14 14 14 14
15 [illegible] 19 15 16 16 17 21 27 24 17 15 14 17 15
15 16 [illegible] 17 15 17 17 [illegible] 29 25 19 28 [illegible] 19
14 15 16 20 25 22 15 14 17 21 26 [illegible] 23 23 21 15 [illegible] 15
14 15 16 14 [illegible] 16 17 18 16 16 16 15 14 13 13 12 12 12
15 20 19 14 21 [illegible] 29 [illegible] 17 16 16 14 15 14 14 14 13
17 [illegible] 19 16 15 [illegible] 29 28 26 24 25 26 24 15 13 13 13 14 13

DIAGONAL POINTS OF AREA 1018 147 1024 152

BAND 4

35 34 34 34 34 38 35
37 34 34 37 39 37 37
29 32 34 36 32 36 34
31 27 25 25 25 31 32 LAKE
33 33 32 29 28 26 29
35 35 36 37 31 32 39

BAND 5

34 30 33 33 33 37 33
33 32 32 33 35 36 33
26 29 32 32 27 35 33
26 20 19 19 20 29 32
33 32 24 24 22 21 26 LAKE
32 35 35 24 24 29 41

BAND 6

35 33 33 33 33 37 31
36 34 31 34 32 34 34
31 31 33 37 31 37 33
30 21 [illegible] 21 33 33
33 31 [illegible] 20 23 26 LAKE
34 34 34 15 21 31 38

BAND 7

17 17 15 15 17 17 16
16 17 16 17 17 17 17
16 17 17 17 15 17 16
13 [illegible] 15 16
16 14 [illegible] 11 LAKE
16 17 13 [illegible] 14 19

Figure 2.1.16 Numerical Data for Site #58 Areas.

2.2 REDUCTION AND PROCESSING OF LANDSAT TAPES (CCT)

2.2.1 STANSORT: Philosophy and Operational Use

2.2.1.1 Introduction

With the increasing application of ERTS multispectral scanner data in the field of agriculture, forestry, geology and landuse management, urban studies and hydrology, a need has developed for a system which will allow any user, from the most experienced to the novice, with any (or no) level of training in computing and programming to use ERTS tapes with minimal effort and cost. It is also desirable that he have at his disposal all of the techniques which have been developed for reduction, interpretation, and evaluation of such data, for example, density-slicing of images, inter-band ratioing, clustering and classification techniques, plus the removal of instrumental and atmospheric effects. For speed, flexibility and ease of operation, an interactive program is the most appropriate form.

For these reasons STANSORT, a fully interactive tape reading program was developed. The program has been written so that the operation is self-instructive, the user being queried prior to each step and being required to input short answers at the terminal, depending on his requirements. The user may examine output from earlier stages of the program to assist him in his decision to the current query. Because of the 'tutorial' nature of the program, it has been used also for the instruction of graduate students in the use of ERTS data (AES classes 294, 133, etc.).

2.2.1.2 STANSORT Program Philosophy

The program was developed on a PDP-10 computer at the Institute for Mathematical Studies in the Social Sciences at Stanford University. The source language is SAIL, an ALGOL-type language taking advantage of many of the PDP-10 features. The programs are broken into basic procedures, giving an open structure in which any new techniques may be simply inserted with a minimum of program change. The IMSSS PDP-10 operates under the TENEX monitoring system, so some small changes would have to be made to the program to implement it on any other PDP-10 operating under the DEC operating system.

2.2.1.2.1 Principal Aspect - Detailed Analysis of 20 km^2 (7.7 mi^2 areas)

It should be stressed that STANSORT is designed for the detailed analyses of a small area on a large scale (approximately 1:20,000) of sections of the ERTS images. Additional areas may be added simply to cover more extensive scenes. It is assumed that the users will have located (at least to within several miles) the area in the ERTS image in which they are interested. Such a decision may be arrived at by examination of the complete image, or from enlarged portions (1:210,000 scale) of the image produced from the tape using the Stanford image generation program IMAGE (SRSL 74-12, Honey, 1974, 75-4, Levine, 1975).

2.2.1.3 ERTS System and CCT Tapes

The ERTS system consists of satellites in a sun-synchronous, almost polar orbit, at an altitude of 920 kilometers. Either satellite crossses the equator, traveling in a southerly direction at 0942 local time. Every 18 days the satellite covers the same ground track, so that sequential coverage of any ground scene is available, with an 18-day period. The instrument package on the satellite consists of three ReturnBeam Vidicon (RBV) cameras, a Multispectral Scanner (MSS), a Data Collection System (DCS), and two wide band Video Tape recorders.

The RBV cameras, sensitive in the ranges 475-575 nm (blue-green, channel 1) 580-680 nm (red, channel 2) and 690-830 nm (near infrared, channel 3) have not been utilized due to an early electrical malfunction. These instruments will not be described further. Such 3-band data would also require modification to the STANSORT (4-band) programs.

The MSS is a four-band scanner, with bandpasses of 500-600 nm (green, channel 4), 600-700 nm (red, channel 5), 700-800 nm (infrared, channel 6), and 800-1100 nm (infrared, channel 7). These wavelengths are in the reflected region of the spectrum - no thermal radiation is detected, although ERTS-C (1977 launch) will carry this as a fifth channel. Each of the bands has a bank of six detectors to assist the scanning speeds. Across-track (E-W) scanning of 185 km is achieved by means of an oscillating mirror in the optical path. Six scan lines are imaged at once in each of the four bands. The video outputs are multiplexed and either stored on the video tape recorders, or, if in range of a ground receiving station, encoded and transmitted. Recorded data is encoded and transmitted later. Both of the tape recorders in ERTS-1 have failed, but ERTS-2 is making recordings to be dumped.

Each image is made from 2340 scan lines each of 185 km length. A scan line consists, after processing, of 3240 digital units (picture elements, pixels) which are packed as 8-bit bytes on tape. In addition 56 bytes of calibration information are included at the end of each record on bulk tape. Thus for each image there are about 3×10^7 bytes of information. A set of computer compatible tapes for a scene consists of four tapes, each tape representing one quarter of an image, a strip 46·25 km E-W and 185 km N-S. Each tape contains $7{\cdot}71 \times 10^6$ bytes to date, with a 40-byte scene identification and a 624-byte annotation record appearing as the first two records.

Each data record on the tape consists of 2340 bytes of data, representing 4 channels for one quarter of the image. The data is in an interleaved format, as indicated below:

BYTE NO.	1	2	3	4	5	6	7	8	....
CHANNEL NO.	4	4	5	5	6	6	7	7	....
PIXEL NO.	1	2	1	2	1	2	1	2	....

Each pixel in a scene represents an area of 57×79 m^2 (approximately 0.4 hectare, or one acre).

2.2.1.4 Operational Use of the STANSORT Program

2.2.1.4.1 Initial Steps

The user is required to have logged in, mounted his tape and carried out any preliminary measurements to determine the location of his area (Appendix 1). He is then queried by the main program for basic information regarding the tape. The program reads the Header and Annotation records and displays identifying information on the screen - Scene ID, date of acquisition

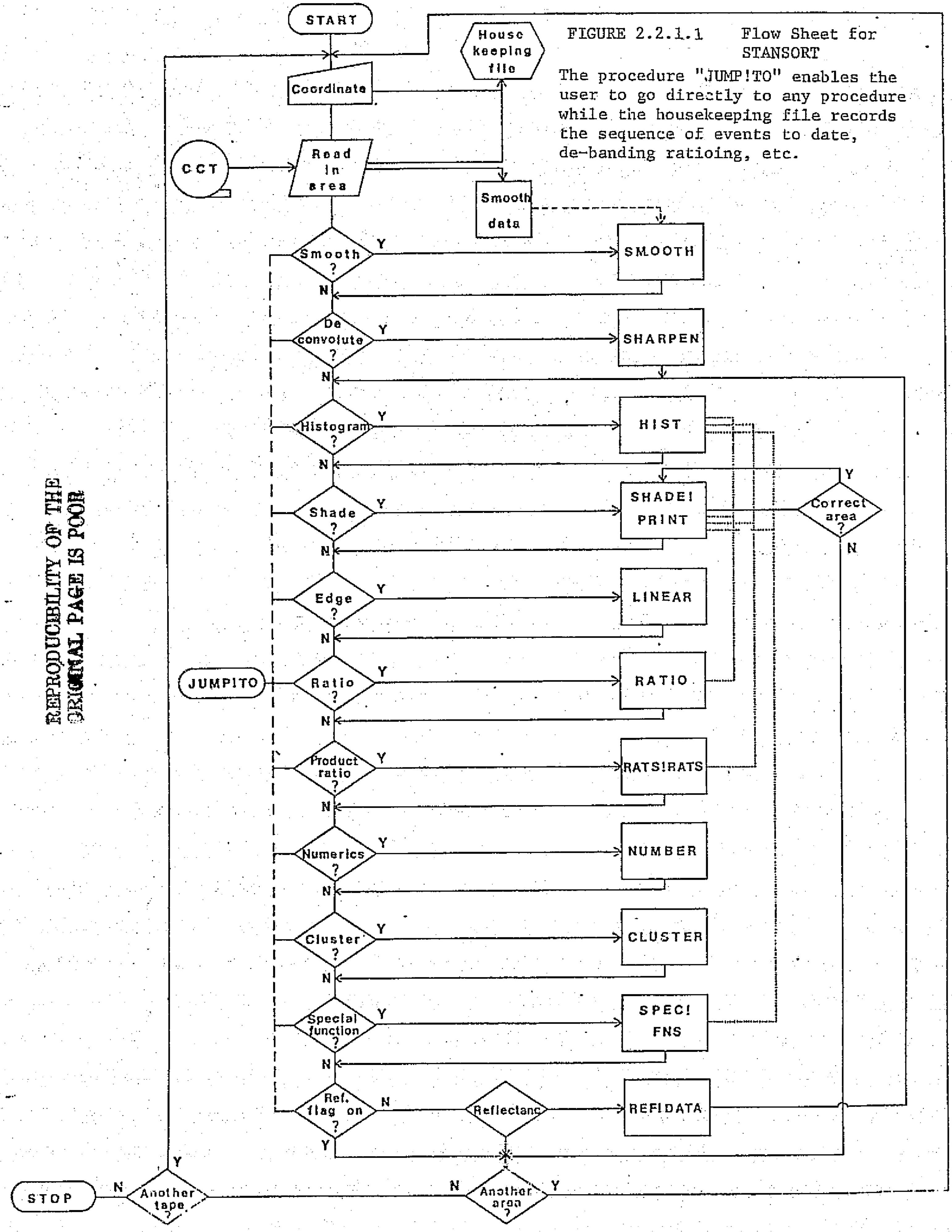

FIGURE 2.2.1.1 Flow Sheet for STANSORT

The procedure "JUMP!TO" enables the user to go directly to any procedure while the housekeeping file records the sequence of events to date, de-banding ratioing, etc.

of data and which tape (of the set of four) is being read. This necessary stage prevents mounting the wrong tape and subsequent (costly) confusion! If the tape is correct, then the "Yes" answer causes relevant information from the header and annotation records to be stored in the housekeeping file. This sequence of actions is typical-data shown from the tape, a question, which requires decisive action by the user.

The user than enters the co-ordinate of the position on the tape (image) and the size of the area. The program checks the coordinates to be sure they exist on that tape, then the tape advances to the area which is read in and repacked. The program then enters a series of procedures, querying the user and proceeding according to the response.

The Flowsheet outlined in Figure 1 illustrates the cperations and their normal sequence of execution. This sequence was derived during development of the program as the most common one a new user would follow. For the more experienced user, or for a re-examination of a scene as with another algorithm the "JUMP! TO" operation may be utilized. With this feature the operator may skip forward or back to any procedure and break the normal sequence.

2.2.1.4.2 Header

The Housekeeping File stores the user-designated title for the area, the ERTS tape identifier and dates, the relevant information from the header and annotation records, such as frame-center coordinates, sun elevation and azimuth and satellite heading. This information appears at the top of every output as indicated in Figure 2.

The majority of the queries and the effect of the replies are evident from the flowsheet. We will proceed with the sequence and a brief description of each procedure will be given. More detailed description are presented in Section V.

STANFORD REMOTE SENSING LABORATORIES

STANFORD UNIVERSITY

CALIFORNIA

U.S.A.

Tel. (415) 497-2747 F.R.HONEY

+++

ERTS tape 1273-1818300 Tape number 2 of 4
Exposure date 22 APR 1973
Coordinates of frame center N37-37/W122-02
Sun elevation 55
Sun azimuth 129
Satellite heading 190

Area begins at row 1299,pixel 1293 of frame

SCALE : HORIZ (E-W) 1: 22440 ; VERT (N-S) 1:18670

REDWOOD CITY TEST FOR AES 133 CLASS

Shadeprint of 5
ERTS raw data,debanded, deconvoluted to 'sharpen image'
Levels and their symbols:

```
B=7 - 8
▒=9 - 10
M=11 - 12
▓=13 - 14
0=15 - 16
S=17 - 18
%=19 - 20
==21 - 22
+=23 - 24
;=25 - 26
-=27 - 28
\=29 - 30
.=31 - 32
 =33 - 34
```

NOTE: Minimum value of area is 7, D.C. level of 7 taken from values.

Figure 2.2.1. 2 Header showing Housekeeping Information

Some of the procedures interact with each other. For example, histograms of ratios may be obtained by a "jump" thereby presenting the histogram procedure data in ratioed form. Such interactions are presented by dotted lines on the flowsheet.

For speed and efficiency all arithmetic operations are performed in integer arithmetic, except where the roundoff would seriously affect the result of the procedure. A great deal of careful consideration was taken to minimize any unnecessary time consuming operations within the procedures, for therein lie the principal cost generators.

After reading in the tape data representing his area, the user may deband the data. This function attempts to remove much of the "striping" of the scanner data.

2.2.1.4.3 Deconvolute

The data may then be "deconvoluted", a procedure included in an attempt to remove the effect of the overlapping fields of view of the scanner across a scan line. This appears to provide significant image improvement, particularly when searching for fine details such as roads, rivers, airports, etc.

2.2.1.4.4 Histogram

Histograms of the data may be obtained at this point. The histograms are almost indispensible for a clear interpretation of the data, and as an indicator for some of the subsequent procedures, such as shadeprinting, ratioing and clustering. We feel however that automatic use of histograms to control the grey scale of a shadeprint is not advisable, and prefer to leave this option available to the user. This is a particularly attractive aspect of an interactive program.

2.2.1.4.5 Shade Print

The next procedure, SHADE PRINT, ~~presents~~ the user with his first look at the data in a 'map' form on the display screen. Typically the experienced user "jumps" to SHADE initially to make sure of his location and to quickly refine the co-ordinates if necessary. He is queried as to the correctness of the current location: if not correct, the program skips to the step of asking for a new area; if correct the user may print the shadeprint with various levels of slicing (stretching or enhancement) for any of the channels.

2.2.1.4.6 Edge

Edge detection is included to enable a search for high-contrast changes as may occur at boundaries such as land-water interfaces or, possibly, of curvilinear geologic features such as faults or intrusives, or a vegetation changes.

2.2.1.4.7 Ratio

Interband-ratioing allows the user to select the numerator band, denominator band and the levels at which slicing is to be performed. The result also may be displayed in 'map' form with a shadeprint representing the ratio values printed.

2.2.1.4.8 Numerics

Numeric data from either raw data (or data converted to reflectance) may be printed for more detailed examination, by a call to NUMBER.

2.2.1.4.9 Clustering

A cluster analysis may then be performed on the data in an attempt to separate population classes, or if some information about expected classes is available a supervised classification may be performed.

2.2.1.4.10 Special Function

The special functions procedure (not implemented to date) will act as a run-time compiler, allowing the user to insert any new (special) function by which the data will be evaluated. This will provide an extremely versatile and powerful otpion for testing new ideas on manipulation of the data.

2.2.1.4.11 Reflectance

The data flag is then checked to see if the data is already in the form of reflectance. If not, the user may convert data to reflectance provided he has certain standard measurements to insert. After conversion of of the data to reflectance the program recycles through the entire sequence (D-I).

2.2.1.4.12 New Area, New Tape

Having satisfied himself that no more information can be obtained for the current area, the user may then move to another area of the tape, or to another tape and repeat the sequence of operations.

2.2.1.4.13 Scale of Lineprinter Output

A note on the printout format from SHADE! PRINT, RATIO and CLUSTER. The N-S scale is approximately 1:19,000, the E-W scale approximately 1:22,000. The skewing (3.5 degrees) due to rotation of the earth has not been taken into account, as the resulting "map' is slightly distorted, both in the magnitude and direction of its axes. This in no way interferes with the interpretation steps as all the output is similarly distorted in precisely the same way.

2.2.1.5 Detailed Description of Each Procedure

2.2.1.5.1 Debanding (Removal of Banding or Striping)

Noise on the satellite data appears to take two forms. The first, of a fairly random nature, arises apparently from digitization on the satellite, followed by calibration (which necessitates floating point numbers). For Channels 4, 5 and 6, noise is introduced during decompression of the data, by using the look up table (Thomas 1973) which has missing values. An examination of the histograms for the three decompressed channels shows much more apparent noise than for Channel 7, thus it would appear that the majority of the random noise arises during the decompression process. The second form of noise, a less random, banding with a six-scan line period, probably arises from error used in the calibration expression for each of the tour detectors in the bank of six per spectral band.

The first form, by far the least significant of the two, is the most difficult to remove. One crude approach is to convolute the data with a smoothing function, thereby reducing any noise spikes, but in the process effectively 'defocusing' the image by lowering the spatial resolution. This technique obviously also removes most of the banding. Because of its effect on the resolution, however, it is an undesirable approach when looking for fine details but has attraction in some regional geochemical studies (Lizaur, 1975). For examination of targets with no high-frequency information expected, such as areas of shallow (< 20 m) water to estimate depths, this approach may be employed. This technique was used in our initial studies but was abondoned in favor of a "debanding" algorithm. True smoothing is being re-introduced, after debanding, in the new "STANSORT 3", as a branching option relative to deconvolution. One thus has a three-way branch - raw data, smoothed data or deconvoluted (sharpened) data.

The problem of 'striping' (banding) of the imagery has been considered by Algazi (1973), who presents an algorithm for removal of this noise. In this technique, the mean and variance for each channel across a whole tape record (810 pixels), and for a large number of scan lines of the image are calculated. The means and variances for each line are calculated as the data is being read in, and comparison with the global means and variances, provides an offset and gain factor to be applied to each scan line for each channel. This appears to effectively remove the banding, but does not affect the random noise discussed above. For intermediate and high radiance targets i.e. where this random noise is low relative to the signal, the image quality is improved substantially.

Debanding is generally a necessary step if ratioing is to be performed on the data as the noise effects are increased noticably by the ratios.

It may be more appropriate to automatically smooth the data using Algazi's algorithm as the data is read in; at present this is a later option, the debanding factors being calculated, not for every line, but as a set using the first twelve lines of the area of the image under study, the factors being stored, and printed out for reference.

If the data is debanded a flag is set, and the housekeeping file is modified to indicate debanded data on output.

2.2.1.5.2 Sharpen (Deconvolution)

The area sampled by the scanner across the ground track is nominally 79.3 x 79.3 meters^2, but has an overlap because of oversampling. This overlap is 21.8 meters, if one assumes constant mirror velocity* There is, ideally, no overlap between adjacent scan lines, although this may be disputed at the extremities of each line due to slight broadening of the ground footprint of the field of view.

This overlap of pixels results in a slight degradation of the image. This may be reduced dramatically by 'deconvolution' of the data to remove some of the effects of the overlap.

The un-normalized digital function performing this operation may be represented diagramatically by

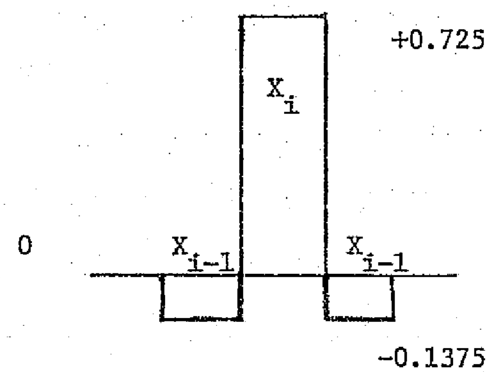

*The mirror velocity is not constant but is a fixed, continously varying function directly related to the E-W position of the pixel. We make a simplifying assumption that it averages 13.75%.

For any pixel X_i (across the scan line), the enhanced value is given by

$$X_i' = N(0.725\,X_i - 0.1375\,(X_{i-1} + X_{i+1})),\ i = 2\ldots n-1, \qquad (1)$$

where N is a normalization gain factor given by

$$N = \frac{\left(\sum_{i=2}^{n-1} X_i'\right) + X_i + X_n}{\sum_{i=1}^{n} X_i}$$

The normalization factor may be evaluated by the program. For average radiance targets it has been found to have a value of 2.0.

This enhancement procedure has been found to give greatly improved quality in recreated imagery, though for use with line-printer output the enhancement is not immediately obvious. Image contrast is heightened as well as apparent spatial resolution.

2.2.1.5.3 Histogram

This procedure provides output on the screen, (and if desired, on the lineprinter) the present type of data being processed — either raw or smoothed data, enhanced data or ratioed. The histograms are scaled for the width of our line printer to have a maximum ordinate value of 68. The frequencies of counts for each level are printed down the right hand margin on the line printer.

The procedure itself is straightforward, but provides a powerful tool in the interpretation and planning of processing of the data at later stages of the program. As mentioned above we differ in program concept from many

other groups and do not use the histogram areas to automatically control the next SHADEPRINT step. We reserve this for an operator-decision.

2.2.1.5.4 SHADE! PRINT (Map-like Output)

The shadeprinting procedure enables the user to display on the screen a symbolic 'map' of his area, with approximate gray scale lines being indiated by appropriate alphanumeric characters (no graphic terminal is available at present , although we are reprogramming an IMLAC unit for this purpose). The shadeprint may be printed in either a replica of the screen image, or overprinted twice per raster line to give better gray scale representation,with the appearance of a over-enlarged newspaper illustration. (See below).

FIGURE 2.2.1.5.1

FIGURE 2.2.1.5.2

41

Enhanced "digital image" using conventional ERTS imagery at an approximate scale of 1:87,000. Original ERTS 1:1,000,000 scale print is included for comparison (lower right)

DN-Offset. Two functions may be performed on the data at this stage to improve the presentation. The first, removal of a DN (digital number or counts) offset allows the user to have a lower cutoff level for the data. In the case of raw data, for the visible channels (4 and5) there is a significant contribution due to radiation backscattered by the atmosphere. For Channel 4, this may reach 18 digital counts. This may be removed to allow better slicing intervals, and to look at another useful range of the data. Another user may be interested in only looking at very high radiance targets, for example snow and clouds (Itten, 1975). All data below 120 may be disregarded, and with intervals of 1, the remaining screen counts will allow partial differentiation of wet and dry snow.

Stretch. The second function involves variations in different levels of slicing, or changes in the grey scale increments. Although each of the levels are the same (i.e. "linear stretch") this allows the user to produce the optimum 'map' of his scene on the screen and in the subsequent printout. Varying the DN offset and the slicing interval, allows the user to look at specific types of scene- water, forest, rangeland, or snow.

No attempt has been made to implement the more automatic 'histogram corrected' form of shadeprinting, wherein equal areas of the frequency curve are allotted to equal grey scale intervals. We felt that some small but (possibly important) details may be lost using this technique, and each user must make the decision which best fits his data set.

2.2.1.5.5 Linear

In most applications of photogeology, linear and curvi-linear features are selected based upon the concept that such boundaries are structurally-controlled features. A search may be made for those boundaries, which show as contrast-edges between materials of different reflectivities, using the edge-detection algorithm. In this algorithm an attempt is made to eliminate single-pixel noise, by requiring that any contrast change be present simultaneously in at least two of the channels. If a pixel-pair possesses this contrast

their position is marked by an asterisk symbol, chosen so as to appear non-directional to the eye of the observer, and hence will not influence his decision of linear joins.

The user may decide the contrast change (or tolerance level) required to define a boundary for each of the channels. A'map' then appears on the screen, and the levels may be changed to produce greater or lesser detail. The product may then be printed.

We have not used this spectral-lineation detector as much as we had hoped. The technique works satisfactorily for obvious delineations. It has the advantage of removing unwanted (presumably) information. One possible application being investigated is the automatic "contouring" of shallow (< 20 m) water data to prepare bathymetric maps, by using the known spectral aspects of water to define depths in clear sediment-free bays.

2.2.1.5.6 Ratio

The application of interband-ratioing to enhance and accentuate features is a well established technique in several remote sensing groups. For enhancement of alteration zones in mineralized areas ratios of Channel 4 (green) over Channel 5 (red) yields some excellent results (Rowan, et. al, 1974). For vegetation studies ratios of $\frac{CH7}{CH5}$ or $\frac{CH7}{CH4}$ give a good indication of vigor, although some subtle changes may be brought out by $\frac{CH5}{CH4}$ (Lyon, et.al., 1975).

The user selects his numerator and denominator channels. Maximum and minimum values for the ratios are displayed, and the user may request a histogram of the ratioed data. After examination of the histogram (and, if required, printing), a DN level and a slicing interval are selected. A shade-printed map is presented of the results which may be modified before and after printing. Any number of ratios may be examined in this way, and hard-copy produced as desired.

2.2.1.5.7 Ratio of Ratios (RATS!RATS)

Ratios (or products) of ratios effectively provides a combination of the form

$$\frac{\text{(channel n) X(channel m)}}{\text{(channel i) X(channel j)}}$$

This technique was implemented on the request of P. Lizaur, in an attempt to increase discrimination of the data, in particular in alteration zones. The results of a study using this method are presented in Lizaur (1975).

The procedure is very similar to RATIO - the required channels are typed in, histograms may be examined and a shadeprint prepared, examined and printed. At present this proceedure is being replaced by a more general (+, -, X, or ÷) algorithm to manipulate matrix-pairs.

2.2.1.5.8 Number

This procedure outputs the data in its current form as it occurs in memory, i.e. raw data, debanded or deconvoluted, or reflectance data. The quantity of output is large, so that the use of NUMBER is only recommended when some definite study requiring the numeric information is to be attempted.

2.2.1.5.9 Cluster

Clustering of the image information into unique classes while using a fully-interactive mode is one of the most important aspects of the program. The algorithm used is extremely straight forward and fast, although it lacks the statistical rigor of the more usual clustering techniques. Some of these techniques will be discussed before describing <u>our</u> clustering procedure.

Classification of data may be carried out in two modes. One is the so-called "supervised" classification, whereby previously defined populations with their representative spectra input to the program, are assigned to these known types according to some nearest-neighbor or least-distance criterion.

This can either involve some preprocessing of the data to eliminate unncessary data (Andrews, 1972, Sebestyan 1962) followed by testing with the distance criterion, or the use of "table look-up" techniques in which a range of data is input for each pre-determined class and the data sorted by comparison (Eppler, 1974). The second of the two techniques is extremely rapid and is somewhat similar to our clustering algorithm described herein.

The second mode of classification, "non-supervised" classification (or clustering) uses natural differences in the data to classify them into arbitrary groups (Andenburg 1971). Several types of rigorous, but time - consuming statistical proceudres, are available for the clustering of data (Prelat, 1974).

The technique used in STANSORT is to divide four-dimensional space into hyper-rectangular "pigeon-holes", whose locations in space are determined from the data. The significant difference with our approach is that the size of the rectangular "pigeon-holes" are determined interactively by the user. The data is then sorted into its appropriate position. Inspection of the shade-printed 'map' allows the user to preserve the patterns or to redo them with variable pigeon-hole sizes (tolerances).

In examining an initial area, the user selects the tolerance (or gate-width) he will allow around each band of the spectrum of any class. The program then begins to cycle through the data, the first pixel being arbitrarily assigned as the first class ("A"). The remainder of the data is then compared with the spectrum of the first class. If the spectra fit within the tolerance, they are assigned as the same class. After examining all member of the array, the program recycles, taking the first pixel, unassigned from a previous cycle and classifies it with the next symbol, comparing all remaining unassigned pixel spectra to the current 'standard'. The program continues to cycle in this manner until all data has been classified, or until no classes remain (maximum 26 with all others assigned to a blank symbol). A classification 'map'

appears on the screen, and the user decides if the result is satisfactory: if yes, then he may print; if no, the tolerance may be varied. The final set of 'standard' patterns i.e. the mean of each class, are printed out, and stored for classification of subsequent areas. The printed output may be used to evaluate each class. Sometimes these spectra are found to be closely similar, although just outside the tolerance range. The technique appears to over-classify some data which could possibly be merged into one large class, perhaps during a subsequent hand-analysis stage (coloring, etc).

The classification is sensitive to the starting spectrum. If it is started at a different position, the 'standards' and classes will be different. However, the gross clustering remains very similar - only the assigned symbol and partially, the 'standard' spectra for an area will vary.

It should be emphasized that this clustering procedure is used mainly for smaller areas, for example summing up to 4000 to 5000 pixels. It can be modified for examination of complete tapes or sets of tapes, and would remain a very fast technique, but at present we are more interested in detailed analyses of small areas (~200 square miles) with mining interest.

The clustering procedure may be used in four modes, un-normalized or normalized on raw data, and similarly on reflectance data. In addition, for reflectance data, the procedure may be used in a classification form to search for materials with known reflectance spectra which are typed into the program. Such spectra would, perhaps, result from field measurements in the area.

It is found that for surfaces with undulating topography, that the spectra of similar materials are virtually identical, but the relative magnitudes of the spectra vary according to whether the pixel is on a sun-facing slope or on a partially-shaded slope. For moderate variations in slopes it is found that normalizing (or ratioing) to one of the channels removes most of the effect due to topography. Without normalization, two similar spectra may be classified

differently. For extensive areas of uniform slopes, or horizontal areas (coastal plains, lakes or ocean scenes), the necessity for normalization is removed, so computation times may be reduced by avoiding normalization. Both are present in STANSORT as readily-available options. In addition, in the un-normalized mode, the user may choose to discard a channel, particularly if that channel is excessively noisy.

In conclusion, it should be emphasized again that this algorithm was chosen primarily for its rapidity and comparatively low cost. Testing of the procedure against other techniques has been limited, but one case (Itten 1974) produced virtually identical clustering results to a procedure in LARSYS, at a fraction of the cost, in a much shorter time.

2.2.1.5.10 Special Function

Using this procedure the user could type in any form of manipulatory algorithm he wished. This procedure has not been implemented as yet, but its basic aim is to provide an extremely versatile facility by which to evaluate functional approaches to enhance the data, and for feature extraction, without the necessity for writing a separate program for each function.

2.2.1.5.11 Reflectance

The digital data present on the ERTS tapes represent the radiance signal received at the sensors. This signal is composed of atmospheric backscattered radiation, and radiation reflected from the ground target. The magnitudes of both of these signals are a function of sun angle, and their relative values may vary significantly. For inter-season comparisons therefore, it is preferrable to have the data in a more standard form, such as relative reflectance. To achieve this, several standard targets must be available within each scene. These targets should be extensive (over 9 pixels in size) with near-constant reflectivity throughout the year, and easily locatable. Once the standards are chosen their bidirectional reflectivities should be measured relative to some laboratory standards (barium sulfate or smoked

magnesium oxide). The user may then search for these targets on the tape, extract the digital readings for the areas and derive regression coefficients for the conversion of the satellite data to reflectances. It is desirable to have several such areas of known reflectance within a scene so that the converted data may be checked, as atmospheric effects over a scene may vary (Duggin, 1974).

With the data now converted to reflectance the user may then perform all of the previously described functions on the data. A reflectance 'flag' is set by the program for each area to avoid attempts at conversion of areas already in a reflectance form.

2.2.1.5.12 Completion of a Study

Having completed all of the required steps above, the user is then asked if he wishes to examine another area on the current tape. If so, then he inserts the relative position and size of the new area. The system checks the coordinates to be sure they are valid for that tape and then the tape is repositioned. Data for the new area are read in. Should another area not be required on the current tape, the user may then look at another area on another tape, which must be mounted. For both of these steps, control is stored (such as clustering standards and ranges) along with the relevant header information.

If the user does not wish to continue, he may exit from the program. Any printout the user may have requested exists as separate files on disc, and must be printed with a separate program.

2.2.2 AN INTERACTIVE PROGRAM FOR PRODUCING COMPUTER-ENHANCED ERTS IMAGES ("IMAGE") PART II - METHODOLOGY DEVELOPMENT

2.2.2.1 Introduction

This paper covers the operational or applications phase of the imagine software program during which the methodology was finalized. A series of black and white and color-composite images of several areas in California and Nevada, generated during this phase, are presented and discussed.

It should be emphasized, that it is the operational simplicity and the interactive nature of the program, utilizing the PDP-10 computer and a keyboard controlled CRT display that represents the core and the strength of the program. The best capabilities of both man and machine are utilized. With IMAGE it is possible for the operator/investigator to initiate functions and react quickly to each step in the program. Parameter changes may be made rapidly to optimize the final enhancment, a tape generated and the required images made by use of the DICOMED Image Recorder*. Used in conjunction with the SRSL STANSORT Program (Honey, Lyon, 1974) for preliminary investigative purposes, computer-enhanced ERTS images may be produced economically and quickly.

A general discussion of the initial phase in which the need, criteria and evolution of the Stanford Remote Sensing Laboratory interactive program (IMAGE) for producing computer-enhanced ERTS images are covered by F. R. Honey in SRSL Report 74-12.

---

*Made available to us by the courtesy of NASA Ames Research Center, Moffett Field, California.

2.2.2.2 Image Generating Program Functions

The image generating program was designed to reformat the interleaved image data on the ERTS CCTs in such a fashion that it could be manipulated, as desired, to enhance areas of interest and then generate digital tapes that are compatible with a CRT recording instrument (such as the DICOMED D47 Image Recorder). These tapes then contain the necessary intensity information to produce enhanced black and white, or, by using 2 or 3 such black and white images, to make color composite images of the areas of interest. The images obtained are recorded on standard 4 X 5 inch Polaroid or Ektacolor film, covering an area of 300 pixels horizontally and 250 vertically at a scale of 1:210,000 approximately.

As indicated in SRSL Report 74-12 the image program, which is an interactive one, designed for use with a PDP-10 computer, locates the area of interest and then makes a series of mathematical functions and operations available which the user may apply to study the area before generating the final image. These functions will be discussed below in a sequential fashion as they appear in the program.

2.2.2.2.1 The program initially makes geometric corrections in the image format due to the lateral skewing of the progressive lines of the scanning device, caused by the orbital inclination, rotation of the earth, and the higher sampling rate in the scan direction vs. the flight direction.

2.2.2.2.2 After locating the area of interest and specifying its extent, a debanding function is made available. This option selects 6 lines of data, a full 810 pixels wide and determines their 6 "average means". The "debanding factors" then are the quantities necessary to make all the average means up to equal average intensity. The striped pattern

is due to the imperfection of the on-board sensor radiometric calibration which results in a banding pattern repeat at six line intervals in the recorded images.

2.2.2.2.3 A deconvolution function is also supplied which tends to eliminate the scan line overlap of pixels due to the over-high sampling rate, thus strengthening their contrast.

2.2.2.2.4 Since the scanning system is designed to cover a large dynamic range (due to wide variations of scene albedo and sun angle) the brightness range of any particular image may only cover a part of the dynamic range. Contrast enhancement of the image is made possible by stretching this brightness range. This program presently provides a linear stretch (uniform contrast increase) over the entire range of the image.

2.2.2.2.5 To facilitate determination of the desired limits, a histogram of the scene, showing the frequency distribution of the image digital numbers (scene brightness) now stretched between 0 and 255 DN may be obtained. Study of the histogram then enables setting the most desirable limits for optimum contrast or enhancement of a particular scene element or area. To assist in this determination maximum and minimum values, means, and standard deviations are also provided in a print out. A DN value subtraction may be made which effectively zeros the left hand extreme of the histogram.

2.2.2.2.6 Amplification of the remaining values is made linearly to coincide with the 255 DN value limit (or beyond), at the operators discretion should more white or more black seem desireable for a particular problem.

2.2.2.2.7 Individual channels may be enhanced and imaged or ratioed pixel-by-pixel to show the variations in the slopes of the spectral reflectivity of the two bands. Ratio stretching tends to enhance the spectral reflectivity differences and also minimize radiance differences due to albedo and topography or slope. The histogram capability, the DN subtraction and linear amplification are also provided to facilitate enhancement in the ratio mode.

2.2.2.2.8 After generation of the image tapes they are then utilized to control the output recording of the DICOMED D47 Image Recorder to produce enhanced black and white images. This unit may also be utilized to produce enhanced color composite images of two or more channels or ratios of channels in which the color variations represent differences in spectral reflectivity. Interchange of the channel or ratio with the colors selected is also possible by the user to maximize color contrast, and improve interpretability.

2.2.2.3 Methodology Study

After the desired functions and flexibility had been designed into the image enhancement and image generating program, a series of images were produced which covered areas under investigation by the SRSL. These studies covered (a) the ERTS-ground correlation site in the hills adjacent to Stanford University (Stanford Grassland Site), (b) serpentines adjacent to Crystal Springs Reservoir and the San Andreas Fault in central California, (c) the Yerington, Nevada open pit copper mine and (d) a geobotanical anomaly related to a molybdenum-rich area in the Pine Nut Mountains, Nevada.

The development of the methodology evolved, as images were generated relating to these studies. Detailed analysis of the enhanced images and the results of these studies are covered in Section IV of this report. A discussion of these images as they relate to the methodology and the application of the program in producing computer enhanced images follows.

2.2.2.4 IMAGE ANALYSIS

Initially a preliminary study of the area of interest was made, with STANSORT, to pin point the location and assess the problem. The first image generated on the full 4 X 5 inch polaroid format is geometrically corrected but unenhanced (see Figure 1, 6, and 11).

With all our images the full 4 X 5 inch Polaroid format was utilized (300 by 250 pixels of ERTS data) which produces about a 1:210,000 scale. Histograms are then generated for each of the 4 channels and selected ratios that are believed would contain information of significance. By studying these histograms one may decide upon the DN levels which it would be desireable to use, to stretch by a DN subtraction, with an amplification of the remaining levels. Figures 1 thru 20 indicate various combinations that were used for enhancement and show the images generated. During this preliminary phase many more images were generated then required for analysis in order to gain a more complete understanding of the capabilities and limitations of the system. In general our review of the images shows an overall improvement in contrast with a DN subtraction and amplification (stretching). A comparison of Figure 1 and 2, 6 and 8, 11 and 12, illustrate this improvement. However, it should also be noted that an increase in amplification often will eliminate information by boosting data beyond the 255 DN range. This can be seen in Figures 9D, 13 A,B,C and 18 B,C. Of course, this is not universally true through the entire image or for every channel. In fact, some areas appear to be optimized; therefore, the specifics of a problem must be considered and often the aesthetics are sacrificed to the enhancement and specific information content obtained.

Review of the ratioed images where by each channel is divided by Ch 4 and particularly Figures 10, 14 and 19 illustrate the minimizing of

radiance differences which appears to flatten the topography. With the DN subtraction and amplification the contrast improvement is again evident (compare Figures 14 and 15; and 19 and 20). The possible loss of information content with increased amplification (stretching) is shown in Figures 16C and 21C. It should be noted that the images presented here only show integer amplification values. The program was subsequently modified to include the greater flexibility of floating point values. After generating the computer enhanced tapes for the area of interest the best combinations of straight channel data or ratios were selected for the generation of the <u>color composites</u> which are then available for further study. The colors assigned to the various channels or ratios can be varied to suit the investigator and possibly improve image analysis. A cursory review of the color composites presented as Figures 22 through 23 indicate the improvement in interpretability by the superposition of the various bands or ratios and the addition of the color dimension.

It is obvious from the above that continued optimiziation of the enhancement process will occur as additional type areas are studied and more understanding is gained of the relationshp between terrain types and spectral behavior.

2.2.2.4.1 Stanford-NASA/Ames, (1075/18154; October 6 1972 image)

In this series of images, Figures 1-5 a progression of DN subtraction and amplifications were applied to individual ERTS channels as well as ratioed channels in order to optimize or enhance the information content. In Figure 1, it can be seen that the image generated from the raw ERTS data is generally of low contrast(particularly channels 4 and 5, with 5 somewhat better than 4). Features such as the turbidity of the bay, the wooded areas as well as watered (bright) grassy areas (golf courses, etc), runways, main highways are evident but require careful scrutiny to distinguish them from the background. In channel 7 the contrast is better with the reservoirs, bay, bayland ponds and road networks quite evident; however, the topography of the hills is poorly defined. The turbidity of the shallower creeks and the inshore areas of the bay can also be seen by contrast with the darker adjacent salt ponds.

The DN subtraction and amplification demonstrated in Figures 2 and 3 improve the overall contrast with the turbidity features of the bay and its shores more sharply defined. Felt Lake in the lower central area of the image is now very evident in channel 5; however, close examination of Figure 3 indicates that the clipping of the DN level has effected the outline (reduced) by eliminating the damp transitional areas of the shoreline. The wooded areas on the left and bottom side of the images are now easier to see in channel 5 as well as the road network and watered grassy areas of channel 7.

Figures 4 and 5 contain images obtained by ratioing channels. Study of these images indicate both a gain and a loss of information content as a result of the ratioing and enhancement procedures. For instance, in Figure 5, at the higher DN clipping and amplification levels a peculiar salt and pepper effect tends to blend features in the 5/4 ratio. Oversaturation (over amplification)

of the signal in the 6/4 ratio while emphasizing the .anford Linear Accelerator because of the background brightness of the lower left quadrant of the image tends to obliterate other detail in that area. In general, the topographic relief is subdued in all images of Figure 5, which tends to emphasize the cultural features such as the developed areas and road networks. The DN and amplification levels of Figure 4 seem to be more optimum, as the salt and pepper effect is not apparent, the topographic detail is more subdued but the highlights are more apparent without appearing washed out. The road networks and cultural features also seem optimized as well as the bay and bay land features.

CH 4 RAW DATA

CH 5 RAW DATA

CH 7 RAW DATA

1075-18154 October 6, 1972

STANFORD - NASA/AMES

FIGURE - 2.2.2.2.1

CH 4 (-40 DN) AMP 3

CH 5 (-40 DN) AMP 3

CH 7 (-40 DN) AMP 3

1075-18154 October 6, 1972

STANFORD - NASA/AMES

FIGURE - 2.2.2.2.2

CH 4 (-50 DN) AMP 4

CH 5 (-50 DN) AMP 4

CH 7 (-50 DN) AMP 4

1075-18154 October 6, 1972

STANFORD - NASA/AMES

FIGURE - 2.2.2.2.3

RATIO 5/4 (-40 DN) AMP 3

RATIO 6/4 (-40 DN) AMP 3

RATIO 7/4 (-40 DN) AMP 3

1075-18154 October 6, 1972

STANFORD - NASA/AMES

FIGURE - 2.2.2.2.4

RATIO 5/4 (-50 DN) AMP 4

RATIO 6/4 (-50 DN) AMP 4

RATIO 7/4 (-50 DN) AMP 4

1075-18154 October 6, 1972

STANFORD - NASA/AMES

FIGURE - 2.2.2.2.5

2.2.2.4.2 Crystal Springs Reservoir, California
1075-18154, October 6, 1972 images

In this study, an investigation was made relative to the possibility of differentiating, serpentine outcrops and soils to the east of Crystal Springs Reservoir, the surface manifestation of the San Andreas fault in this area. In this series of images Figures 6-10, the effect of increasing amplification with a fixed (optimum) DN subtraction on specific information content can be seen. In Figure 6, the raw data was utilized to generate the images. As before, the contrast level in generally poor in channel 4 and 5. It is in channel 6 and 7 that the serpentine area, east of Crystal Springs and south of the Crystal Springs Golf Course (bright area in center of image) can be detected. The initial DN subtraction shown in Figure 7 has the overall effect of darkening the overall aspect of the images with some detectable contrast increase in channels 4 and 5. In Figure 8 the amplification increase to 2 improves the contrast and tends to isolate the serpentine area somewhat, particularly in channel 7. An increase in amplification to 3 in Figure 9, further isolates the serpentine in channel 7 but the oversaturation reduces the information content elsewhere by the general increase in brightness level. With progressive amplification it is possible to emphasize the difference in character of the topography and ground cover east and west of the fault zone. This is seen best in channel 5 of Figure 8. Also evident with this increase in amplification is the increase in contrast of the watered grassy (bright) areas (golf courses, cemeteries, parks etc) in channel 6 and 7, the bay turbidity in channel 5, and the road networks in channel 7. The shore outlines of the bay and Crystal Springs are sharpened appreciably as the contrast is improved.

Ratioed images are presented in Figure 10. It is evident that while the display of the serpentine area is optimized in the 7/4 ratio further DN subtraction and amplification would only tend to eliminate information content elsewhere.

CH 4 (-0 DN) AMP 1

CH 5 (-0 DN) AMP 1

CH 6 (-0 DN) AMP 1

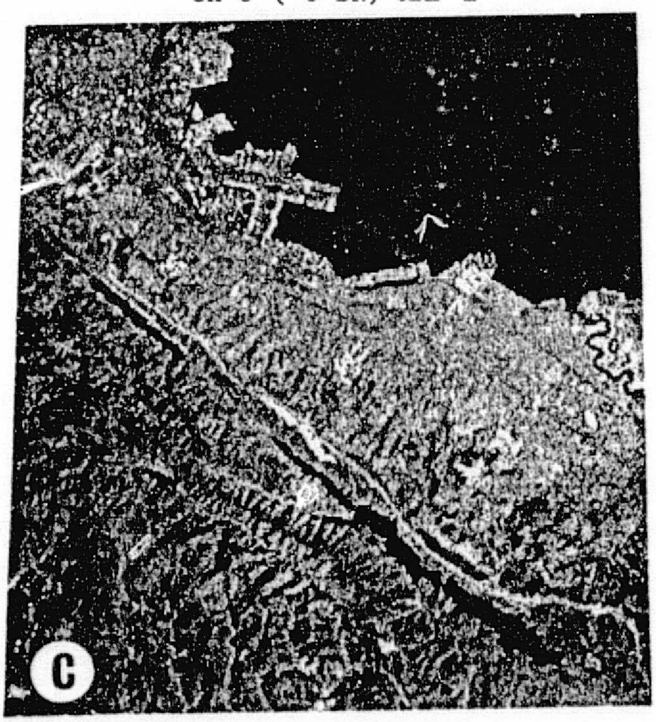

CH 7 (-0 DN) AMP 1

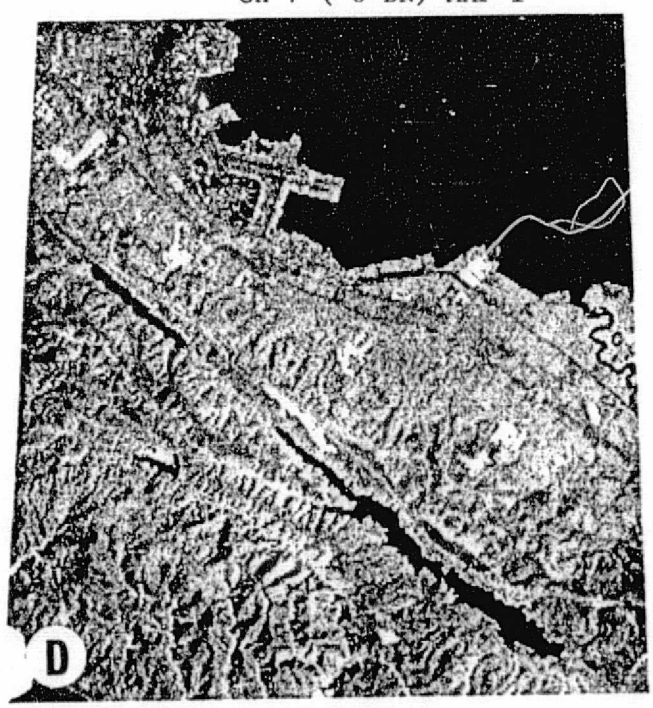

1075-18154 October 6, 1972

CRYSTAL SPRINGS RESERVOIR, CALIFORNIA

FIGURE - 2.2.2.2.6

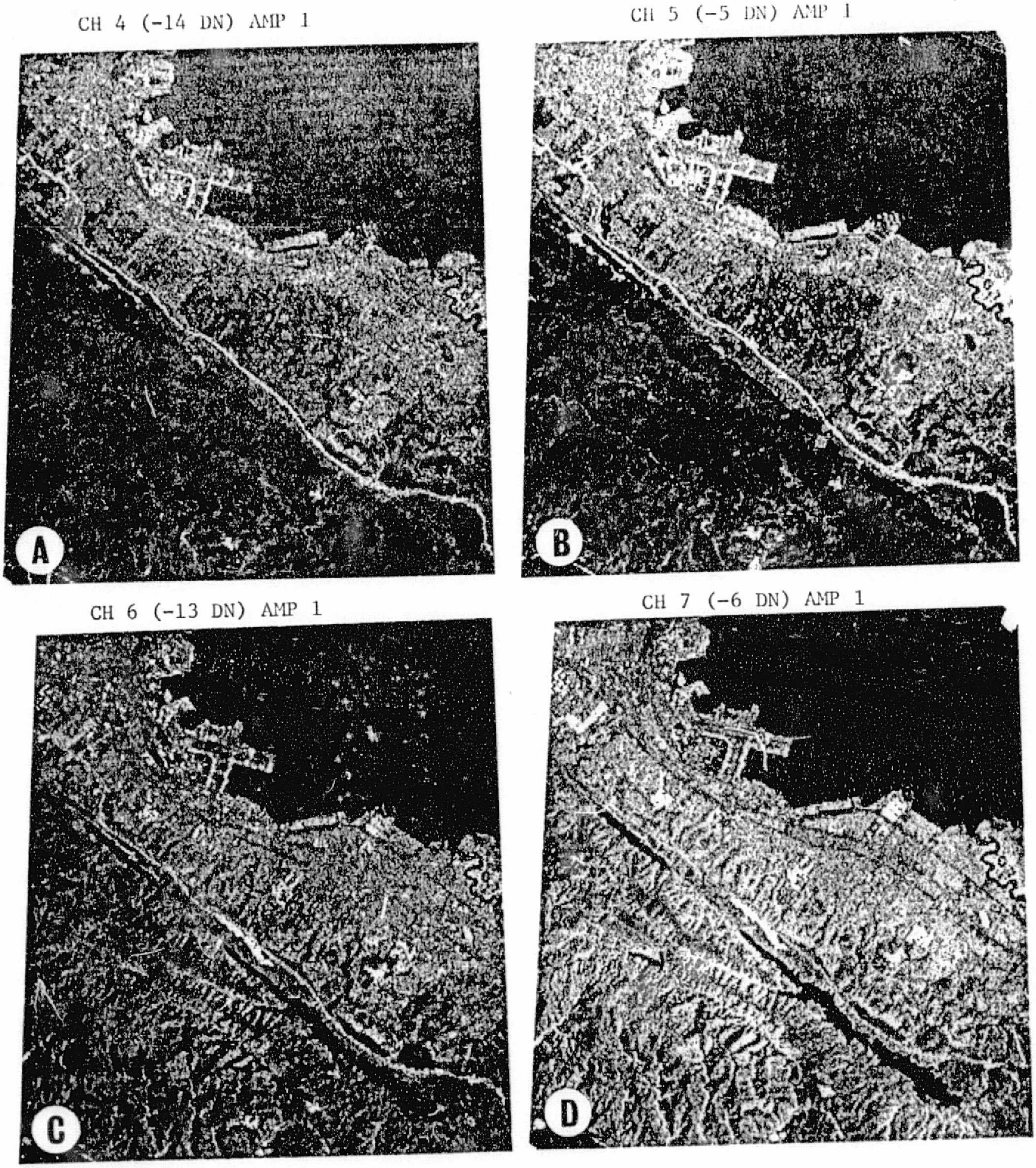

1075-18154 October 6, 1972

CRYSTAL SPRINGS RESERVOIR, CALIFORNIA

FIGURE - 2.2.2.2.7

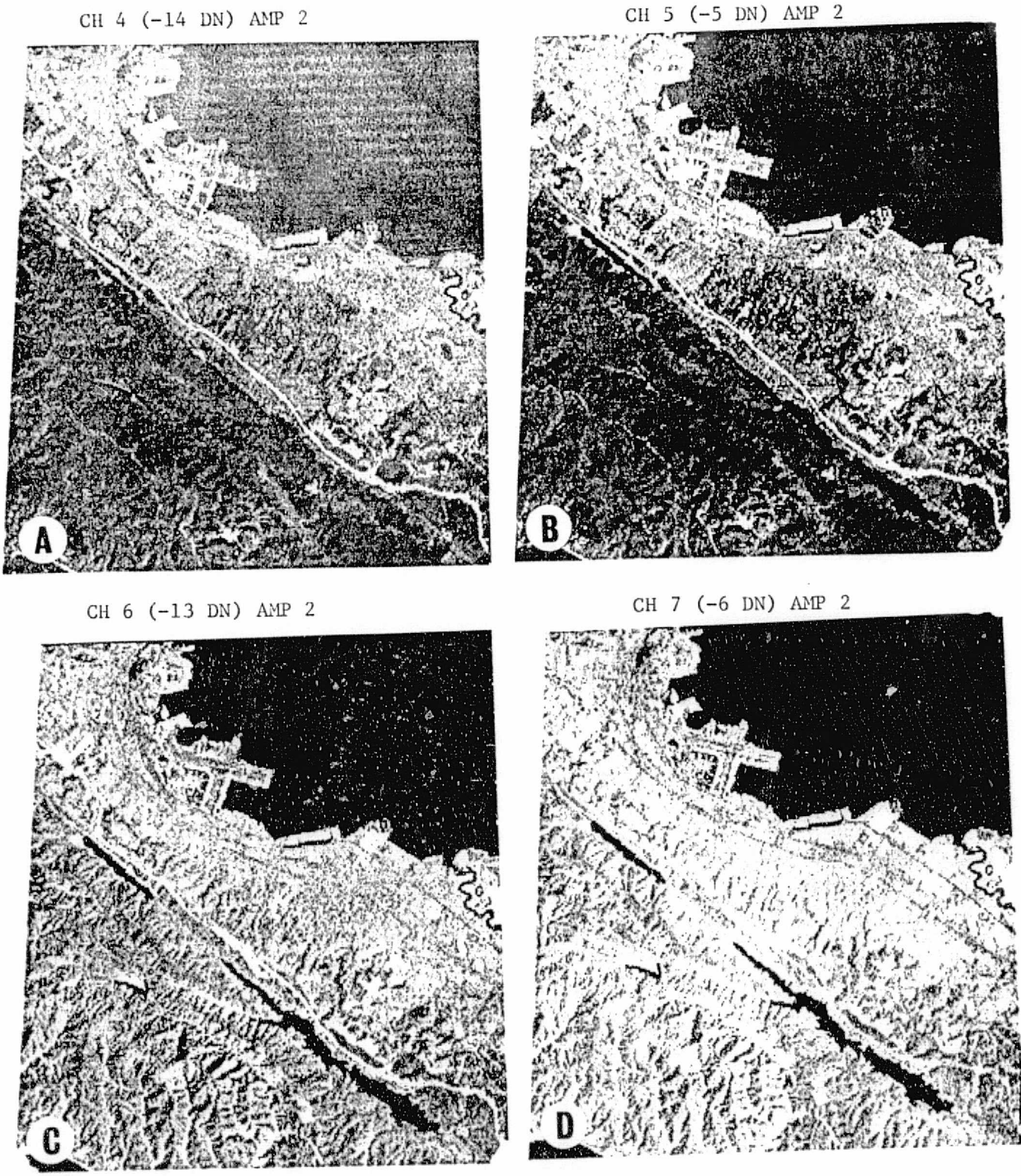

1075-18154 October 6, 1972

CRYSTAL SPRINGS RESERVOIR, CALIFORNIA

FIGURE - 2.2.2.2.8

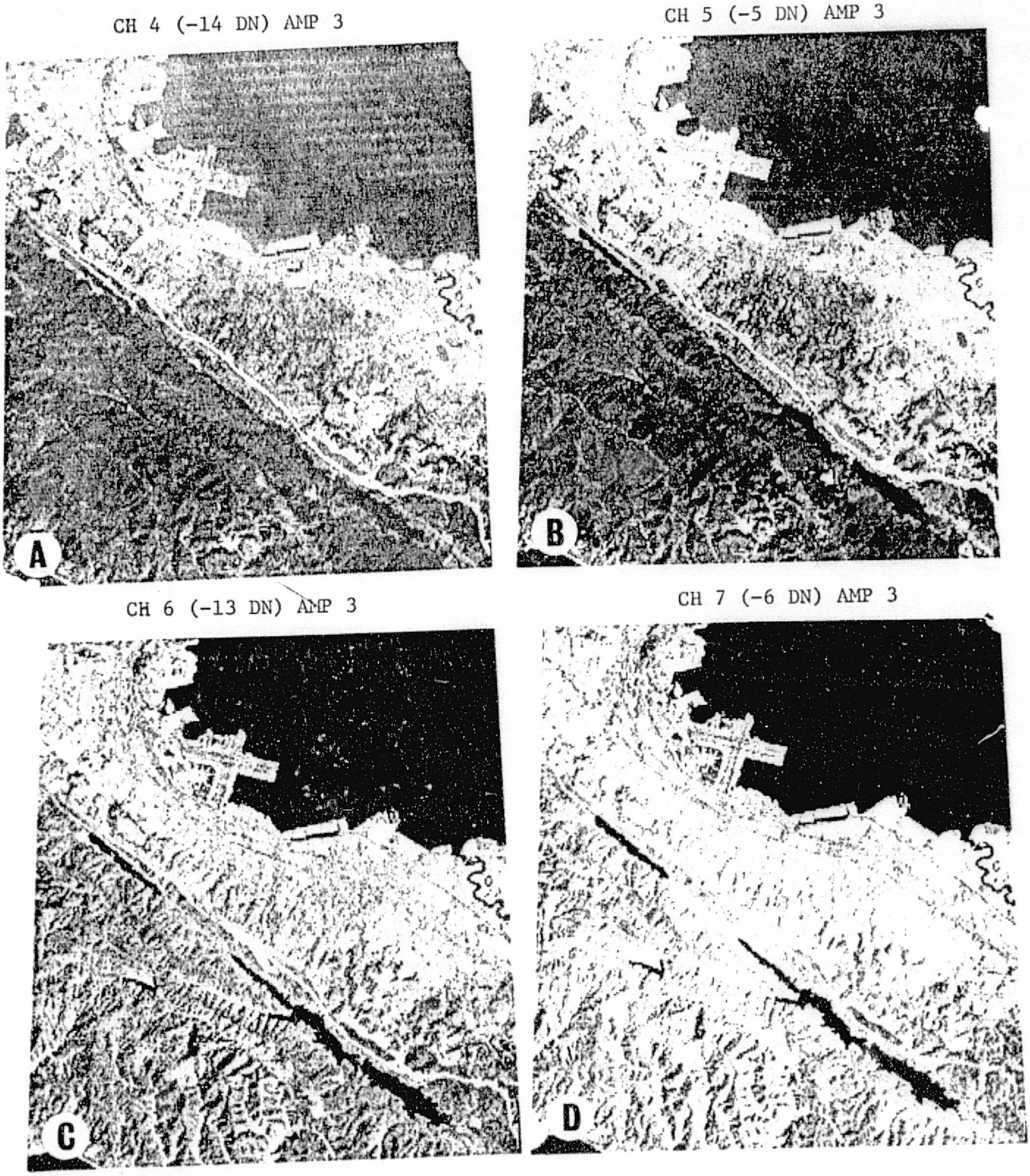

1075-18154 October 6, 1972

CRYSTAL SPRINGS RESERVOIR, CALIFORNIA

FIGURE - 2.2.2.2.9

RATIO 5/4 (-0 DN) AMP 1

RATIO 6/4 (-0 DN) AMP 1

RATIO 7/4 (-0 DN) AMP 1

1075-18154 October 6, 1972

CRYSTAL SPRINGS RESERVOIR, CALIFORNIA

FIGURE - 2.2.2.2.10

2.2.2.4.3 Yerington Pit, Nevada, 1397-18154, August 24, 1973

2.2.2.4.3.1 Bands 4, 5, 6 and 7

Figures 11-16 represent images made from ERTS tape 1397-18051, from August 24, 1973. This tape was selected for study because it was made by ERTS only 13 days after a RB57 underflight (for SKYLAB SL3) obtained excellent photographic coverage with B/W and color films. In addition the high sun elevation (67°) of this date aids the spectral content.

All four bands have been processed on each figure. In sequence Figure 11 represents the 4 raw data images, Figure 12 shows them with suitable digital values (DN) removed, but still with amplifications of 1.0. In Figure 13 the amplification has been raised to 3.0, stretching the data linearly. (By this point Channel 5 (-45DN; amp 3) is starting to show a ragged appearance, due to noise.

At first glance there is little difference between any of the four images, except in the obvious vegetation at the right hand margin, of the irrigated crops (alfalfa etc.) of the flat, agriculturally-rich Mason Valley, in which the town of Yerington lies off the image to the lower right. A few small areas of vegetation may be seen similarly north of the shorelines of the mostly dry, Artesia Lake playa. Elsewhere in the Singatse Range, centrally running N-S through the image, no obvious spectral differences exist. The banana-shaped patch at the central right best seen on Channel 4 and 5, represents the gardens and housing of the mine.

The black and darker grey triangles in the upper right are noticeably different in Channels 4, 5 and 6. The area darkest in Channel 4 is acidified ferric sulfate leach liquor, used to extract "oxide" copper from the adjacent piles of mineralized rock. It has a deep rust-red color to the eye and here is black even in Channel 4, regardless of its depth. The cigar shaped patch, best seen in Channel 6 and 7 is a shallow pond of water at the lowr end (northern) of the tailings pond. This pond becomes essentially transparent in Channel 4.

Clipping suitable digital values (DN) off the data sets seems to bring the values into a better portion of the grey scale of the (Polaroid Type 107) film. It does somewhat increase the information content, but not their spectral differences. Further amplification to 3.0, with the same DN offsets, serves to

brighten the whole scene, although now the lightest areas are hopelessly overexposed.

A <u>false color</u> (CIR) image was made using the following settings of the 3 best images, and colored using the filters as indicated;

Ch 7	(-17DN), amp 2	RED
Ch 6	(-42DN), amp 3	GREEN
Ch 5	(-45DN), amp 3	BLUE

A black and white representation of the original color print is shown in Figure 22A.

2.2.2.4.3.2 <u>Ratio of Bands</u> (R5/4, R6/4, R7/4)

Comparisons between ratio images (Figures 14, 15 and 16), with the raw data sets (Figures 11-13) show immediately that most of the topographic effects have been removed, providing a "flat image". Figures 14, 15 and 16 represent successive steps in DN subtraction and increasing "stretch" (amplification).

The ratio images now differ slightly from each other (which makes the color print show differences). Of these one now sees a darker patch in the lower right center now appearing which correlates with the granite (Kg) on the geological map and is terminated by a roughly E-W line (fault). The best simple ratio for lithological purposes is Ch 6/4.

Figure 22 (even in its B and W form in this report) shows these contrasts clearly, particularly those which result from the beneficial removal of topographic effects and the heightened degree of the rock type discrimination.

CH 4 (-0 DN) AMP 1

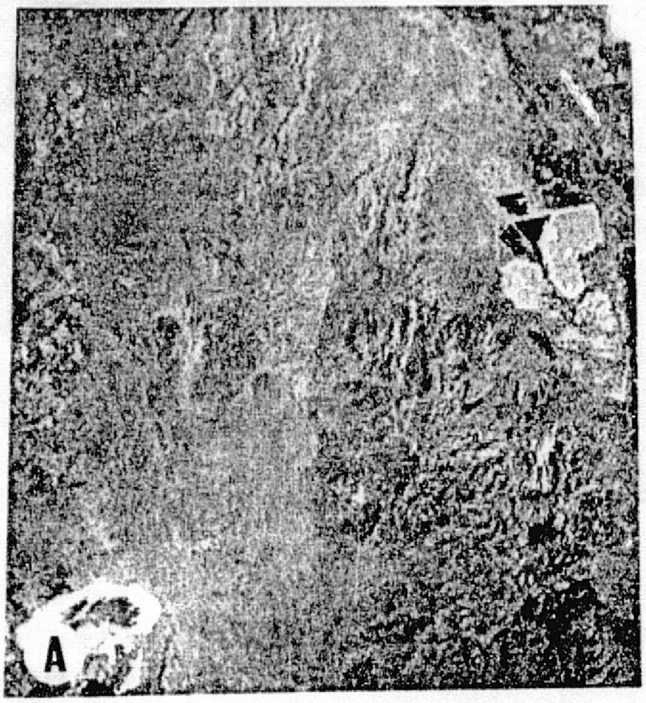

CH 5 (-0 DN) AMP 1

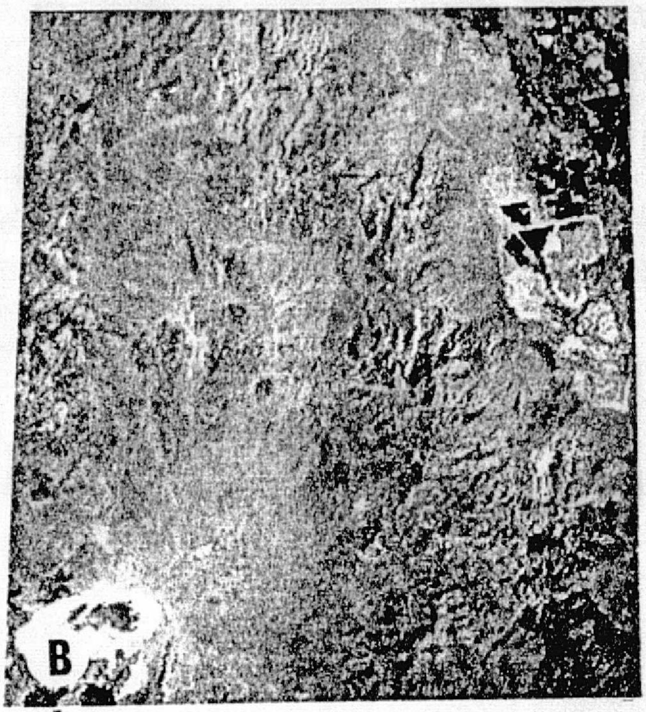

CH 6 (-0 DN) AMP 1

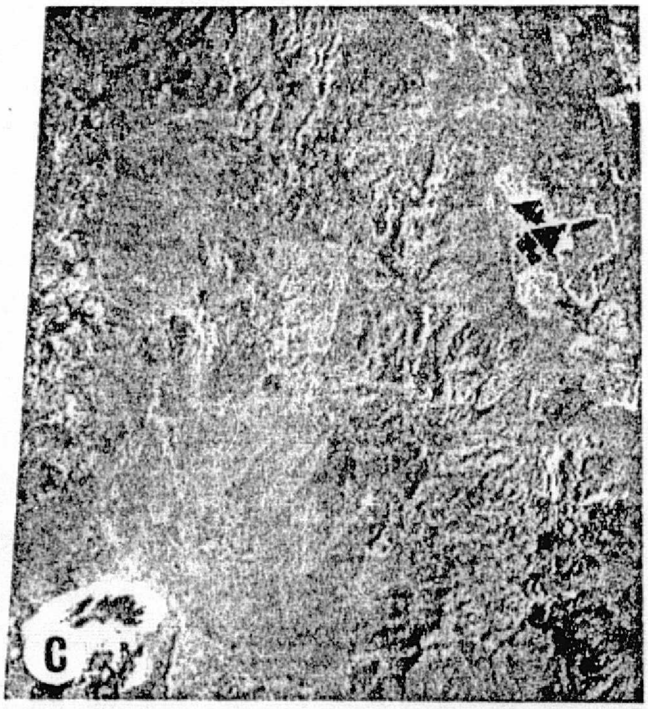

CH 7 (-0 DN) AMP 1

1397-18051 August 24, 1973

YERINGTON PIT, NEVADA

FIGURE - 2.2.2.2.11

CH 4 (-41 DN) AMP 1

CH 5 (-45 DN) AMP 1

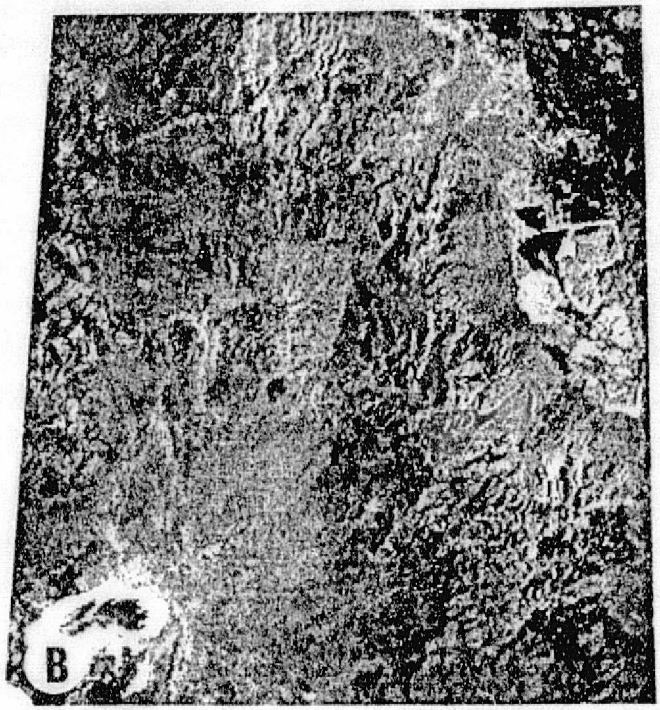

CH 6 (-42 DN) AMP 1

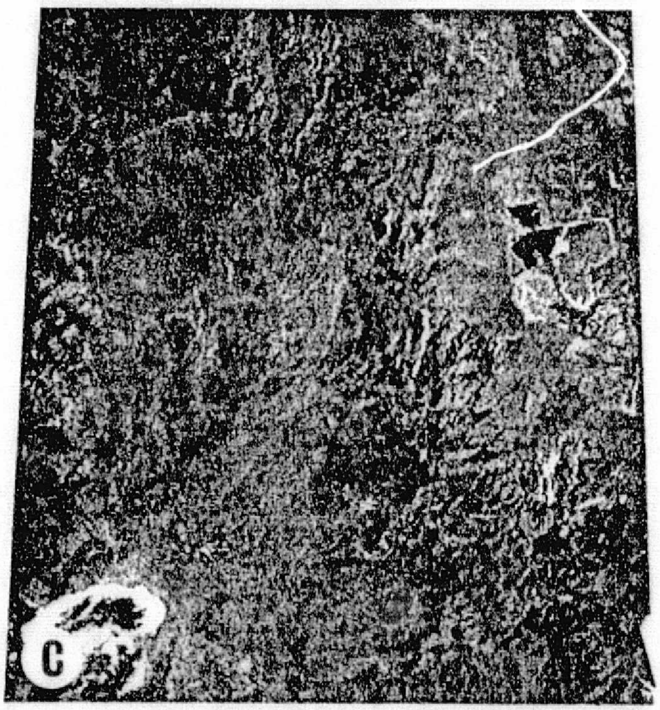

CH 7 (-17 DN) AMP 1

1397-18051 August 24, 1973

YERINGTON PIT, NEVADA

FIGURE - 2.2.2.2.12

CH 4 (-41 DN) AMP 3

CH 5 (-45 DN) AMP3

CH 6 (-42 DN) AMP 3

CH 7 (-17 DN) AMP 3

1397-18051 August 24, 1973

YERINGTON PIT, NEVADA

FIGURE 2.2.2.2.13

RATIO 7/5 (-0 DN) AMP 1

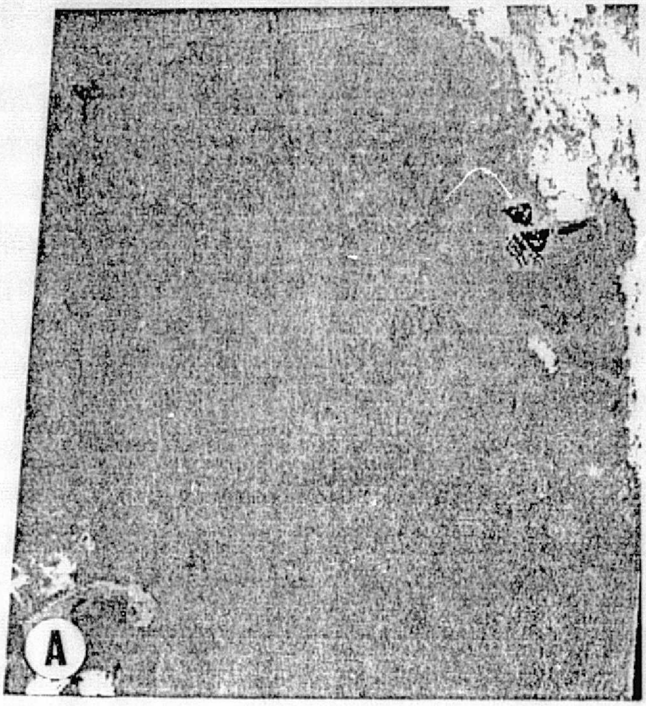

RATIO 6/5 (-0 DN) AMP 1

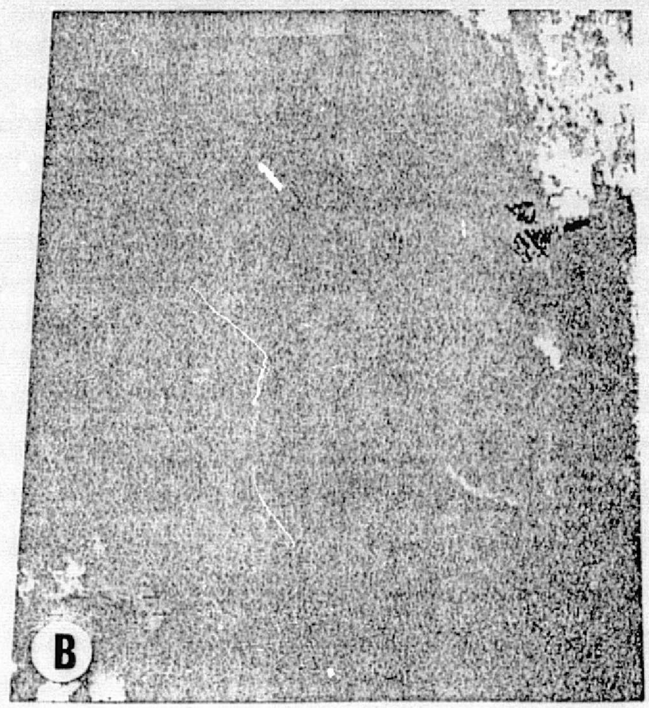

RATIO 7/6 (-0 DN) AMP 1

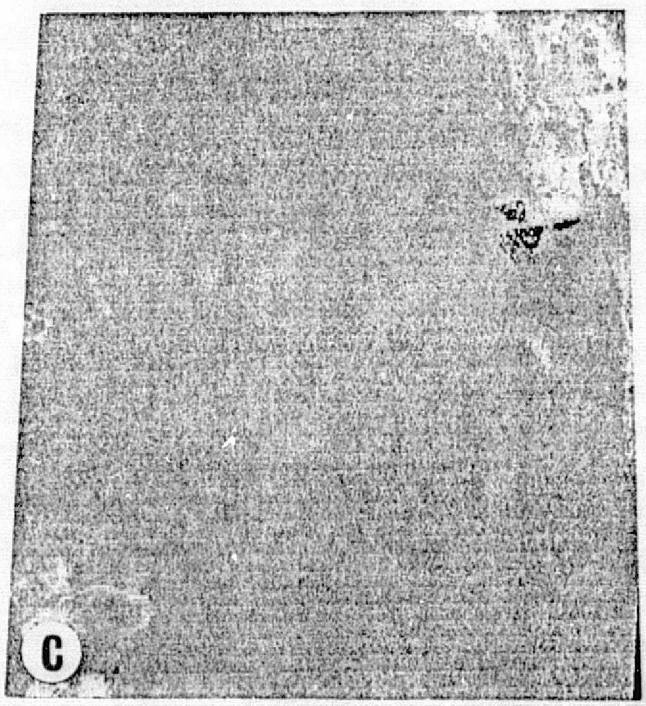

1397-18051 August 24, 1973

YERINGTON PIT, NEVADA

FIGURE 2.2.2.2.13A

R4

RATIO 5/4 (-0 DN) AMP 1

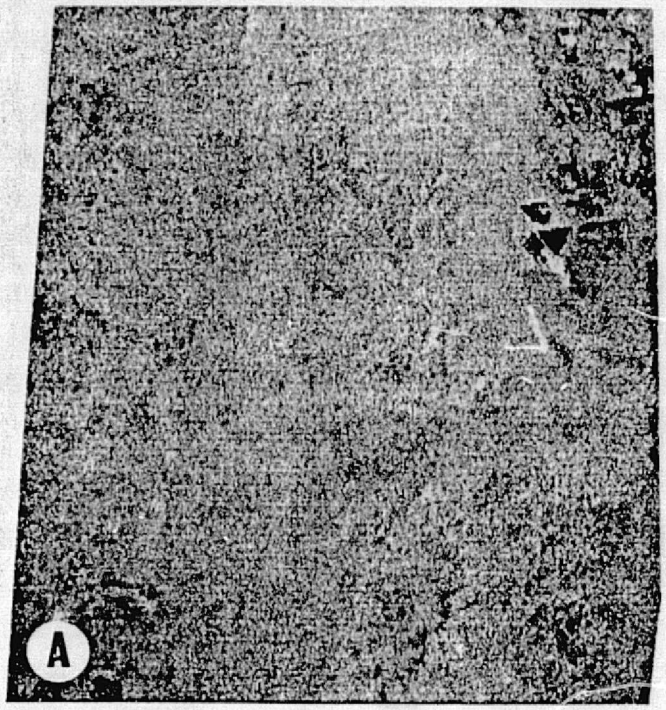

R5

RATIO 6/4 (-0 DN) AMP 1

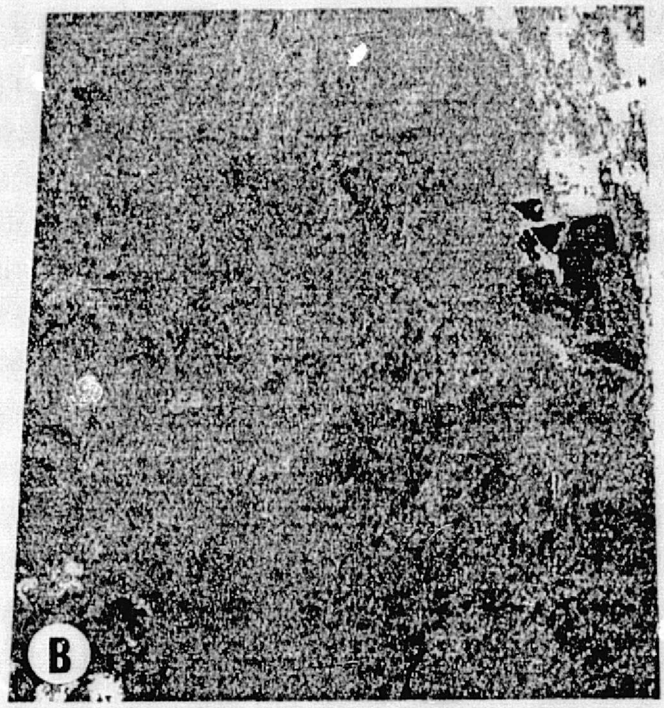

RATIO 7/4 (-0 DN) AMP 1

R6

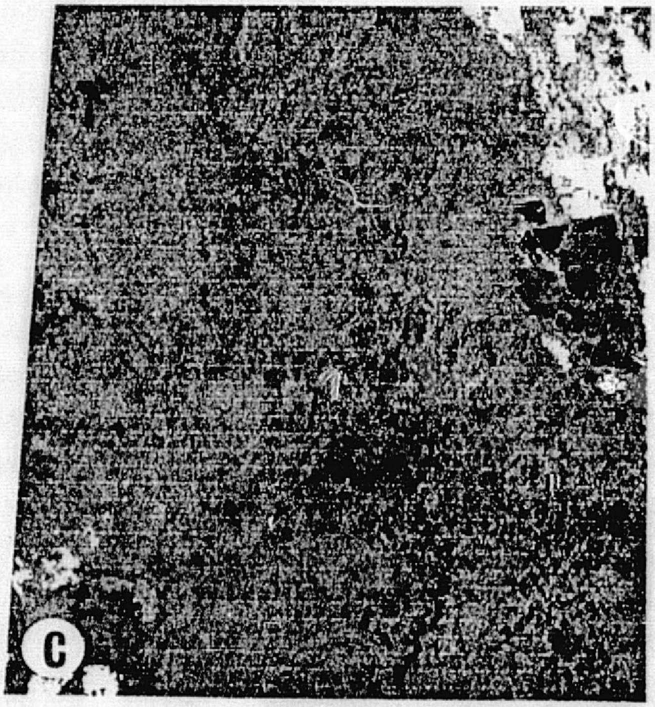

1397-18051 August 24, 1973

YERINGTON PIT, NEVADA

FIGURE - 2.2.2.2.14

RATIO 5/4 (-66 DN) AMP 1

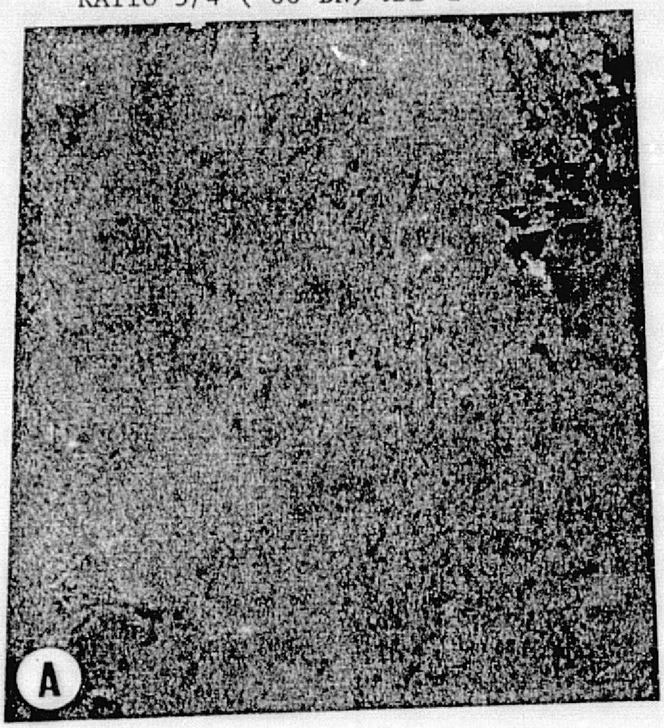

RATIO 6/4 (-63 DN) AMP 1

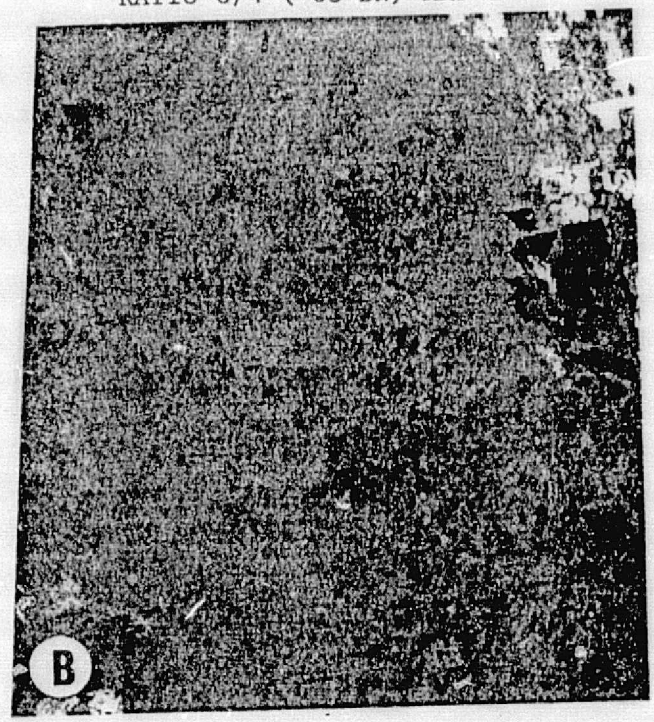

RATIO 7/4 (-25 DN) AMP 1

R6

1397-18051 August 24, 1973

YERINGTON PIT, NEVADA

FIGURE - 2.2.2.2.15

RATIO 5/4 (-66 DN) AMP 3

RATIO 6/4 (-63 DN) AMP 3

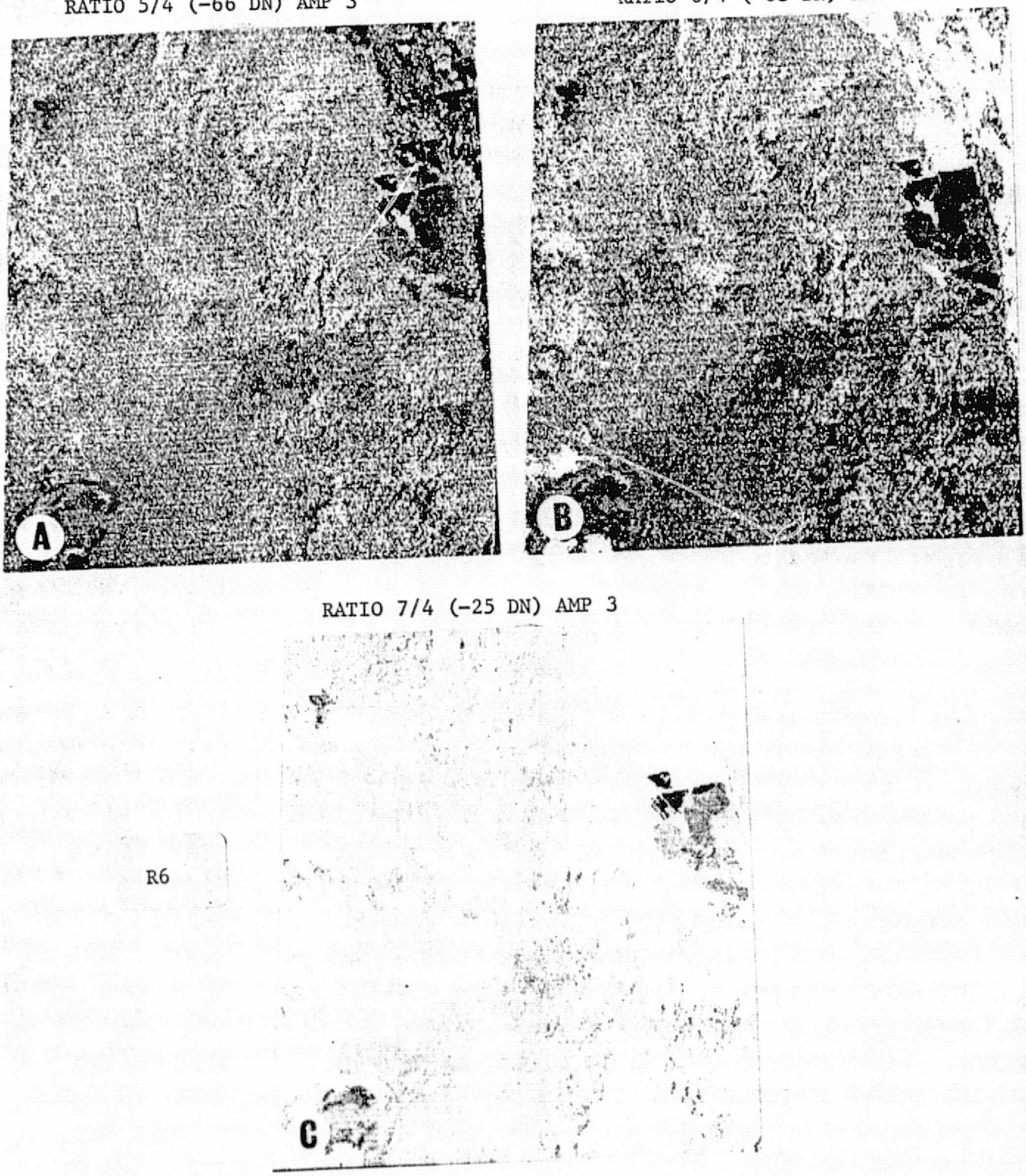

RATIO 7/4 (-25 DN) AMP 3

R6

1397-18051 August 24, 1973

YERINGTON PIT, NEVADA

FIGURE 2.2.2.2.16

2.2.2.4.4 Pine Nut Mountains, Nevada (Molybdenum-vegetation anomaly)
1289-18063, May 8, 1973

A similar series of images for Channels 4, 6 and 7 appear in Figures 17 and 18 with DN subtraction and increasing amplification (stretch). A large area of snow, taking up most of the right hand (E) edge of the image dominates the scene. Because the ERTS system clips all data values above 127DN the snow brightness variability (now reduced evenly to 127DN counts) causes problems in subsequently ratioing steps. (In addition while making these particular images the NASA/ARC DICOMED unit was suffering "electronic-overshoot" problems resulting in blacks anomalously appearing in the snow). Notice also that the areal extent of the "white" snow is larger on Ch 4 > Ch 5 > Ch 7, in accord with the known spectral pattern for late spring snow melting.

Several localities are keyed to symbols on the figures,

Figure 17 (a) -- Mo/vegetation lies (1 cm) to left (w) of this letter (Figure 17c).

(b) -- Sugar Loaf Hill, andesitic plug intrusive

(c) -- Suspected caldera (outlined by arrow points) of Double Springs Flat traversed by Highway 395.

Figure 18 (a) -- Small farming area E-W patch (Figure 18b)

Figure 19 (b) -- Trace of 3-5 year old fire, which burned off the pines and junipers, now replaced by sagebrush.

Figure 23 shows the false color (CIR) composite print (here is black and white) of these images.

Rationing (in areas outside the snow problem) again removes the topography allowing the observer to concentrate on spectral differences. Figure 19 has zero DN offset, Figure 20 has the best DN offset, and Figure 21 increases the stretch (amplification) from 1.0 to 2.0. Figure 23 (B/W copy) shows the effect of composite-color-ratios.

The best simple ratio is again Ch 6/4, in which the (sparse) broad-leaved vegetation (near Spring of Wales) shows white patches. The spotty white/black pixel in the snow are due to the "overshoot" problem.

Water in Double Springs Flat shows black spectrally in the 7/4 and 6/4 ratios (lower left corner). The fire trace (b) does not appear in Ch 5/4 but is emphasized in Ch 6/4 and Ch 7/4.

Channel 5/4 ratio however does show patterns in the geology in the upper right corner correlatable with the published geological maps.

The Mo-vegetation anomaly is not easily seen but may be discerned about 1 cm to the left of (b) in Figure 21B, as a grey rounded patch.

CH 4 (-21 DN) AMP 2

CH 6 (-23 DN) AMP 2

CH 7 (-13 DN) AMP 2

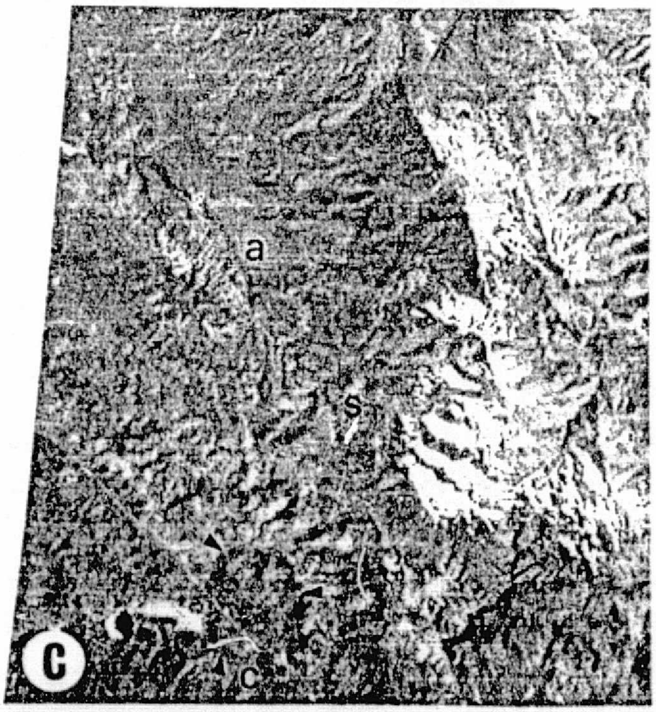

1289-18063 May 8, 1973

PINE NUT MTNS, NEVADA

FIGURE - 2.2.2.2.17

CH 4 (-21 DN) AMP 3

CH 6 (-23 DN) AMP 3

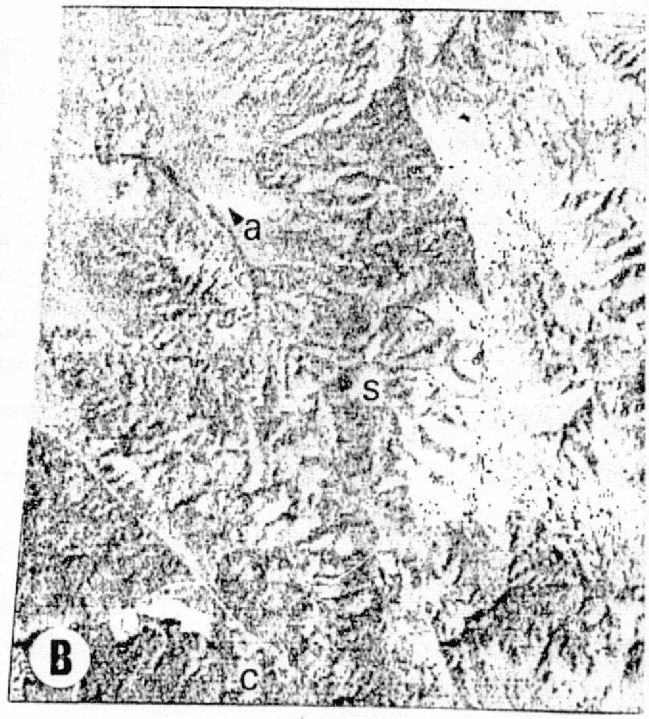

CH 7 (-13 DN) AMP 3

1289-18063 May 8, 1973

PINE NUT MTNS, NEVADA

FIGURE 2.2.2.2.18

RATIO 5/4 (-0 DN) AMP 1

RATIO 6/4 (-0 DN) AMP 1

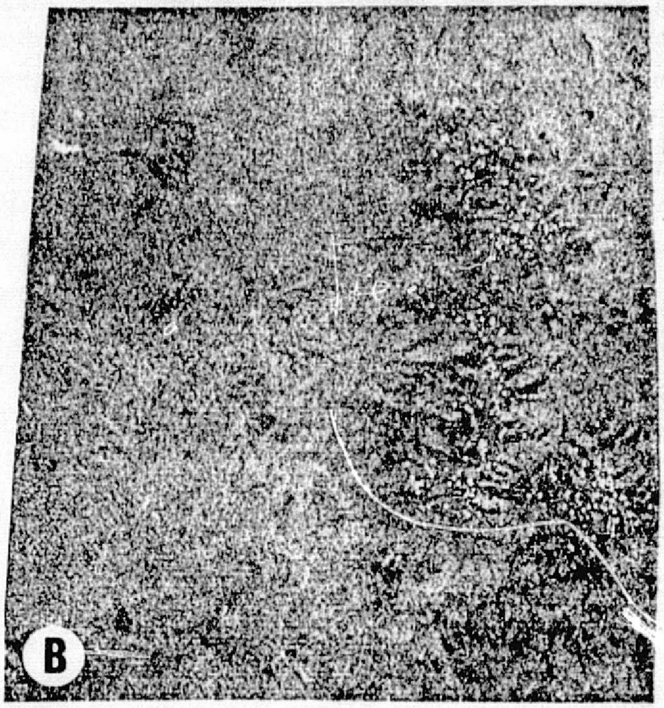

RATIO 7/4 (-0 DN) AMP 1

1289-18063 May 8, 1973

PINE NUT MTNS, NEVADA

FIGURE - 2.2.2.2.19

RATIO 5/4 (-41 DN) AMP 1

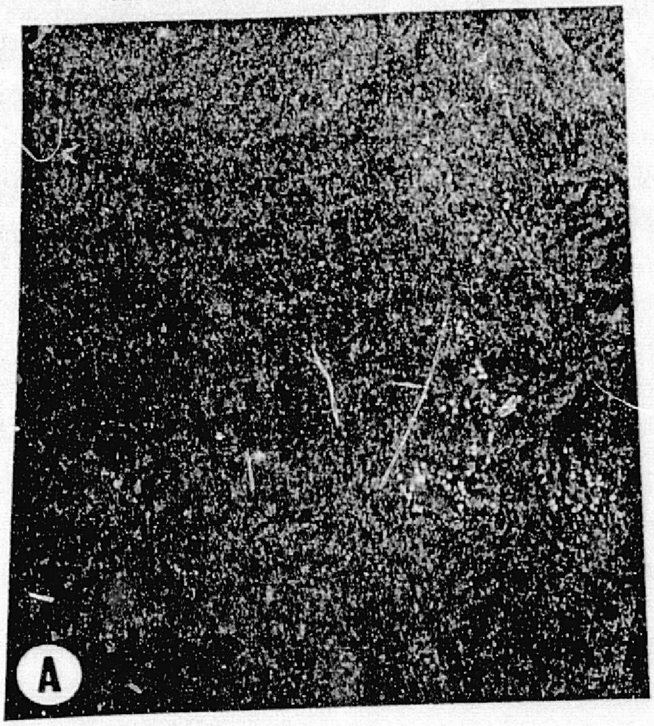

RATIO 6/4 (-63 DN) AMP 1

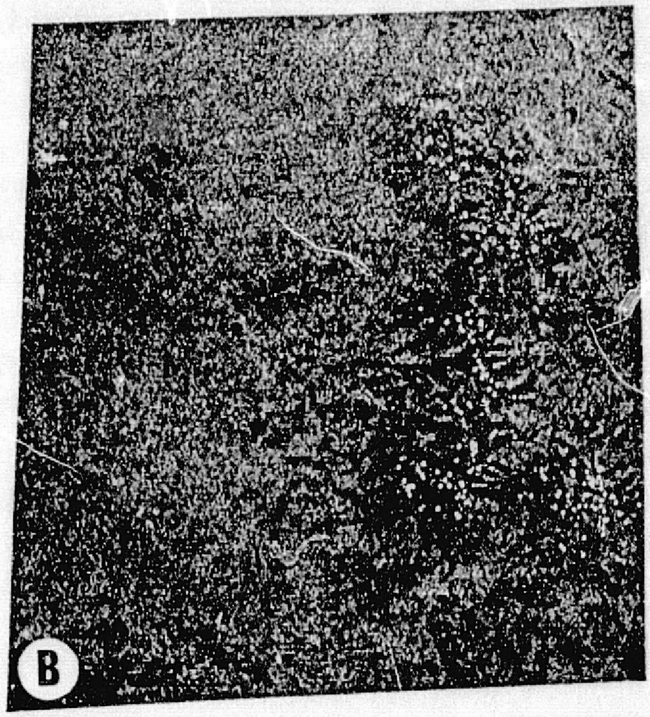

RATIO 7/4 (-28 DN) AMP 1

1289-18063 May 8, 1973

PINE NUT MTNS, NEVADA

FIGURE - 2.2.2.2.20

RATIO 5/4 (-41 DN) AMP 2

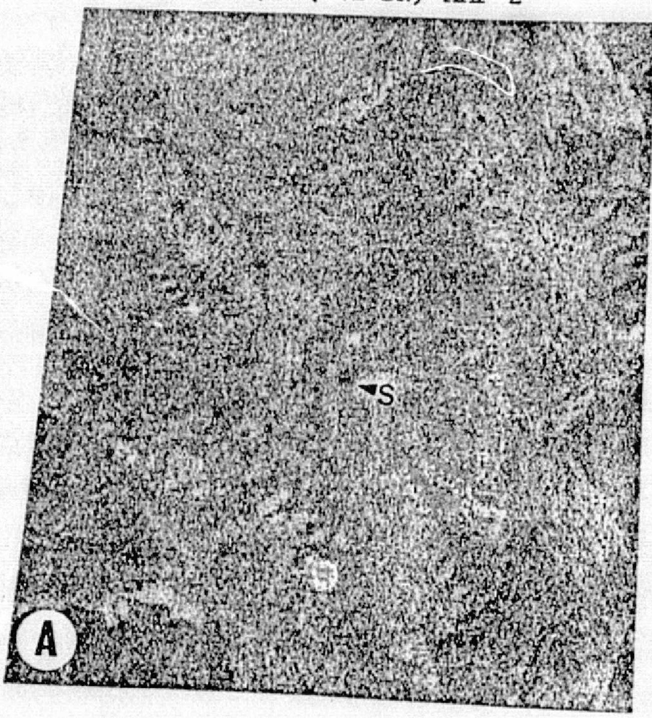

RATIO 6/4 (-63 DN) AMP 2

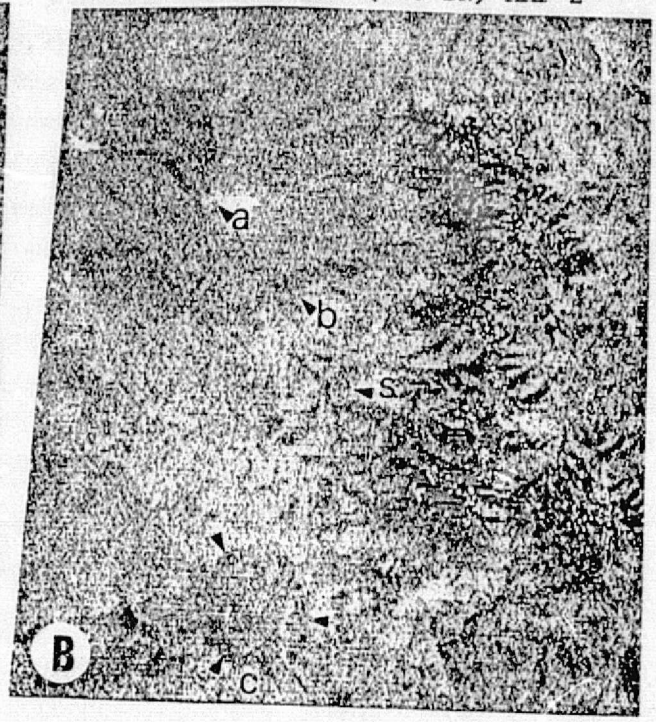

RATIO 7/4 (-28 DN) AMP 2

1289-18063 May 8, 1973

PINE NUT MTNS, NEVADA

FIGURE 2.2.2.2.21

CH 7 (-17 DN) AMP 2 (RED)
CH 6 (-42 DN) AMP 3 (GREEN)
CH 5 (-45 DN) AMP 3 (BLUE)

A

RATIO 7/4 (-25 DN) AMP 3 (GREEN)
RATIO 6/4 (-63 DN) AMP 3 (RED)
RATIO 5/4 (-66 DN) AMP 3 (BLUE)

B

1397-18051 August 24, 1973

YERINGTON PIT, NEVADA

FIGURE 2.2.2.2.22

86

2.2.2.5 Conclusions

The rapid interactive and iterative nature of the program leads to the continuing development of applications technique as experience is gained in an expeditious fashion. An integration of the SRSL STANSORT program with the image enhancement program (IMAGE) would improve the efficiency of the process. Although, at the expense of lowering the overall speed drastically. Also recommended is the use of an on line, real time TV viewing system so that the computer enhancement may be viewed, modified as desired, and finalized images produced more rapidly.

2.3 INTERPRETATION OF LANDSAT DIGITAL TAPES

2.3.1 ATMOSPHERIC EFFECTS

With multiple coverages available from LANDSAT-1, it has been possible to effect a calibration procedure, using an approximately 45 acre target, in the northern part of San Francisco Bay. This target is composed of carbon black, a waste product of oil refining nearby, and was found by searching Channel 5 and 7 iamges for very black targets -- this target was very black inboth.

The following is an abstract of a published paper (appearing in Appendix A), detailing the use of black targets for atmospheric correction. The simultaneous use of a "bright" target of known bidirectional reflectance (using the 4 LANDSAT filter bandpasses) can transform the radiance data sets to reflectance data sets. This has obvious use in comparing ground-measured reflectances, and in searching for matching spectra elsewhere in a LANDSAT tape.

88

2.3.1.1 Abstract of Published Paper
(in Appendix A)

A COMPARISON OF OBSERVED AND MODEL-PREDICTED ATMOSPHERIC PERTURBATIONS ON TARGET RADIANCES MEASURED BY ERTS

by

R.J.P. Lyon
F. R. Honey

Stanford Remote Sensing Lab
Stanford University
Stanford, California 94305

SUMMARY

In order to be able to compare results from ERTS MSS data over a series of tapes, the perturbing effects of a variable contribution due to radiation scattered by the atmosphere into the detector field of view, and of the variation in the irradiance on a target with solar zenith angle, must be eliminated. These two effects may be compensated for, or entirely removed, by studying selected targets in a scene, one (or more) of low (zero) reflectance, one (or more) or high, known reflectance. In some scenes, however, suitable reflectance targets may not be obtained. When this occurs, atmospheric modelling must be employed to arrive at some values for the atmospheric scattering contribution, and for the irradiance on the scene.

Two targets of measured, constant reflectivity in the area of San Francisco, California are studied. The first standard, a waste products treatment pond at an oil refinery near Suisan Bay, having an area of approximately 0.3 square miles, and bandpass reflectances of <0.5% in all four bands, is assumed to have a zero contribution to the radiance recorded by ERTS. The radiance observed then arises entirely from atmospheric scattering. The variation in these radiance values as a function of solar zenith angle is compared with models for atmospheric scattering.

A second target, a concrete parking apron for aircraft at Moffett Field, California, assuming that it remains dry during the period of study has constant reflectances of 27.8, 31.0, 30.0, and 32.3 percent bandpass reflectances in four MSS equivalent channels. Using these values, the radiance observed by ERTS may be corrected for the atmospheric contribution, and thus values for the irradiance on the target may be calculated. Thes values may be studied as a function of solar zenith angle and compared with results from models.

The technique of using standard targets within a scene is applied to a specific scene which contains an area of measured reflectivity.

2.3.2 GEOLOGY AND SOILS OF THE STANFORD GRASSLANDS SITE

2.3.2.1 Introduction

The foothills behind the Stanford campus are exemplary of the rolling topography encountered the length of the San Francisco Peninsula. The rocks are predominately of marine origin and have undergone considerable deformation since their lithification. Local relief is substantial with hills rising to elevations above 500 feet. Topography is rolling as a result of structural control and a well developed soil profile.

2.3.2.2 The Project Area

The area is characterized by a rolling hill and swale topography indicative of the climate and geological structure of the region. Vegetation is predominantly annual grasses; a few large oaks dominate the grassy knolls. Slopewash deposits and soils are thick enough to conceal most of the bedrock. Outcrops occur on steep slopes where erosion is able to remove surficial material faster than its production. Faults express themselves in minor control of topography. The 64-year rainfall average is 15 inches on the east (lower) side and 20 inches on the western (higher) side. Over 80% of this falls between December and March. Streams occupy deeply incised valleys. Rejuvenated headward erosion in these valleys indicates a change in runoff conditions. This is interpreted as the result of overgrazing by cattle.

2.3.2.3 Geology, Rock Units

The rock types encountered in the project are marine in origin. During part of the early Tertiary, these rocks must have accumulated in an off shore environment. A schematic statigraphic section is included in the appendices.

2.3.2.3.1 Butano Formation (Eocene, Tbu)

This unit is composed of medium grained sandstone beds averaging 60 feet in thickness and dark grey-green shales averaging 60 feet in section.

The sandstone is massive, fragments angular, poorly sorted, and arkosic. Relatively thin beds (1 - 2 ft.) of grey silt and mudstone are included in these larger beds. Outcrops weather to a yellow buff color and are much harder than unweathered rock.

The shale beds of this unit are greenish to brown grey and contain a predominate proportion of clay minerals. Atchley and Grose (1960) state that core specimens contained as much as 50% mc :tmorillinite. Those which appeared dry would shrink upon exposure to the atmosphere. The resultant cracks represented a minimum of 5% of the original volume.

Edwards (1961) examined microfossils from the mudstones of the unit and placed it in the Eocene.

The unit is probably more than 2000 feet in section. Alon, Francisquito Creek at Searsville Lake there are more than 4000 fe vertical section exposed.

Detailed Discussion:

The unit is of marine sedimentary origin and is dated by fossil content as Eocene age. It presently occupies the core of a faulted anticlinal fold and is overlain with angular unconformity by younger Miocene rocks. The unit has undergone at least two major episodes of burial, deformation, uplift, and erosion. The component sediments, originally sand and clay mud, were lithified to sandstone and clay shale and subsequently deformed and distorted.

The lithology of the unit is characterized by irregular alternation of sandstone beds and clay shale beds. The individual beds vary in thickness from 1 foot to more than 100 feet, and within any given section the ratio of sandstone to shale may vary from 70:30 to 30:70.

The Eocene sandstones typically are fine-to-medium grained, poorly sorted, and variably cemented. Beds of mappable continuity are commonly 30 to 90 feet thick and often contain 1 to 2 foot thick interbeds of shale. The contacts are irregular and the attitudes of the beds may vary abruptly. Individual beds of sandstone or shale may pinch or swell in thickness, terminate abruptly, or coalesce with adjacent beds.

The sandstones consistently are light grey in color when fresh; they generally weather to white or light brown with conspicuous iron stains on fracture and bedding planes. Outcrops generally are "case-hardened" and are often harder than fresh rock. Road cuts along Junipero Serra Blvd. show criss-cross joints which yield 2 to 3 foot blocks in the weathered, case-hardened rock. The Eocene sandstones tend to be somewhat harder than the Miocene sandstones.

The Eocene shales consist perdominantly of clay rocks, but include minor sandy clays, silty clays and marls. Most of the clay rocks have the appearance of mudstone, but thinly laminated shale is also found. The degree of distortion in the shales varies from severe shearing to blocky fracturing. The common distortion of the clay beds appears to be primarily the result of wide-spread, intra-bed movement during deformation and folding and only in small part the result of shearing associated with fault movement.

Mappable shale beds range in thickness from 20 feet to rarely over 100 feet. Individual beds usually contain a mixture of several varieties of shale and commonly 2 to 3 foot interbeds of sandstone. In several core intervals, tectonic mixing of sandstone and clay was noted.

Several varieties of clay shale were recognized in the drill cores but none of these could be correlated with the weathered varieties exposed in the trenches. The dominant variety observed in the drill cores is a blocky, hard, dry, medium-dark olive-grey or brownish-grey clay with occasional thin horizons of sheared, light green-grey clay. This light grey clay was analyzed by X-ray diffraction and found to contain approximately 50% montmorillonite. Somewhat less abundant is a moderately stiff, hard, dark, greenish-grey chloritic clay shale.

Most of the shales appear "dry" when first cored, but on exposure to air, they further dry out and develop extensive shrinkage cracks amounting to as much as 5% of the original volume. Many of the clay horizons contain variable amounts of authigenic pyrite which, in the weathered zone, oxidizes to form abundant secondary gypsum. Practically all of the clay shales are abundantly fossiliferous.

2.3.2.3.2. Page Mill Basalt (Miocene, Tpb)

This unit is a series of separate volcanic flows. Detailed study by Atchley and Grose (1954) delineated the sequence of flows and mapped their locations. The basalt of the 9 flows they identify have three distinctly different textures. (See Map II and Appendix II.)

The massive basalt is fine grained and very hard. However, it is extensively fractured and columnar jointed. The vesicular flow is tuffaceous, massive, and well statified by horizons of gritty pumiceous debris. The breccia has fragments of various sizes incorporated into it. Outcrops weather to a distinctive brown.

Cummings (1956) concluded that this unit was contemporaneous with the Mendigo diabase and tuff exposed in Woodside.

Poland (1939) recognized the submarine environment of deposition of the basalt without finding chilled pillows.

The unit varies in thickness. It is as much as 400 feet thick in the Quarry off of Page Mill Road.

Detailed Discussion:

The Miocene volcanics include three principal rock types: fine-grained flow basalt, blocky volcanic agglomerate, and local volcanic tuff and tuffaceous sandstone. Previous mapping distinguished the basalt flows from the agglomerate. The present map further refines the distribution of the basalt flows; the tuffaceous rocks were mapped as part of the agglomerate unit. The volcanic agglomerate occurs sporadically intermixed with basalt flows in the Page Mill quarry, and as a thin capping on the slopes and hilltops immediately west of Page Mill Road.

The agglomerate is a composite mixture of fragmental volcanic debris imbedded in a matrix composed principally of hardened ash and mud. It appears to be a mixture of volcanic fragments, mud flow sediment, and landslide debris, such as is often found on the flanks of active volcanoes. It contains angular to subangular fragments of volcanic rock, usually vesicular basalt, which range in size from one to several inches across. The agglomerate is a soft weak rock and its dominant occurrence in the Page Mill quarry gives an erroneous impression of conditions in the volcanic rock sections.

The basalt flows, four of which are recognized, are well exposed in the Page Mill quarry. Along the west limb of the anticline, they lens into a single flow which thins and swells in thickness along a narrow band extending beyond Alpine Road. Where penetrated by tunnels, the basalt unit consists of a single flow, complete with vesicular flow surface and baked lower contact. The rock is an extremely hard, dense, fine-grained basalt but is highly fractured, jointed, and transected by hair-line cracks which result in easy breakage. The basalt flows typically contain abundant pyrite disseminated within the rock or filling cross-cutting fractures. There is considerable chloritic-type alteration along the fractures associated with the pyrite mineralization.

The tuffaceous rocks consist of massive, well-stratified horizons of gritty pumiceous debris mixed locally with coarse sandy materials. Much of this rock appears to be water-deposited, but some of it is clearly of volcanic origin. The rock itself is variable in hardness, density, color and composition, and generally forms conspicuous brown-stained outcrops.

2.3.2.3.3. Lower and Middle Miocene Sandstone (Un-named; Ts)

The lower part of this unit is richly fossiliferous and rests unconformably on the volcanic unit. Fragments of marine invertebrate shells (such as barnacles and pelecypods) are abundant. Calcareous cement makes this course grained, well sorted, feldspathic sandstone more resistant to erosion than the upper part of the unit. Hogg (1963) concluded that the presence of megafossils indicated a shallow environment of deposition. Weathered rock is case hardened.

Higher in the section the sands are finer and moderately well sorted. The rocks are yellow-grey to olive green and quite friable, lacking the calcareous cement seen lower in section. Calcareous concretions are large. Shell fragments form resistant beds. This rock weathers to a light grey. Outcrops are rare and slopewash cover thick. Antonnen (1966) concluded that the sorting and feldspathic nature of the sandstone indicated a relatively immature sand being deposited near the source.

Los Trancos Formation has been proposed as a name for this unit but remains unadopted.

Detailed Discussion:

The unit is composed predominately of massive, thick-bedded, fine-grained to silty sandstone which is poorly to moderately cemented. Some of the rock is very poorly cemented, almost a firmly compacted sand. Interstratified are local 1 to 5-foot beds and lenses of coarse-grained sandstone which also varies in hardness and cementation. Clay or shale strata are virtually absent. The moderately cemented sandstones constitute the bulk of the rock, but even these are relatively soft and cores

can be broken by hand or with light hammer blows. Much of the softer rock can be crushed by finger pressure. Only a small percentage of the sandstones can be classed as hard to very hard, such that a 2-inch core would require several hammer blows to fragment. The harder rocks include thin beds of calcite-cemented fossiliferous sandstone scattered through the lower portion of the unit, and occasional boulder-size calcareous concretions.

The fine-grained sandstones are medium grey in color, weathering to light buff or light brown, and are quite friable. Most of the sands are fairly well sorted, with generally subangular grains, and are only slightly permeable. Many of the sandstones are "arkosic" or "feldspathic" as they contain a variable, though high, percentage of feldspar minerals. Distinctive features of the Miocene sandstones are their massive character, the general scarcity of shale horizons, and the presence of thin fossil-fragment beds. Near the western part of the area the sandstones are interbedded with the Miocene volcanic sequence and are found beneath the basalt flows.

2.3.2.3.4. Upper Miocene Silicious Siltstone

This unit is represented at the southern boundary of the project area. The lower sandstones grade into it conformably. The silicious cement indicates a much deeper, calcium deficient environment of deposition. The chert is very fractured, Weathering then produces fragmented debris.

2.3.2.3.5. Early Pleistocene (Santa Clara) Formation

The Santa Clara formation, of widespread occurrence along the margins of the Santa Clara Valley, is commonly described as a terrestrial deposit of Plio-Pleistocene age. In the Stanford Foothills, this formation is partly of marine origin and probably perdominantly of early Pleistocene age. Along Arastadero Road south of Felt Lake, nearly flat lying beds of sands and gravels of this formation are well exposed. These beds are near the base of the formation and have fossil horizons containing a marine pelecopod fauna. Similar beds are found in the hills south of the intersection of Page Mill and Arastadero Roads. This fauna has been identified by Dr. Keen (personal communication, July, 1959) as being no older than Pleistocene. Thus, in the central part of the mapped area, the Santa Clara rocks would appear to be essentially Pleistocene in age though rocks of Pliocene age may occur furtherto the southeast.

The Santa Clara formation consists perdominantly of poorly bedded unconsolidated sandstone with layers and lenses of interbedded sandy gravels. The gravel is mostly of small size, from 1/4" to 2", but larger sizes are not uncommon. The rocks are generally similar to local deposits of recent alluvium although there are some obvious differences in the source areas of the gravels. The Santa Clara commonly shows evidence of accumulation from local sources such as the Eocene sandstone and the Miocene basalt.

The Santa Clara rocks rest unconformably on all of the older formations and at one time may have covered most of the area. Remnants of gravel are found almost everywhere even though the bulk of the formation has been eroded from most of the hill areas. The Santa Clara rocks are gently folded in the central part of the area, but they have been greatly affected by

faulting along the San Andreas zone and have been extensively folded and faulted along with the underlying Miocene rocks, near the border of the alluvial plain, northeast of Junipero Serra Boulevard.

Some late Pleistocene and Recent terrace gravels were mapped with the Santa Clara rocks since, in the absence of good exposures, the two are practically indistinguishable. The thickness of the Santa Clara rocks in the mapped area is not known; however the formation is several thousand feet thick in the region immediately southwest of the San Andreas fault.

2.3.2.3.6 Recent Alluvium

Recent alluvium is present in the foothill area only along the stream valleys; it forms no deep valley fillings except along the San Andreas rift zone. Extensive thick deposits of alluvium are present along the northeast margin of the foothills.

2.3.2.4 Structure

The rocks described above are all involved in local distortion resulting from folding during the Late Miocene orogeny which produced the coast ranges.

The project area is dominated by an anticlinal fold which has been breached by erosion.

Atchley and Dobbs (1960) point out that the complexity of distortions obscures the structure. However, one can recognize the dip of certain beds in the Butano Formation and the dip of the Lower Miocene Sandstones.

Reverse faults displace parts of the volcanic unit and involve the Lower Middle Miocene Sandstones as well. This structural irregularity is expressed in valleys cutting across the inclined beds of the Butano Formation.

2.3.2.5 Geometric Considerations of ERTS Imagery

The common approach for dealing with areally distributed (two-dimensional) data is to prepare an appropriately scaled base (usually orthographic topography) ,,,on which different data types can be plotted.

The ERTS scanning system presents certain technical problems to this approach. The actual ground area for which spectral reflectance is sampled is a rectangle approximately 187 by 259 feet East-West and North-South respectively. Because the orbit of the satellite is not exactly polar, these rectangles are oeiented approximately 10°E of North. In addition, the MSS collects six such lines of data simultaneously. Each successive scan takes place after the earth has rotated to the east slightly (60 ft). Hence, every six lines are offset to the west almost 1/2 one such element. The images produced by Goddard are rectified to compensate for these geometric characteristics and hence, are almost completely orthogonal. Finally, during a subsequent overflight the picture element may be collected as much as 50% both North and East of the pixel from the previous overflight.

The Stanford ERTS-tape reading system presents the data on a simple line printer (10 characters per inch horizontally and 6 characters vertically). The results is a skewed and stretched "image" with scales of 1:18482.64 and 1:22171.32 E-W. In order to locate particular sites within such "images" it is necessary to find recognizable features such as bodies of water or highways (best seen in band 7) and interpolate between them. This difficulty is compounded when one wishes to collect

the actual numeric value for one pixel as numeric printouts are stretched horizontally X3 in order to legibly present double digits. And, of course, when images from different overflights are to be compared this is the final problem of determining just what piece of ground was sampled.

Costly and time-consuming efforts would be necessary to develop a system to present various shade-prints geometrically corrected and at appropriate scale. It would be even more difficult to present numeric data in a form compatible with an orthogonal base map.

One alternative to converting the "image" to orthogonality is to convert the orthogonal base to the geometry of the printouts. Such skewed and stretched maps could be layed directly over printouts.

Another approach is to construct templates for collecting discrete data points from either type of data format.

2.3.2.6 Soil Sampling

Once actual locations of sites were established in the field their positions were plotted on a topographic map with a scle of 1:2400. Distance measurements made to features appearing on the map (such as road intersections, structures, hill-tops, etc.) made it possible to locate sites to within a few feet.

Samples of soil were taken at each site. The percent of weight comprised by water was determined by oven drying. Color of soil was determined by comparison with the Geological Society of America Rock-Color Chart.

The soil type and bed-rock for each site was determined on the basis of field reconnaissance and mapping, consultation of literature on the area, and physical examination of samples. The actual procedures used are described in the Appendices. The individual sites were plotted on a template for numeric printout. When the dam of Felt Lake and several clumps of trees are located on both printouts (band 7 shade prints are darker and numerics have lowest numbers at these locations). Statistical analysis of the data should reveal the relationships, if any, which exist between geologic characteristics and spectral reflectance as measured by ERTS.

Detailed Techniques Used

2.3.2.6.1 Soil Samples

A block of top soil was excavated with pick-hammer and shovel. Following trimming a fist size sample was placed in a plastic bag with a label and sealed.

2.3.2.6.2 Soil Moisture

A small amount of each sample was cut from each block, placed in crucible, weighed, and dried in an oven at 120°C for 8-10 hours, and weighed again while still hot. The difference was used to calculate the percent of original weight which the moisture represented.

2.3.2.6.3 Color

The dried samples were set next to the color chips in the Rock-Color Chart and the Munsell number of that which was most like the soil was recorded.

2.3.2.6.4 Soil Type

Local — Local variations of soil types result from down slope movement of surficial materials and the resulting differential distribution of clay size particles. The classification in this category was made on the basis of field examination as well as textural study of samples.

Soil Conservation Service — The SCS Soils Report for Santa Clara County describe different soil types and shows their areal distribution on photomaps of scale 1:12000. A portion of this mapping is shown in Appendix VIII. The descriptions of the classifications are given in Table I.

2.3.2.6.5 Bed Rock Units

The geologic unit for each site was determined by fieldwork as well as using existing maps. Descriptions are included in the section on Rock Units.

2.3.2.6.6 Inclination and Slope Azimuth

With site locations plotted on the small-scale topographic map it was a simple matter to determine gross slope characteristics. A line was constructed perpendicular to adjacent contour lines. Its azimuth was noted. The distance between contour lines was then used to trigonometrically calculate dip of surface below horizontal. These measurements appear in Table I.

2.3.2.6.7 Elevation and Lambert Coordinates

These were determined by simple interpolation on the grided topographic map. These are noted in Table I as well.

TABLE 2.3.2.6.1

STANFORD FOOTHILLS
ERTS-A TEST SITES

STAT NO.	SOIL DESCRIPTOR 1 2 3	DRY COLOR HUE 4 5	% SOIL MOISTURE 11/15/74	TOPOGRAPHIC SLOPE INCL AZMTH	ELEV FT	LAMBERT CO-ORD (ZONE III) NORTH	EAST
B-029	SLR-GME/TBU	/	.	14.0/175SSE	380	1516262	335158
B-030	FIL-GME/TBU	5YR 5/1	5.4	4.7/243SWW	360	1516349	335034
B-031	CSW-GME/TBU	5YR 4/1	11.8	11.3/338NNW	374	1516425	334905
B-032	CSW-GME/TBU	5YR 3/1	10.1	9.5/003NNE	390	1516451	334801
B-033	CLR-LTD/TPB	5YR 4/1	11.9	5.7/012NNE	444	1516454	334502
B-035	CLR-LTD/TPB	10YR 4/2	10.7	6.3/335NNW	467	1516476	334297
C-041	CLR-LTD/TPB	/	.	4.0/200SSW	476	1516596	334078
C-042	CSW-LTD/TPB	10YR 2/2	9.9	3.2/201SSW	468	1516569	333951
C-045	CSW-LTD/TPB	5Y 4/1	16.6	2.3/145SEE	466	1516572	333886
C-046	CSW-LTD/TPB	5Y 3/1	20.1	2.8/089 E	468	1516507	333847
C-047	CLR-LTD/TPB	5YR 3/2	11.2	4.1/095 E	480	1516321	333739
C-049	CLR-LTD/TPB	10YR 2/2	17.2	5.2/094 E	493	1516128	333642
D-051	CLR-LTD/TPB	10YR 3/2	10.9	3.6/076 E	512	1515877	333482
D-053	CLR-LTD/TPB	/	.	4.8/074 E	523	1515690	333295
D-054	CLR-LTD/TPB	/	.	2.3/135SE	516	1515557	333097
D-055	CLR-LTD/TPB	10YR 2/2	13.9	3.6/080 E	519	1515464	332941
D-056	CLR-LTD/TPB	10YR 4/2	9.0	3.2/083 E	528	1515412	332758
E-060	CSW-DAE/TBS	5YR 4/1	17.0	0. /320NW	457	1514286	333305
F-070	SLR-DAE/TUS	10YR 4/2	7.2	7.1/028NNE	475	1514202	333057
F-072	SLR-DAE/TUS	10YR 3/2	10.6	14.0/030NNE	496	1514311	332906
F-073	SLR-DAE/TUS	10YR 4/2	7.2	9.5/111SWE	486	1514450	332666
G-080	SLR-DAE/TUS	5Y 5/1	8.3	3.2/288SW	483	1514382	332563
G-082	SLR-DAE/TUS	5Y 4/1	15.1	11.3/307NWW	498	1514296	332406
G-084	SLR-DAE/TUS	10YR 4/2	5.8	9.5/237SWW	480	1514242	332134
G-086	SLR-DAE/TUS	10YR 5/2	6.6	8.1/253SWW	454	1514197	331815
H-091	SLR-DAE/TUS	10YR 4/2	7.9	4.7/104SEE	452	1514096	331612
H-092	CSW-DAE/TUS	10YR 3/2	9.3	8. /056 E	445	1514058	331451
H-094	SLR-DAE/TUS	5Y 5/1	10.1	4.1/061NEE	467	1513964	331246
H-096	CLR-DAE/TM	5Y 5/1	11.2	7.1/074NEE	477	1513839	331103
I-005	CLR-DAE/TM	7YR 4/1	10.4	0.5/190 S	473	1513772	330962
I-006	CLR-DAE/TM	5Y 5/1	10.4	6.5/205SSW	466	1513719	330783
I-008	CLR-DAE/TM	10YR 5/2	8.7	0.5/204SSW	435	1513610	330562
I-009	CLR-AVD/QSC	10YR 6/2	8.3	13. /207SSW	405	1513456	330400
I-010	CSW-AVD/QSC	10YR 4/2	9.3	14. /235SWW	360	1513318	330322

Table 2.3.2.6.1 (Cont'd)

STAT NO.	SOIL DESCRIPTOR 1 2 3	DRY COLOR HUE 4 5	% SOIL MOISTURE 11/15/74	TOPOGRAPHIC SLOPE INCL AZMTH	ELEV FT	LAMBERT CO-ORD (ZONE III) NORTH	EAST
J-020	CLR-AVD/QSC	10YR 5/4	7.9	10. /130SE	340	1513606	329426
J-019	CLR-AVD/QSC	10YR 5/2	6.9	5.5/200SSW	358	1513400	329510
J-016	CLR-AVD/QSC	10YR 4/2	6.9	9.5/141SE	370	1513081	329558
J-014	CLR-AVD/QSC	10YR 5/4	6.9	4.5/194 S	368	1512779	329482
K-030	CSW-AVD/QSC	10YR 5/2	9.2	5.7/123SE	368	1512606	329331
K-031	CLR-AVD/QSC	10YR 5/4	7.8	3.8/190 S	397	1512327	329278
K-032	CLR-AVD/QSC	10YR 4/2	8.6	5. /044NE	393	1512066	329231
K-034	CLR-AVD/QSC	10YR 4/2	8.6	1. /285NWW	400	1511816	329245
K-035	CLR-AVD/QSC	10YR 4/2	7.2	10. /284NWW	372	1511557	329295
M-052	CLR-AVD/QSC	5Y 5/1	7.1	4.1/312NW	404	1510937	328267
M-054	CLR-AVD/QSC	10YR 4/2	8.2	2.5/316NW	423	1511102	328403
N-001	SCL-PRD/QAL	10YR 5/4	6.8	2.8/068NEE	381	1510230	330275
N-002	SCL-PRD/QAL	/	.	1.0/267 W	383	1510136	330160
N-003	SCL-PRD/QAL	10YR 7/4	5.5	5. /275 W	382	1510072	329943
N-004	SCL-PRD/QAL	/	.	1. /064NEE	392	1510173	329624
N-006	SCL-PRD/QAL	/	.	6.3/132SEE	386	1510211	329378
N-008	SCL-PRD/QAL	/	.	3.3/095 E	382	1510180	329083
N-010	SCL-PRD/QAL	/	.	2.0/085 E	381	1510177	328760
N-012	SCL-PRD/QAL	/	.	4.5/105SEE	381	1510150	328515
N-014	SCL-PRD/QAL	/	.	6.3/090 E	383	1510124	328216
N-016	SCL-PRD/QAL	/	.	0.5/323NNW	384	1510000	327914

TABLE 2.3.2.6.1 (Cont'd)

1 LOCAL SOIL TYPE -
FIL= MAN PLACED FILL OF MIXED TEXTURES
SLR= SANDY LOAM RESIDUAL
CLR= CLAY LOAM RESIDUAL
SSW= SANDY SLOPEWASH
CSW= CLAYEY SLOPEWASH
SCL= SANDY CLAY LOAM

2 SOIL CONSERVATION SERVICE SOIL NAMES -
GME= GAVIOTA-LOS GATOS COMPLEX
GCE= GAVIOTA LOAM
LTD= LOS TRANCOS STONY CLAY
DAE= DIABLO CLAY
AVD= AZULE SILTY CLAY
PRD= POSITAS-SARATOGA LOAM

3 GEOLOGIC BEDROCK NAME -
TBU= BUTANO FORMATION (SANDSTONE AND SHALE)
TPB= PAGE MILL BASALT (MASSIVE, BRECCIA, AND TUFF FLOWS)
TBS= BARNICLE BED SANDSTONE
TUS= UNNAMED SANDSTONE
TM = MONTEREY SHALE (SILICIOUS)
QSC= SANTA CLARA GRAVELS
QAL= OLD AND RECENT ALLUVIAL DEPOSITS

4 VALUE (LIGHTNESS)

5 CHROMA (SATURATION)

MUNSELL NUMBER		NAME
5Y	3/1	= BETWEEN 'OLIVE BLACK' AND 'OLIVE GRAY'
5Y	4/1	= 'OLIVE GRAY'
5Y	5/1	= BETWEEN 'LIGHT OLIVE GRAY' AND 'OLIVE GRAY'
5YR	4/1	= 'BROWNISH GRAY'
5YR	5/1	= BETWEEN 'LIGHT BROWNISH GRAY' AND 'BROWNISH GRAY'
5YR	3/2	= 'GRAYISH BROWN'
7YR	4/1	= BETWEEN 'LIGHT BROWN' AND 'YELLOWISH BROWN'
10YR	2/2	= 'DUSKY YELLOWISH BROWN'
10YR	3/2	= 'GRAYISH YELLOWISH BROWN'
10YR	4/2	= 'DARK YELLOWISH BROWN'
10YR	5/2	= 'YELLOWISH BROWN'
10YR	6/2	= 'PALE YELLOWISH BROWN'
10YR	5/4	= 'MODERATE YELLOWISH BROWN'
10YR	7/4	= 'GRAYISH ORANGE'

TABLE 2.3.2.6.2

GENERALIZED STRATIGRAPHIC COLUMN

ROCK UNITS ENCOUNTERED IN THE DISH HILL AREA

(no vertical scale)

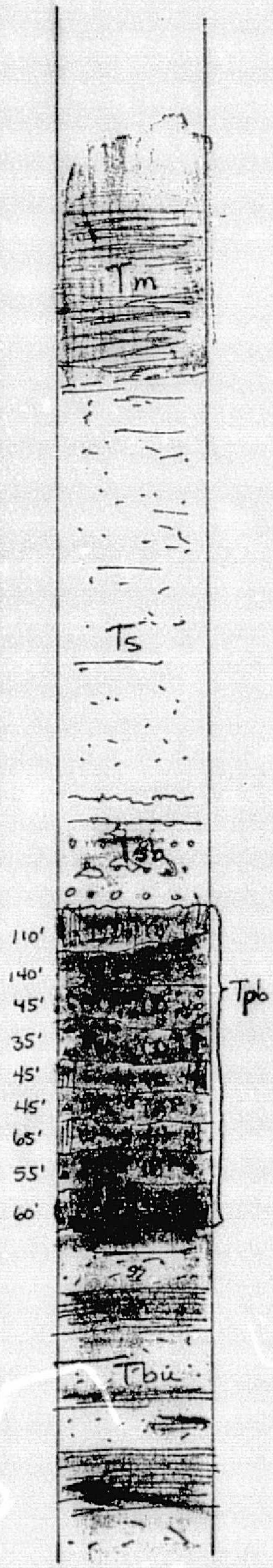

<u>Upper Miocene Silicious Siltstone</u>

fine grained, well statified,
clay and mudstones with silicious
cementation.
chert concretions numerous
dark grey weathers to light buff

<u>Middle Miocene Sandstone</u>

olive-grey arkos
scarcely interbedded with light
grey clay and shale.
very friable
few fossil beds

<u>Lower Miocene Sandstone</u>

fine grained, moderately well sorted,
well cemented, fossiliferous,
feldspathic with basalt pebbles,
weathers light brown and case hardened

<u>Lower Miocene Volcanics</u> (Page Mill Basalt)

series of flows ranging:

1) massive, hard, fractured,
columnar jointing
2) tuffaceous, massive, well sorte
statified horigons of gritty
pumiceous debris
3) volcanic breccia , fragments of
variable size

<u>Eocene Sandstone and Shale</u> (Butano Formation)

fine to medium grained, poorly sorted,
variably cemented sandstone, beds 30-90 ft.
interbedded with dark green shale, beds
20-100 ft.

TABLE 2.3.2.6.3

STATIGRAPHIC COLUMN OF ROCK UNITS

DISH HILL, STANFORD,
(no vertical scale)

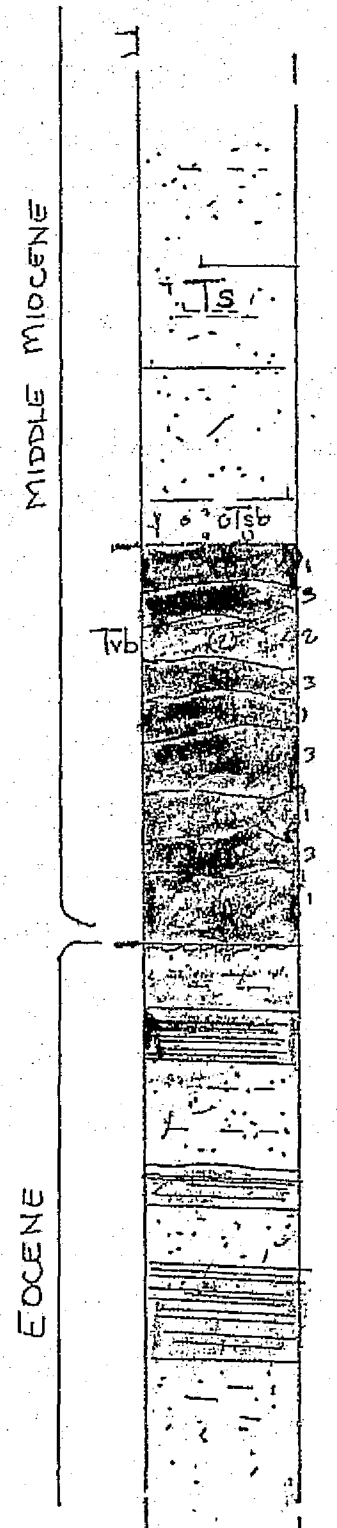

Unnamed Sandstone (Los Trancos Formation*)
700 feet

fine grained, moderately well sorted, well cemented, fossiliferous, feldspathic sandstone

grading up into calcium deficient, friable, grey to olive-grey arkos scarcely interbedded with light grey clay and shale near center of section

Page Mill Basalt 300+feet

series of volcanic flows ranging

1. massive, extremely hard, extensively fractured and jointed
2. tuffaceous, massive, well stratified horizons of gritty pumiceous debris
3. breccia with fragments of variable size

Butano Formation 2000+ feet

fine to medium grained, poorly sorted, variably cemented sandstone beds (30-90 ft) with dark grey claystone seams (2-3 ft) composed of 50% montmorillinite

interbedded with medium dark olive-grey to brownish shale seamed with course to fine sand (1-2 ft)

Sandstone weathers to case-hardened, buff outcrpos
Shale renders a dark black, clayrich soil

composit after Atchley & Grose,(1954),Antonen (1966),Edwards (1961) SBB

* a proposed name still unadopted

110

THIS PAGE IS INTENTIONALLY BLANK

THIS PAGE IS INTENTIONALLY BLANK

2.3.3 THE VEGETATION OF THE STANFORD GRASSLAND SITE: A BIOMASS STUDY

2.3.3.1 Description of the Study

A study of the vegatation at selected sites in the Stanford grassland has been undertaken to aid in the interpretation of reflectance data from those sites.

The Stanford grassland is a typical representative of the California Valley Grassland plant community (Munz and Keck, 1965). It has been subjected to grazing by cattle for decades which has changed the species composition entirely. Few of the original native species remain. Most of the species of grasses and broad-leaved plants found in the grassland today have been introduced from the Mediterranean region (Thomas, 1961; McNaughton, 1968).

A preliminary study was done to determine the species of the grasses and broad-leaved plants growing at the study sites. (Figs. 2.3.3.1 - 3). Plants were collected in early May in various stages of flower and seed formation. The plants were identified to the level of genus or species using local floras. The nomenclature is that of Munz and Keck. Specimens of each 3 species were dried and pressed for a permanent reference collection. The major plant species found in the Stanford grassland study sites are:

	Botanical Name	Common Name	Figures
Grasses:	Bromus mollis	Soft chess	5, 10
	Avena barbata	Slender Wild Oats	4, 11
	Lolium multiflorum	Ryegrass	9, 12
	Bromus rigidus	Ripgut grass	6, 13
	Hordeum leporinum	Foxtail	7, 14
	Hordeum hystrix	Mediterranean barley	8, 15

A description and drawing of each grass species is attached (Table I).

Broad-leaved Plants:	Erodium sp.	Filaree, needle plant	16
	Geranium sp.	Geranium	17
	Medicago sp.	Bur clover	18
	Convolvulus arvensis	Morning glory, bindweed	19
	Bellardia trixago	Bellardia	20
	Eschscholzia californica	California poppy	21
	Rumex sp.	Sorrel	22

Initial observations also revealed that the vegetation at the study sites was variable in species composition, plant size, percent cover and time of onset of senescence and drying.

TABLE 2.3.3.1

Description of the major grass species

Grass species are identified by the characteristics of their flowers and, to a lesser extent, their leaves. The flower head is borne on a culm, or stalk, which raises it above the leaves. The rachis, or main axis, of the head may be branched in a variety of patterns and bears the spikelets, the basic unit of grass flower structure. At the base of each spikelet is a pair of glumes, modified leaf structures whose shape and texture are important in species identification. The glumes subtend one to many florets, small modified flowers. The floret consists of an outer lemma and palea enclosing a small inner flower. Glumes, lemmas and paleas may terminate in slender bristles called awns.

The grass leaf consists of a lower sheath, which surrounds the stem, and an upper blade which diverges from the stem. At the junction of the sheath and blade is the ligule, a hairy or membranous extension of the sheath. The margin of the leaf at the junction may be extended laterally into auricles, or lobes. See Fig. 2.3.3.1 - 2.3.3.3

Avena barbata Brot. Slender Wild Oat (Fig. 2.3.3.4)

Annual; culm 30-60 cm. tall; flower head open, loosely branched; spikelets large and drooping at maturity; florets 2; lemma hairy, bearing a prominant bent awn 3 cm. long.

Bromus mollis L. Soft Chess; Soft Brome (Fig. 2.3.3.5)

Annual; culm 10-80 cm. tall; softly hairy all over plant; flower head compact, 4-10 cm. long, few short branches; spikelets compact, slightly flattened laterally, 15-20 cm. long; florets 6-12 per spikelet; lemma rounded on back, with soft awn 5-9 mm. long.

Bromus rigidis Roth. Ripgut Grass; Ripgut Brome (Fig. 2.3.3.6)

Annual; culm 30-70 cm. tall; flower head branched, open, 6-18 cm. long; spikelets 2-5 cm. long; florets 5-7 per spikelet; lemmas 2.5-3 cm. long, tipped with a stiff awn 3.5-5 cm. long; both lemmas and awns covered with stiff short hairs pointing toward the tip.

Hordeum hystrix Roth. Mediterranean Barley (Fig. 2.3.3.8)

Annual; culms sometimes bent, 12-35 cm. tall, foliage hairy; leaf blade lacks auricle; flower head 1.5-3 cm. long, unbranched, with bottle brush appearance due to radiating awns; glumes rigid and divergent, lacking hairs on margin; spikelets in 3's; florets 1 per spikelet.

Fig. 2.3.3.1 from Crampton (1974)
Fig. 2.3.3.2 from Munz and Keck (1965)
Fig. 2.3.3.4 from Abrans (1940)

<u>Hordeum</u> <u>leporinum</u> Link. Foxtail (Fig. 2.3.3.7)

Annual; culm 15-60 cm. tall; leaf with auricle; flower head 5-9 cm. long, unbranched, with bottle brush appearance due to radiating awns; spikelets in 3's; florets 1 per spikelet; glumes with hairs on margin.

<u>Lolium</u> <u>multiflorum</u> Lam. Ryegrass; Italian Ryegrass; Australian Ryegrass (Fig. 2.3.3

Annual, culm 25-100 cm. tall; blades with auricles at base; flower head 10-20 cm. long, unbranched narrow spike; spikelets flattened, close to and alternating on rachis; 10-20 florets per spikelet; glumes shorter than spikelet; lemmas with awns.

2.3.3.2 BIOMASS AND REFLECTANCES STUDIES

From May 15 to May 22 a detailed study of the vegetation at 44 sites was made to determine the species composition, biomass and stage of plant growth. At each site the vegetation was treated in the following manner:

1. A square, 0.5 m. on a side, was marked off at a randomly selected site.
2. Reflectance relative to $BaSO_4$ was recorded.
3. The plant species were determined.
4. The percent contribution of each species to the total biomass was estimated by eye.
5. All vegetation within the square was cut off at ground level and put in an airtight plastic bag and taken to the lab.
6. Reflectance after cutting was recorded.
7. Total fresh weight of the vegetation at each site was measured.
8. All plant material was dried in ovens at $100^{o} \pm 5^{o}$C. for 48 hours.
9. Total dry weight was measured.

The reflectance at each site was measured before and after the removal of the vegetation cover, using the ERTS radiometer, 15^{o}FOV bidirectional geometry (Tab. 2.3.3.2)The sites vary considerably with regard to species composition, fresh weight, dry weight (biomass) and the ratio, dry weight/ fresh weight.(Tab. 2.3.3.2 and 2.3.3.3). The dry weight/fresh weight measurement indicates the degree to which the plants have dried out. As the vegetation dries, the green color is lost and the leaves turn to yellow-green then tan. The ratio of dry weight to fresh weight is therefore, an indirect measure of the "greeness" of the vegetation. These data will be used to interpret the reflectance data taken at the same sites.

A statistical study of the correlations between species, biomass, biomass ratio and reflectance, appears elsewhere as SRSL Technical Report No. 74-7.

TABLE 2.3.3.2

STANFORD GRASSLANDS

Site Number	Total wet weight (g)	Total dry weight (g)	Dry weight / Wet weight
946	158.3	78.9	.495
942	117.3	52.8	.450
941	105.0	62.8	.598
947 (green)	213.2	120.0	.563
947 (dry)	79.7	57.3	.719
949	119.3	71.0	.595
951	150.0	81.9	.546
953	131.1	82.7	.631
954	83.9	55.5	.662
955	70.1	54.6	.779
980	342.4	138.4	.404
982	421.8	173.0	.410
914	282.5	121.0	.428
916	306.4	128.2	.418
917	184.6	103.2	.559
920	193.9	104.6	.539
930	333.7	160.0	.479
931	271.7	155.0	.570
932	406.5	180.0	.443
934	307.3	130.1	.423
940	344.8	122.3	.355
942	430.8	149.1	.346
943	313.9	138.5	.441
944	290.0	132.3	.456
905	354.5	168.2	.474
906	168.0	50.1	.476
908	209.5	95.8	.457
909	192.5	113.6	.590
991	220.4	98.9	.449
992	463.5	175.7	.379
994	404.3	165.4	.407
996	423.2	197.2	.466
986	411.0	152.4	.371
984	317.7	126.4	.398
950	325.5	127.1	.390
952	403.5	145.3	.360
954	367.1	164.2	.447
970	86.5	45.1	.521
972	152.0	74.1	.488
973	354.9	171.4	.483
929	191.7	81.8	.427
931	294.6	131.4	.446
933	86.2	48.2	.559
936	60.3	42.2	.700

TABLE 2.3.3.3 Stanford Grassland – Species Composition

TABLE III

STANFORD GRASSLAND SPECIES COMPOSITION

Site #	Grasses: Soft Chess (Bromus mollis) (green)	Ryegrass (Lolium multiflorum) (green)	Wall barley (Hordeum hystrix) (yellow-green)	Foxtail barley (H. leporinum) (purplish)	Slender Wild oat (Avena barbata) (dark green)	Ripgut grass (Bromus rigidis) (green)	Broad-leaved plants: Morning glory (Convolvulus) (gray-green)	Needle (Erodium) (slightly reddish)	Sheep sorrel (Rumex) (reddish green)	Other broad-leaved plants
946	30	30	30							10
942		10	80							10
941	80	10			10					
947	10	20		60						10
947 dry	10	50	20							20
949	70	20								10
951	5	5	90							
953	70	20			10					
954	5		95							
955	40	5	40							15
980	95	5								
982	20	15	60				5			
II.										
914	30	20	40		5					5
916	30	10	30		30					
917	60	20			10		5			5
920	10	70			10					10
930	5	30	60							5
931	10	30	40	10	10					
932	25	25			40		5	5		
934	40	40			20					
940		40	30		20					10
942	30	30	20	20						
943	30	30	30							10
944	20	40			40					
III.										
905	50	40		5	5					
906	50	40			10					
908	20	30			50					
909	45	45						10		
991	30	20	35		5		5			5
992	25	50		25						
994	30	60	10							
996	10	30		60						
986	30	30		40						
984	30	60				5				5
IV.										
950	5	5	5		80		5			
952	10	20	20		30		20			
954	20	10			40		10		10	10
970	50	30	20							
972	40	40			10				10	
973	5	20			70	5				
929	20	20	10	10	30	10				
931		50	50							
933	20	20			50					10
936	30				30			40		

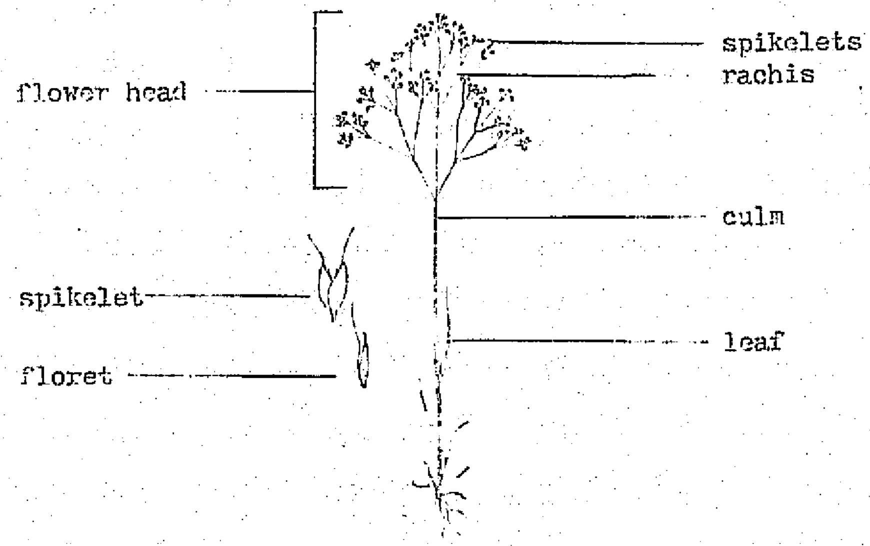

Fig. 2.3.3.1 A grass plant

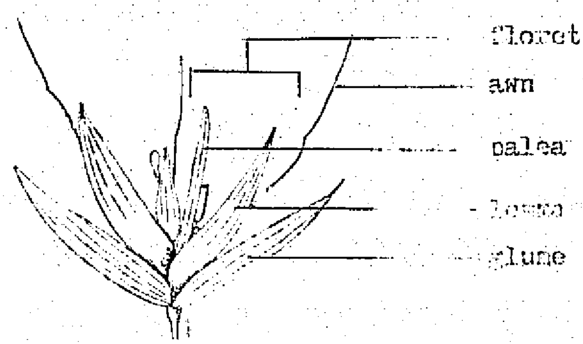

Fig. 2.3.3.2 A grass spikelet

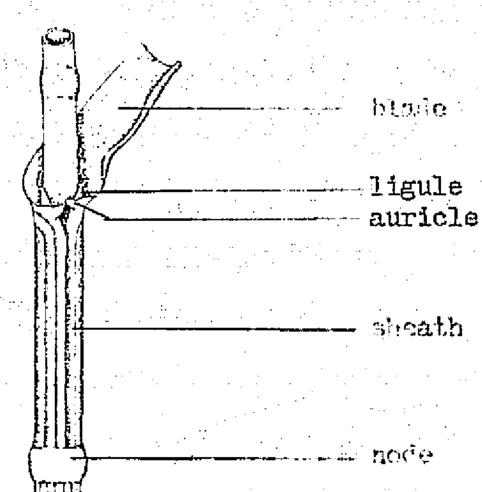

Fig. 2.3.3.3 A grass leaf

Fig. 2.3.3.4 Avena barbata

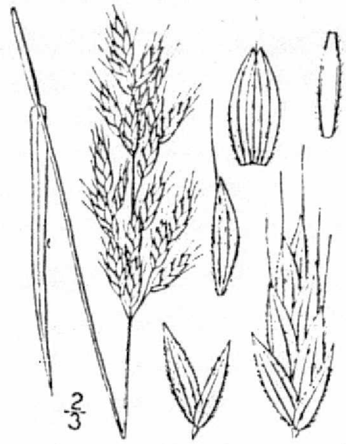

Fig. 2.3.3.5 Bromus mollis

Fig. 2.3.3.6 Bromus rigidis

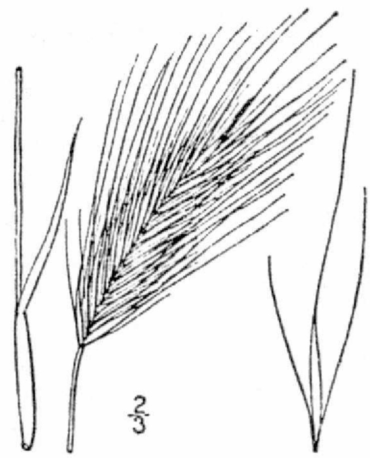

Fig. 2.3.3.7 Hordeum leporinum

Fig. 2.3.3.8 Hordeum hystrix

Fig. 2.3.3.9 Lolium multiflorum

Fig 2.3.3.10 Bromus mollis, Soft Chess grass

Fig. 2.2.3.11 Avena barbata, Slender Wild Oats

Fig. 2.2.3.12 Lolium multiflorum, Ryegrass

122

Fig. 2.3.3.13 Bromus rigidis, Ripgut Grass

Fig. 2.3.3.14 Hordeum leporinum, Fox tail barley

Fig. 2.3.3.15 Hordeum hystrix, Mediterranean barley.

Fig. 2.3.3.16 Erodium sp., Filaree, Needle plant

Fig. 2.3.3.17 Geranium sp., Geranium

Fig. 2.3.3.18 Medicago sp., Bur clover

Fig. 2.3.3.19 Convolvulus arvensis, Morning Glory, bindweed.

Fig. 2.3.3.20 Bellardia trixago, Bellardia

Fig. 2.3.3.21 Rumex sp., Sorrel

2.3.4 STATISTICAL CORRELATION OF BIOMASS DATA VERSUS BI-DIRECTIONAL REFLECTANCE:

2.3.4.1 INTRODUCTION

When the biomass data from the 42 sites of the Stanford Grassland study became available, a statistical study was started by Prelat, using both the "scatter diagram" (2 variable plot) program (BMDO2D), and the stepwise discriminant program (BMDO7M).

Selected examples of the output have been included in this section.

2.3.4.2 COMPUTATIONAL METHOD (BMDO2D)

As stated by Sears in the preceding Section 0.5m x 0.5m quadrants were selected at random near the measurement stations on the Grassland traverse over the period May 15-18, 1974. These stations were at intervals of about 80m along a 5 Km N-S traverse across the 4 main rock/soil types in the Grassland site.

For the biomass portion of the study, the grass was clipped off the quadrant, and weighed (wet and dried) in the lab, where species counts were also prepared.

Immediately prior to the clipping, however, the bi-directional reflectance measurements were taken, relative to $BaSO_4$, using an ERTS-bandpass radiometer (EXOTECH Model 100). The measurements were repeated after clipping, to give an appreciation of what "stubble" reflectance (grass roots + stem bases + soil) might look like as seen from ERTS.

2.3.4.2.1 The following ground measurement variables were available for statistical analysis (both before and after clipping):

1. Ch 4, 5, 6, 7. brightness (radiance)
2. Ch 4, 5, 6, 7. reflectance (bi-directional)
   (or R4, R5, R6, R7)
3. Ratios: R7/R6, R7/R5, R7/R4, R6/R5, R6/R4 and R5/R4. (or R76, R75, R74, R65, R64, R54)
4. Ratios: R74, R64, R54 (used to diminish the effect of sunlit and shaded-sides of hills).

The following biomass variables were available for each of the same 42 stations:

1. Wet weight grass

2. Dried weight grass (Biomass, weight/m^2)
3. "Deadness" (Biomass ratio = Dried/wet weight
4. Species (10) determination

The following soil variables were available:

1. Soil type, color, etc.

2. Soil moisture (although not taken until November 1974, at the end of a dry summer, the relative moisture-holding capabilities should be consistent).

3. Azimuth and slope of hill at the station.

From careful location of the ERTS CCT outputs we were able to give an approximate ERTS-radiance figure to each site, for 7 overpasses of the satellite. However, in common with many other experiments, we did not have tapes for the year of 1974, but had to make do with those of 1973, unfortunately a more wet year. Obviously this is not a suitable situation but it was all we had with which to work.

The analyses proceeded using four (4) main data sets. (Prelat worked only with Set 1, the present author used all 4).

2.3.4.2.1.1 Data Set 1: Eleven variables - 42 stations

Biomass data, plus ground reflectance, before and after clipping. See Table 2.3.4.1.

Data Set 2: Nine variables - 42 stations

Same data set, now normalized to Channel 4, before and after clipping. See Table 2.3.4.2.

2.3.4.2.1.2 Data Set 3: Thirty-three variables - 42 stations

Grass color, biomass data, ground radiance reflectance and ratios, soil parameters and species data.

See Table 2.3.4.3.

Data Set 4: Seventy-six variables - 42 stations

ERTS-radiance, ERTS-reflectance (calculated) and ground (truck) reflectance, from 8 ERTS overpasses and 3 truck traverses.

Cross correlation matricies were prepared for each data set, and those showing meaningful correlations selected for scatter diagram plotting.

Typical matricies were:

Ground Data

	R4	R5	R7	
	.	-.77	.71	Wet wt.
	.	-.62	.	Dry wt.
	.70	.90	.	Biomass ratio

Data Set 1

	$\underline{\underline{r}}$
Biomass ratio to R5 (ground)	+0.90
Biomass (dry) to R5	- .62

Ground Data

Dry	Biomass rat.	R54	R64	R74	
.95	-.79	.	.77	.80	Wet wt.
	-.61	-.50	.65	.67	Dry wt.
		.50	-.81	-.82	Biomass ratio
			.	.	R54
				.96	R64

Data Set 2

	$\underline{\underline{r}}$
Biomass ratio to	
R74	- .82
R64	- .81
Biomass (dry) to	
R74	.67

Ground Data

Dry wt.	BP5*	R5	R75	R74	R65	R64	
.95	.	-.74	.82	.76	.	.	Wet wt.
	.87	.82	-.83	-.82	.	.77	Biomass rat.
		.61	.	.	.	.	Soil moisture
		.35	.	.	.	.	Broadleaf
					.45	.	Morning Glory sp.

Data Set 3

* = Channel 5, bandpass radiance

CORRELATION MATRIX WITH ERTS SATELLITE DATA

(NOTICE THE DATES REPRESENTED IN THE MATRIX)

1973 - Wet ERTS 1309 May 28, 1973	1973 - Drier ERTS 1669 May 23, 1974			Data Set 4
BP7	BP5	R5	R6	
.	.71**	.70	.	"Deadness" Biomass ratio - ground May 15-18, 1974
.	.	−.63	.	Truck R75 - ground (3 dates)
.	.	.70	.	R5: ERTS 1309 May 28, 1973
.	.	.	.88	R6
.80	.	.	.	BP7: ERTS 1165 Jan. 4, 1973 (wet year)

** - linear

r = 0.71; see figure 2.3.4.19 for actual plot shape

TABLE 2.3.4.1 Five Soil (+Grass) Types in Discriminant Analysis
Stepwise Choice Sequence

	Single	Pair	Trio	Quartet	Quintet	
A 1 5 steps	Station Altitudes	BP4 ERTS-74 5/23/74	BP4 ERTS-73 12/30/73	Plant Species 6 (Ripgut)	BP7 ERTS-74 1/4/74	
Success	52%	69%	93%	93%	100%	Fig. 2.3.4.2.3
A 2 10 steps	Station Altitude	BP4 ERTS-74 5/23/74	BP4 ERTS-73 12/30/73	Ground ratio R76 5/18/74	-	
Success	72%	92%	100%	100%	(100%)	Fig. 2.3.4.2.4
B1 5 steps	BP4 ERTS-74 5/23/74	Biomass ratio (D/W) 5/15/74	BP4 ERTS-73 12/30/73	Station Slope	BP7 ERTS-73 5/28/73	
Success	60%	69%	90%	86%	88%	Fig. 2.3.4.2.5
B 2 34 var.	BP4 ERTS-73 5/28/73	Biomass (Dry wt.) 5/15/74	Station slope°	R7 ERTS-73 5/28/73	R5 ERTS-74 5/23/74	
Success	45%	69%	79%	86%	88%	Fig. 2.3.4.2.6
C 34 var. Reflectance	BP4 ERTS-73 5/28/73	R5 ERTS-74 5/23/74	R7 ERTS-73 5/28/73	R6 ERTS-73 1/4/73	R4 ERTS-73 12/30/73	
Success	45%	[illegible]	88%	88%	98%	Fig. 2.3.4.2.7

NOTE: Crosshatching indicates selection of ERTS data

Table 2.3.4.2 Strategy of Groupings used in Discriminant Analysis

	Groups	Steps	Variables Used	Deletions
A 1	5	5	65	-
A 2	3+ (Two tests)	10	65	
B 1	5	5	54	Altitude + Plants
B 2	5	5	34	Altitude + Plants and all band pass brightnesses
B 3	5	5	34	" "

Table 2.3.4.3 Stepwise Choices: F-Value Results at End

	Single	Pair	Trio	Quartet	Quintet
A 1	40	11	14	8	8
A 2	67*	21	16	14	9
B 1	15	10	9	7	5
B 2	14	10	7	6	4
C	14	8	10	6	5

* Highest Discriminability

2.3.4.2.2 Data Set 1 (Reflectance Variables)

The following date were available from the biomass and ground reflectance measurements at the 44 stations in the Grassland Survey. (See Table 2.3.4.4)

TABLE 2.3.4.4 BI-DIRECTIONAL REFLECTANCES

Variable 1 = total wet weight grass in 0.25 m^2

Variable 2 = total dry weight grass in 0.25 m^2

Variable 3 = ratio dry weight/wet weight

Variable 4 = reflectance channel 4 before cutting

Variable 5 = reflectance channel 5 before cutting

Variable 6 = reflectance channel 6 before cutting

Variable 7 = reflectance channel 7 before cutting

Variable 8 = reflectance channel 4 after cutting

Variable 9 = reflectance channel 5 after cutting

Variable 10= reflectance channel 6 after cutting

Variable 11= reflectance channel 7 after cutting

TABLE 2.3.4.5 Station Data for eleven Variables

ID	variables 1	2	3	$R4_B$	$R5_B$	$R6_B$	$R7_B$	$R8_{4A}$	$R9_{5A}$	$R10_{6A}$	$R11_{7A}$
942	117.3	52.8	0.450	0.057	0.089	0.241	0.338	0.192	0.144	0.224	0.299
941	105.0	62.8	0.590	0.064	0.111	0.209	0.281	0.098	0.149	0.224	0.297
947	213.2	120.0	0.563	0.065	0.111	0.239	0.337	0.128	0.187	0.251	0.321
947	79.7	57.3	0.719	0.078	0.130	0.206	0.278	0.119	0.173	0.257	0.301
949	119.3	71.0	0.595	0.072	0.105	0.218	0.284	0.105	0.152	0.214	0.279
951	150.0	81.9	0.546	0.057	0.093	0.230	0.335	0.123	0.175	0.251	0.316
953	131.1	82.7	0.631	0.067	0.114	0.206	0.287	0.099	0.151	0.213	0.286
954	83.9	55.5	0.662	0.087	0.143	0.239	0.300	0.147	0.208	0.279	0.351
955	70.1	54.6	0.779	0.091	0.149	0.213	0.296	0.129	0.184	0.245	0.331
980	342.4	138.4	0.404	0.054	0.065	0.243	0.414	0.095	0.139	0.209	0.297
982	421.8	173.9	0.410	0.066	0.071	0.293	0.474	0.103	0.142	0.199	0.265
914	282.5	121.0	0.428	0.055	0.070	0.253	0.360	0.198	0.162	0.226	0.289
916	306.4	128.2	0.418	0.057	0.068	0.246	0.338	0.097	0.142	0.214	0.268
917	184.6	103.2	0.559	0.051	0.097	0.199	0.314	0.098	0.146	0.214	0.283
920	193.9	104.6	0.539	0.048	0.085	0.187	0.281	0.093	0.144	0.203	0.272
939	333.7	160.6	0.479	0.053	0.085	0.218	0.382	0.096	0.124	0.194	0.265
931	271.7	155.0	0.579	0.058	0.097	0.221	0.339	0.115	0.171	0.232	0.294
932	406.5	180.0	0.443	0.051	0.076	0.204	0.327	0.107	0.167	0.233	0.315
934	307.3	130.1	0.423	0.059	0.076	0.211	0.335	0.089	0.128	0.185	0.244
940	344.8	122.3	0.335	0.039	0.042	0.219	0.325	0.109	0.146	0.207	0.263
942	430.8	149.1	0.346	0.051	0.055	0.269	0.409	0.115	0.168	0.255	0.347
943	313.9	132.5	0.441	0.069	0.093	0.288	0.458	0.101	0.150	0.201	0.284
944	290.0	132.3	0.456	0.069	0.083	0.242	0.356	0.098	0.138	0.195	0.253
905	354.5	168.2	0.474	0.083	0.105	0.257	0.369	0.116	0.187	0.236	0.328
906	168.0	50.1	0.476	0.062	0.113	0.226	0.329	0.106	0.131	0.165	0.219
908	209.5	95.8	0.457	0.046	0.074	0.162	0.258	0.116	0.177	0.251	0.284
909	192.5	113.6	0.590	0.068	0.108	0.252	0.328	0.099	0.149	0.211	0.288
991	220.4	98.9	0.449	0.056	0.075	0.215	0.341	0.056	0.084	0.123	0.162
992	463.5	175.7	0.379	0.039	0.045	0.192	0.322	0.102	0.148	0.212	0.295
994	404.3	165.4	0.407	0.068	0.084	0.273	0.388	0.118	0.170	0.243	0.359
996	423.2	197.2	0.466	0.048	0.089	0.251	0.366	0.122	0.175	0.253	0.349
984	317.7	126.4	0.398	0.043	0.064	0.178	0.299	0.114	0.163	0.251	0.335
950	325.5	127.1	0.390	0.054	0.062	0.270	0.382	0.091	0.143	0.206	0.272
952	403.5	145.3	0.360	0.041	0.049	0.248	0.398	0.106	0.194	0.229	0.309
954	367.1	164.2	0.447	0.068	0.081	0.264	0.365	0.109	0.173	0.247	0.339
970	86.5	45.1	0.521	0.059	0.099	0.195	0.278	0.093	0.144	0.216	0.299
972	152.9	74.1	0.488	0.061	0.099	0.225	0.317	0.117	0.183	0.251	0.338
973	354.9	171.4	0.483	0.059	0.089	0.245	0.354	0.109	0.159	0.231	0.301
929	191.7	81.8	0.427	0.061	0.099	0.220	0.309	0.119	0.155	0.211	0.295
931	294.6	131.4	0.446	0.054	0.080	0.246	0.349	0.118	0.179	0.259	0.321
933	86.2	48.2	0.559	0.083	0.130	0.192	0.274	0.109	0.165	0.227	0.301
936	60.3	42.2	0.700	0.076	0.118	0.187	0.269	0.096	0.148	0.203	0.286

Fig. 2.3.4.1 Biomass ratio (Dry/Wet) versus R5 (r=0.90)

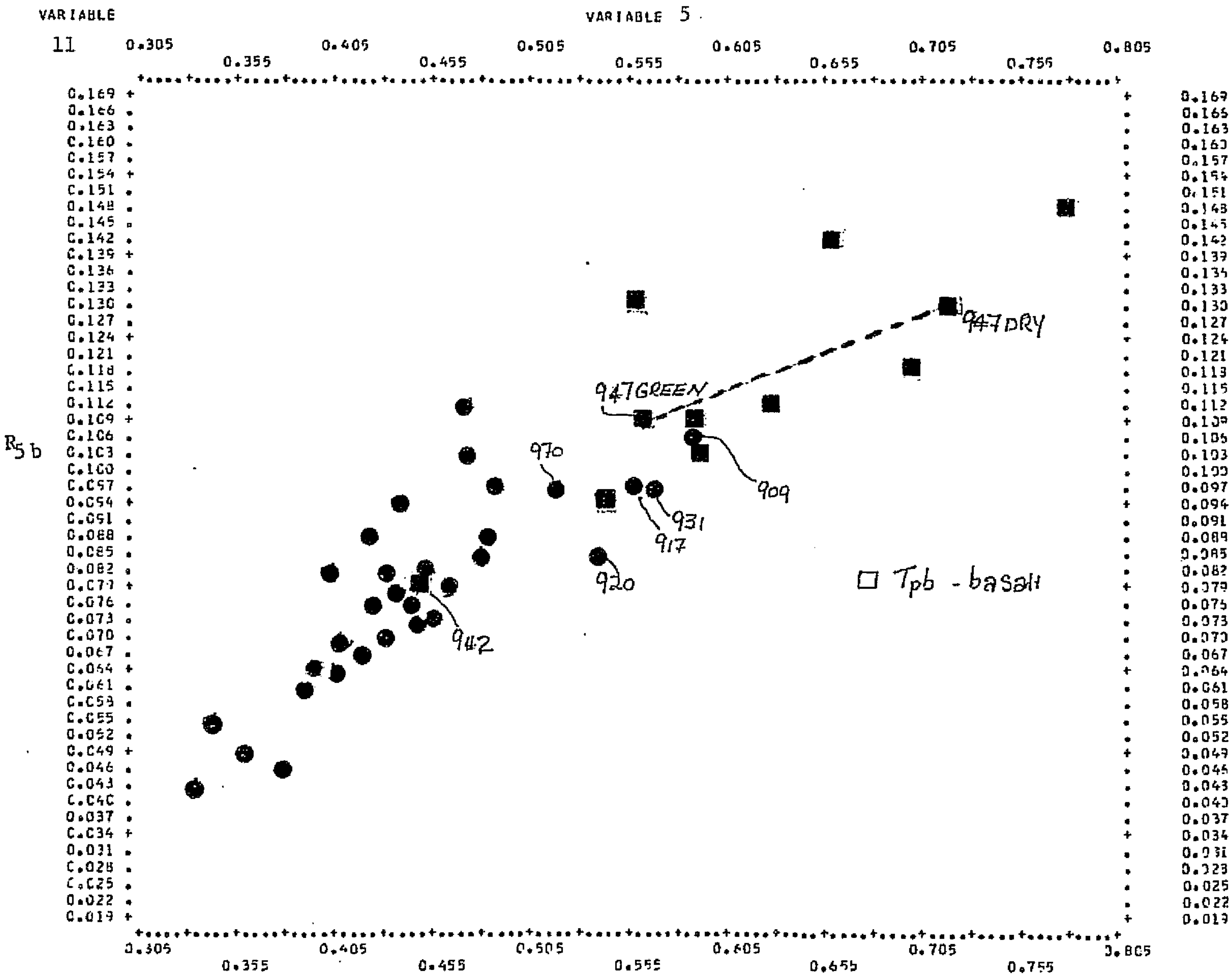

Fig. 2.3.4.2 Wet weight versus CH 5 (r=-0.77)

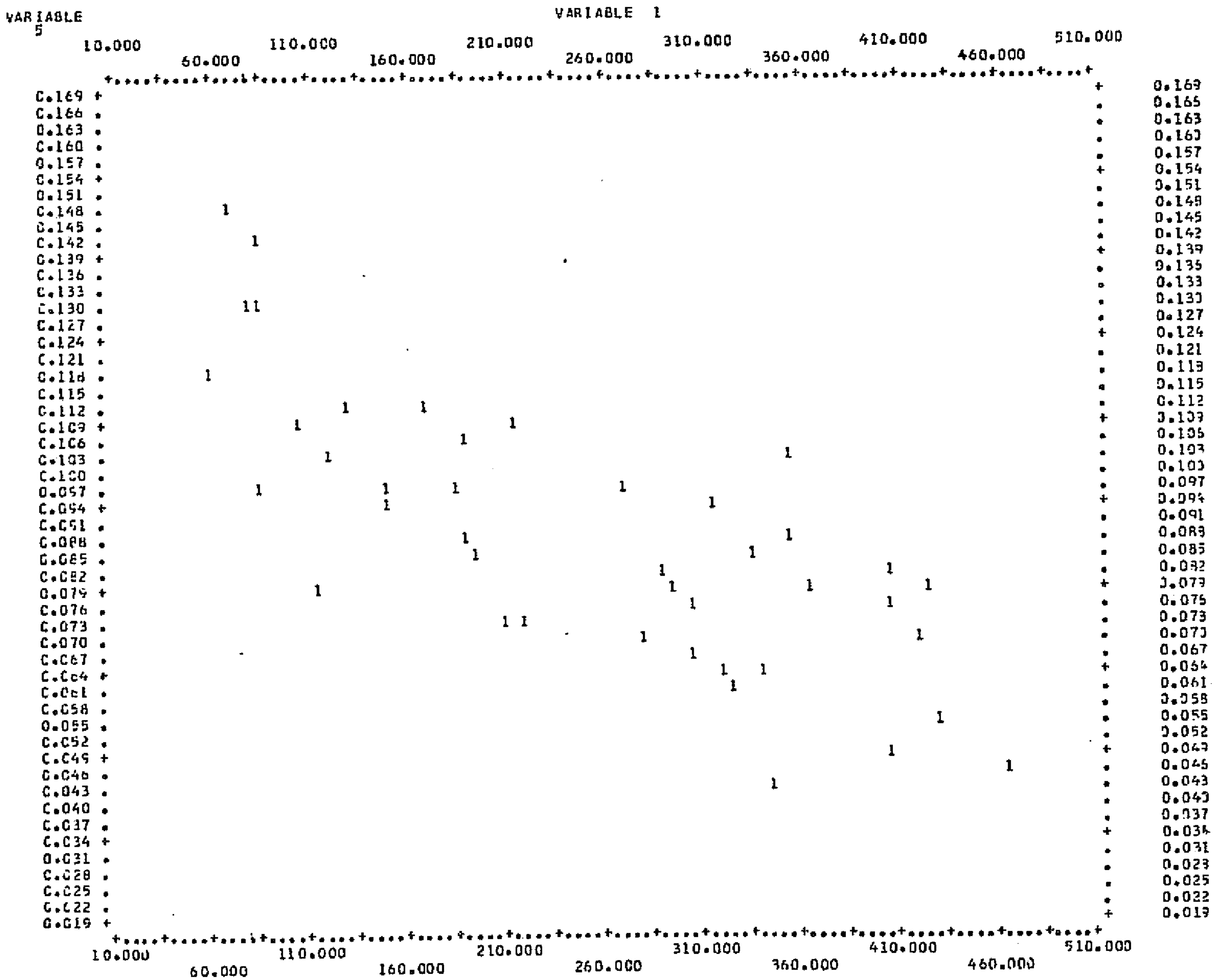

Fig. 2.3.4.3 Wet weight versus CH 7 (r=0.71)

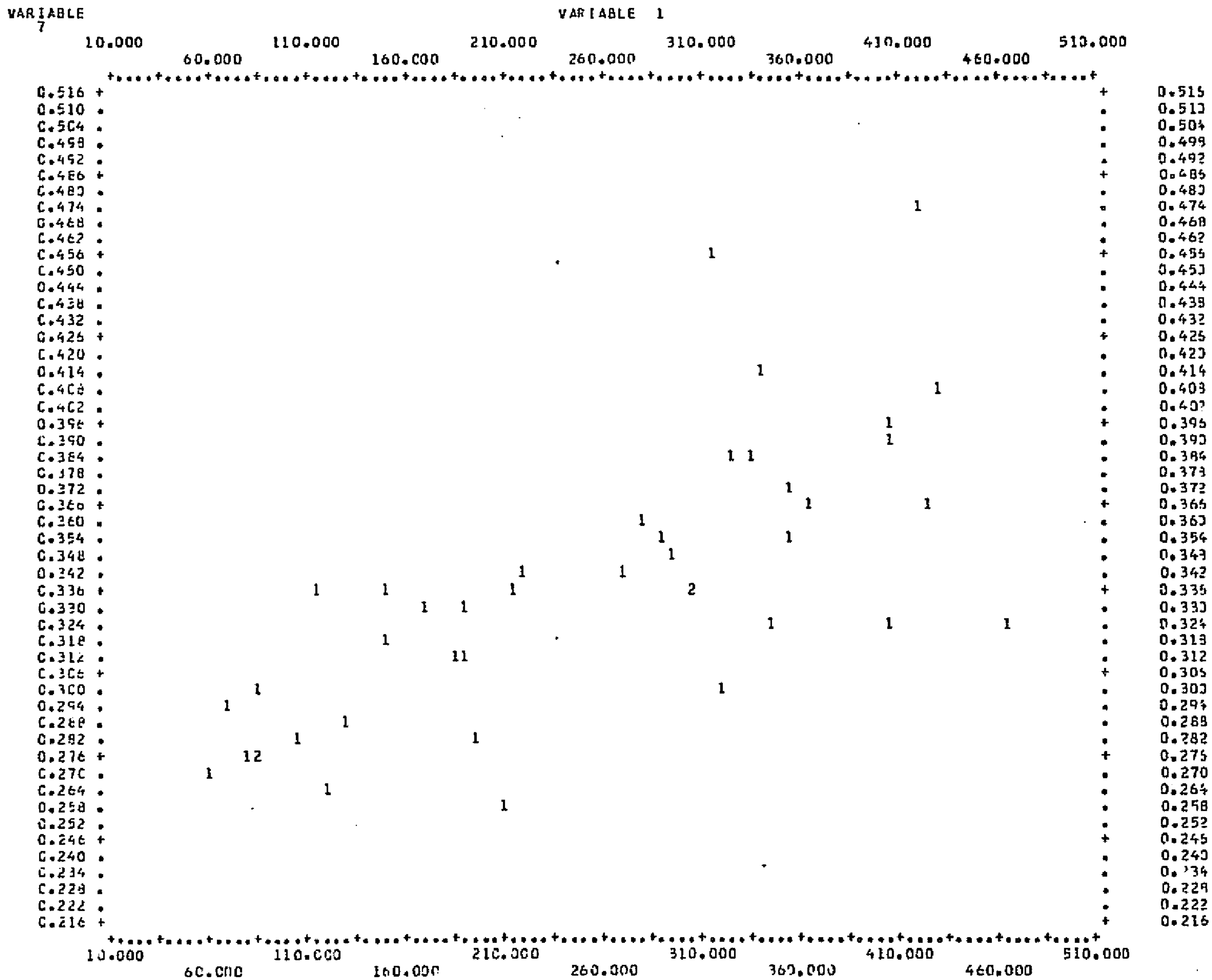

Fig. 2.3.4.4 "Deadness" (Biomass ratio, or Dry/Wet) versus R 4 (r=0.70)

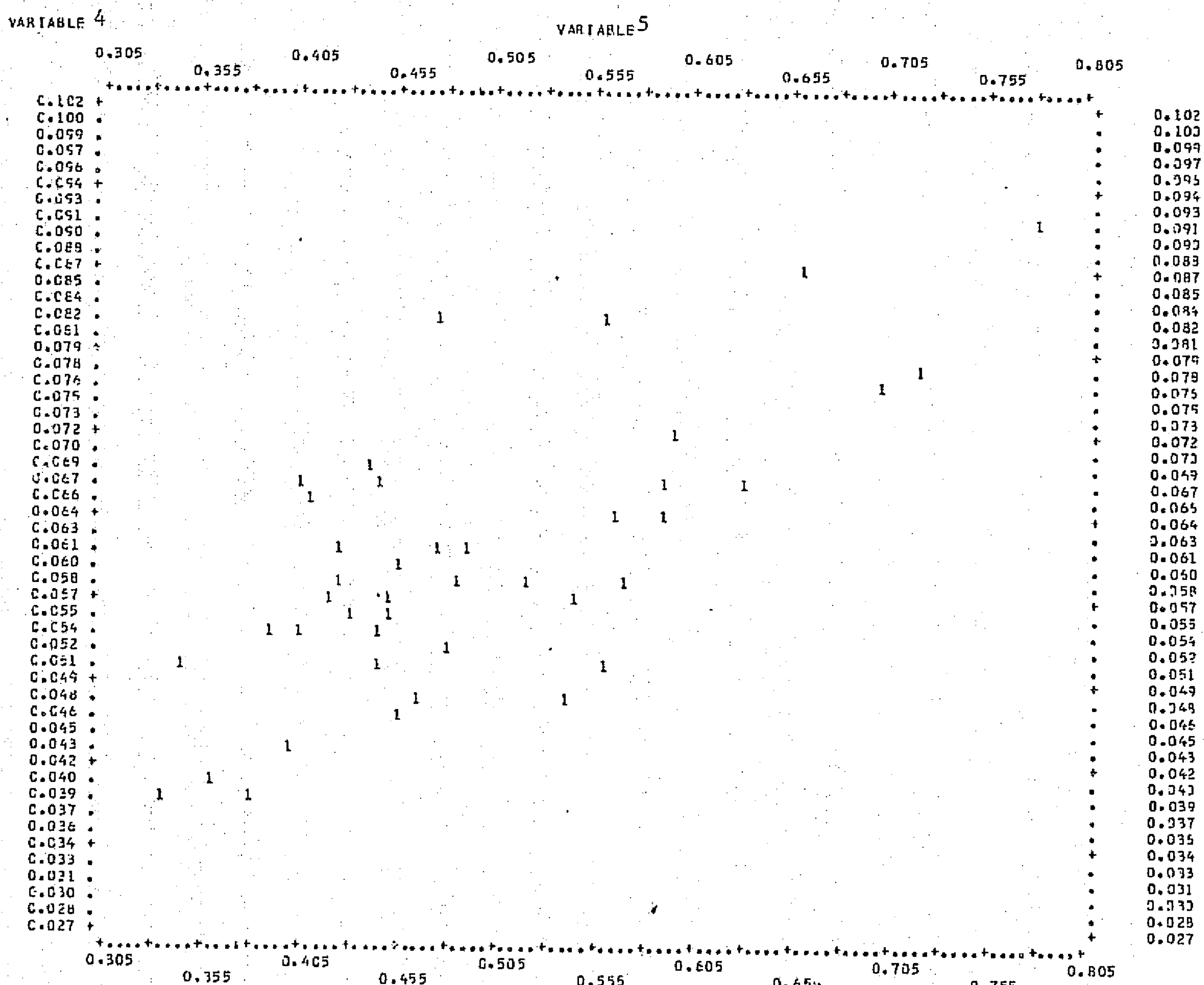

Fig. 2.3.4.5 Dead weight (Biomass) versus R 5 (r=-0.62)

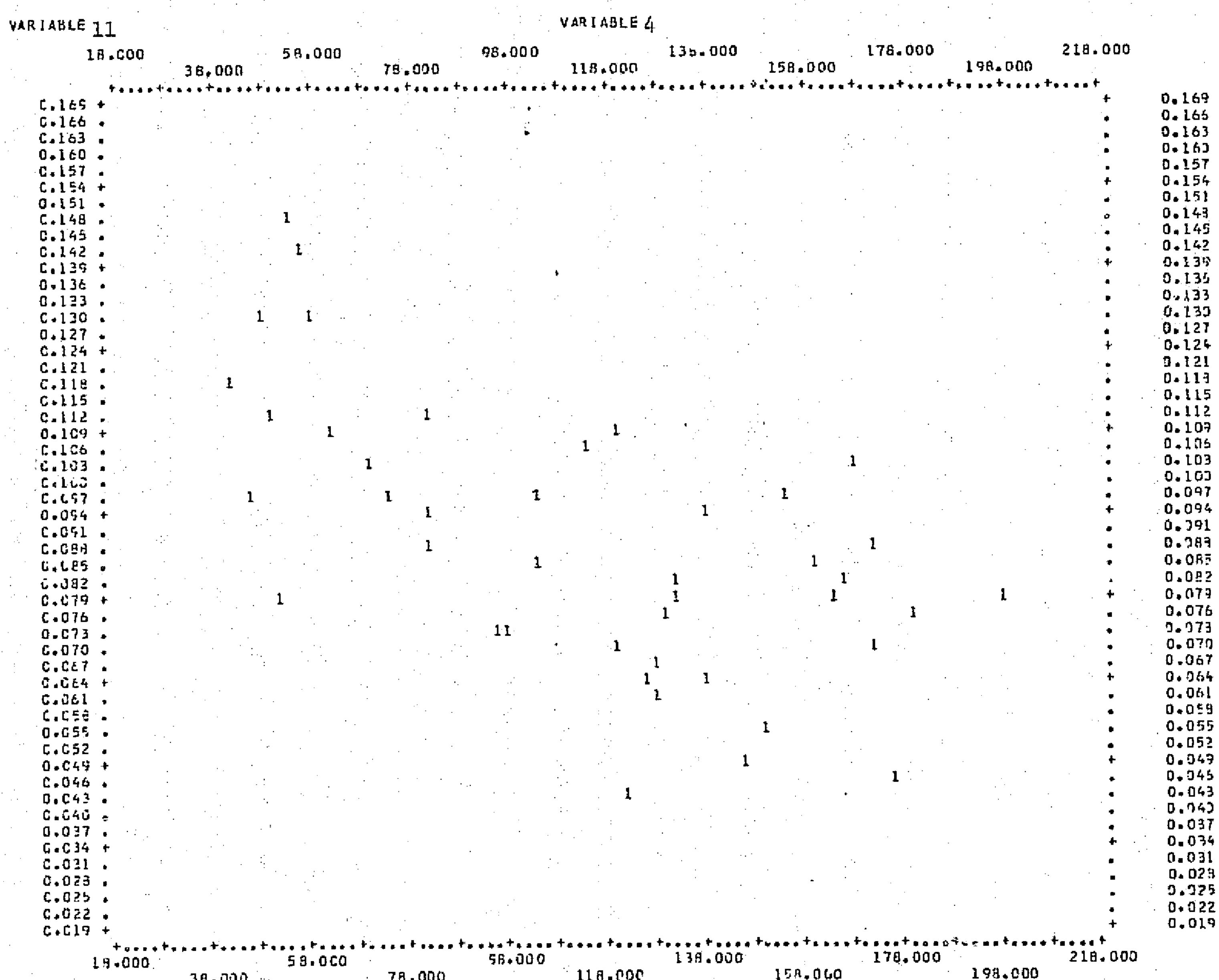

2.3.4.2.3 Data Set 2 (9 Variables)

The data set after normalization to Channel 4 (for reduction of lighting effects and preliminary atmospheric correction. (See Table 2.3.4.6)

TABLE 2.3.4.6 BI-DIRECTIONAL REFLECTANCE DATA NORMALIZED TO CHANNEL 4

Variable 1 = total wet weight grass in 0.25 m^2

Variable 2 = total dry weight grass in 0.25 m^2

Variable 3 = ratio dry weight/wet weight

Variable 4 = reflectance channel 5/4 before cutting

Variable 5 = reflectance channel 6/4 before cutting

Variable 6 = reflectance channel 7/4 before cutting

Variable 7 = reflectance channel 5/4 after cutting

Variable 8 = reflectance channel 6/4 after cutting

Variable 9 = reflectance channel 7/4 after cutting

TABLE 2.3.4.6 cont. Preceding Set Normalized to Channel 4

VARIABLES

ID	WET	DRY	D/W	R5/4B	R6/4B	R7/4B	R5/4A	R6/4A	R7/4A
	1	2	3	4	5	6	7	8	9
942	117.3	52.8	0.450	1.388	4.202	5.894	1.419	2.191	2.922
941	105.0	62.8	0.590	1.717	3.242	4.364	1.523	2.294	3.039
947	213.2	120.0	0.563	1.704	3.679	5.179	1.453	1.954	2.502
947	79.7	57.3	0.719	1.666	2.631	3.551	1.456	1.999	2.536
949	119.3	71.0	0.595	1.466	3.937	3.690	1.472	2.069	2.793
951	150.0	81.9	0.546	1.615	4.020	5.849	1.417	2.034	2.565
953	131.1	82.7	0.631	1.708	3.071	4.290	1.531	2.165	2.899
954	83.9	55.5	0.662	1.636	2.642	3.446	1.413	1.897	2.379
955	70.1	54.6	0.779	1.639	2.335	3.249	1.426	1.998	2.509
980	342.4	138.4	0.404	1.193	4.471	7.635	1.461	2.201	3.074
982	421.8	173.0	0.410	1.067	4.406	7.131	1.389	1.958	2.581
914	282.5	121.9	0.428	1.265	4.691	6.543	1.492	2.099	2.662
916	306.4	128.2	0.418	1.192	4.313	5.932	1.457	2.195	2.759
917	184.6	103.2	0.559	1.929	3.925	6.196	1.486	2.191	2.978
920	193.9	104.6	0.539	1.779	3.897	5.953	1.542	2.179	2.912
930	333.7	159.0	0.479	1.593	4.096	7.194	1.293	1.916	2.753
931	271.7	155.0	0.570	1.666	3.778	5.996	1.471	1.992	2.525
932	406.5	180.0	0.443	1.499	4.019	6.438	1.551	2.373	2.934
934	307.3	130.1	0.423	1.298	3.696	5.723	1.449	2.096	2.759
940	344.8	122.3	0.355	1.072	5.398	8.372	1.358	1.999	2.419
942	430.[illegible]	149.1	0.346	1.070	5.229	7.951	1.479	2.222	3.026
943	313.9	138.5	0.441	1.352	4.102	6.670	1.491	1.982	2.902
944	290.0	132.3	0.456	1.381	4.054	5.955	1.409	1.996	2.641
995	354.5	168.2	0.474	1.266	3.112	4.473	1.611	2.035	2.922
996	168.0	59.2	0.476	2.823	3.634	5.299	1.239	-1.553	3.077
998	209.5	95.8	0.457	1.622	3.531	5.638	1.519	2.154	2.438
999	192.5	113.6	0.590	1.579	3.679	4.796	1.516	2.139	2.921
991	220.4	98.9	0.449	1.341	3.849	6.113	1.599	2.299	2.997
992	463.5	175.7	0.379	1.158	4.922	8.255	1.449	2.067	2.880
994	404.3	165.4	0.407	1.234	4.016	5.713	1.482	2.195	2.955
996	423.2	197.2	0.466	1.081	5.265	7.665	1.442	2.081	2.797
984	317.7	126.4	0.398	1.499	4.156	7.092	1.438	2.232	2.952
959	325.[illegible]	127.1	0.399	1.152	4.995	7.075	1.562	2.350	2.974
952	403.[illegible]	165.3	0.360	1.186	6.056	9.686	1.550	2.091	2.839
954	367.1	164.2	0.447	1.186	3.853	5.337	1.586	2.262	3.024
970	86.5	45.1	0.521	1.000	3.273	4.681	1.543	2.311	3.299
972	152.0	74.1	0.488	1.617	3.659	5.161	1.567	2.146	2.896
973	354.9	171.4	0.483	1.500	4.135	5.975	1.456	2.112	2.756
929	191.7	81.8	0.427	1.479	3.628	5.109	1.549	2.194	2.843
931	294.6	131.4	0.446	1.483	4.543	6.467	1.517	2.054	2.723
933	86.2	48.2	0.559	1.560	2.398	3.295	1.515	2.083	2.758
936	60.3	42.2	0.700	1.552	2.462	3.542	1.531	2.110	2.968

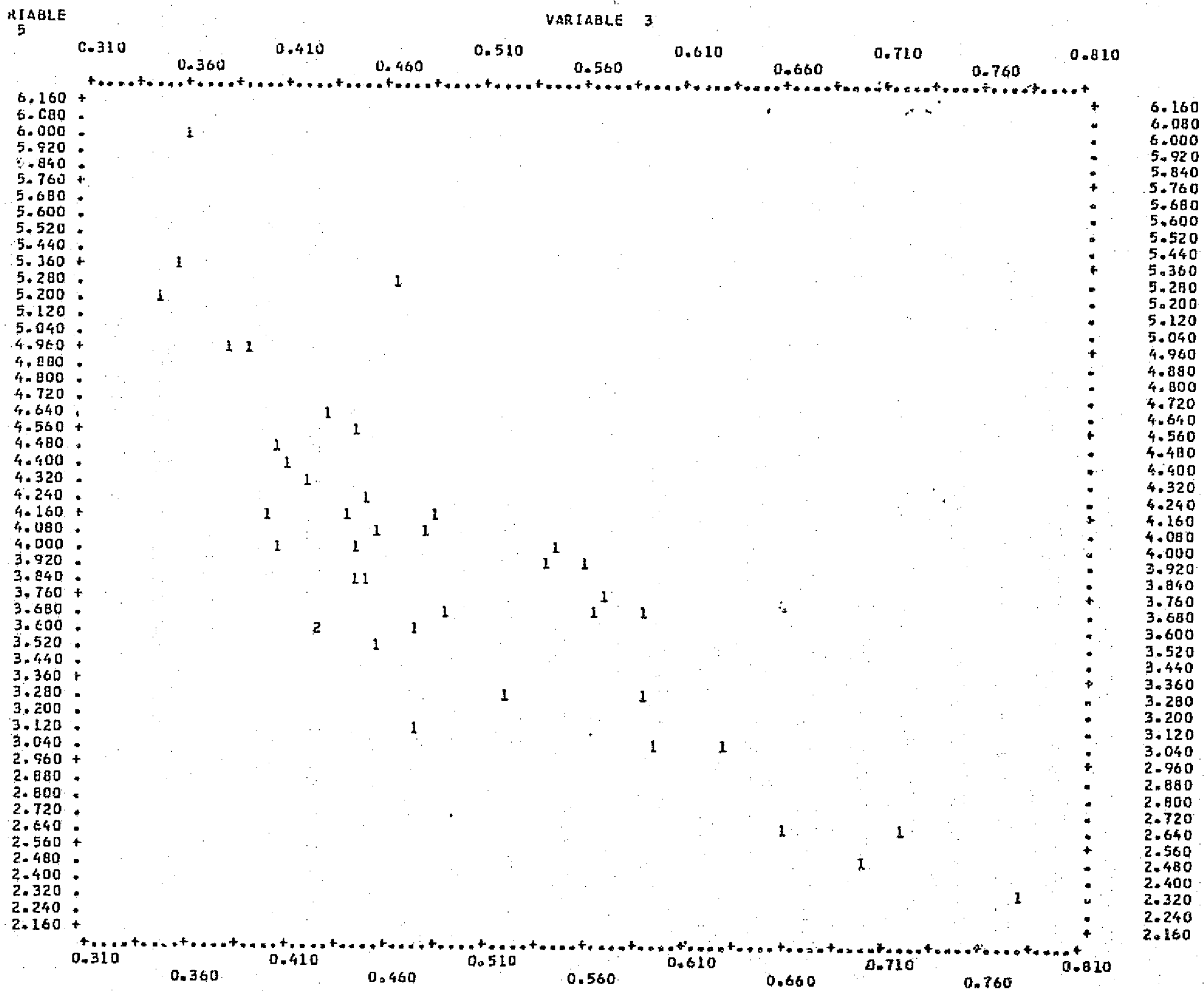

2.3.4.6 "Deadness" versus R 64 (r=-.81)

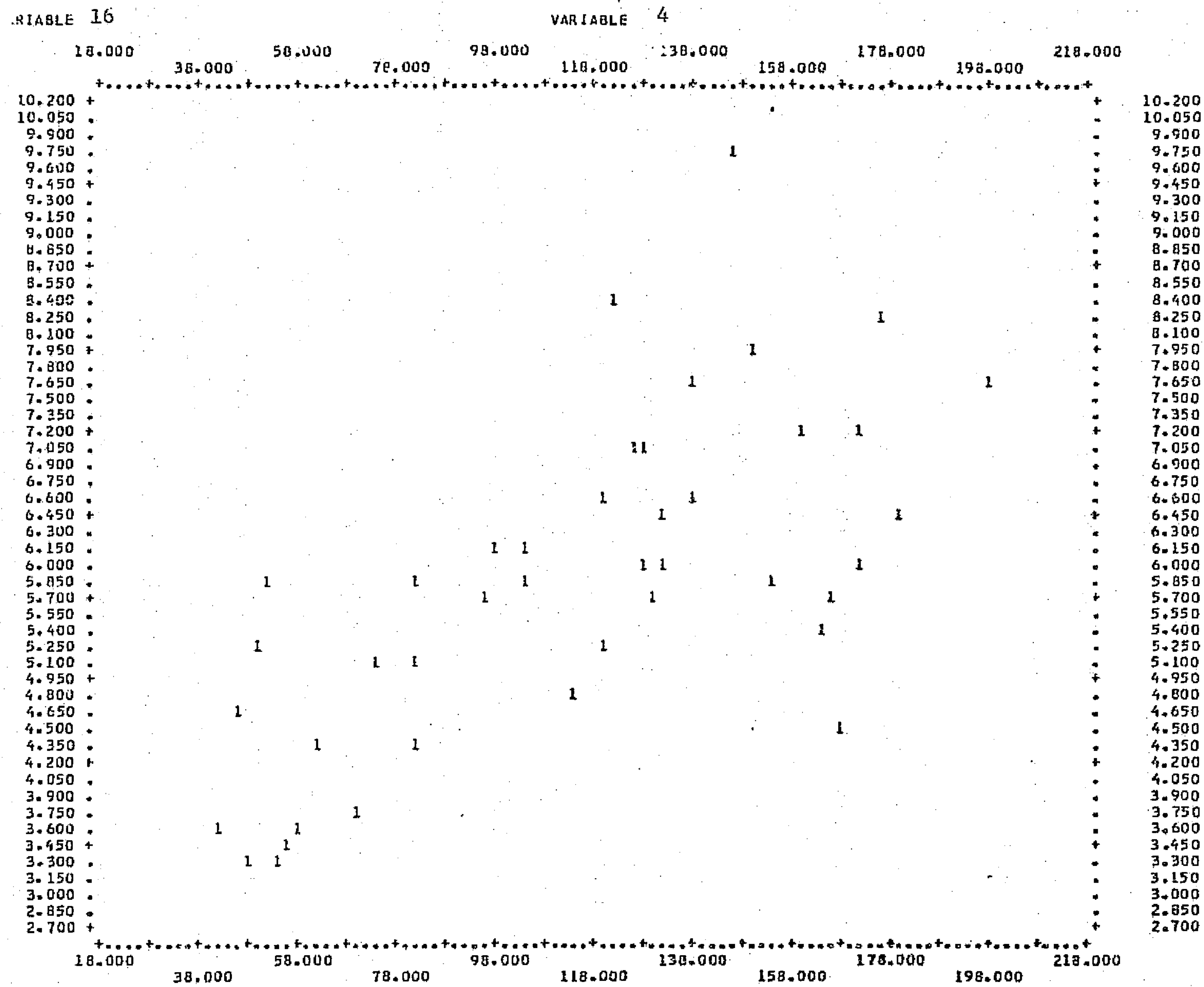

2.3.4.7 Dead weight (Biomass) versus R 74 (r=.68)

2.3.4.2.4 Data Set 3; Original set; plus biomass, plus species and soil types (see Table 2.3.4.7)

TABLE 2.3.4.7 BI-DIRECTIONAL REFLECTANCE, CHANNEL BRIGHTNESS, BIOMASS DATA, ETC.

VARIABLE	LINE NO.	DESCRIPTION
1.	2 1	Pseudo-C.I.E. coordinates "RASNX"
2.	2 2	Pseudo-C.I.E. coordinates "RASNY"
3.	2 3	Wet weight of grass/0.25 m^2
4.	2 4	Dry weight of grass/0.25 m^2
5.	2 5	Biomass ratio= "deadness" = D/W (3/4)
6.	3 2	CH 4 radiance(w/ cm^2 /bandpass ERTS filter)
7.	3 3	CH 5 " "
8.	3 4	CH 6 " "
9.	3 5	CH 7 " "
10.	3 6	Reflectance R 4
11.	3 7	R 5
12.	3 8	R 6
13.	3 9	R 7
14.	4 1	Ratio R7/R6
15.	4 2	R7/R5
16.	4 3	R7/R4
17.	4 4	R6/R5
18.	4 5	R6/R4
19.	4 6	R5/R4
20.	5 6	Moisture percentage,Nov 1973
21.	5 7	Dip of slope,degrees
22.	5 8	Azimuth of slope ,degrees from north
23.	5 9	Altitude,feet/sea level
24.	6 2	Species count,percent, of soft chess(Bromus mollis)
25.	6 3	Ryegrass(Lolium multiflorum)
26.	6 4	Wall barley(Hordeum hystrix)
27.	6 5	Foxtail barley(H. leporinum)
28.	6 6	Slender wild oat(Avena barbata)
29.	6 7	Ripgut grass(Bromus rigidis)
30.	6 8	Morning Glory(Convolvulus sp.)
31.	6 9	Needle (Erodium sp.)
32.	6 10	Sheep sorrel(Rumex sp.)
33.	6 11	All other broad leaved plants.

TABLE 2.3.4.7 cont.

```
1.942; 92700    1.C   0.19C   0.290   1.0   0.860   1.285   0.515   15. GRASS UP HILL TO NE MW
2. ;   0.180      0.226 117.3  52.8 C.450; 942,:RASNY
3.; 942 0.412 0.675 1.647 3.034 0.059 0.078 0.254 0.337
4.; 1.327 4.344 5.716 3.272 4.307 1.316
5. C-942;CSW-LTB/TPB              10YR 2/2     9.9     3.2/201SSW   468 1516569 333951
6. 942  --    10   80          --                      10
------------------------------------------------------------------
- 941;  94600    1.0   0.24C   0.470   1.0   0.820   1.167   0.515   15. GRASS NR MW TRAILER HIL
  ;   0.200      0.317 105.0  62.8 C.590; 941,:RASNY
  ; 941 0.514 1.057 1.566 2.762 0.066 0.108 0.220 0.280
  ; 1.274 2.599 4.232 2.041 3.322 1.628
  C-941;CLR-LTB/TPB              (10YR 2/2)   (9.8)   4.0/200SSW   476 1516596 334078
  941  80   10   --         10                        --
------------------------------------------------------------------
  947; 100000    1.0   0.25C   0.480   1.0   0.985   1.505   0.515   15. GREEN GRASS SITE 4
  ;    0.180      0.281 213.2 12C.0 C.563; 947,:RASNY
  ; 947 0.534 1.078 1.900 3.541 0.067 0.108 0.252 0.336
  ; 1.335 3.109 5.022 2.328 3.761 1.615
  C-947;CLR-LTB/TPB               5YR 3/2     11.2     4.1/095 E    480 1516321 333739
  947  10   20   --   60   --                         10
------------------------------------------------------------------
  947; 101000    1.0   0.350   0.665   1.0   0.937   1.337   0.515   15. VERY DRY ADJ PATCH 4DRY
  ;    0.224      0.345  79.7  57.3 C.713; 947,:RASNY
  ; 947 0.736 1.471 1.803 3.154 0.080 0.127 0.217 0.277
  ; 1.277 2.18C 3.443 1.7C7 2.697 1.579
  C-947;CLR-LTB/TPB               5YR 3/2     11.2     4.1/095 E    480 1516321 333739
  947  10   50   20         --                        20
------------------------------------------------------------------
  949; 102200    1.0   0.30C   0.500   1.0   0.940   1.220   0.515   15. SITE 6 NR OAK TREESNW
  ;    0.227      0.309 119.3  71.0 C.595; 949,:RASNY
  ; 949 0.635 1.120 1.809 2.885 0.C74 0.102 0.229 0.263
  ; 1.150 2.574 3.578 2.239 3.112 1.390
  C-949;CLR-LTB/TPB              10YR 2/2     17.2     5.2/C94 E    493 1516128 333642
  949  70   20   --         --                        10
------------------------------------------------------------------
  951; 103400    1.0   0.26C   0.475   1.0   1.060   1.650   0.515   15. SHORT GRASS NR OCT FNCE
  ;    0.178      0.264 150.C  81.9 0.546; 951,:RASNY
  ; 951 0.554 1.067 2.052 3.875 0.059 0.090 0.243 0.334
  ; 1.377 3.703 5.672 2.65C 4.120 1.532
  D-951;CLR-LTB/TPB              10YR 3/2     10.9     3.6/076 E    512 1515877 333482
  951   5    5   5C         --                        --
------------------------------------------------------------------
  953; 104900    1.C   0.310   0.6C0   1.0   0.960   1.428   0.515   15. GRASS SITE 8 SHRT BLKTI
  ;    0.205      0.322 131.1  82.7 C.631; 953,:RASNY
  ; 953 0.655 1.333 1.850 3.364 0.C69 0.112 0.217 0.286
  ; 1.319 2.562 4.151 1.943 3.147 1.620
  D-953;CLR-LTB/TPB              (10YR 2/2)   (9.8)   4.8/074 E    523 1515690 333295
  953  70   20   --         10                        --
------------------------------------------------------------------
  954; 110000    1.0   0.41C   0.747   1.0   1.090   1.510   0.515   15. GS SITE 9 CRX RD GRY F
  ;    0.23C      0.341  83.9  55.5 C.662; 954,:RASNY
```

TABLE 2.3.4.7 cont.

```
; 954 0.857 1.645 2.113 3.553 0.090 0.139 0.242 0.299
; 1.234 2.154 3.342 1.745 2.707 1.551
D-954;CLR-LTB/TPB            (10YR 2/2)   (9.8)    2.3/135SE    516 1515557 333097
954   5    --  95          --                         --
----------------------------------------------------------------------------
955; 111000   1.0   0.450   0.830   1.0   1.070   1.537   0.515   15. SITE 10 HLF TO TOP DEAD
 ;   0.236      0.354  70.1  54.6 0.779; 955,:RASNY
; 955 0.938 1.821 2.073 3.615 0.094 0.147 0.207 0.293
; 1.413 1.950 3.119 1.408 2.207 1.568
D-955;CLR-LTB/TPB             10YR 2/2     13.9    3.6/080 E    519 1515464 332941
955  40    5   40          --                         15
----------------------------------------------------------------------------
980; 112500   1.0   0.260   0.340   1.0   1.195   2.105   0.515   15. SITE 11 ACROSS Y FORK
 ;   0.164      0.179 342.4 138.4 0.404; 980,:RASNY
; 980 0.554 0.781 2.326 4.924 0.056 0.064 0.236 0.409
; 1.733 6.421 7.327 3.704 4.227 1.141
G-980;SLR-DAE/TUS              5Y  5/1      8.3    3.2/288SW    483 1514382 332563
980  95    5   --          --                         --
----------------------------------------------------------------------------
982; 114000   1.0   0.320   0.375   1.0   1.450   2.510   0.515   15. SITE 12 TO W OF 11 GREE
 ;   0.170      0.166 421.8 173.0 0.410; 982,:RASNY
; 982 0.675 0.855 2.843 5.857 0.068 0.070 0.285 0.468
; 1.644 6.705 6.846 4.079 4.165 1.021
G-982;SLR-DAE/TUS              5Y  4/1     15.1   11.3/307NWW   498 1514296 332406
982  20   15   60          --           05            --
----------------------------------------------------------------------------
914;  93000   1.0   0.190   0.270   1.0   0.980   1.540   0.516   15. GRASS PH#2
 ;   0.163      0.193 282.5 121.0 0.428; 914,:RASNY
; 914 0.412 0.632 1.890 3.622 0.052 0.068 0.267 0.359
; 1.346 5.288 6.873 3.930 5.108 1.300
J-914;CLR-AVD/QSC             10YR 5/4      6.9    4.5/194 S    368 1512779 329482
914  30   20   40           5                         05
----------------------------------------------------------------------------
916;  95000   1.0   0.210   0.275   1.0   1.000   1.495   0.516   15. GRASS PH #4
 ;   0.179      0.196 306.4 128.2 0.418; 916,:RASNY
; 916 0.453 0.643 1.931 3.518 0.059 0.066 0.259 0.337
; 1.301 5.091 5.752 3.912 4.420 1.130
J-916;CLR-AVD/QSC             10YR 4/2      6.9    9.5/141SE    370 1513081 329558
916  30   10   30          30                         --
----------------------------------------------------------------------------
917; 101000   1.0   0.190   0.415   1.0   0.820   1.370   0.516   15. GRASS PH #6
 ;   0.159      0.280 184.6 103.2 0.559; 917,:RASNY
; 917 0.412 0.940 1.566 3.230 0.052 0.095 0.210 0.313
; 1.494 3.300 6.008 2.209 4.023 1.821
J-917;CLR-AVD/QSC             10YR 4/2      6.9    9.5/141SE    370 1513081 329558
917  60   20   --          10           5             05
----------------------------------------------------------------------------
920; 101850   1.0   0.210   0.420   1.0   0.880   1.400   0.516   15. GRASS PH# 8
 ;   0.170      0.275 193.9 104.6 0.539; 920,:RASNY
; 920 0.453 0.951 1.687 3.299 0.049 0.083 0.197 0.280
; 1.421 3.382 5.676 2.379 3.993 1.678
J-920;CLR-AVD/QSC             10YR 5/4      7.9   10. /130SE    340 1513606 329426
920  10   70   --          10                         10
----------------------------------------------------------------------------
930; 102800   1.0   0.220   0.380   1.0   1.395   1.850   0.516   15. GRASS PH#10 AT T FELT L
 ;   0.153      0.216 333.7 160.0 0.479; 930,:RASNY
; 930 0.473 0.866 2.123 4.336 0.052 0.082 0.249 0.382
; 1.533 4.642 7.303 3.028 4.764 1.573
K-930;CSW-AVD/QSC             10YR 5/2      9.2    5.7/123SE    368 1512606 329331
930   5   30   60          --                          5
```

TABLE 2.3.4.7 cont.

```
-------------------------------------------------------------------------
931; 104200   1.0   0.250   0.470   1.0   1.000   1.670   0.516   15. GRASS PH# 12 TO LAKE
 ;   0.171      0.262 271.7 155.0 0.570; 931,:RASNY
; 931 0.534 1.057 1.931 3.921 0.060 0.095 0.233 0.338
; 1.454 3.564 5.630 2.452 3.872 1.579
K-931;CLR-AVD/QSC                    10YR 5/4     7.8     3.8/190 S    397 1512327 329278
931  10   30   40   10   10                            --
-------------------------------------------------------------------------
932; 105700   1.0   0.225   0.370   1.0   0.960   1.637   0.516   15. GRASS PH# 14
 ;   0.169      0.227 406.5 180.0 0.443; 932,:RASNY
; 932 0.483 0.845 1.850 3.845 0.052 0.074 0.214 0.326
; 1.519 4.419 6.243 2.909 4.109 1.413
K-932;CLR-AVD/QSC                    10YR 4/2     8.6     5. /044NE    393 1512066 329231
932  25   25   --        40          5    5            --
-------------------------------------------------------------------------
934; 111400   1.0   0.260   0.370   1.0   0.980   1.605   0.516   15. GRASS PH# 16
 ;   0.191      0.224 307.3 130.1 0.423; 934,:RASNY
; 934 0.554 0.845 1.890 3.772 0.060 0.074 0.223 0.334
; 1.502 4.509 5.550 3.002 3.696 1.231
K-934;CLR-AVD/QSC                    10YR 4/2     8.6     1. /285NWW   400 1511816 329245
934  40   40   --        20                            --
-------------------------------------------------------------------------
940; 113100   1.0   0.180   0.205   1.0   1.017   1.680   0.516   15. GRASS AT LAKE PH#18-TRK5
 ;   0.154      0.150 344.8 122.3 0.355; 940,:RASNY
; 940 0.392 0.494 1.965 3.944 0.040 0.041 0.221 0.324
; 1.467 7.988 8.118 5.443 5.532 1.016
M-940;CLR-AVD/QSC                     5Y  5/1    (7.1)    4.1/312NW    404 1510937 328267
940  --   40   30        20                            10
-------------------------------------------------------------------------
942; 114000   1.0   0.240   0.284   1.0   1.320   2.160   0.516   15. GRASS PH# 1 NEW ROLE
 ;   0.156      0.155 430.8 149.1 0.346; 942,:RASNY
; 942 0.514 0.662 2.580 5.050 0.053 0.054 0.262 0.404
; 1.544 7.456 7.634 4.828 4.944 1.024
M-942;CLR-AVD/QSC                     5Y  5/1    (7.1)    4.1/312NW    404 1510937 328267
942  30   30   20   20   --                            --
-------------------------------------------------------------------------
943; 120400   1.0   0.340   0.513   1.0   1.460   2.460   0.516   15. GS VRY WNDY PH 4
 ;   0.171      0.212 313.9 138.5 0.441; 943,:RASNY
; 943 0.716 1.148 2.864 5.742 0.071 0.091 0.280 0.453
; 1.618 4.951 6.405 3.059 3.958 1.294
M-943;CLR-AVD/QSC                    10YR 4/2    (8.2)    2.5/316NW    423 1511102 328403
943  30   30   30        --                            10
-------------------------------------------------------------------------
944; 121700   1.0   0.305   0.467   1.0   1.270   1.960   0.516   15. GRASS PH# 6 WINDY
 ;   0.183      0.230 290.0 132.3 0.456; 944,:RASNY
; 944 0.645 1.050 2.478 4.590 0.061 0.081 0.235 0.352
; 1.494 4.331 5.720 2.900 3.829 1.321
M-944;CLR-AVD/QSC                    10YR 4/2    (8.2)    2.5/316NW    423 1511102 328403
944  20   40   --        40                            --
-------------------------------------------------------------------------
905;  93500   1.0   0.280   0.390   1.0   0.900   1.340   0.521   15. PH# 7 NO WIND DAY 3
 ;   0.220      0.253 354.5 168.2 0.474; 905,:RASNY
; 905 0.594 0.887 1.728 3.161 0.085 0.102 0.271 0.368
; 1.360 3.613 4.337 2.657 3.190 1.200
I-905;CLR-DAE/TM                      7YR 4/1    10.4     0.5/190 S    473 1513772 330962
905  50   40   --    5    5                            --
-------------------------------------------------------------------------
906;  94800   1.0   0.230   0.480   1.0   0.880   1.340   0.521   15. SPARSE GS PH# 9 + SOIL
 ;   0.180      0.303 168.0  50.2 0.476; 906,:RASNY
; 906 0.493 1.078 1.697 3.161 0.064 0.111 0.238 0.328
```

TABLE 2.3.4.7 cont.

```
; 1.377 2.966 5.128 2.154 3.724 1.729
I-906;CLR-DAF/TM                  5Y  5/1    10.4    6.5/205SSW  466 1513719 330783
906  50   40   --          10                        --
-----------------------------------------------------------------
908; 100200   1.0   0.170   0.310   1.0   0.660   1.080   0.521   15. PH# 12 HILL SLOPNG W
 ;   0.179        0.266 209.5  95.8 0.457; 908,:RASNY
; 908 0.372 0.717 1.241 2.562 0.047 0.072 0.170 0.257
; 1.510 3.553 5.467 2.352 3.619 1.539
I-908;CLR-DAE/TM                10YR 5/2     8.7    0.5/204SSW  435 1513610 330562
908  20   30   --          50                        --
-----------------------------------------------------------------
909; 101600   1.0   0.250   0.450   1.0   0.950   1.315   0.521   15. PH# 14 LAST BFR FRWY
 ;   0.197        0.288 192.5 113.6 0.590; 909,:RASNY
; 909 0.534 1.014 1.829 3.103 0.070 0.105 0.265 0.326
; 1.231 3.099 4.641 2.517 3.770 1.498
I-909;CLR-AVD/QSC               10YR 6/2     8.3    13. /207SSW  405 1513456 330400
909  45   45   --          --              10        --
-----------------------------------------------------------------
991; 103300   1.0   0.240   0.360   1.0   0.990   1.590   0.521   15. ACRX DIRT RD PH 16
 ;   0.182        0.224 220.4  98.9 0.449; 991,:RASNY
; 991 0.514 0.823 1.910 3.737 0.057 0.074 0.209 0.336
; 1.609 4.563 5.862 2.836 3.642 1.284
H-991;SLR-DAE/TUS               10YR 4/2     7.9    4.7/104SFE  452 1514096 331612
991  30   20   35          5           5             5
-----------------------------------------------------------------
992; 104800   1.0   0.140   0.160   1.0   0.840   1.330   0.521   15. VRY GRN VALLEY PH# 18
 ;   0.153        0.151 463.5 175.7 0.379; 992,:RASNY
; 992 0.311 0.399 1.606 3.138 0.040 0.045 0.197 0.317
; 1.608 7.113 7.905 4.424 4.917 1.111
H-992;CSW-DAE/TUS               10YR 3/2     9.3    8. /056 E    445 1514058 331451
992  25   50   --    25   --                         --
-----------------------------------------------------------------
994; 110400   1.0   0.300   0.410   1.0   1.270   1.910   0.521   15. PH 20 CLR SKY UP HILL
 ;   0.189        0.213 404.3 165.4 0.407; 994,:RASNY
; 994 0.635 0.929 2.478 4.474 0.070 0.083 0.266 0.426
; 1.601 5.145 6.082 3.214 3.800 1.182
H-994;SLR-DAE/TUS                 5Y  5/1    10.1    4.1/061NFE  467 1513964 331246
994  30   60   10          --                        --
-----------------------------------------------------------------
996; 111700   1.0   0.220   0.420   1.0   1.230   1.865   0.521   15. PH 1 CLR SKY SHRT OF DR
 ;   0.149        0.231 423.2 197.2 0.466; 996,:RASNY
; 996 0.473 0.951 2.397 4.371 0.049 0.079 0.244 0.361
; 1.478 4.574 7.357 3.095 4.978 1.608
H-996;CLR-DAE/TM                  5Y  5/1    11.2    7.1/074NFE  477 1513839 331103
996  10   30   --    50   --                         --
-----------------------------------------------------------------
984; 115500   1.0   0.200   0.330   1.0   0.880   1.410   0.521   15. PH 4
 ;   0.172        0.233 317.7 126.4 0.398; 984,:RASNY
; 984 0.433 0.760 1.687 3.322 0.044 0.063 0.173 0.295
; 1.709 4.681 6.716 2.739 3.930 1.435
G-984;SLP-DAE/TUS               10YR 4/2     5.8    9.5/237SWW  480 1514242 332134
984  30   60   --          --   05                   5
-----------------------------------------------------------------
950;  53200   1.0   0.160   0.200   1.0   0.870   1.300   0.522   15. GREEN AT LAKE TRK 6 PH6
 ;   0.167        0.177 325.5 127.1 0.390; 950,:RASNY
; 950 0.352 0.484 1.667 3.069 0.056 0.061 0.284 0.381
; 1.340 6.278 6.861 4.685 5.119 1.093
M-950;CLR-AVD/QSC                 5Y  5/1     7.1    4.1/312NW   404 1510937 328267
950   5    5    5          80      5                 --
-----------------------------------------------------------------
```

TABLE 2.3.4.7 cont.

```
952; 94800   1.0   0.140   0.180   1.0   0.930   1.620   0.522   15. GREEN W MRNG GLRY CRPR B
 ;   0.132     0.144 403.5 145.3 0.360; 952,:RASNY
; 952 0.311 0.441 1.789 3.806 0.042 0.048 0.262 0.397
; 1.517 8.354 9.392 5.505 6.189 1.124
M-952;CLR-AVD/QSC              5Y  5/1    7.1    4.1/312NW   404 1510937 328267
952  10   20   20        30        20            --
-----------------------------------------------------------------------------------
954; 100100   1.0   0.250   0.330   1.0   1.040   1.530   0.522   15. SEEMS DRIER PH 10
 ;   0.195     0.214 367.1 164.2 0.447; 954,:RASNY
; 954 0.534 0.760 2.012 3.599 0.070 0.079 0.278 0.364
; 1.310 4.603 5.175 3.513 3.949 1.124
M-954;CLR-AVD/QSC              10YR 4/2    8.2    2.5/316NW   423 1511102 328403
954  20   10   --        40        10      10     10
-----------------------------------------------------------------------------------
970; 102600   1.0   0.240   0.450   1.0   0.820   1.220   0.522   15. VRY SPARSE GS NR T/SCPE
 ;   0.198     0.302  86.5  45.1 0.521; 970,:RASNY
; 970 0.514 1.014 1.566 2.885 0.061 0.096 0.205 0.277
; 1.349 2.883 4.539 2.137 3.364 1.574
F-970;SLR-DAE/TUS              10YR 4/2    7.2    7.1/028NNE  475 1514202 333057
970  50   30   20        --                      --
-----------------------------------------------------------------------------------
972; 103600   1.0   0.270   0.500   1.0   1.020   1.515   0.522   15. SPARSE GS WITH CLAYS
 ;   0.189     0.284 152.0  74.1 0.488; 972,:RASNY
; 972 0.574 1.120 1.971 3.564 0.063 0.097 0.237 0.316
; 1.335 3.263 5.004 2.445 3.750 1.534
F-972;SLR-DAE/TUS              10YR 3/2   10.6   14.0/030NNE  496 1514311 332906
972  40   40   --        10                10    --
-----------------------------------------------------------------------------------
973; 105200   1.0   0.260   0.450   1.0   1.110   1.680   0.522   15. PH 1 SHRT BUNCHED OATS
 ;   0.178     0.251 354.9 171.4 0.483; 973,:RASNY
; 973 0.554 1.014 2.154 3.944 0.061 0.087 0.238 0.349
; 1.464 3.992 5.731 2.727 3.914 1.436
F-973;SLR-DAE/TUS              10YR 4/2    7.2    9.5/111SWE  486 1514450 332666
973   5   20   --        70   5                  --
-----------------------------------------------------------------------------------
929; 111300   1.0   0.275   0.470   1.0   1.045   1.540   0.522   15. NR SOLR TSCPE OFF RD
 ;   0.193     0.269 191.7  81.8 0.427; 929,:RASNY
; 929 0.584 1.057 2.022 3.622 0.062 0.088 0.214 0.306
; 1.426 3.459 4.894 2.426 3.432 1.415
B-929;SLR-GME/TBU                   /     (9.8)  14.0/175SSE  380 1516262 335158
929  20   20   10   10   30   10                 --
-----------------------------------------------------------------------------------
931; 112500   1.0   0.250   0.420   1.0   1.170   1.750   0.522   15. DOWN VALLEY BTM GRN
 ;   0.171     0.235 294.6 131.4 0.446; 931,:RASNY
; 931 0.534 0.951 2.275 4.106 0.056 0.079 0.239 0.345
; 1.444 4.372 6.206 3.027 4.298 1.420
B-931;CSW-GME/TBU               5YR 4/1   11.8   11.3/338NNW  374 1516425 334905
931  --   50   50        --                      --
-----------------------------------------------------------------------------------
933; 113800   1.0   0.385   0.685   1.0   0.910   1.320   0.522   15. JST SHRT BSLT RDGE FLOAT
 ;   0.239     0.346  86.2  48.2 0.559; 933,:RASNY
; 933 0.807 1.513 1.748 3.115 0.085 0.128 0.187 0.270
; 1.448 2.117 3.161 1.462 2.184 1.493
B-933;CLR-LTB/TPB               5YR 4/1   11.9    5.7/012NNE  444 1516454 334502
933  20   20   --        50                      10
-----------------------------------------------------------------------------------
936; 115200   1.0   0.360   0.640   1.0   0.890   1.315   0.522   15. DEAD BRD LF+THIN OATS
 ;   0.233     0.337  60.3  42.2 0.700; 936,:RASNY
; 936 0.756 1.417 1.708 3.103 0.078 0.116 0.182 0.266
; 1.459 2.288 3.398 1.568 2.329 1.485
B-936;CLR-LTB/TPB              10YR 4/2   10.7    6.3/335NNW  467 1516476 334297
936  30                  30              40      --
```

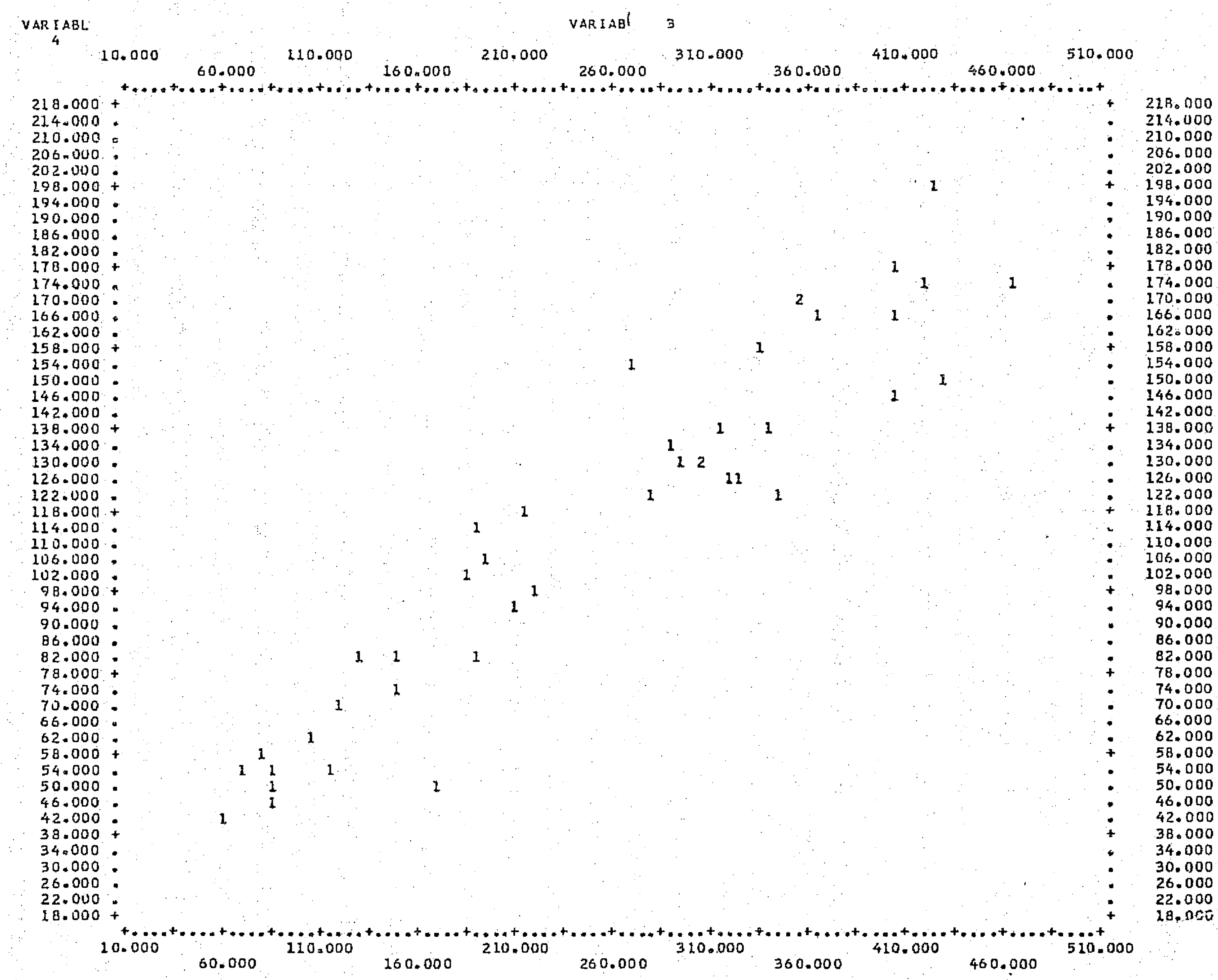

2.3.4.8 Wet weight versus dead weight (r=0.95)

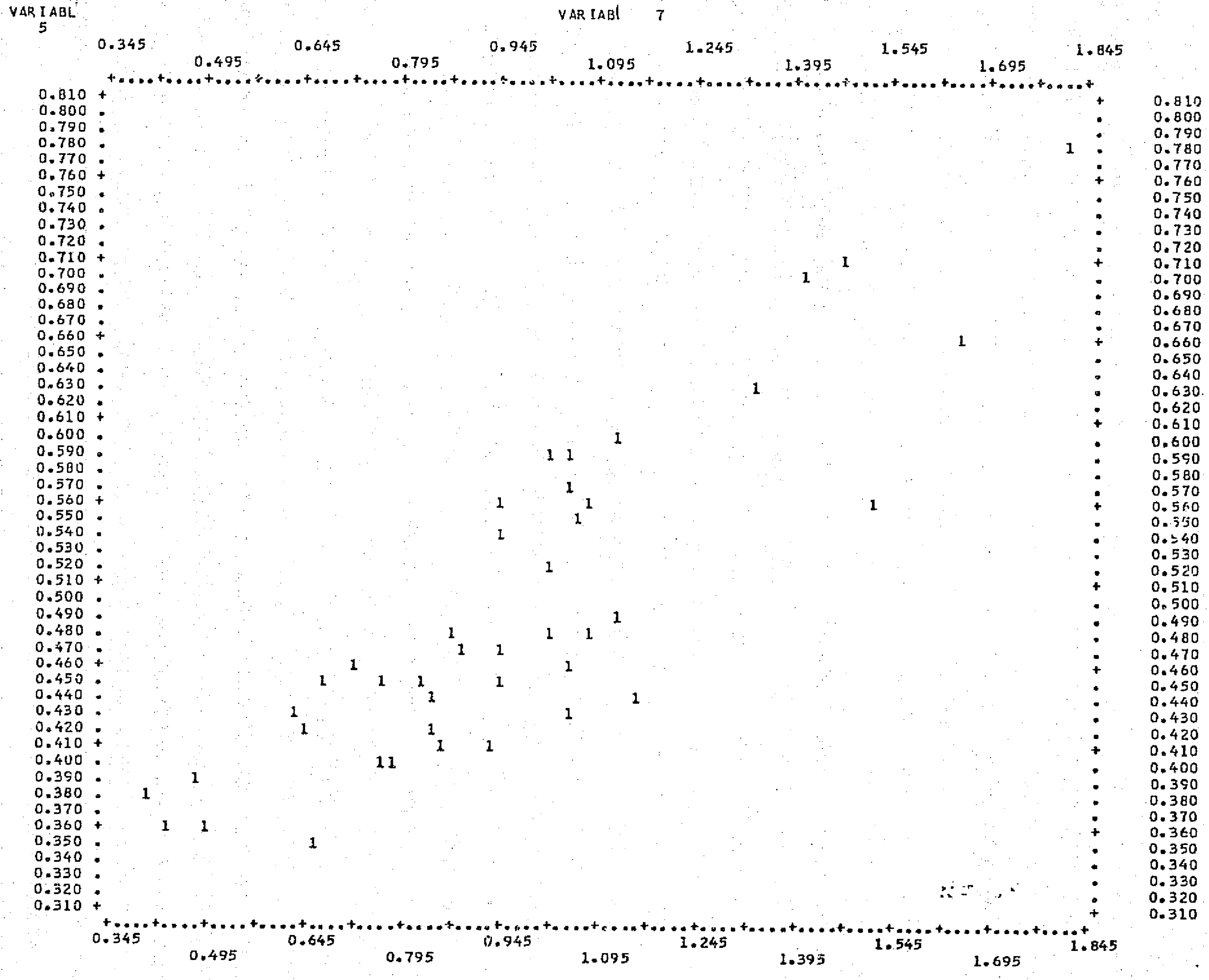

2.3.4.9 "Deadness" versus CH 5 (BP 5)(r=0.87)

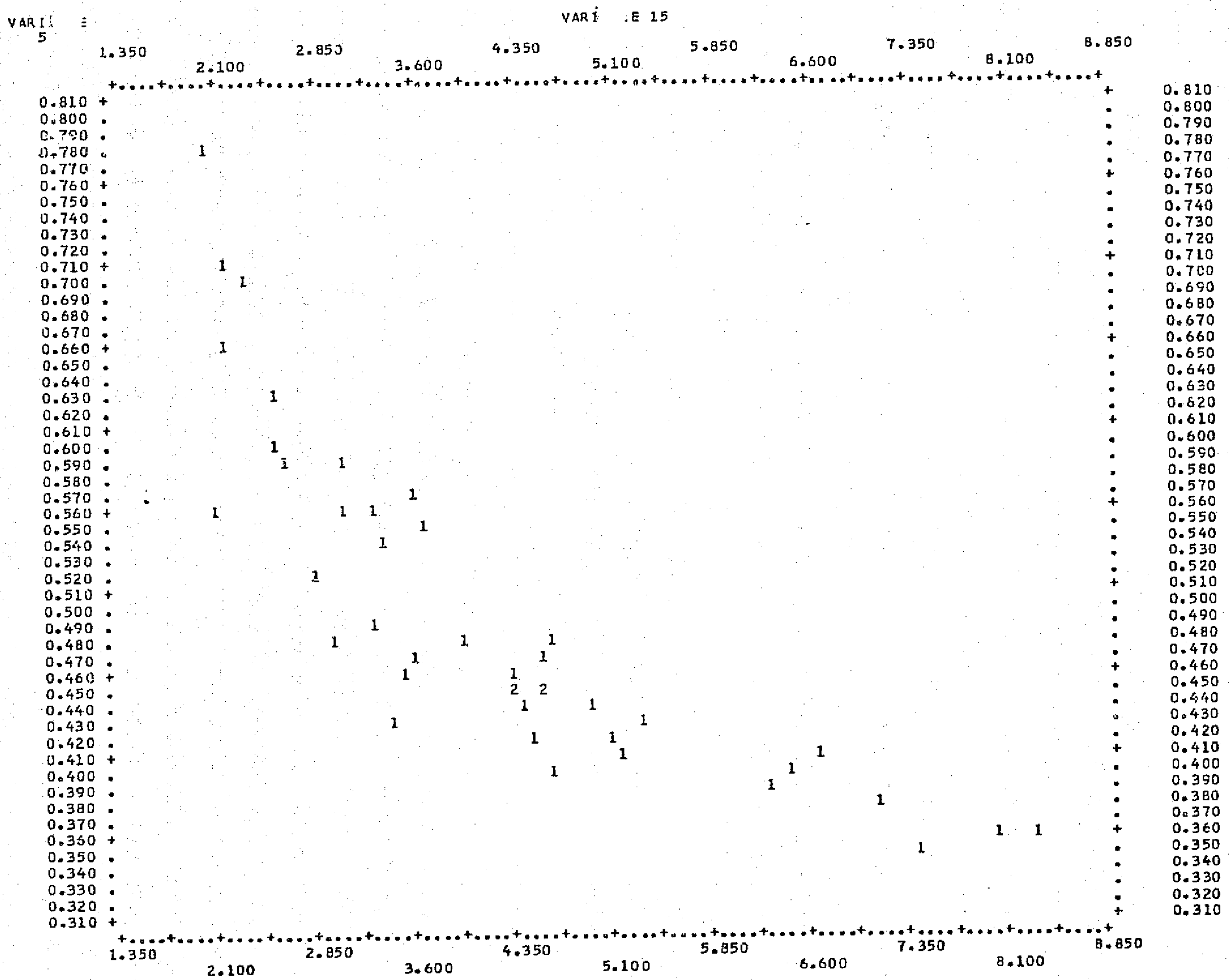

2.3.4.10 "Deadness" versus R 75 (r=-.83)

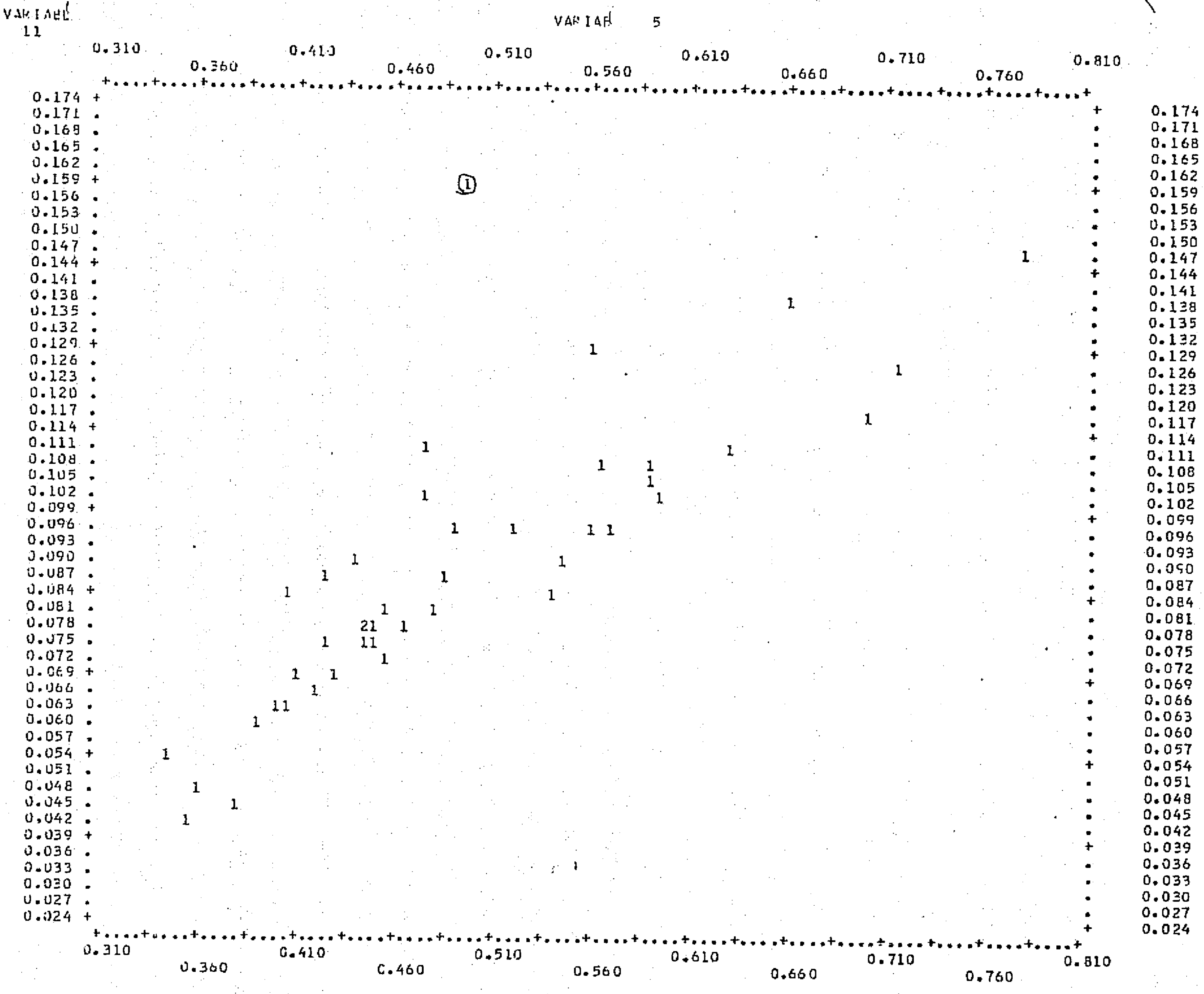

2.3.4.11 "Deadness" versus R 5 (r=.82)

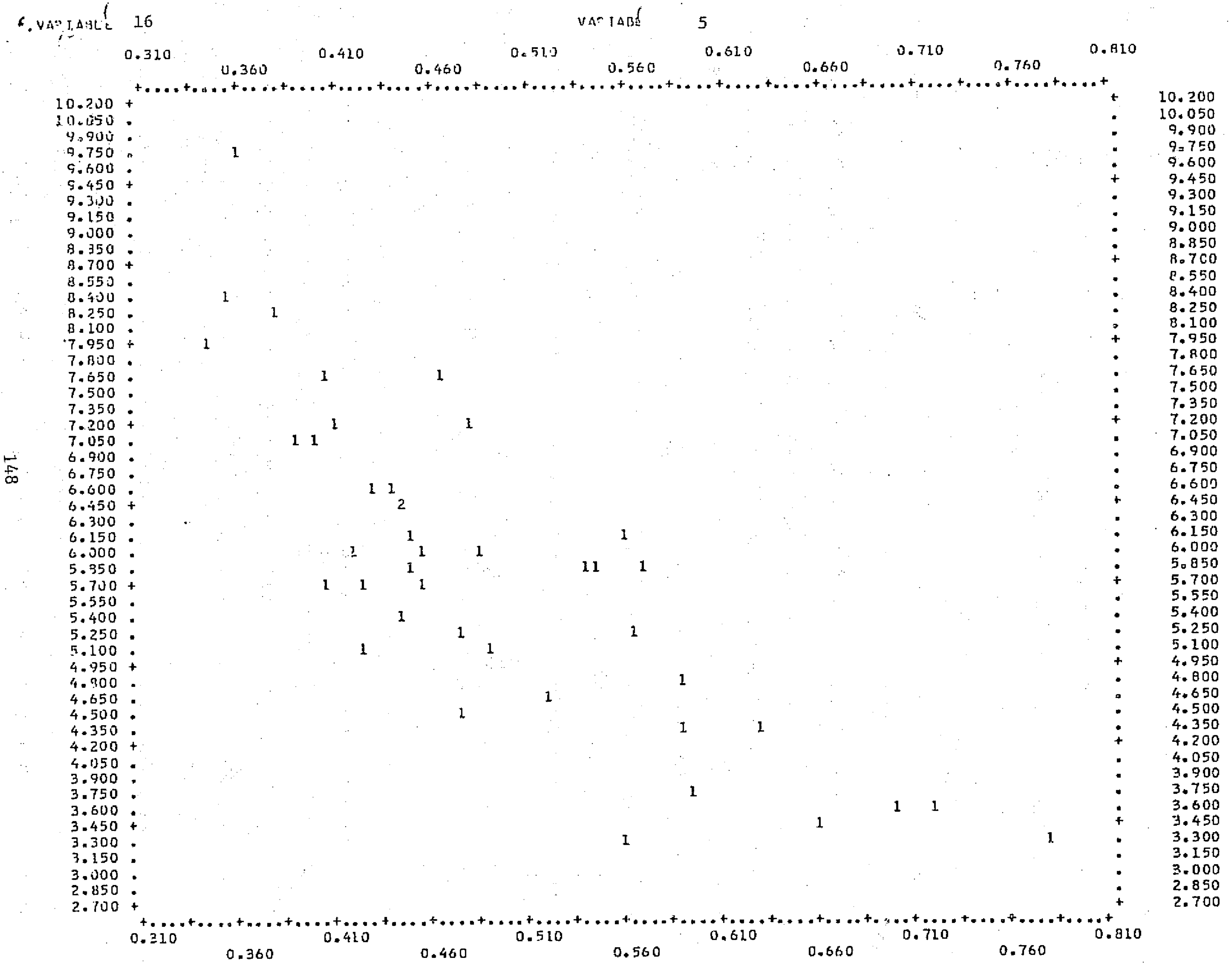

2.3.4.12 "Deadness" versus R 74 (r=-.82)

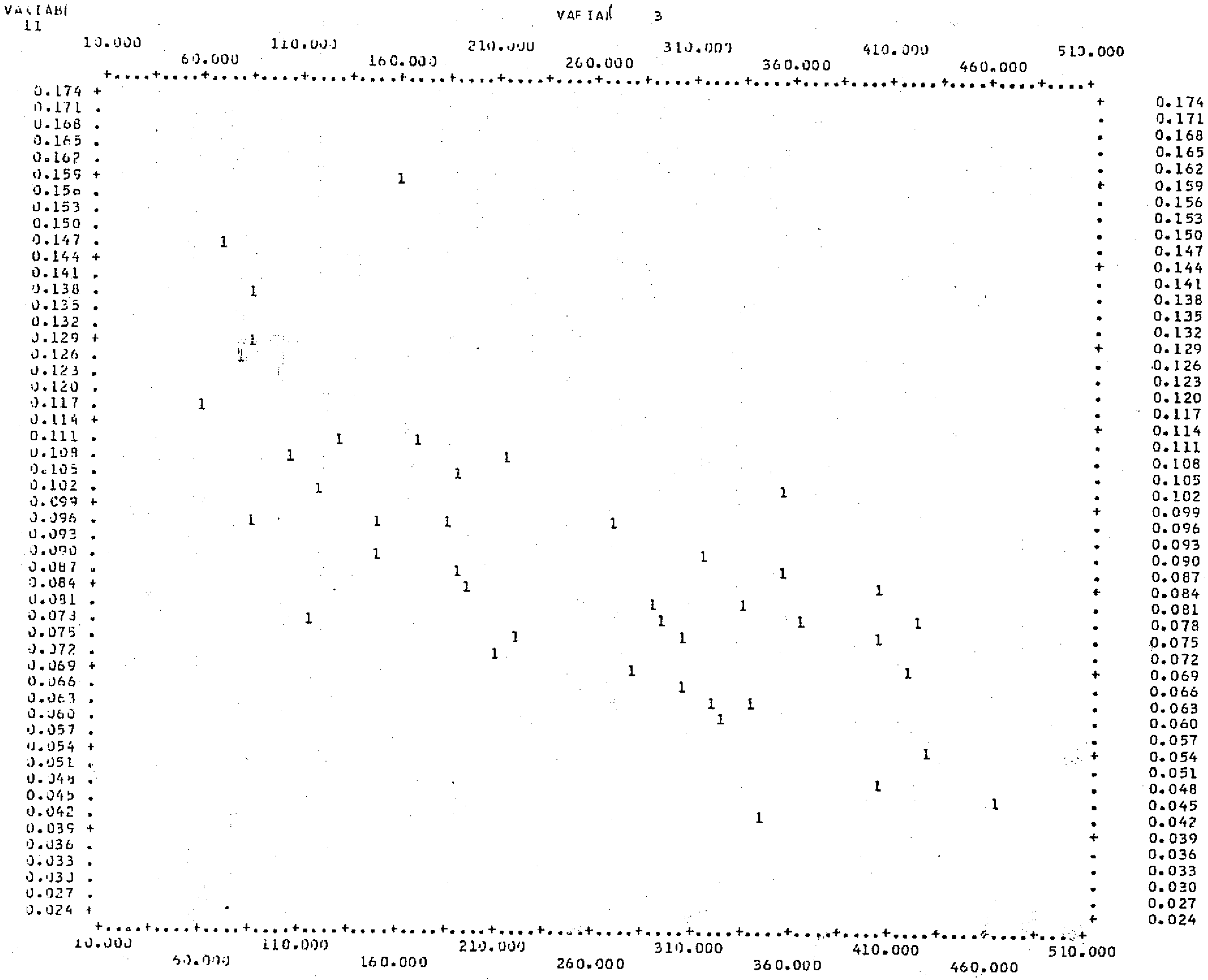

2.3.4.13 Wet weight versus R 5 (r=-.74)

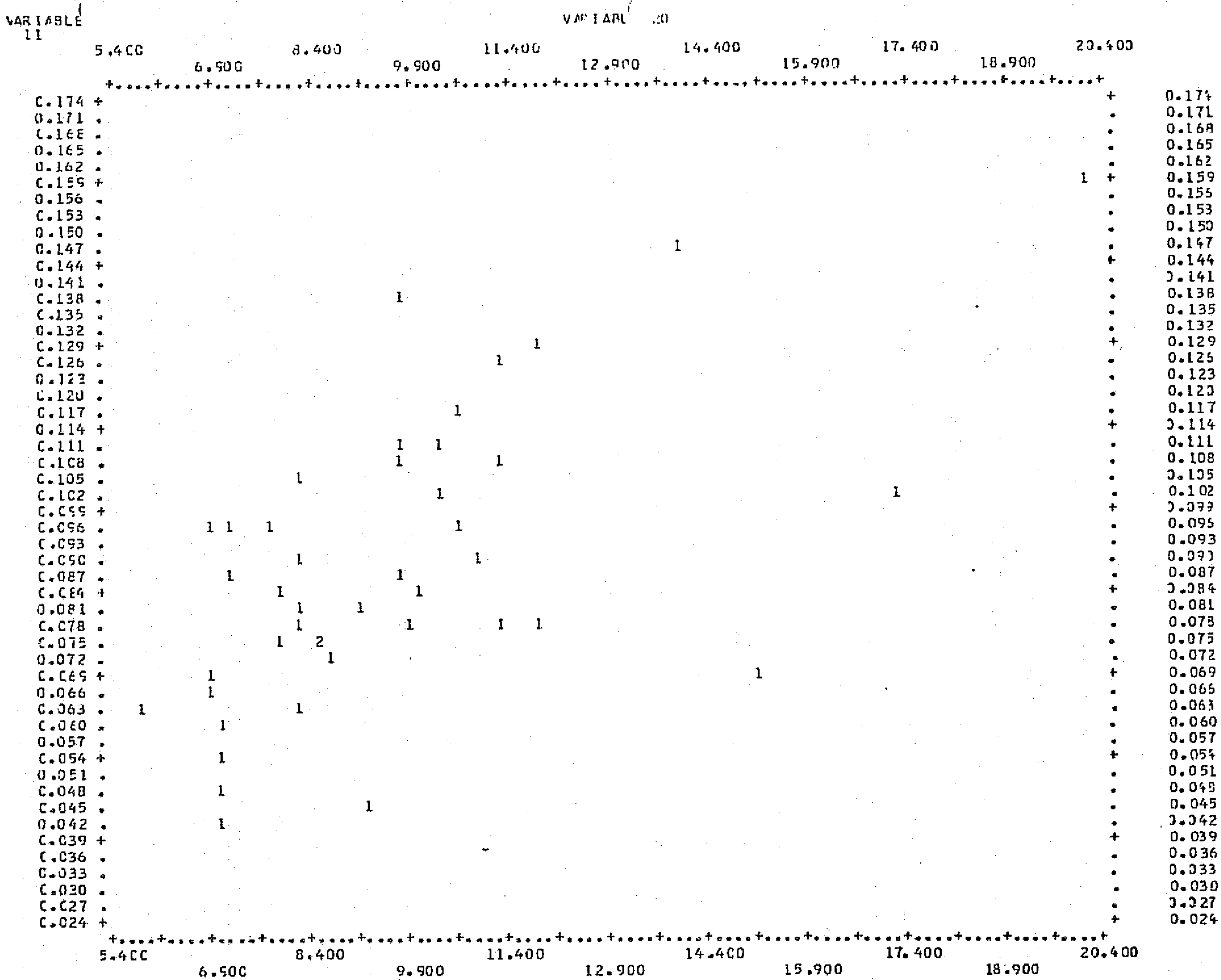

2.3.4.14 Soil moisture versus R 5 (r=.61)

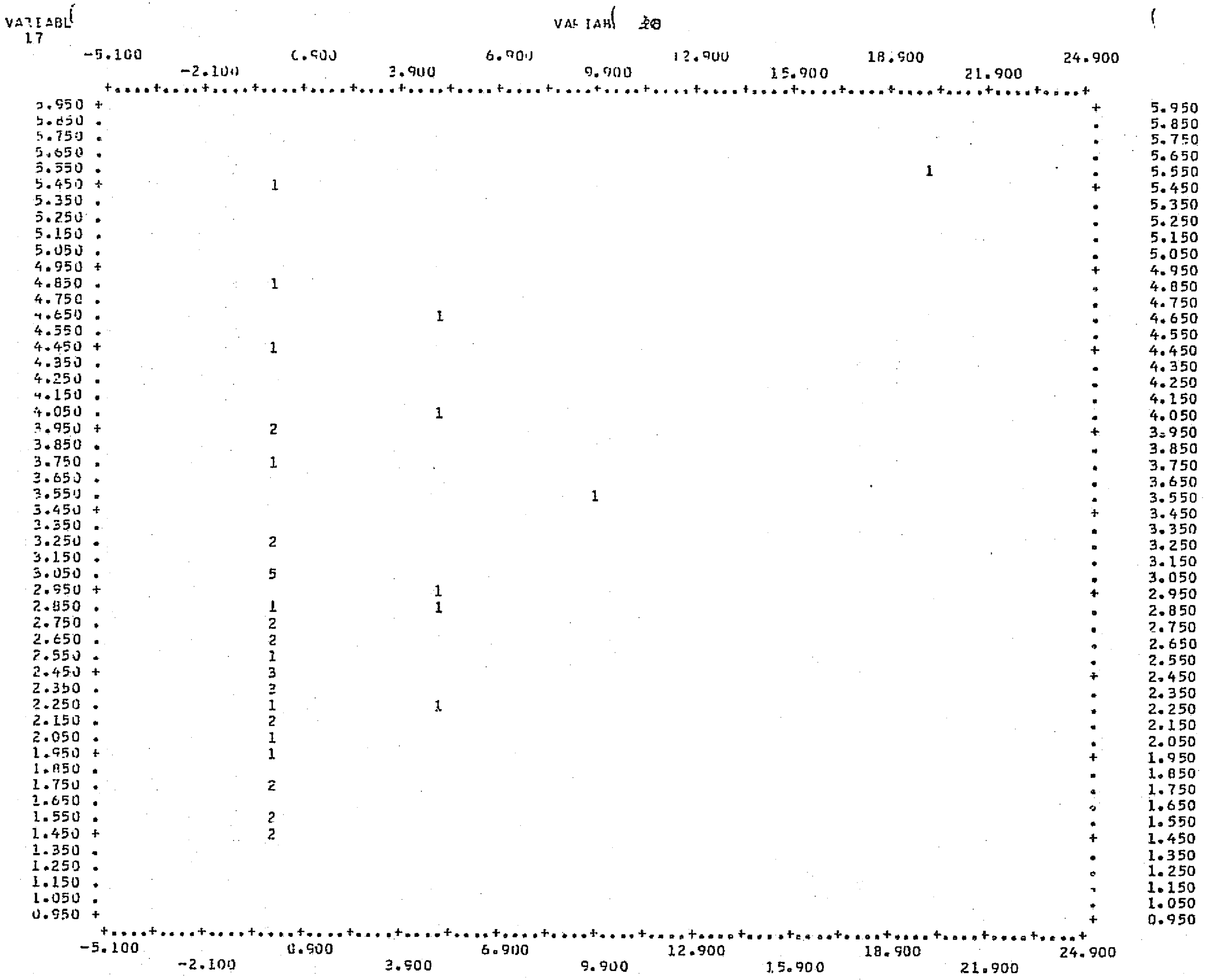

2.3.4.15 Morning Glory (sp.) versus R 65 (r=.45)

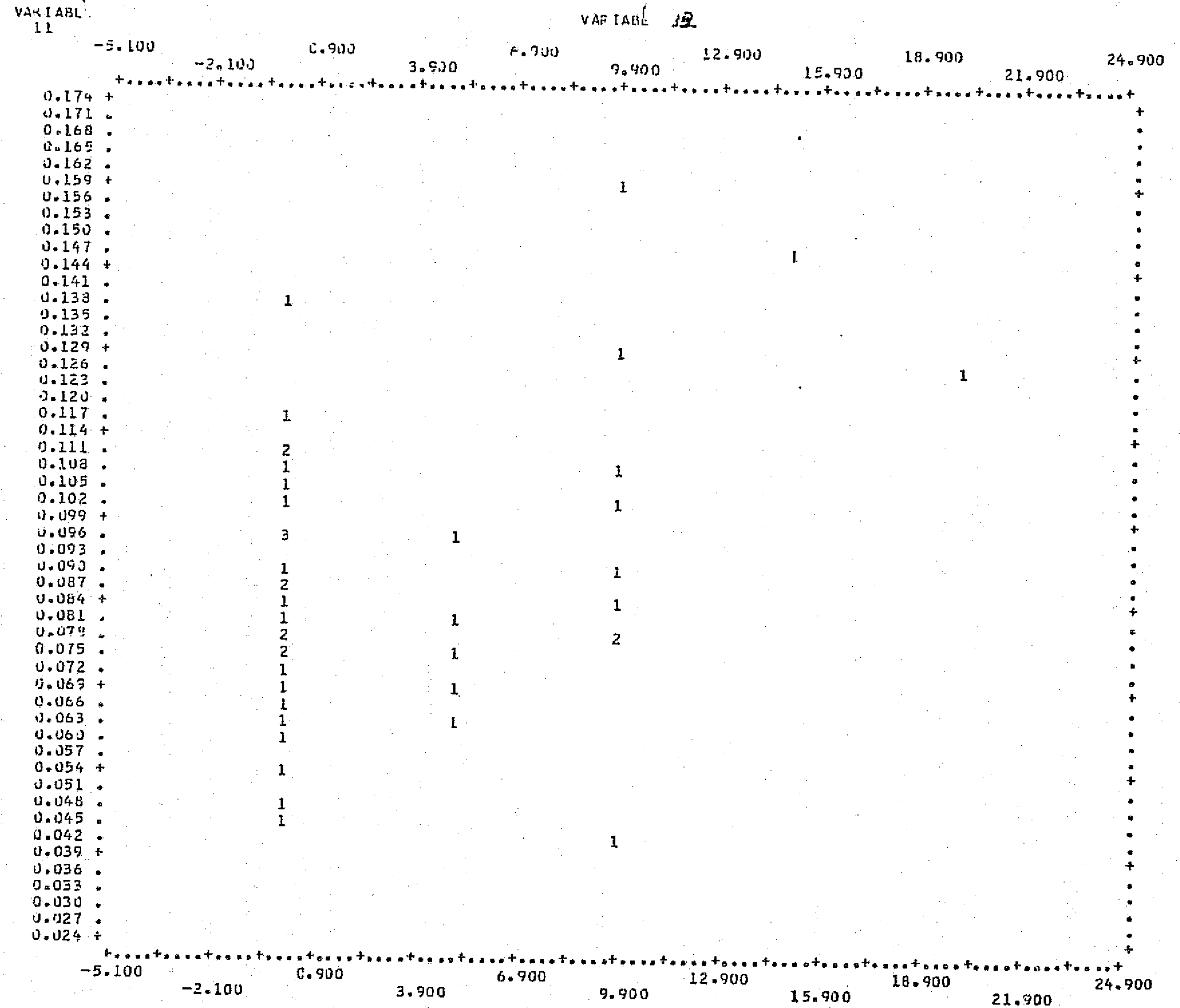

2.3.4.16 Broad leaved plants versus R 5 (r=.35)

2.3.4.2.5 Data Set 4 (76 Variables); Original set of ground data plus ERTS brightness and reflectance.

TABLE 2.3.4.8 ERTS BRIGHTNESS, ERTS REFLECTANCES AND GROUND REFLECTANCES

(TOTAL OF 76 VARIABLES).

LRTS BRIGHTNESS   ERTS REFLECTNCE.   GROUND REFLECTNCE

ERTS 1075 Oct 6,1972 1309 May 28,1973 1489 Nov 24,1973
1165 Jan 4,1973 1399 Aug 26,1973 1525 Dec 30 ,1973
#34 1669 May 23 1974 1687 June 6,1974

2.	C29	29	29	31	18	7	11	15	28	137	179	228	299	ERTS1075
3.	029	18	13	33	19	6	5	33	50					ERTS1165
4.	C29	32	33	47	25	6	10	20	29					ERTS1309
5.	C29	29	51	45	36	8	16	22	35					ERTS1399
6.	C29	13	26	13	18	7	8	25	36					ERTS1489
7.	029	16	10	23	14	3	3	21	37					ERTS1525
8.	C29	36	37	52	29	8	12	23	37	55	86	208	305	ERTS1669
9.	C29	35	36	55	28	6	10	23	34	85	137	181	266	ERTS1687
10.														
11.	030	30	28	30	165	75	105	145	26	113	148	194	269	ERTS1075
12.	030	15	95	20	11	2	15	18	29					ERTS1165
13.	C30	295	285	43	235	5	8	18	275					ERTS1309
14.	C30	265	495	41	355	85	14	215	32					ERTS1399
15.	C30	95	195	12	17	45	5	15	235					ERTS1489
16.	030	105	85	18	145	15	15	15	25					ERTS1525
17.	C30	335	325	51	285	65	95	22	365	86	136	294	402	ERTS1669
18.	030	36	37	555	285	7	11	225	35	98	152	215	294	ERTS1687
19.														
20.	C31	31	29	295	16	8	11	145	25	89	108	143	180	ERTS1075
21.	031	15	85	145	75	2	5	115	195					ERTS1165
22.	031	285	275	42	215	45	75	175	25					ERTS1309
23.	C31	24	48	385	345	75	13	21	29					ERTS1399
24.	C31	8	18	10	175	4	4	11	17					ERTS1489
25.	031	65	75	115	13	C	5	75	17					ERTS1525
26.	C31	335	30	49	275	65	85	21	35	69	92	222	315	ERTS1669
27.	031	32	29	47	26	45	7	18	32	69	107	166	235	ERTS1687
28.														
29.	032	31	29	28	16	8	11	14	25	121	148	185	234	ERTS1075
20.	032	16	9	16	8	3	1	13	21					ERTS1165
31.	C32	30	31	43	21	5	9	18	24					ERTS1309
32.	C32	24	48	40	36	8	14	21	29					ERTS1399
33.	032	9	19	10	18	4	4	12	16					ERTS1489
34.	032	7	8	12	13	0	1	8	18					ERTS1525
35.	C32	36	34	50	27	8	10	22	34	79	104	260	347	ERTS1669
36.	032	33	31	47	26	5	8	18	32	73	113	154	215	ERTS1687
37.														
38.	033	27	27	25	125	6	10	12	195	121	148	185	234	ERTS1075
39.	033	155	95	185	105	25	15	165	195					ERTS1165
40.	C33	33	38	435	245	7	12	18	285					ERTS1309
41.	033	245	48	44	355	8	16	205	295					ERTS1399
42.	C33	11	235	115	18	4	5	165	235					ERTS1489
43.	033	10	9	20	16	3	2	17	26					ERTS1525
44.	C33	38	40	56	285	9	14	25	365	83	113	245	338	ERTS1669
45.	033	385	46	545	295	85	15	223	365	102	146	186	260	ERTS1687
46.														
47.	035	30	27	29	13	8	10	14	20	123	150	180	224	ERTS1075
48.	035	17	10	25	13	4	2	24	34					ERTS1165
49.	C35	34	38	43	23	7	12	18	27					ERTS1309
50.	C35	25	52	44	37	5	16	23	30					ERTS1399
51.	C35	13	24	13	18	5	6	21	32					ERTS1489
52.	035	11	10	23	15	2	3	21	29					EPTS1525
53.	C35	38	41	51	29	9	14	22	37	96	142	208	324	ERTS1669
54.	035	42	51	54	27	10	17	22	33	71	117	169	234	ERTS1687
55.														
56.	C41	303	285	278	135	8	11	14	21	143	174	278	287	ERTS1075
57.	041	178	113	26	14	53	33	25	418					ERTS1165
58.	C41	34	395	443	24	7	128	185	28					EPTS1309
59.	C41	26	533	475	358	1C5	175	233	315					ERTS1399

TABLE 2.3.4.8 cont.

60.	041	135	248	135	115	55	68	203	343					ERTS1489
61.	041	125	10	25	165	35	3	23	33					ERTS1525
62.	041	383	41	515	285	93	138	225	363	94	143	258	355	ERTS1669
63.	041	423	508	558	288	103	178	23	353	116	165	235	307	ERTS1687
64.														
65.	042	29	30	30	14	7	12	15	22	116	162	195	263	ERTS1075
66.	042	19	13	27	15	7	5	26	42					ERTS1165
67.	042	34	40	44	24	7	13	18	28					ERTS1309
68.	042	27	56	49	41	8	18	25	33					ERTS1399
69.	042	14	265	14	19	6	8	21	34					ERTS1489
70.	042	14	11	245	17	4	4	22	41					ERTS1525
71.	042	40	40	52	27	10	13	23	34	77	128	247	359	ERTS1669
72.	042	41	49	55	30	10	17	23	37	81	126	175	241	ERTS1687
73.														
74.	047	32	31	32	14	9	12	16	22	136	168	220	281	ERTS1075
75.	047	18	12	28	17	6	4	27	45					ERTS1165
76.	047	37	37	51	27	9	16	22	32					ERTS1309
77.	047	29	59	55	44	13	21	27	35					ERTS1399
78.	047	13	27	14	19	6	6	24	36					ERTS1489
79.	047	16	10	29	18	6	3	27	42					ERTS1525
80.	047	39	46	59	30	10	16	27	39	94	141	294	380	ERTS1669
81.	047	45	52	60	30	12	18	25	37	125	187	240	319	ERTS1687
82.														
83.	047	32	31	32	14	9	12	16	22	136	168	220	281	ERTS1075
84.	047	18	12	28	17	6	4	27	45					ERTS1165
85.	047	37	37	51	27	9	16	22	32					ERTS1309
86.	047	29	59	55	44	13	21	27	35					ERTS1399
87.	047	13	27	14	19	6	6	24	36					ERTS1489
88.	047	16	10	29	18	6	3	27	42					ERTS1525
89.	047	39	46	59	30	10	16	27	39	94	141	294	380	ERTS1669
90.	047	45	52	60	30	12	18	25	37	125	187	240	319	ERTS1687
91.														
92.	049	315	29	295	15	85	11	145	24	141	168	219	267	ERTS1075
93.	049	165	11	265	16	35	3	255	42					ERTS1165
94.	049	35	42	49	275	75	14	21	32					ERTS1309
95.	049	29	585	55	425	12	21	265	355					ERTS1399
96.	049	15	29	13	185	65	6	245	405					ERTS1489
97.	049	155	95	275	17	45	25	255	41					ERTS1525
98.	049	37	465	58	30	85	165	265	385	97	153	268	349	ERTS1669
99.	049	42	505	595	295	105	175	25	37	92	146	188	263	ERTS1687
100.														
101.	051	305	27	275	14	8	10	13	22	165	214	252	322	ERTS1075
102.	051	165	105	23	13	35	25	215	345					ERTS1165
103.	051	365	44	50	255	85	15	215	295					ERTS1309
104.	051	26	585	43	37	9	15	21	315					ERTS1399
105.	051	175	305	125	205	55	55	22	36					ERTS1489
106.	051	13	105	235	16	3	35	21	34					ERTS1525
107.	051	365	41	555	30	85	135	25	39	123	181	340	399	ERTS1669
108.	051	395	49	59	29	9	17	25	355	94	149	181	244	ERTS1687
109.														
110.	053	31	28	26	14	8	11	12	22	137	172	225	294	ERTS1075
111.	053	17	10	22	13	4	2	20	34					ERTS1165
112.	053	37	42	51	25	8	14	22	29					ERTS1309
113.	053	26	48	47	36	8	17	21	32					ERTS1399
114.	053	16	30	13	19	6	6	24	36					ERTS1489
115.	053	17	10	23	14	4	3	21	37					ERTS1525
116.	053	37	43	57	30	9	15	26	39	115	174	278	373	ERTS1669
117.	053	39	48	53	28	8	16	21	34	98	143	204	278	ERTS1687
118.														
119.	055	325	30	285	14	9	12	14	22	127	159	216	273	ERTS1075

TABLE 2.3.4.8 cont.

120.	C55	17	105	22	125	45	25	205	33					ERTS1165
121.	055	355	425	48	26	8	145	20	30					ERTS1309
122.	C55	28	545	52	40	105	195	24	345					ERTS1399
123.	C55	165	32	12	185	6	6	245	35					ERTS1489
124.	C55	16	95	24	13	3	25	22	345					EPTS1525
125.	C55	39	445	575	26	95	155	24	36	1C5	146	283	397	ERTS1669
126.	C55	385	47	555	275	85	155	23	335	89	134	176	237	ERTS1687
127.														
128.	056	33	313	31	145	93	128	145	23	1C6	143	183	240	ERTS1075
129.	C56	178	103	25	138	53	23	238	363					ERTS1165
130.	C56	348	42	473	26	75	143	198	30					ERTS1309
131.	C56	288	473	545	428	12	21	258	353					ERTS1399
132.	056	155	24	125	19	65	6	228	358					ERTS1489
133.	056	168	93	283	145	4	23	268	383					ERTS1525
134.	056	395	46	578	3C5	98	153	26	395	126	182	288	375	ERTS1669
135.	C56	408	525	595	297	98	21	27	368	78	135	187	265	ERTS1687
136.														
137.	057	335	325	31	15	95	135	15	24	156	2C8	246	328	ERTS1075
138.	C57	18	10	28	15	6	2	27	395					ERTS1165
139.	C57	34	415	465	26	7	14	195	30					ERTS1309
140.	C57	3C5	60	57	455	135	225	275	36					ERTS1399
141.	057	15	26	13	19	7	6	21	365					ERTS1489
142.	C57	175	9	325	16	5	2	315	42					ERTS1525
143.	C57	40	46	58	33	10	16	26	43	61	73	237	345	ERTS1669
144.	C57	44	58	635	32	11	21	225	40	96	143	203	279	ERTS1687
145.														
146.	070	33	32	29	16	9	13	14	25	129	167	198	250	ERTS1075
147.	70	20	14	25	13	8	7	24	34					ERTS1165
149.	7C	34	36	41	21	7	12	17	24					ERTS1309
149.	C7C	4C	46	50	25	11	17	22	30					ERTS1399
150.	070	18	13	25	14	5	5	18	29					ERTS1489
151.	70	18	13	21	8	6	6	18	21					ERTS1525
152.	70	38	36	53	32	9	11	23	42					ERTS1669
153.	070	44	48	54	25	11	16	22	30	76	128	177	263	ERTS1687
154.														
155.	C72	32	30	31	16	9	12	15	25	123	152	190	253	ERTS1075
156.	72	18	11	27	16	6	3	26	42					ERTS1165
157.	72	36	42	45	26	8	14	19	30					ERTS1309
158.	C72	41	48	53	29	11	18	24	35					ERTS1399
159.	C72	19	14	24	12	6	7	18	27					ERTS1489
160.	72	17	12	27	15	4	5	25	40					ERTS1525
161.	72	36	38	54	32	8	12	24	42					ERTS1669
162.	C72	41	49	58	33	10	17	24	41	72	1C0	119	169	ERTS1687
163.														
164.	073	315	295	305	155	85	115	15	245	162	2C4	255	329	ERTS1075
165.	73	18	12	31	175	6	4	31	465					EPTS1165
166.	73	35	375	46	26	75	135	195	305					ERTS1309
167.	C73	38	465	535	29	10	17	24	355					ERTS1399
168.	073	19	13	25	13	6	7	185	295					ERTS1489
169.	73	165	115	235	125	35	45	215	33					ERTS1525
170.	73	35	345	575	325	75	105	26	425					ERTS1669
171.	C73	42	495	59	33	105	17	245	41	99	151	221	3C9	ERTS1687
172.														
173.	C80	318	31	295	148	85	123	145	243	126	166	214	277	ERTS1075
174.	80	165	108	298	178	33	28	293	47					ERTS1165
175.	8C	355	398	47	275	75	133	213	323					ERTS1309
176.	C80	375	46	505	273	93	168	245	33					ERTS1399
177.	C80	185	13	24	13	55	68	18	32					ERTS1489
178.	8C	155	103	213	115	25	33	188	328					ERTS1525
179.	80	358	36	603	328	8	113	27	43	56	80	214	336	ERTS1669

TABLE 2.3.4.8 cont.

180.	080	408	488	62	328	98	165	26	408	106	158	226	303	ERTS1687
181.														
182.	082	32	31	29	14	9	12	14	22	97	133	164	223	ERTS1075
183.	82	15	10	28	16	2	2	27	42					ERTS1165
184.	82	36	41	51	29	8	14	22	34					ERTS1309
185.	082	34	43	45	25	7	15	19	30					ERTS1399
186.	082	18	14	23	13	5	6	17	25					ERTS1489
187.	82	155	10	19	10	2	3	16	26					ERTS1525
188.	82	36	37	59	33	8	12	27	43	93	132	309	438	ERTS1669
189.	082	38	46	64	31	8	15	27	38	85	125	183	249	ERTS1687
190.														
191.	084	32	29	31	17	9	11	15	27	143	166	221	261	ERTS1075
192.	84	17	11	34	20	4	3	34	53					ERTS1165
193.	84	34	39	55	28	7	13	24	33					ERTS1309
194.	084	36	45	50	26	8	16	22	32					ERTS1399
195.	084	21	13	27	14	6	7	19	29					ERTS1489
196.	84	16	10	22	13	3	3	20	34					ERTS1525
197.	84	36	38	63	36	8	12	29	48	124	144	401	553	ERTS1669
198.	084	39	47	56	32	8	16	23	40	149	211	265	349	ERTS1687
199.														
200.	086	30	30	31	16	8	12	15	25	104	139	187	252	ERTS1075
201.	86	16	10	26	16	3	2	25	42					ERTS1165
202.	86	34	35	50	29	7	11	21	34					ERTS1309
203.	086	34	44	49	26	7	16	21	32					ERTS1399
204.	086	18	14	26	12	5	5	20	29					ERTS1489
205.	86	14	8	18	9	1	1	15	24					ERTS1525
206.	86	36	32	67	37	8	9	31	49	161	199	380	498	ERTS1669
207.	086	36	44	57	32	7	14	24	40	126	190	248	337	ERTS1687
208.														
209.	091	315	32	315	165	85	13	155	26	109	134	192	247	ERTS1075
210.	91	17	10	325	205	4	2	325	54					ERTS1165
211.	91	355	36	49	28	8	12	21	33					ERTS1309
212.	091	37	45	50	265	9	165	22	325					ERTS1399
213.	091	20	14	27	155	7	65	22	36					ERTS1489
214.	91	17	12	285	14	4	5	265	37					ERTS1525
215.	91	38	36	62	365	9	11	285	485	83	114	323	482	ERTS1669
216.	091	42	51	62	325	10	18	26	405	93	136	198	273	ERTS1687
217.														
218.	092	303	31	303	16	78	125	15	253	84	117	174	239	ERTS1075
219.	92	17	10	313	19	43	2	313	503					ERTS1165
220.	92	358	365	49	275	8	12	208	323					ERTS1309
221.	092	37	453	505	273	9	165	22	333					ERTS1399
222.	092	185	13	253	137	58	63	195	305					ERTS1489
223.	92	17	115	253	133	4	45	238	37					ERTS1525
224.	92	37	35	613	353	85	103	28	465	74	91	261	390	ERTS1669
225.	092	415	50	618	325	10	175	26	425	96	145	200	280	ERTS1687
226.														
227.	094	29	30	28	15	7	12	14	22	61	71	114	148	ERTS1075
228.	94	18	9	30	18	6	1	30	48					ERTS1165
229.	94	36	37	50	26	8	15	21	30					ERTS1309
230.	094	37	48	51	28	9	18	22	34					ERTS1399
231.	094	17	12	23	11	6	7	17	25					ERTS1489
232.	94	17	11	22	13	4	4	20	35					ERTS1525
233.	94	36	35	61	35	8	11	28	46	58	129	319	477	ERTS1669
234.	094	41	49	63	36	10	17	27	45	88	132	189	264	ERTS1687
235.														
236.	096	32	32	32	16	9	13	16	25	98	127	168	223	ERTS1075
237.	96	17	12	33	22	4	4	33	58					ERTS1165
238.	96	37	43	53	28	9	15	23	33					ERTS1309
239.	096	39	45	52	27	10	16	23	33					ERTS1399

TABLE 2.3.4.8 cont.

240.	096	17	14	23	12	6	7	17	29					ERTS1489
241.	96	18	11	26	14	6	4	24	37					ERTS1525
242.	96	36	36	68	36	8	11	32	48	91	122	306	463	ERTS1669
243.	096	46	54	63	35	12	19	27	44	100	147	218	297	ERTS1687
244.														
245.	005	32	32	32	16	9	13	16	25	117	143	193	251	ERTS1075
246.	05	17	12	33	22	4	4	33	58					ERTS1165
247.	05	37	43	53	28	9	15	23	33					ERTS1309
248.	005	39	45	52	27	10	16	23	33					ERTS1399
249.	005	17	14	23	12	6	7	17	29					ERTS1489
250.	05	18	11	26	14	6	4	24	37					ERTS1525
251.	05	36	36	68	36	8	11	32	48	110	144	373	530	ERTS1669
252.	005	46	54	63	35	12	19	27	44	125	177	245	320	ERTS1687
253.														
254.	006	23	35	33	18	9	15	17	28	147	185	224	288	ERTS1075
255.	06	16	11	36	23	3	3	36	61					ERTS1165
256.	06	38	44	56	30	9	15	24	35					ERTS1309
257.	006	36	41	49	26	6	16	21	32					ERTS1399
258.	006	20	14	25	12	7	8	20	29					ERTS1489
259.	06	17	10	22	13	4	3	20	34					ERTS1525
260.	06	36	36	63	35	8	11	29	46	80	128	247	356	ERTS1669
261.	006	41	51	70	34	10	18	31	42	140	202	248	343	ERTS1687
262.														
263.	008	33	34	335	178	95	14	168	28	125	159	204	265	ERTS1075
264.	08	178	108	375	23	55	28	38	613					ERTS1165
265.	08	375	435	548	303	9	15	235	355					ERTS1309
266.	008	383	50	525	285	10	163	245	323					ERTS1399
267.	008	185	125	233	103	58	68	188	268					ERTS1489
268.	08	175	118	24	125	5	48	22	33					ERTS1525
269.	08	363	373	59	32	83	12	263	418	95	150	246	337	ERTS1669
270.	008	385	403	555	313	8	163	235	388	104	174	218	343	ERTS1687
271.														
272.	009	31	34	35	19	8	14	18	30	158	210	271	355	ERTS1075
273.	09	18	11	34	21	6	3	34	56					ERTS1165
274.	09	39	45	54	31	9	16	23	36					ERTS1309
275.	009	37	46	51	28	9	17	22	34					ERTS1399
276.	009	18	12	23	10	6	8	20	29					ERTS1489
277.	09	18	13	26	13	6	6	24	34					ERTS1525
278.	09	36	39	58	31	8	13	26	40	113	175	285	382	ERTS1669
279.	009	38	48	54	31	8	16	22	38	88	156	228	357	ERTS1687
280.														
281.	010	325	343	34	173	10	143	173	273	103	146	182	245	ERTS1075
282.	010	195	133	293	173	68	148	265	482					ERTS1165
283.	010	385	385	495	268	92	145	21	235					ERTS1309
284.	010	388	47	52	273	103	173	228	253					ERTS1399
285.	010	193	138	245	12	63	68	185	268					ERTS1489
286.	010	188	14	24	103	68	7	22	295					ERTS1525
287.	010	373	388	553	298	9	138	245	383	66	105	224	332	ERTS1669
288.	010	413	475	523	26	213	158	98	318	86	149	201	294	ERTS1687
289.														
290.	020	345	34	335	16	105	145	17	25	147	215	253	390	ERTS1075
291.	20	165	135	235	13	6	6	22	345					ERTS1165
292.	20	315	33	46	25	6	10	195	29					ERTS1309
293.	020	40	47	495	245	105	17	21	295					ERTS1399
294.	020	12	225	16	205	75	85	17	27					ERTS1489
295.	20	185	12	19	10	6	5	16	26					ERTS1525
296.	20	365	30	48	255	9	125	205	32	111	161	383	537	ERTS1669
297.	020	395	44	54	28	22	14	9	315	79	130	190	275	ERTS1687
298.														
299.	019	325	33	325	15	9	125	165	235	139	169	239	293	ERTS1075

TABLE 2.3.4.8 cont.

300.	19	17	12	295	165	45	4	29	435					ERTS1165
301.	19	315	32	48	275	6	10	205	325					ERTS1309
302.	C19	40	49	51	26	105	18	225	315					ERTS1399
303.	C19	19	16	22	115	6	85	16	255					ERTS1489
304.	19	175	11	275	15	5	4	255	40					ERTS1525
305.	19	34	37	555	305	7	12	25	395	119	186	364	481	ERTS1669
306.	C19	385	465	605	315	255	155	8	39	88	151	203	296	ERTS1687
307.														
308.	C17	33	37	33	18	9	16	17	28	75	96	149	190	ERTS1075
309.	17	18	12	33	20	6	4	33	53					ERTS1165
310.	17	30	23	47	27	5	10	20	32					ERTS1309
311.	C17	41	56	61	32	11	22	28	39					ERTS1399
312.	C17	18	13	26	14	5	6	22	36					ERTS1489
313.	17	17	11	30	16	4	4	28	42					ERTS1525
314.	17	36	36	59	33	8	11	27	43	80	122	258	352	ERTS1669
315.	C17	38	46	63	33	8	15	27	41	72	116	198	282	ERTS1687
316.														
317.	C15	36	37	37	18	11	16	19	28	91	118	185	243	ERTS1075
318.	15	16	11	33	20	3	3	33	53					ERTS1165
319.	15	32	34	47	28	6	11	20	33					ERTS1309
320.	C15	41	51	51	30	11	19	25	37					ERTS1399
321.	015	18	13	31	17	5	6	24	38					ERTS1489
322.	15	17	11	31	17	4	4	30	45					ERTS1525
323.	15	38	39	59	35	9	13	27	46	78	118	302	457	ERTS1669
324.	015	42	56	70	36	10	20	31	45	69	113	183	274	ERTS1687
325.														
326.	C30	34	33	335	175	10	14	17	275	137	168	250	324	ERTS1075
327.	30	18	12	33	195	6	4	33	515					ERTS1165
328.	30	33	38	50	28	65	125	215	33					ERTS1309
329.	030	405	545	575	315	11	21	26	385					ERTS1399
330.	030	18	125	30	165	55	5	23	36					ERTS1489
331.	30	165	10	32	18	35	3	31	48					ERTS1525
332.	30	375	41	625	365	9	135	285	485	62	85	238	390	ERTS1669
333.	030	415	575	69	37	10	205	30	46	106	172	241	347	ERTS1687
334.														
335.	C31	32	34	34	18	9	14	17	28	123	169	227	307	ERTS1075
336.	31	17	11	32	19	4	3	32	50					ERTS1165
337.	31	33	37	51	28	7	12	22	33					ERTS1309
338.	C31	45	58	65	33	13	23	30	40					ERTS1399
339.	031	15	10	28	15	6	4	25	41					ERTS1489
340.	31	17	10	31	17	4	3	30	45					ERTS1525
341.	31	37	43	63	35	9	15	29	52	145	217	384	464	ERTS1669
342.	C31	41	53	61	35	10	19	26	44	70	119	173	259	ERTS1687
343.														
344.	C33	35	34	34	18	11	14	17	28	102	136	193	260	ERTS1075
345.	33	17	10	27	16	4	2	26	42					ERTS1165
346.	33	33	37	51	28	7	12	22	33					ERTS1309
347.	C33	38	48	57	30	10	18	26	37					ERTS1399
348.	033	19	10	31	18	5	4	25	41					ERTS1489
349.	33	17	10	28	16	4	3	26	42					ERTS1525
350.	33	36	35	63	36	8	11	29	48	66	117	267	425	ERTS1669
351.	C33	39	51	63	34	8	18	27	42	119	191	251	346	ERTS1687
352.														
353.	C34	32	34	30	16	9	14	15	25	139	190	257	342	ERTS1075
354.	34	17	10	23	15	4	2	21	40					ERTS1165
355.	34	33	37	49	27	7	12	21	32					ERTS1309
356.	C34	36	45	50	28	8	16	22	34					ERTS1399
357.	034	18	10	31	18	5	4	22	34					ERTS1489
358.	34	16	10	25	14	3	3	23	37					ERTS1525
359.	34	36	35	58	35	8	11	26	46	166	247	369	457	ERTS1669

TABLE 2.3.4.8 cont.

360.	C34	39	48	63	34	8	16	27	42	85	125	212	304	ERTS1687
361.														
362.	C35	33	34	32	17	95	14	165	268	117	152	214	283	ERTS1075
363.	35	163	85	143	78	42	8	112	202					ERTS1165
364.	35	278	233	305	16	42	3	92	185					ERTS1309
365.	C35	308	313	438	18	5	95	128	213					ERTS1399
366.	C35	19	11	273	153	6	45	205	368					ERTS1489
367.	35	145	75	103	4	15	1	65	11					ERTS1525
368.	35	31	258	453	248	53	73	19	31	63	93	247	391	ERTS1669
369.	035	30	243	253	125	8	5	38	135	73	116	176	247	ERTS1687
370.														
371.	040	283	255	27	143	65	9	13	225	113	156	193	255	ERTS1075
372.	40	155	98	20	11	22	18	18	29					ERTS1165
373.	40	325	333	47	255	65	102	198	295					ERTS1309
374.	C40	415	448	518	265	83	16	228	323					ERTS1399
375.	C40	165	95	215	105	35	35	16	235					ERTS1489
376.	40	155	88	24	118	25	18	185	31					ERTS1525
377.	40	328	343	563	328	6	102	253	428	86	105	373	582	ERTS1669
378.	C40	385	465	61	315	258	155	8	393	94	159	243	346	ERTS1687
379.														
380.	C42	29	27	28	14	7	10	14	22	101	130	201	256	ERTS1075
381.	42	15	10	20	11	1	2	18	29					ERTS1165
382.	42	32	23	47	26	6	10	20	30					ERTS1309
383.	C42	34	40	47	24	7	14	20	29					ERTS1399
384.	042	17	10	23	12	4	4	17	27					ERTS1489
385.	42	16	9	23	14	3	2	21	37					ERTS1525
386.	42	315	29	57	33	6	8	26	43	106	119	351	567	ERTS1669
387.	042	38	46	66	32	28	15	8	40	114	184	243	342	ERTS1687
388.														
389.	043	295	275	285	135	7	10	13	21	101	130	201	256	ERTS1075
390.	43	165	10	23	125	35	2	21	33					ERTS1165
391.	43	31	295	465	26	6	85	195	305					ERTS1309
392.	C43	36	40	455	245	8	145	195	295					ERTS1399
393.	043	165	105	195	105	35	45	145	235					ERTS1489
394.	43	15	105	22	11	2	35	195	29					ERTS1525
395.	43	31	28	56	315	5	7	25	41	107	140	311	483	ERTS1669
396.	043	375	43	575	32	24	135	75	395	79	117	208	283	ERTS1687
397.														
398.	C44	315	295	29	145	85	115	145	23	110	148	211	275	ERTS1075
399.	44	165	95	205	11	3	15	185	29					ERTS1165
400.	44	305	285	445	24	55	8	185	28					ERTS1309
401.	C44	308	345	38	21	65	11	155	25					ERTS1399
402.	044	16	11	19	95	3	5	14	21					ERTS1489
403.	44	155	10	205	10	25	2	18	265					ERTS1525
404.	44	315	26	545	315	55	6	245	41	99	140	276	443	ERTS1669
405.	044	365	38	49	26	19	115	7	315	69	106	208	308	ERTS1687
406.														
407.	C50	29	30	285	275	7	115	14	23	123	167	204	276	ERTS1075
408.	50	155	11	24	125	25	3	23	33					ERTS1165
409.	50	31	23	44	265	55	10	185	31					ERTS1309
410.	C50	36	46	51	28	8	17	22	335					ERTS1399
411.	C50	17	11	225	115	4	45	17	255					ERTS1489
412.	50	16	10	205	12	3	3	18	315					ERTS1525
413.	50	32	30	58	33	6	8	265	43	60	72	256	413	ERTS1669
414.	C50	345	375	535	28	22	115	6	345	133	187	254	321	EPTS1687
415.	C42	38	46	66	32	28	15	8	40	114	184	243	342	ERTS1687
416.	C52	31	31	32	15	8	12	16	24	118	161	207	283	ERTS1075
417.	52	17	12	25	15	4	4	235	40					ERTS1165
418.	52	31	32	49	27	6	10	21	32					ERTS1309
419.	052	37	42	47	26	9	15	20	32					ERTS1399

TABLE 2.3.4.8 cont.

```
052   17   11   20   11    4    5   15   25                         ERTS1489
 52   16   11   24   13    3    4   22   34                         ERTS1525
 52   31   26   59   34    5    6   27   45    79   87  294  248    ERTS1669
052   39   30   65   36   28   17    8   45   124  159  265  374    ERTS1687
- ------------------------------------
054  325  315  308  158    9  125  153   25   106  149  201  275    ERTS1075
 54   16   98  168    9   35   18  142  238                         ERTS1165
 54  265  238  343  188   35    6  135  218                         ERTS1309
054  303  295  313   16   58   85  115   19                         ERTS1399
054   17  113  193   98    4    5   14   22                         ERTS1489
 54  155    9   16    9   25    2  128  235                         ERTS1525
 54  283  228  328  225   42   45  162   28   122  139  276  414    ERTS1669
054   33  295  413  225   20   95    5   27    94  156  214  322    ERTS1687
/*
```

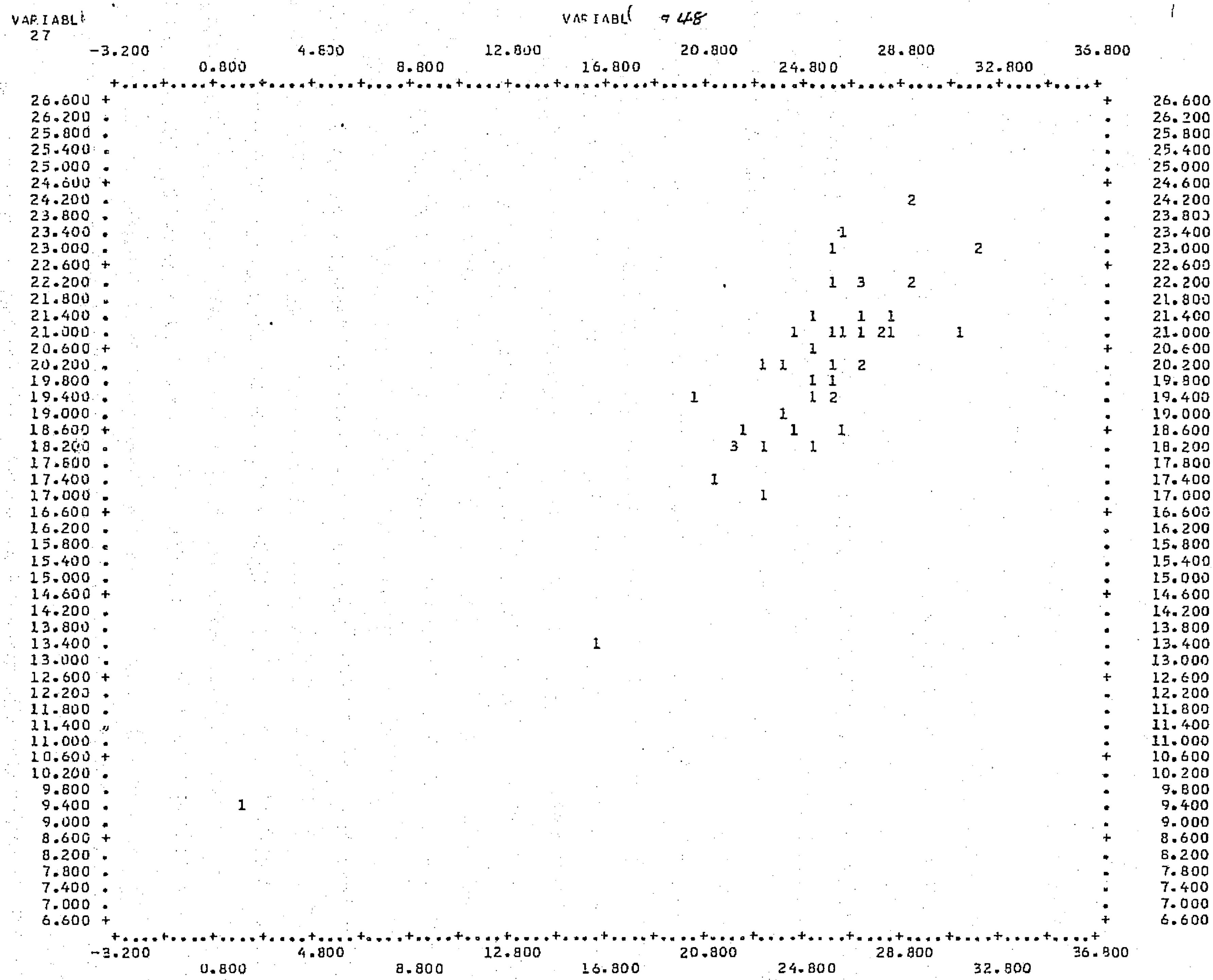

2.3.4.17 ERTS 1669 - R6 versus ERTS 1309 - R6 (r=0.88)

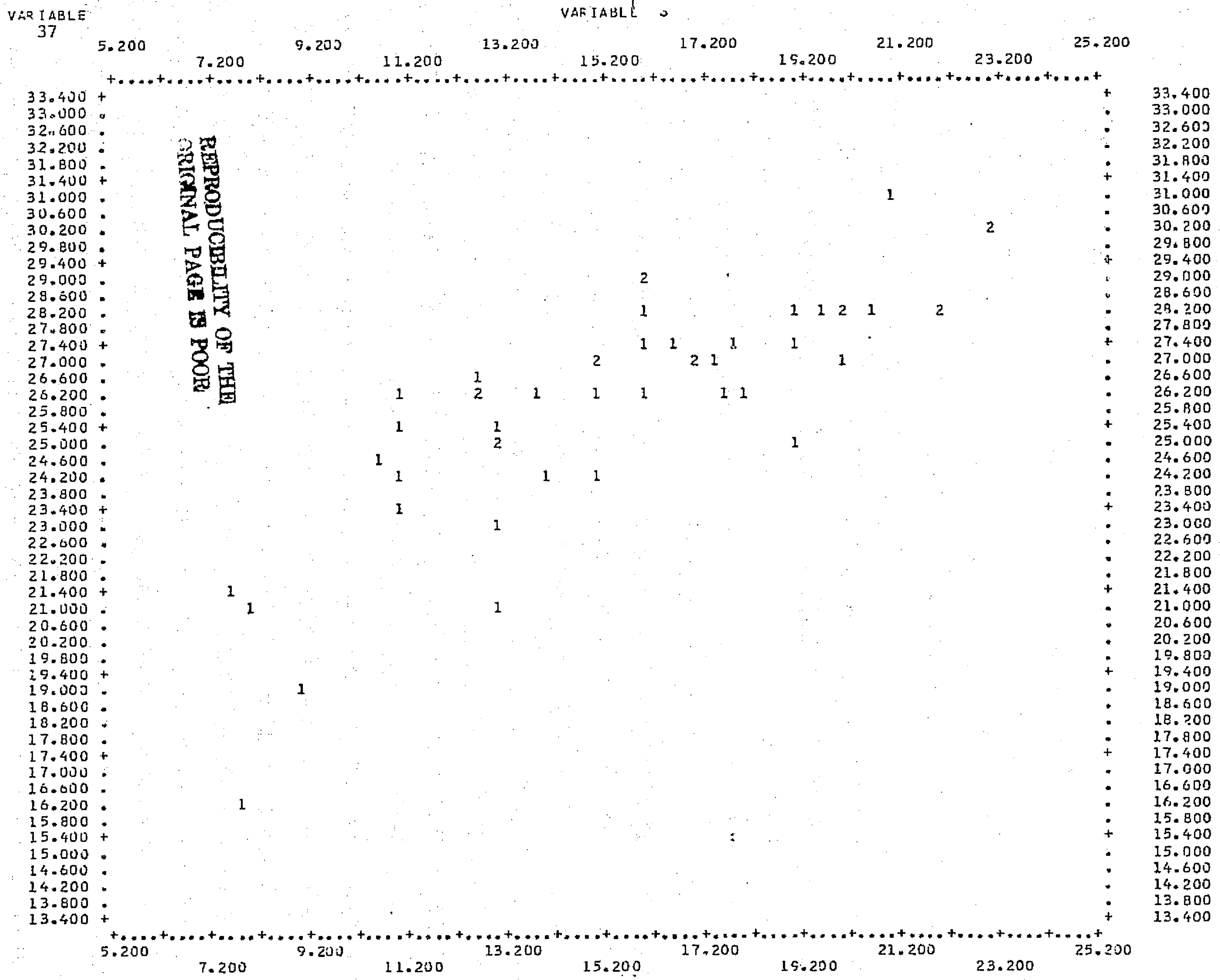

2.3.4.18 ERTS 1165 - BP7 versus ERTS 1309-BP7 (r=0.80)

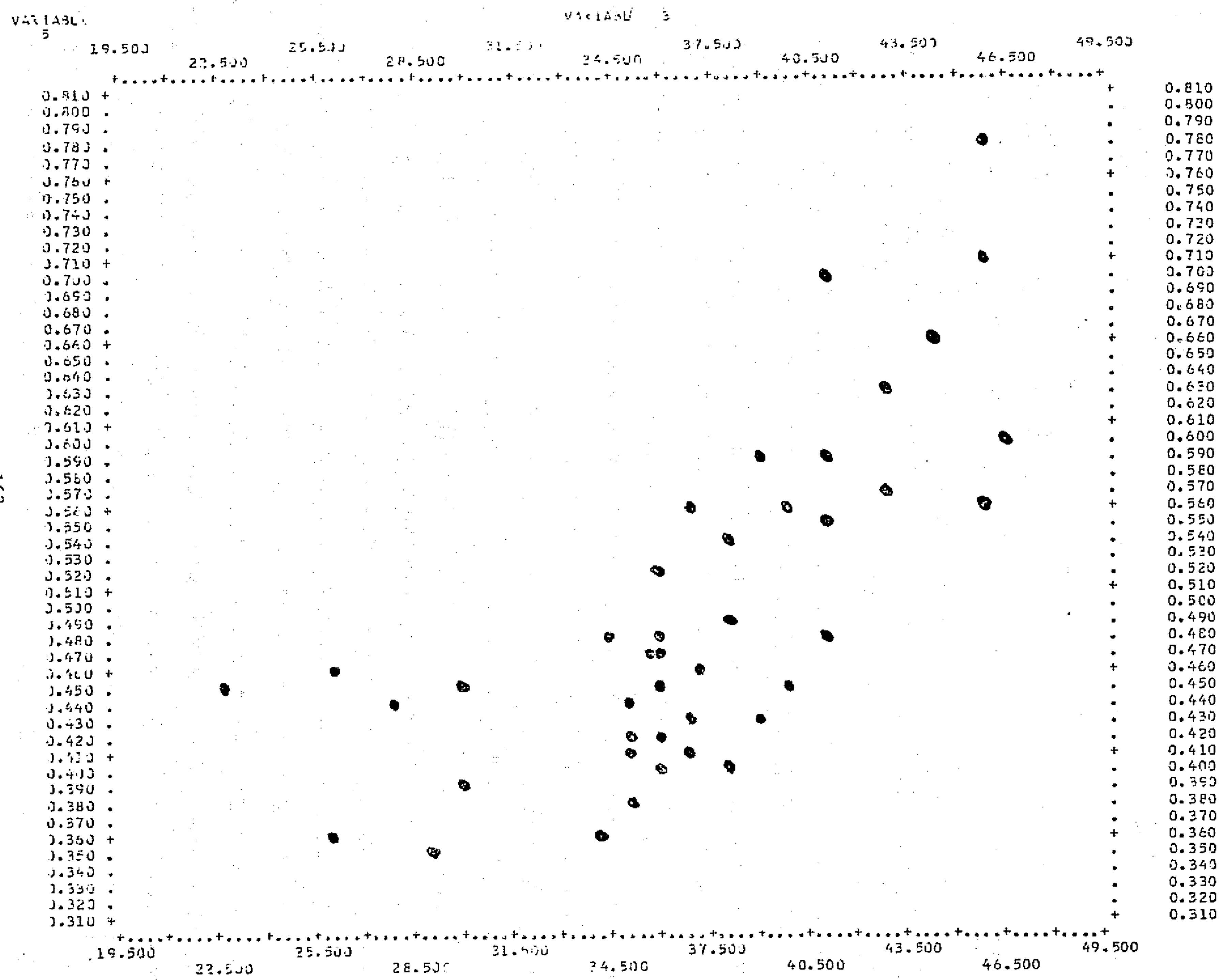

2.3.4.19 ERTS 1669-BP5 versus Biomass ratio ("deadness") (r = 0.71)

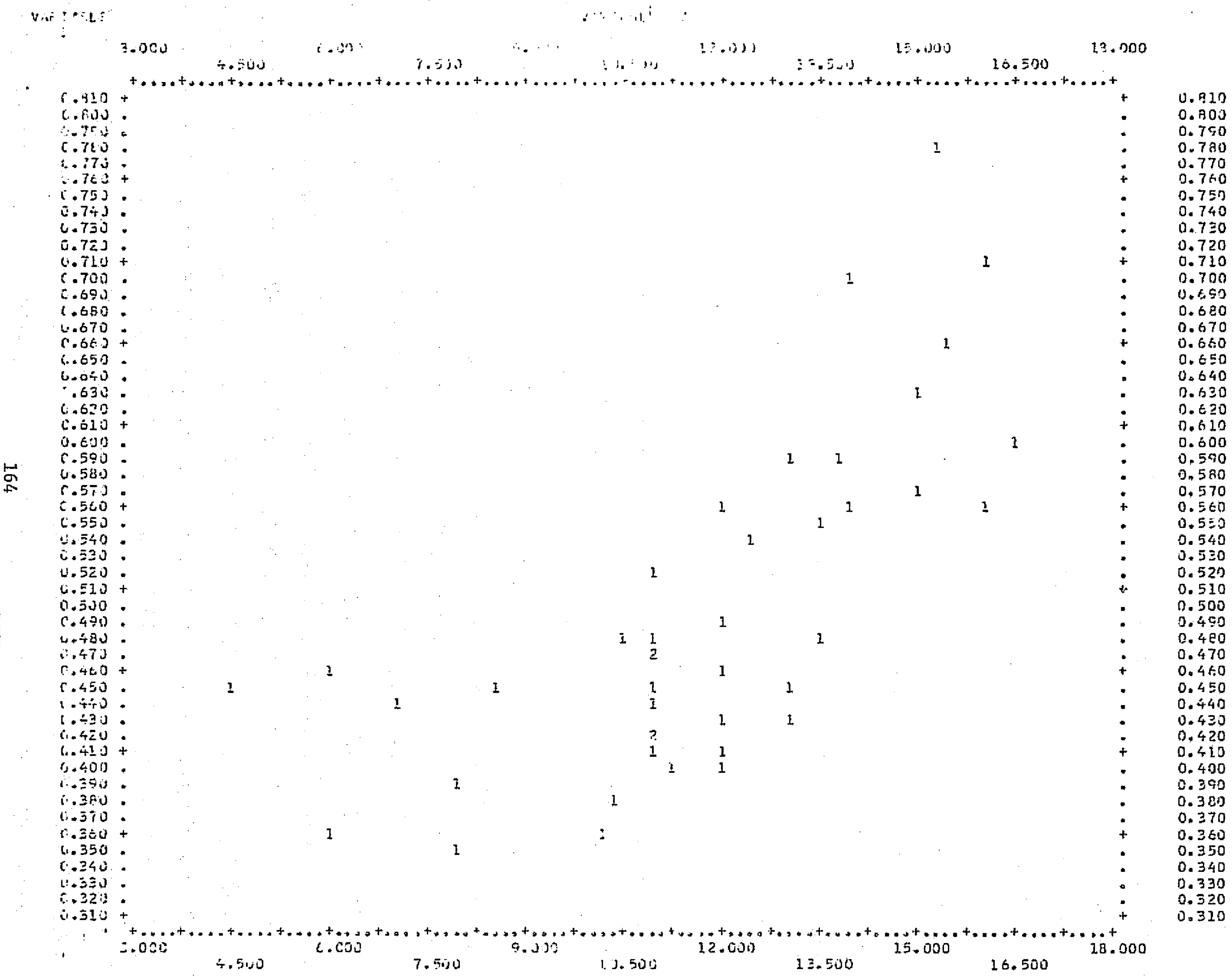

2.3.4.20 ERTS 1669-R5 versus Biomass ratio (r=0.70)

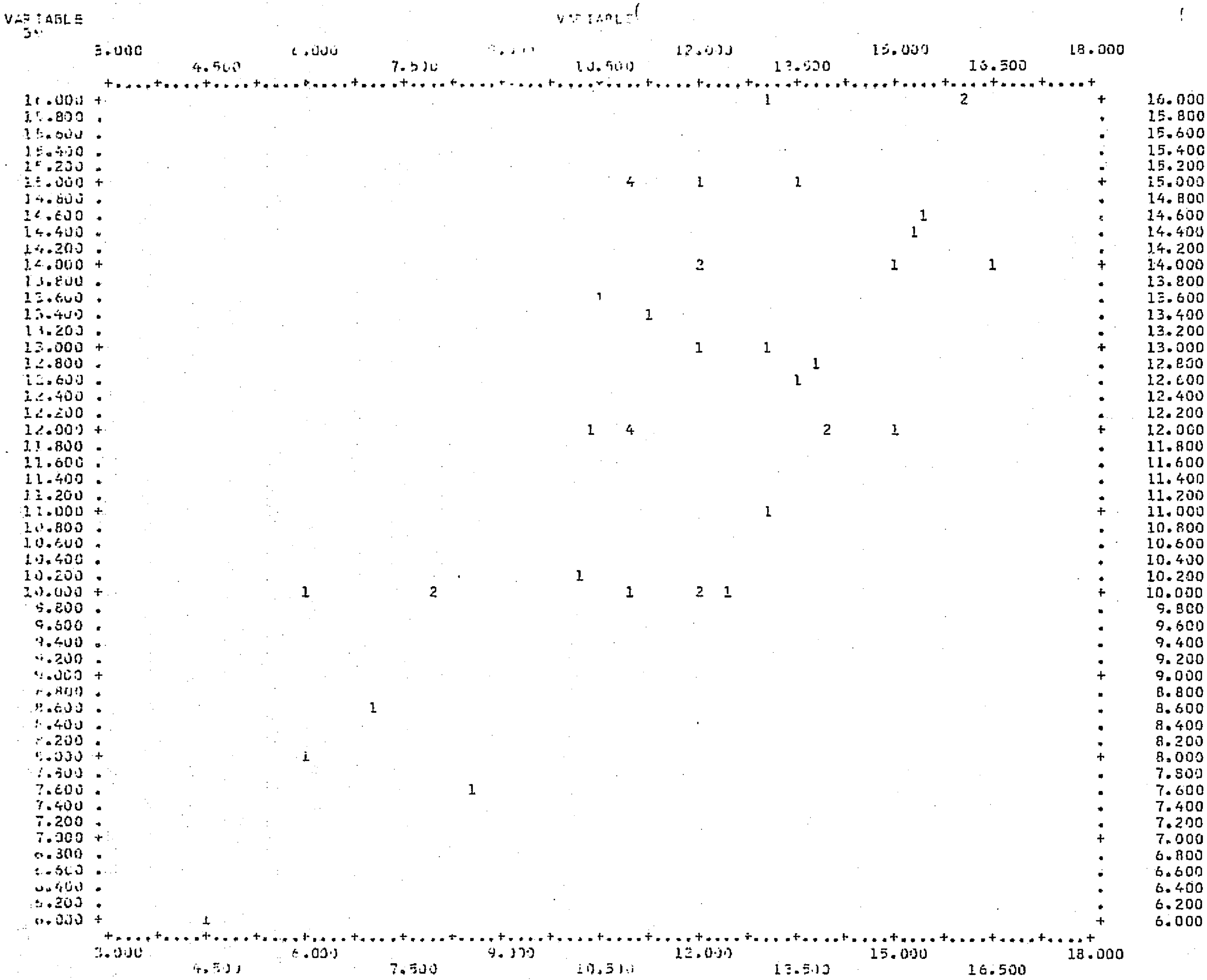

2.3.4.21 ERTS 1669-R5 versus ERTS 1309-R5 (r=0.70)

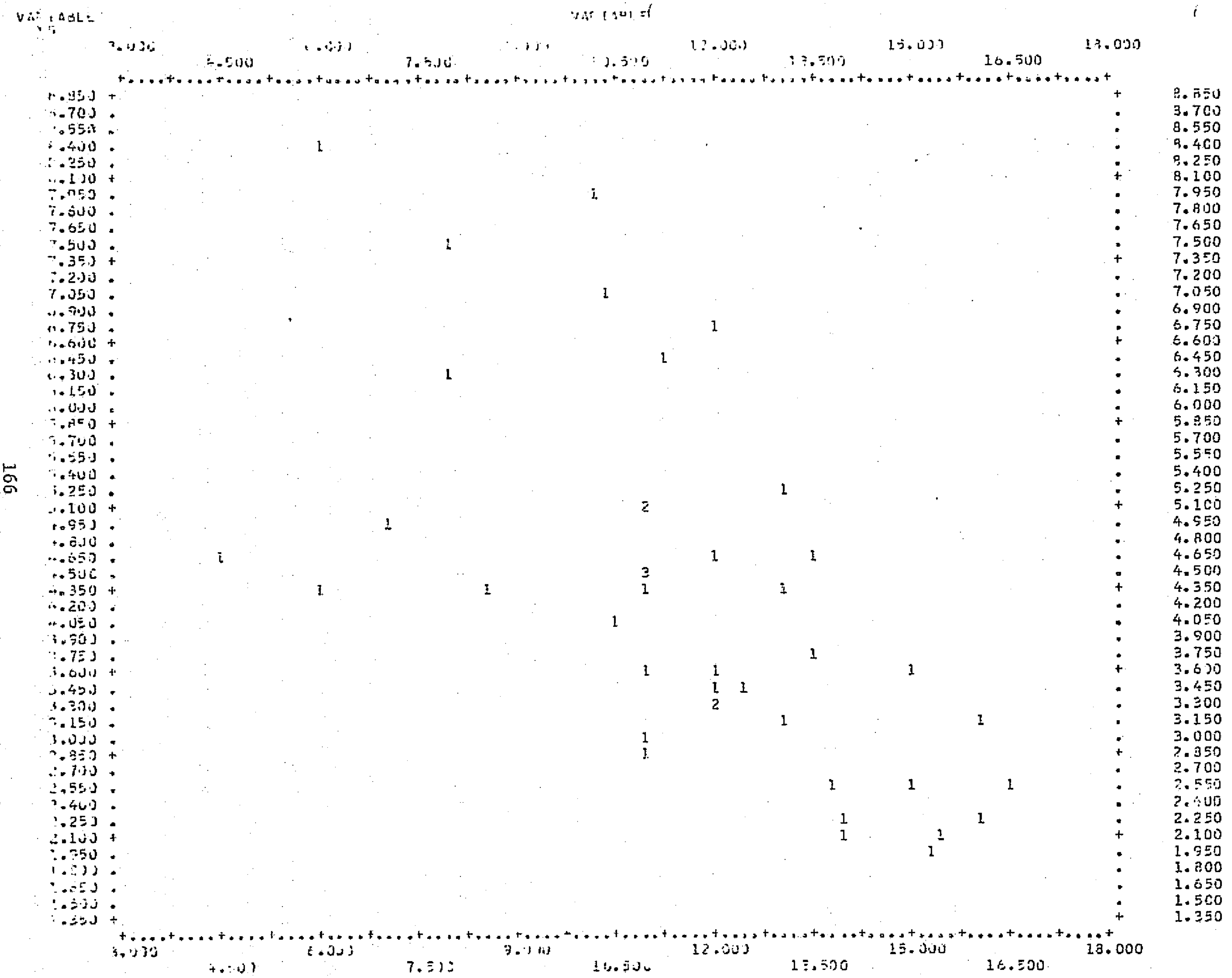

2.3.4.22 ERTS 1669-R5 versus TRUCK R 75 (r=-0.63)

2.3.4.3 Discriminant Analysis using Vegetation on Main Soil Groups (BMDO7M).

Stepwise linear discriminant analysis to calculate canonical transforms of the data (65 variables) was carried out, with results summarized as Tables 2.3.4.1, 2.3.4.2, and 2.3.4.3 above. The programs used were adaptations of the UCLA Biomedical set, generally available on all U.S. computer systems (BMD series).

One pictoral aspect of the output is a two-dimensional plot of the first and second canonical variables, which enable the viewer to see the best-fit-decision plane through the N-dimensional space of the calculation. Such output plots follow here as figures 2.3.4.23 through 2.3.4.26.

2.3.4.4 Computational Procedure Discriminant Analysis (BMDØ7M)

Figure 2.3.4.23	5 groups, 65 variables, 5 steps (A1) no deletions: 100% success in separating the 5 (soil and grass) groups.
Figure 2.3.4.24	3 groups + 2 test groups, (also same as A1), no deletions: 100% success
Figure 2.3.4.25	5 groups, 54 variables (B1) deleted altitude (1) and plant species (10): 88% success, ERTS data included.
Figure 2.3.4.26	5 groups, 51 variables (C), deleted bandpasses (4), altitude (1), and plant species (10): 98% success, ERTS data included.

The CONDEL (control and delete) option was used for Runs B1, B2 (not shown), and C. Table 2.3.4.1 should be read to show the results together with the above figures.

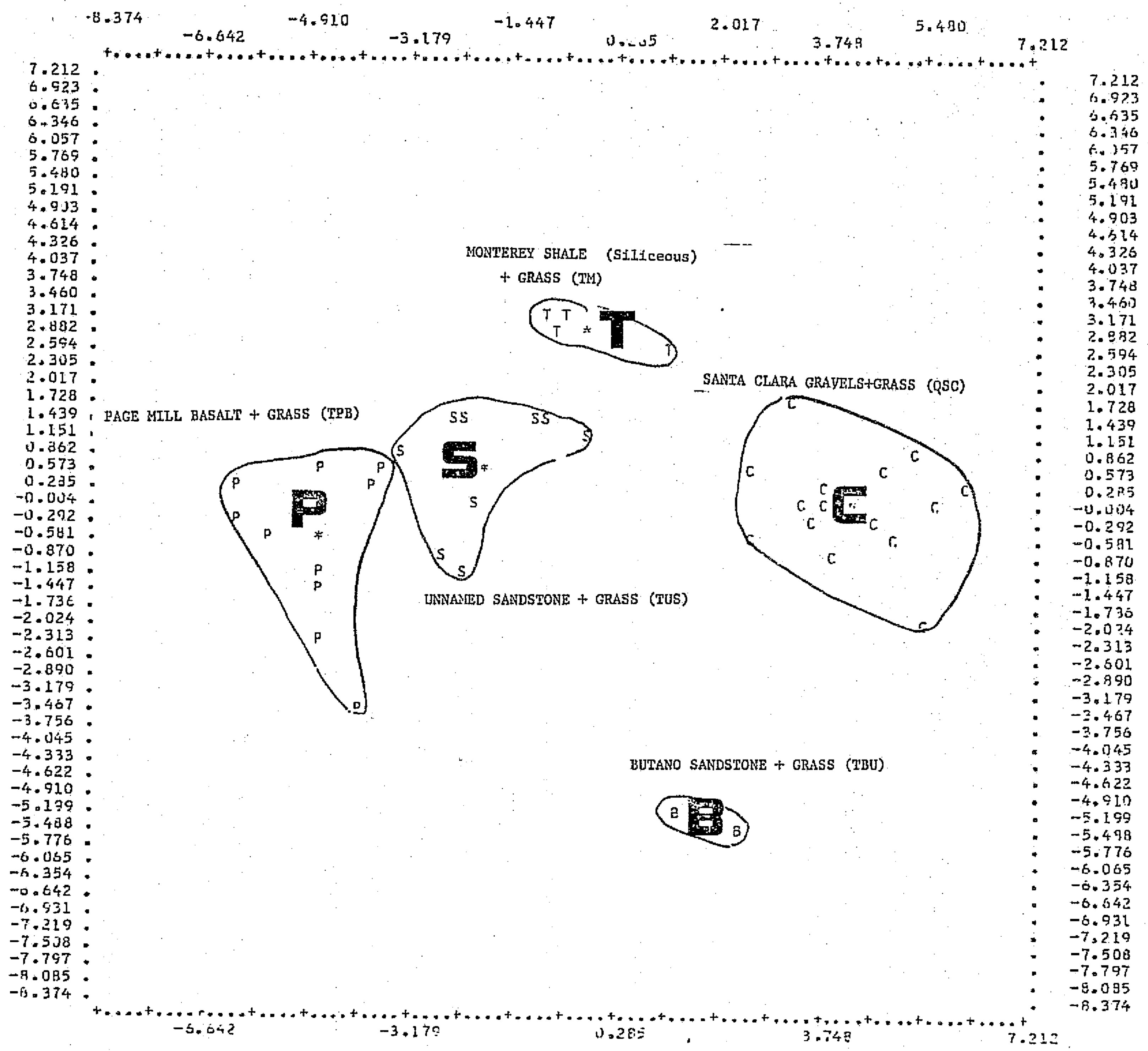

2.3.4.23 Canonical Plot (BMD07M); 5 group separation 65 variables, 5 step.
Run A1, no deletions. (Success = 100%)

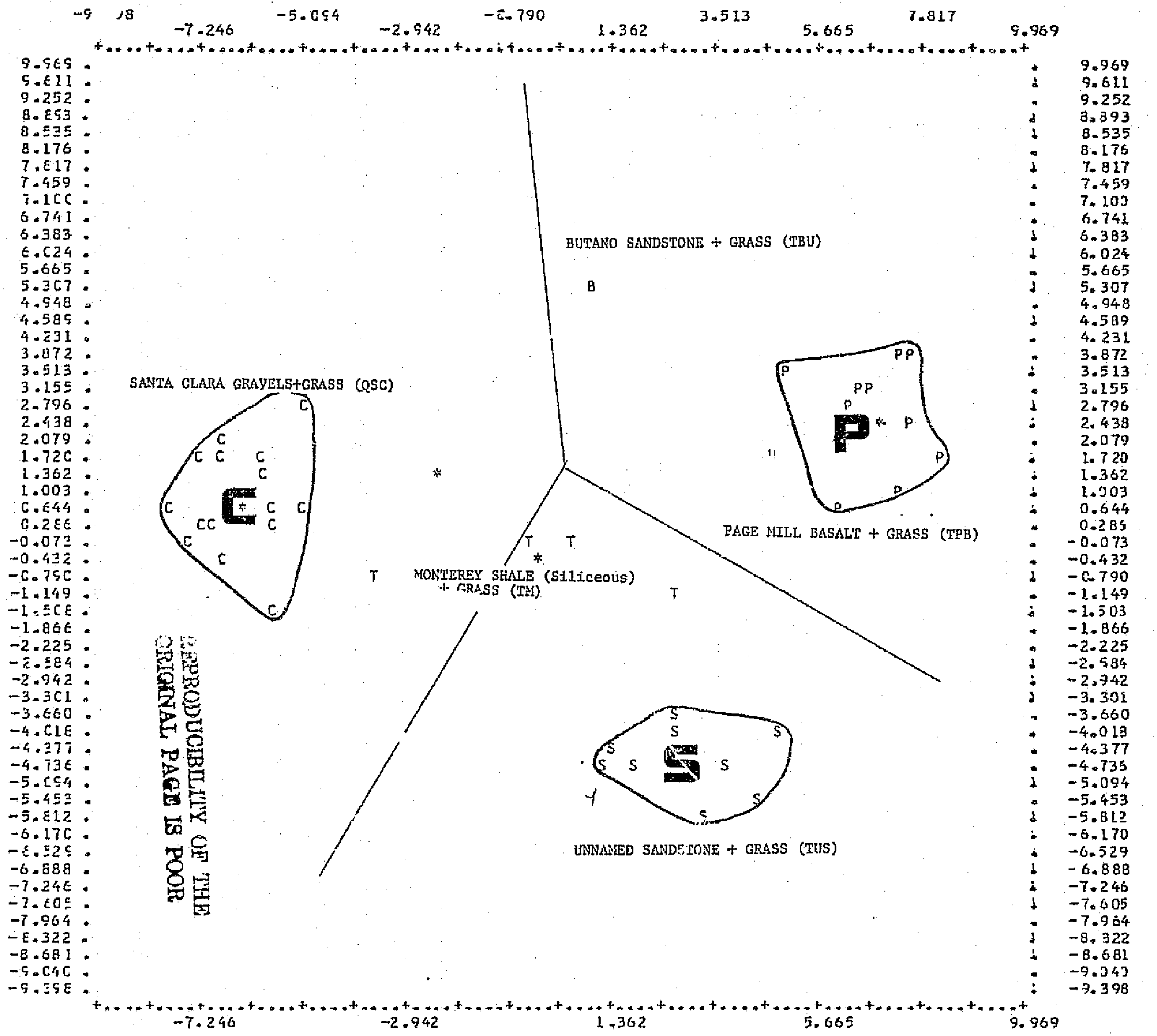

2.3.4.24 Canonical Plot (BMD07M); 3 groups + 2 test groups; 65 variables, 10 step. Run A2, no deletions (Success = 100%)

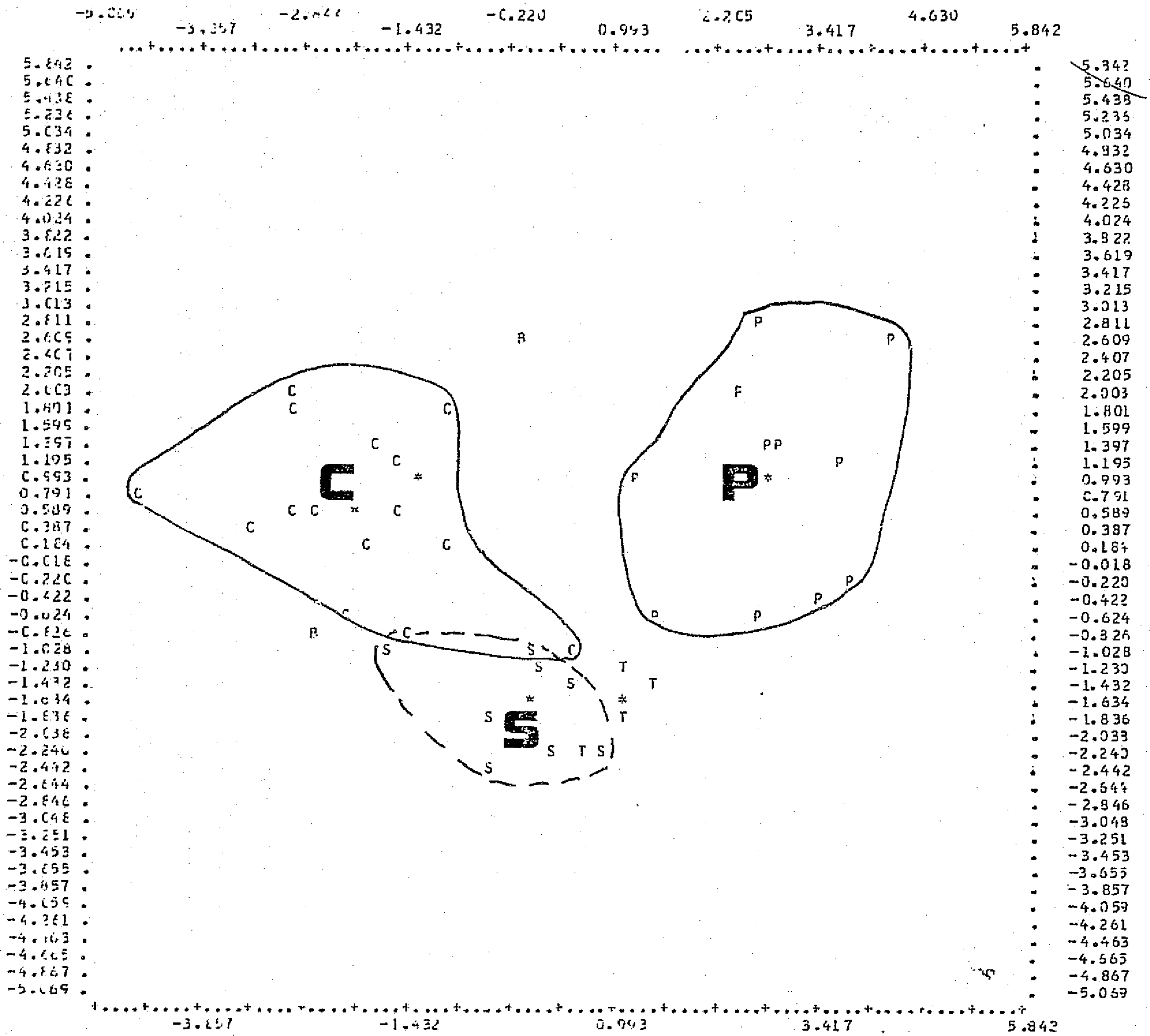

2.3.4.25 Canonical Plot (BMDO7M); 5 groups, 54 variables, 5 step. Run B1,
Deleted Altitude-of-station, and plants species (10)
(Success = 88%)

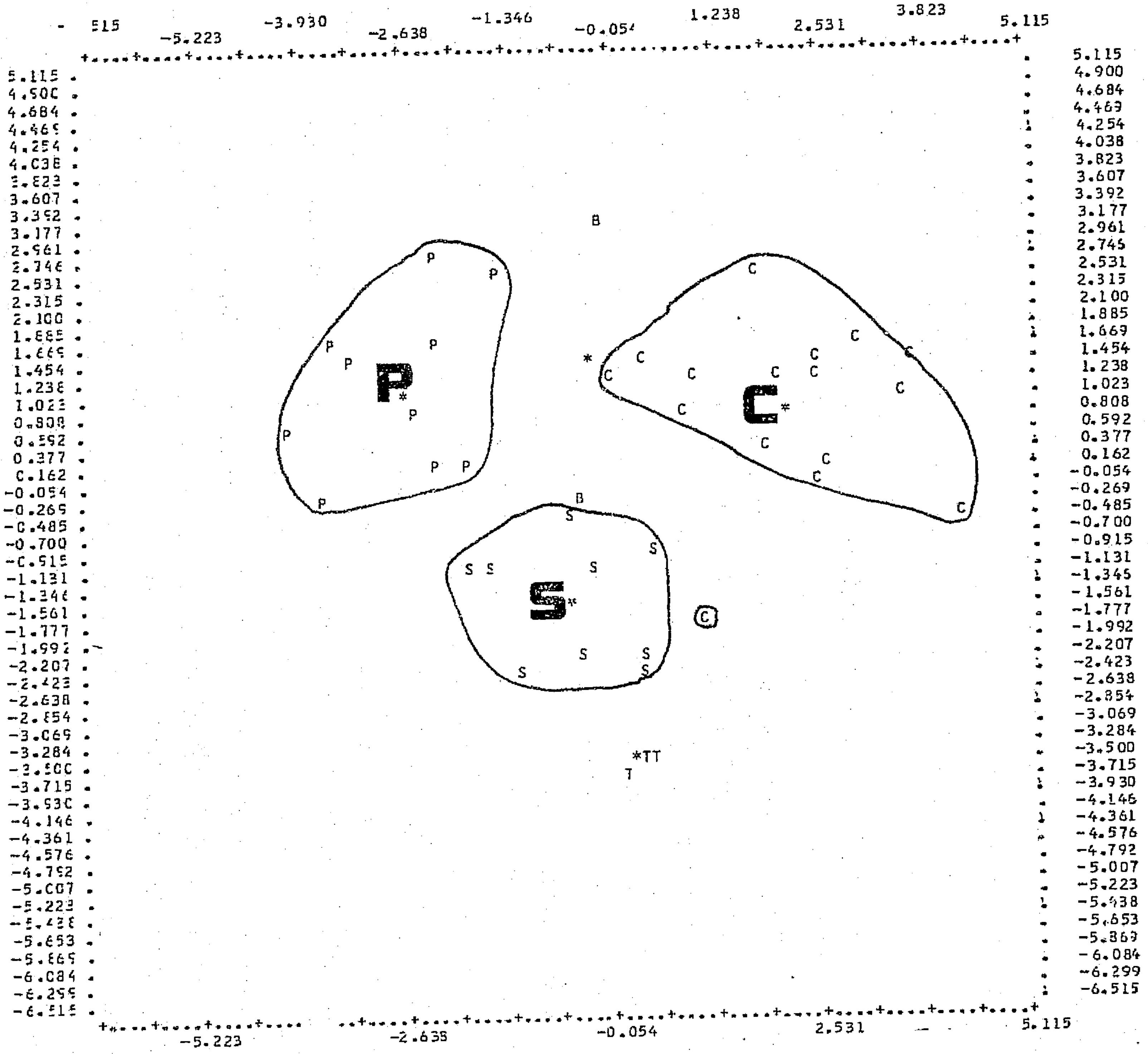

2.3.4.26 Canonical Plot (BMDO7M); 5 groups, 51 variables, 5 step. Run C, deleted bandpasses (4), altitude (1) and plant species (10)

Success = 98%)

182

2.3.5 CORRELATION OF ERTS SPECTRA WITH ROCK/SOIL TYPES IN CALIFORNIA GRASSLAND AREAS

2.3.5.1 ABSTRACT

A seasonal study of ERTS-CCT data, accomplished by means of four band spectra plots of normalized reflectance, indicates that in the San Francisco Bay and adjacent Coast Range grassland areas, soils mapping or classification by computer techniques is possible at the end of the dry or grass dieback season. Excellent correlation is shown between ground reflectance measurements and CCT data at three test sites and two different soil types: serpentine and sedimentary. The uniqueness of their spectra is then demonstrated by the successful application of STANSORT, a computerized classification technique developed by the Stanford Remote Sensing Laboratory.

2.3.5.2 INTRODUCTION

The primary purpose of this investigation was to determine if the serpentine exposures and soils on the San Francisco Peninsula could be detected uniquely by means of ERTS imagery and/or the related CCT data. In doing so it was also hoped to evolve a methodology which would be useful in conducting similar studies in the future. As envisioned, the imagery (individual bands and color composites) were to be studied first to determine if these serpentine areas could be detected visually and then a study made to determine if any uniqueness existed in their four band spectra. This property, if existent, could then be utilized as a basis for the development of a computerized classification program to automize the detection and mapping procedure.

In the course of this investigation, it became evident that the seasonal response of the vegetative cover could be most important in obliterating or enhancing the information relating to the serpentine soil. Therefore, a careful systematic, spectral study of the CCT data for the yearly cycle was undertaken by means of four band radiance and reflectance plots of the test areas. Off season correlations of serpentine soil spectra vs. serpentine soil/grass spectra were also made possible by means of a fortuitous grass fire in the study area which had exposed a large area of bare soil. These correlations ultimately led to the conclusion that the soil/grass spectra were in fact essentially soil spectra at the end of the dry or dieback season.

After an extensive ground measurement program had substantiated the unique character of the serpentine soil spectra the study was expanded to include a sedimentary area on the east side of the Coast Range upon which

a yearly controlled burn occurred. The same seasonal trends were evident and a strong correlation between ERTS reflectance spectra and ground measured spectra was again found. In addition, the spectra of the sedimentary soil was found to be distinguishable from the background as well as the serpentine soils studied on the San Francisco Peninsula.

The clustering program STANSORT developed by the Stanford Remote Sensing Laboratory was then applied to the study areas with significant success.

2.3.5.3 AREAS STUDIED

Two major exposures of serpentine rocks and soils mapped by the USGS, on the San Francisco Peninsula, were selected for study and are shown in Figure 2.351 Area I exposures consist of highly weathered blue-gray serpentine, only a small percentage of which is outcrop, the remainder decomposed fragments, grading to a serpentine soil. These exposures are to the east of, and adjacent to, the Crystals Springs Reservoir segment of the San Andreas Fault Zone. They are surrounded by and occasionally penetrate the various rocks of the Franciscan assemblage. To a large degree the northern section of Area I is obliterated by housing developments and roads. Therefore, the study was focused on the southern section which is largely within the Crystal Springs watershed and is public land.

The vegetation of this site, composed of annual broad leaved herbs and annual grasses, is readily distinguishable from the surrounding grassland on nonserpentine soil. It is marked by a different species composition, smaller

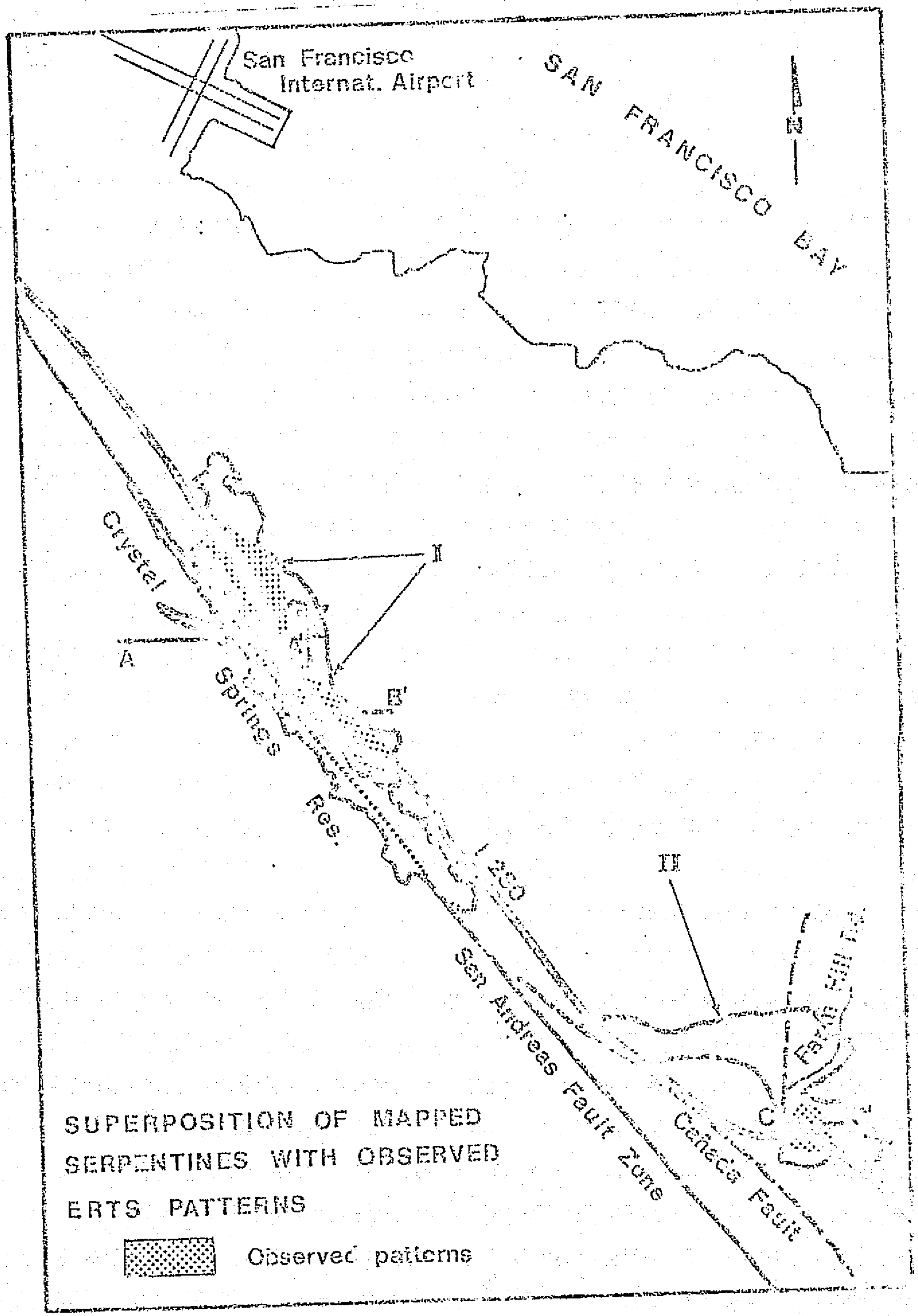

Figure 2.3.5.1 Superposition of Mapped Serpentines with Observed ERTS Patterns

size (height less than one foot), sparser cover and earlier onset of senescence and drying. The dominant broad leaved herbes are Layia platyglossa (tidy tips), Orthocarpus sp. (owl's clover) and Plantago erecta (California plantain) and the dominant grasses are Bromus mollis (soft chess) and Lolium multiflorum (ryegrass).

Area II is approximately 4 miles south of the Crystal Springs Reservoir, again on the east side and adjacent to the San Andreas Fault Zone. Because of the housing developments and roads an open field area of roughly 60 acres at the south end was selected for study. The serpentine is heavily weathered and blue gray in color with only a small percentage of outcrop; the remainder decomposed fragments and serpentine soil. Interstate 280 transverses the south end of the area exposing large amounts of fresh serpentine in the roadcuts.

The serpentine vegetation of the Farm Hill Road site is clearly differentiated from the surrounding nonserpentine vegetation by the same features that distinguish the Crystal Springs Road serpentine vegetation, i.e., a different species composition, smaller size, sparser cover and earlier onset of senescence. It is made up of annual broad leaved herbs and grasses and shares several species in common with the Crystal Springs site. The dominant plants are a grass, Festuca sp. (fescue), and the broad-leaved herbs, Layia platyglossa (tidy tips) and Hemizonia sp. (tarweed).

The third area studied consists of a sedimentary area located in the southeast quadrant of the Midway 7.5' topographic quadrangle (See Figure 2.3.5.2) This area lies within the Lawrence/Livermore Radiation Laboratories Field Test

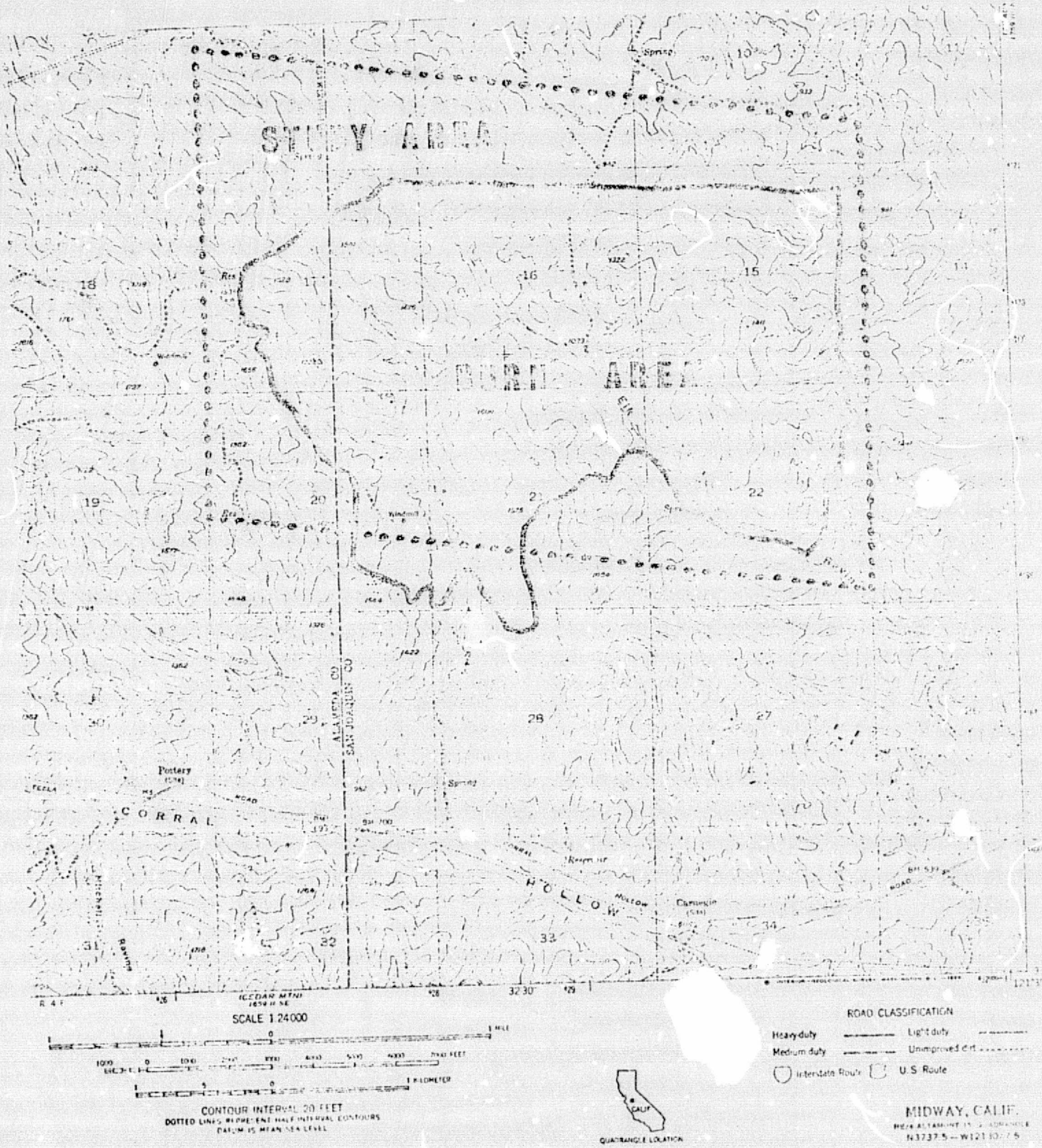

Figure 2.3.5.2 Midway Test Site Location

Site 300 and is largely a yearly controlled burn area. The study site is typical of the rolling grassy eastern foothills of the Coast Range. It is roughly 600 acres in extent, crossing elevations varying from 1000 to 1600 feet. The sediments are semi-consolidated sandstones with the outcrops again a minor percentage compared to the soils derived from the sandstone. The vegetation is that typically described as a California valley grassland community, dominated by annual species of the grasses Bromus (bromegrass), Festuca (fescue), Avena (oat) and others.

2.3.5.4 VISUAL STUDY

A visual study of available ERTS imagery, both the individual bands and color composites covering the San Francisco Peninsula was accomplished. Also included was U-2 imagery taken during the ERTS Simulation Program. It was noted, in the ERTS frame date 6 October 1972, that a distinct dark gray pattern existed which seemed to coincide generally with the Area I serpentine east of Crystal Springs Reservoir. (Fig. 2.3.5.1) Study of the imagery before and after this date indicated that the pattern persisted with diminishing intensity back to 26 July 1972 after which it could not be seen. The pattern was not evident again until 26 August 1973, at which time it was faintly discernible. The appearance and disappearance of the observed pattern seemed to correlate with the die-back and growth cycle of the grass in this area.

Review of the ERTS color composites substantiated the above, with the pattern readily discernible at the dates noted, as a dark purplish tone. In addition, similar tones were also evident within Area II, south of Farm Hill Road, coinciding with the open field mentioned previously.

2.3.5.5 RADIANCE SPECTRA

To study the possible uniqueness of the tones associated with the serpentine areas, the radiance values of ERTS-CCT pixels traversing these and adjacent areas where obtained and their spectra plotted. These pixel traverses, across the Crystal Springs Reservoir and Farm Hill Road areas, are indicated in Figure 2.3.5.1.

Table 2.3.5.1 lists the mean radiance values, standard deviations and coefficients of variation relative to terrain types, across these traverses. Typical spectra are plotted in Fig. 2.3.5.4. Radiance throughout this report is presented as digital or word count levels. Should absolute value of radiance be desired conversion factors must be applied. At this point no atmospheric corrections were made. Fig. 2.3.5.5 contains radiance spectra plots of the traverses indicated in Fig. 2.3.5.1 The location of specific features was accomplished by means of a skewed pixel overlay cf the proper scale and an ortho-photomap (1:24000), as well as aerial photographs of the areas.

It can be seen from examination of the spectra plots that the serpentine and grass areas as well as Interstate 280, water and the forested areas appear to have distinctive spectra. It is interesting to note that while the pixel spectra across the forested area in traverse AA are generally the same shape, peak values are evident at four points. The aerial photographs indicate that these coincide with the hilly terrain across which the traverse was made. Apparently, this effect is caused by the variation in sun angle due to hill slope. The repetitiveness of the individual water spectra is also very striking.

TABLE 2.3.5.1 - - REFLECTANCE STATISTICS PLOTTED FROM SELECTED ERTS PIXEL TRAVERSES AA, BB AND CC

	TREES				WATER				SOIL/GRASS				I 280			
	4	5	6	7	4	5	6	7	4	5	6	7	4	5	6	7
Mean	19.33	11.20	20.88	12.25	19.14	8.89	5.67	1.82	26.53	21.67	20.88	10.12	38.86	36.14	32.4	13.79
Std Dev	1.48	2.09	3.42	2.72	0.90	0.82	1.01	0.57	1.51	1.48	2.13	0.86	3.03	2.88	3.08	1.53
Coef of Var	0.08	0.19	0.16	0.22	0.05	0.09	0.18	0.43	0.06	0.09	0.10	0.08	0.08	0.08	0.10	0.11

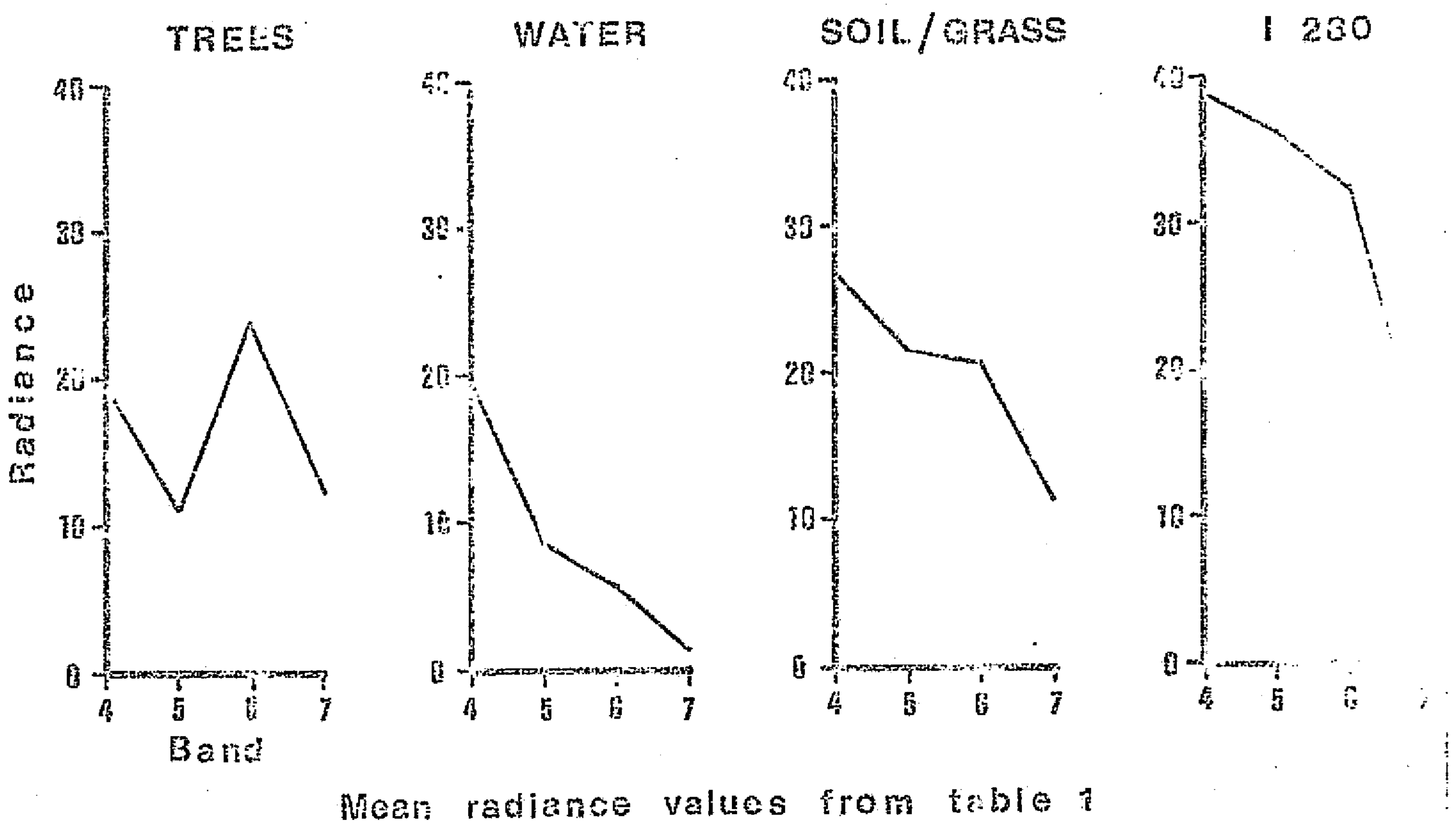

Figure 2.3.5.3 Radiance Spectra - ERTS Frame ID 1075-18173, 6 October 1972

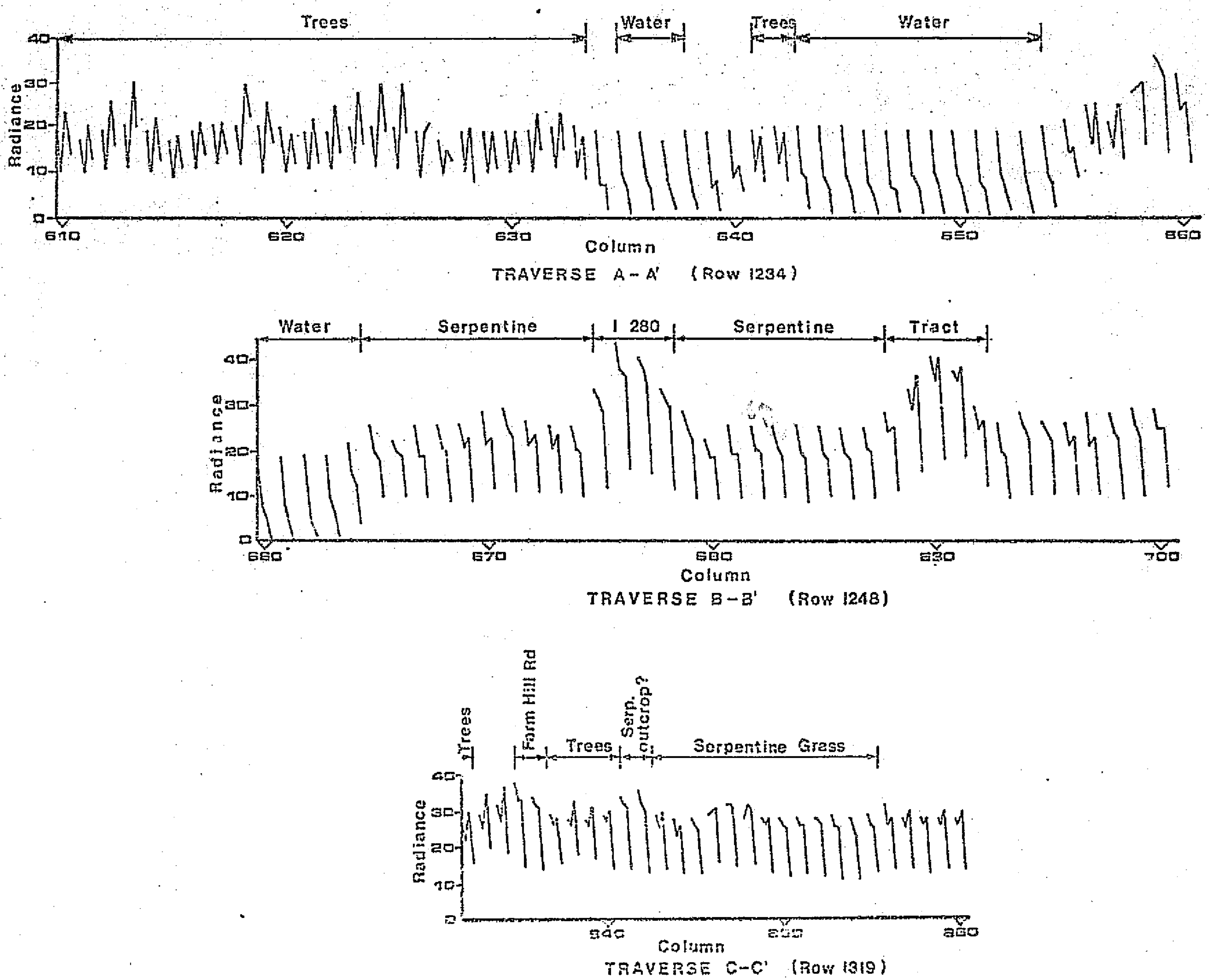

Figure 2.3.5.4 Radiance Spectra Traverses (By Pixel) ERTS Frame ID 1075-18173

In traverse BB, the constancy of the pixel spectra of the serpentine soil/grass area on the east side of Interstate 280 as contrasted to the west can be correlated to the tones evident in the ERTS imagery. The slight variability evident on the west side is attributed to variability in the soil, grass cover or both. It seems apparent that the spectra obtained is a function of the interaction of the soil and degree and type of grass cover which in turn is a function of the season of the year.

2.3.5.6 SEASONAL REFLECTANCE SPECTRAL STUDY

Based on the results of the visual and radiance spectra study it was evident that the serpentine soil/grass signature was unique at the 6 October 1972 date. It also seemed possible that because the grass die back in this part of California, was complete by this date, that the recorded spectra was essentially that of the soil. To substantiate the above, a systematic study of the soil plus grass interaction at the Crystal Springs area through the yearly cycle was instituted. Due to a fortuitous 15 acre grass fire, within Area I which occurred 1 July 1973 and easily seen in the ERTS imagery, it was also possible to include spectra of the devegetated burn area in the study for comparative purposes. This study was accomplished by means of four band spectra plots of the mean ground radiance values of the selected test areas and then the values normalized to band 4. In so far as was possible identical ten pixel areas within the following ERTS frames were utilized, covering an 11 month time interval:

ID 1075-18183	6 October 1972
ID 1165-18175	4 January 1973
ID 1185-18175	22 January 1973
ID 1291-18182	10 May 1973
ID 1309-18181	28 May 1973
ID 1345-18180	3 July 1973
ID 1363-18173	21 July 1973
ID 1399-18170	26 August 1973

In order to be able to compare results from the ERTS multispectral scanner data over these series of tapes, corrections were made for the perturbing effects of radiation scattered by the atmosphere and the variation in irradiance on the scene with solar zenith angle. These effects were removed by studying selected targets of low (zero) reflectance and high known reflectance (Honey and Lyon, 1974). In the scene studied, a waste products treatment pond at an oil refinery near Suisun Bay, with bandpass reflectance of <0.5% in all four bands was utilized as the zero reflectance standard. A concrete parking apron for aircraft at Moffet Field NAS California with reflectances of 27.8, 31.0,30.0 and 32.3 percent bandpass in the four ERTS channels was used for the high reflectance standard. The factors derived were applied as follows:

$$\text{Target Reflectance} = \frac{\text{Target Radiance-Dump Reflectance (Meas)}}{\text{Concrete Radiance-Dump Reflectance(Meas)}} \times \begin{array}{l}\text{Concrete}\\ \text{Reflectance}\\ \text{(Meas)}\end{array}$$

Results obtained are presented in Table II. Radiance plots as well as normalized reflectance are presented in Figure 2.3.5.6.1. Study of this data reveals the following:

2.3.5.6.1 Interpretability of the four band spectra is greatly improved by the

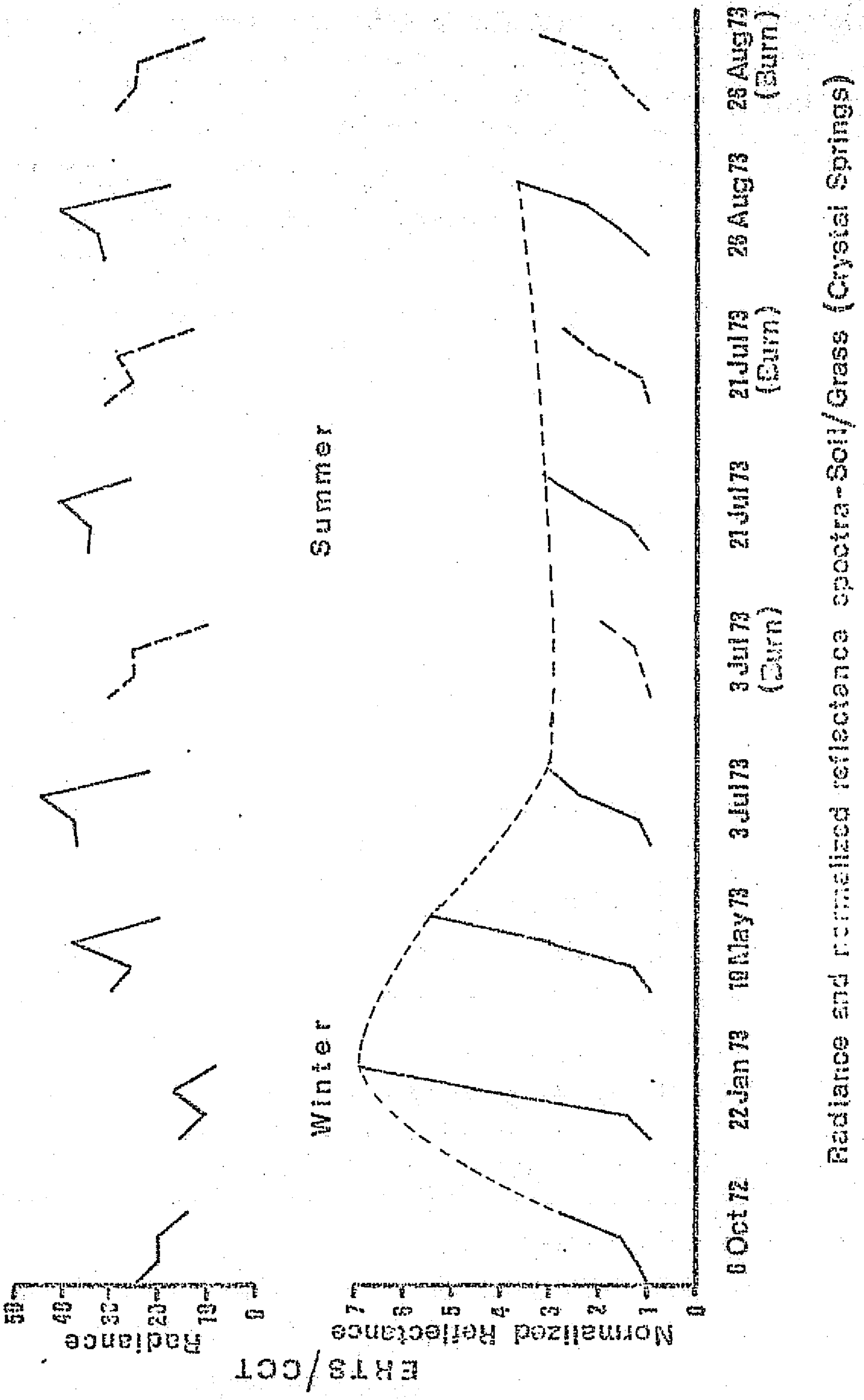

Figure 2.3.5.5 Radiance and Normalized Reflectance Spectra - Soil/Grass (Crystal Springs)

TABLE 2.3.5.2 - ERTS-CCT RADIANCE DATA

GROUP STATISTICS AND NORMALIZED REFLECTANCES

ID 1075-18183 CRYSTAL SPRINGS 6 October 1972

	4	5	6	7
Mean	25.40	20.40	20.20	9.60
Std. Dev.	0.84	1.06	1.55	1.26
Coef. of Var.	0.03	0.05	0.08	0.13
Reflectance	5.11	6.26	8.19	13.97
Norm. Refl.	1.00	1.23	1.58	2.73

ID 1183-18175 CRYSTAL SPRINGS 22 January 1973

	4	5	6	7
Mean	16.80	11.50	17.10	9.10
Std. Dev.	0.63	1.35	1.73	0.99
Coef. of Var.	0.04	0.12	0.10	0.11
Reflectance	3.01	4.43	13.65	20.80
Norm. Refl.	1.00	1.47	4.53	6.90

ID 1291-18182 CRYSTAL SPRINGS 10 May 1973

	4	5	6	7
Mean	29.70	26.20	37.90	21.10
Std. Dev.	1.95	1.93	4.86	2.56
Coef. of Var.	0.07	0.07	0.13	0.12
Reflectance	4.85	7.14	14.45	27.00
Norm. Refl.	1.00	1.47	2.98	5.57

ID 1345-18180 CRYSTAL SPRINGS 3 July 1973

	4	5	6	7
Mean	37.50	37.70	44.20	22.60
Std. Dev.	1.18	3.37	2.25	1.35
Coef. of Var.	0.03	0.09	0.05	0.06
Reflectance	8.63	11.19	20.86	25.60
Norm. Refl.	1.00	1.30	2.42	2.97

TABLE 2.3.5.2 CONTINUED

ID 1345-18180 CRYSTAL SPRINGS (Burn Area) 3 July 1973

	4	5	6	7
Mean	31.00	25.40	25.60	10.60
Std. Dev.	2.45	4.22	6.54	3.6
Coef. of Var.	0.08	0.17	0.26	0.34
Reflectance	5.60	6.03	7.66	11.38
Norm. Refl.	1.00	1.08	1.37	2.03

ID 1363-18173 CRYSTAL SPRINGS 21 July 1973

	4	5	6	7
Mean	35.10	34.60	41.70	21.00
Std. Dev.	2.57	4.40	2.11	1.49
Coef.of Var.	0.07	0.13	0.05	0.07
Reflectance	7.29	10.89	16.80	23.66
Norm. Refl.	1.00	1.49	2.32	3.25

ID 1363-18173 CRYSTAL SPRINGS (Burn Area)

	4	5	6	7
Mean	31.00	25.50	29.20	13.50
Std. Dev.	3.06	3.75	9.08	5.78
Coef. of Var.	0.10	0.14	0.32	0.43
Reflectance	5.36	5.98	10.74	14.82
Norm. Refl.	1.00	1.12	2.01	2.76

ID 1399-18170 CRYSTAL SPRINGS 26 August 1973

	4	5	6	7
Mean	31.50	32.40	35.40	18.60
Std. Dev.	1.27	1.65	1.71	0.52
Coef. of Var.	0.04	0.05	0.05	0.03
Reflectance	5.96	9.90	18.30	21.66
Norm. Refl.	1.00	1.66	3.10	3.63

TABLE 2.3.5.2 CONTINUED

ID 1399-18170 CRYSTAL SPRINGS (Burn Area) 26 August 1973

	4	5	6	7
Mean	28.10	25.10	24.60	12.00
Std. Dev.	1.73	3.00	4.25	3.13
Coef. of Var.	0.06	0.10	0.07	0.26
Reflectance	4.20	6.52	7.93	13.54
Norm. Refl.	1.00	1.55	1.89	3.22

ID 1075-18173 FARM HILL ROAD 6 October 1972

	4	5	6	7
Mean	28.80	25.50	28.30	13.40
Std. Dev.	1.62	1.35	1.49	0.97
Coef. of Var.	0.06	0.05	0.02	0.07
Reflectance	7.28	9.12	12.9	19.5
Norm. Refl.	1.00	1.25	1.72	2.68

ID 1075-18183 MIDWAY 6 October 1972

	4	5	6	7
Mean	32.60	31.73	30.07	13.33
Std. Dev.	3.48	4.77	3.47	2.06
Coef. of Var.	0.11	0.15	0.12	0.15
Reflectance	9.49	12.58	13.89	19.39
Norm. Refl.	1.00	1.33	1.46	2.04

ID 1165-18175 MIDWAY 4 January 1973

	4	5	6	7
Mean	17.73	12.93	22.20	12.60
Std. Dev.	2.15	3.31	5.10	4.36
Coef. of Var.	0.12	0.26	0.23	0.29
Reflectance	3.37	4.93	21.25	28.80
Norm. Refl.	1.00	1.46	6.28	8.55

TABLE 2.?.5.2 CONTINUED

ID 1291-18182 MIDWAY 10 May 1973

	4	5	6	7
Mean	34.80	41.13	52.73	29.93
Std. Dev.	3.36	6.53	8.22	5.54
Coef. of Var.	0.10	0.16	0.16	0.19
Reflectance	7.40	14.15	22.00	37.03
Norm. Refl.	1.00	1.91	2.97	5.00

ID 1309-18181 MIDWAY 28 May 1973

	4	5	6	7
Mean	39.60	51.47	59.13	31.33
Std. Dev.	2.87	4.82	4.55	2.38
Coef. of Var.	0.07	0.09	0.08	0.08
Reflectance	10.30	18.37	26.07	37.13
Norm. Refl.	1.00	1.78	2.53	3.60

ID 1309-18181 MIDWAY (Burn Area) 28 May 1973

	4	5	6	7
Mean	29.40	27.53	26.33	11.27
Std. Dev.	2.47	4.78	6.10	3.08
Coef. of Var.	0.08	0.17	0.23	0.27
Reflectance	5.20	7.76	9.66	13.36
Norm. Refl.	1.00	1.49	1.86	2.57

ID 1345-18180 MIDWAY 3 July 1973

	4	5	6	7
Mean	41.40	53.6	58.53	30.67
Std. Dev.	4.12	7.55	8.86	5.01
Coef. of Var.	0.10	0.14	0.15	0.16
Reflectance	10.45	17.84	22.86	35.16
Norm. Refl.	1.00	1.71	2.19	3.36

TABLE 2.3.5.2 CONTINUED

ID 1345-18180 — MIDWAY (Burn Area) — 3 July 1973

	4	5	6	7
Mean	33.07	33.00	31.60	14.93
Std. Dev.	3.84	6.46	6.99	4.20
Coef. of Var.	0.12	0.20	0.22	0.28
Reflectance	6.57	9.22	10.43	16.51
Norm. Refl.	1.00	1.40	1.59	2.51

ID 1363-18173 — MIDWAY — 21 July 1973

	4	5	6	7
Mean	46.93	60.40	64.27	31.60
Std. Dev.	6.88	11.84	12.07	5.93
Coef. of Var.	0.15	0.20	0.19	0.19
Reflectance	13.00	21.43	27.23	36.27
Norm. Refl.	1.00	1.65	2.09	2.79

ID 1363-18173 — MIDWAY (Burn Area) — 21 July 1973

	4	5	6	7
Mean	33.47	33.07	31.33	14.07
Std. Dev.	3.23	5.51	6.35	3.17
Coef. of Var.	0.10	0.17	0.20	0.23
Reflectance	6.50	9.33	11.29	15.49
Norm. Refl.	1.00	1.44	1.74	2.38

ID 1399-18170 — MIDWAY — 26 August 1973

	4	5	6	7
Mean	43.13	56.93	63.07	30.87
Std. Dev.	3.81	5.43	7.01	3.96
Coef. of Var.	0.81	0.10	0.11	0.13
Reflectance	11.99	21.25	27.49	36.76
Norm. Refl.	1.00	1.77	2.29	3.07

TABLE 2.3.5.2 CONTINUED

ID 1399-18170 MIDWAY (Burn Area) 26 August 1973

	4	5	6	7
Mean	35.93	37.27	37.67	16.60
Std. Dev.	4.61	5.74	7.54	3.40
Coef. of Var.	0.13	0.15	0.20	0.20
Reflectance	8.26	12.16	14.58	19.20
Norm. Refl.	1.00	1.47	1.77	2.32

application of the atmospheric corrections and normalization of the data to band 4.

2.3.5.6.2 The normalized reflectance of the soil/grass is at a maximum (particularly channels 6 and 7) at the height of the rainy season, 22 January 1973; roughly twice as high as that during 6 October 1972, near the end of the dry season.

2.3.5.6.3 The normalized reflectance of the soil/grass gradually diminishes with the end of the rainy season and the entry into the summer dry-out period.

2.3.5.6.4 In the burn area, on 3 July 1973, the normalized reflectance spectra drops to a minimum value, possibly as a result of both the devegetation and the residue of the carbonized-grass remains.

2.3.5.6.5 By 21 July 1973, the normalized reflectance spectra values in the area have increased, probably as a result of the dispersion of the carbonized ash by the wind. They now approximate the values at 6 October.

2.3.5.6.6 A slight increase in the normalized reflectance is noted at 26 August 1973, probably due to some revitalization of the grass in the burn area.

2.3.5.6.7 The 6 October 1972 reflectances are very close to those of the burn area at 3 July and 26 August 1973.

It would appear that based on the above, a strong likelihood exists that the reflectance spectra of 6 October is that of the serpentine soil with little or no reflectance introduced by the dead grass.

A 10 pixel block within the Farm Hill Road test site, (6 October 1972, serpentine soil/grass) was also selected and the normalized reflectance spectra plotted in Fig 2.3.5.7. A strong correlation is found with the

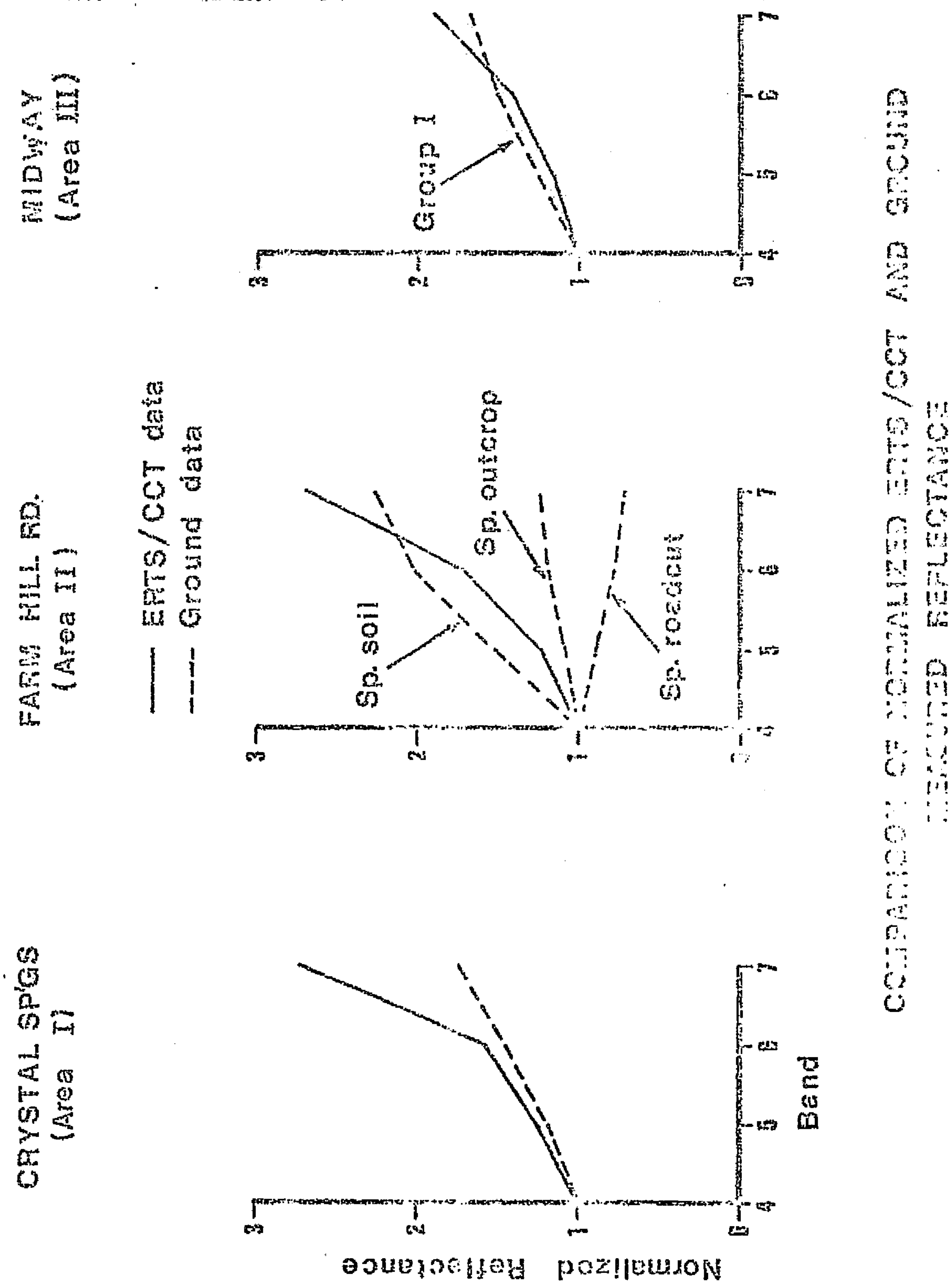

Figure 2.3.5.6 Comparison of Normalized ERTS-CCT and Ground Measured Data

reflectance spectra at Area I at the same time of year. Based on these results, it was decided to broaden the scope of the study somewhat to see if the same trends were obtained at a third site in which the terrain soil was of a different type and at which a similar burn situation existed. This test site (Area III) was located at the Lawrence/Livermore Radiation Laboratories Field Test Site 300 at which controlled burns were used to reduce the likelihood of uncontrolled fires as a result of explosive tests. It is on the east side of the Coast Range, approximately 15 miles east of Livermore. The terrain type had been mapped as marine sediments. In addition to another soil type, a comprehensive verification program of ground reflectance measurements of bare soil was to be accomplished at all three test sites.

The results of the seasonal ERTS-CCT normalized reflectance spectra study at Area III (Midway) is presented in Table 2.3.5.2 and Fig. 2.3.58. Because of the size of this site, approximately 960 acres, a grid pattern, at intervals of 10 pixels, was utilized across the burn area to obtain the reflectance spectra data. It can readily be seen that the same trends exist, as follows:

2.3.5.6.8 The normalized reflectance is at a maximum in the winter, 4 January 1973 and gradually diminishes with the end of the rainy season and entry into the summer dry-out period.

2.3.5.6.9 The 6 October 1972 reflectance spectra and that of the burn area are again comparable.

A comparison of the reflectance spectra for Area III (Marine sediments) and Areas I and II (serpentine soils) indicate that they are considerably different, particularly in bands 6 and 7, thus leading to the conclusion that computerized classification could be applied.

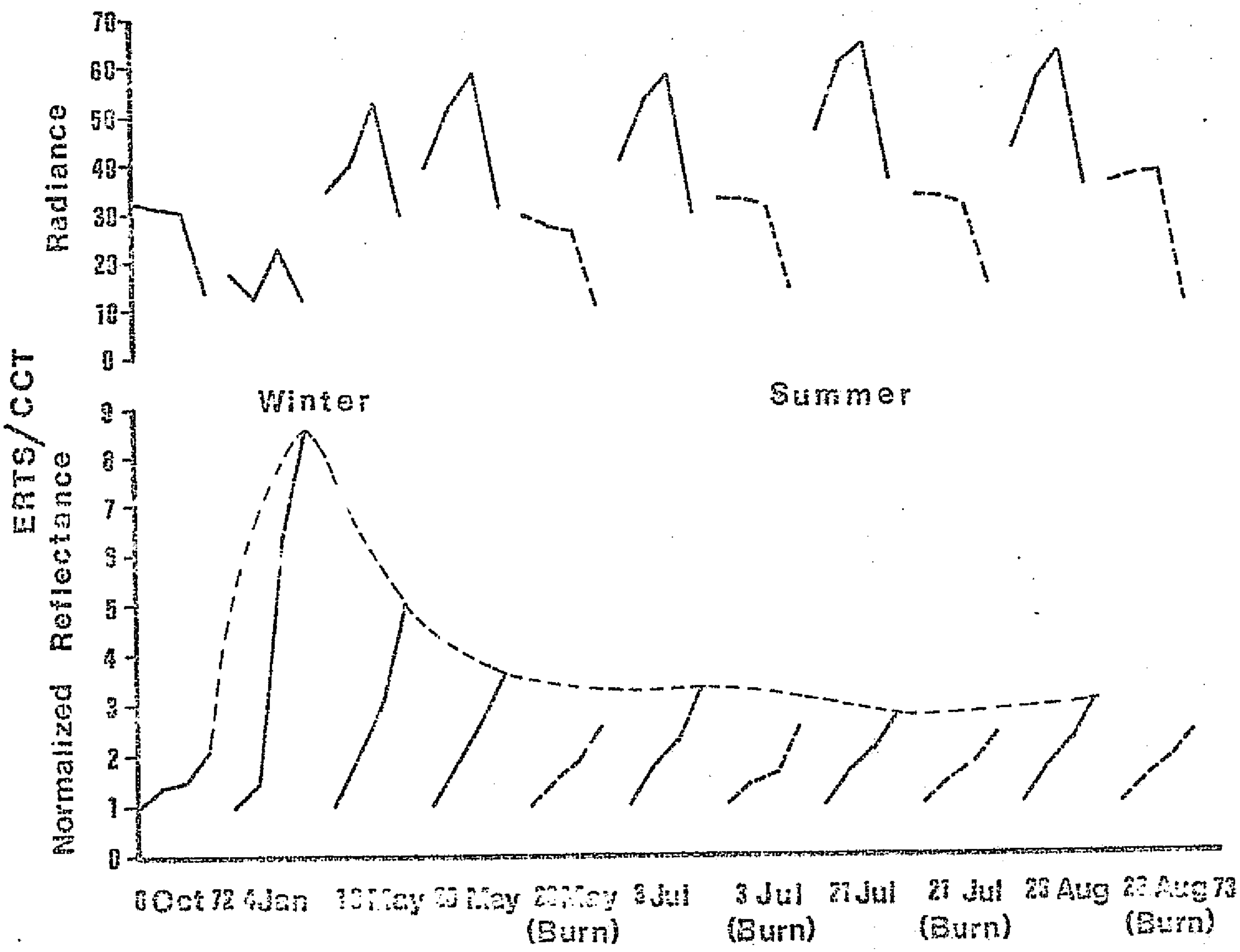

Radiance and normalized reflectance spectra – Soil/Grass (Midway)

Figure 2.3.5.7 Radiance and Normalized Reflectance Spectra - Soil/Grass (Midway)

205

The statistics relative to the ground reflectance measurements taken at the test sites are presented in Table III and Fig. 2.3.5.7. An Exotech ERTS Radiometer and scaled down satellite geometry were utilized to obtain this data. Fig. 2.3.5.7 compares the ERTS-CCT spectra with that obtained above. Study of this data reveals the following:

2.3.5.6.10 The ERTS-CCT normalized reflectance spectra for serpentine soils, at 6 October 1972 are almost identical at Crystal Springs and Farm Hill Road.

2.3.5.6.11 The ground reflectance spectra obtained at Midway correlate very well with that derived from the 6 October 1972 ERTS-CCT data.

2.3.5.6.12 The ground reflectance spectra for serpentine soil at Farm Hill Road compares very favorably with the CCT data. The ground spectra for the roadcut- and outcrop-serpentines, while comparable to each other are substantially different than that of the soil. It is believed that because of the small areal extent of the outcrops as compared to the soil and the limiting resolution of the ERTS system, the outcrops have little integrated effect and essentially only the serpentine soil is detectable on the CCT data.

2.3.5.6.13 The correlation of the ground spectra obtained at Crystal Springs with the ERTS-CCT data is not quite as good. It is believed that this is due to the infiltration of materials from adjacent soils derived from nearby Franciscan sandstone exposures.

2.3.5.6.14 A significant difference is seen in both the ERTS-CCT spectra and the ground spectra for the serpentine soils at Crystal Springs and Farm Hill Road and the sediments at Midway.

In general, from the season/spectral study made and the ground measurements obtained, it can be concluded that the four band ERTS spectra for serpentine soils and sedimentary soils are sufficiently different from each other at the end of the dry or dieback season, to be distinguished from each other and the

TABLE 2.3.5.3 - GROUND MEASURED GROUP REFLECTANCE STATISTICS, AND NORMALIZED REFLECTANCES

CRYSTAL SPRINGS (Group 1)

	4	5	6	7
Mean	8.44	10.26	12.43	14.36
Std. Dev.	2.08	2.17	2.56	2.80
Coef. of Var.	0.25	0.21	0.21	0.19
Norm. Refl.	1.00	1.22	1.47	1.70

CRYSTAL SPRINGS (Group 2)

	4	5	6	7
Mean	10.96	13.34	15.61	17.25
Std. Dev.	0.96	1.60	1.86	3.20
Coef. of Var.	0.09	0.12	0.12	0.19
Norm. Refl.	1.00	1.22	1.42	1.57

FARM HILL ROAD (OUTCROP-Group 1)

	4	5	6	7
Mean	14.99	16.02	17.41	18.37
Std. Dev.	1.29	2.41	2.46	2.85
Coef. of Var.	0.09	0.15	0.14	0.16
Norm. Refl.	1.00	1.07	1.16	1.23

FARM HILL ROAD (OUTCROP-Group 2)

	4	5	6	7
Mean	14.81	15.75	16.53	19.69
Std. Dev.	1.33	1.89	2.24	2.53
Coef. of Var.	0.09	0.12	0.14	0.14
Norm. Refl.	1.00	1.06	1.12	1.19

FARM HILL ROAD (I280 ROAD CUT)

Mean	23.77	20.68	18.29	17.28
Std. Dev.	2.40	1.87	2.23	1.71
Coef. of Var.	0.10	0.09	0.12	0.10
Norm. Refl.	1.00	0.87	0.77	0.73

TABLE 2.3.5.3 - CONTINUED

FARM HILL ROAD (SOIL)

	4	5	6	7
Mean	7.43	11.33	14.96	16.97
Std. Dev.	0.45	0.65	0.58	0.59
Coef. of Var.	0.06	0.06	0.04	0.03
Norm. Refl.	1.00	1.52	2.01	2.28

MIDWAY (SOIL-GROUP 1)

	4	5	6	7
Mean	15.09	18.83	22.95	25.33
Std. Dev.	0.77	0.98	1.79	1.68
Coef. of Var.	0.55	0.05	0.08	0.07
Norm. Refl.	1.00	1.25	1.52	1.68

MIDWAY (SOIL-GROUP 2)

	4	5	6	7
Mean	10.09	12.03	14.22	16.70
Std. Dev.	0.50	0.62	0.93	0.59
Coef. of Var.	0.05	0.05	0.07	0.04
Norm. Refl.	1.00	1.19	1.41	1.66

MIDWAY (SOIL-GROUP 3)

Mean	15.79	18.81	22.02	23.97
Std. Dev.	1.66	1.43	1.78	3.38
Coef.of Var.	0.11	0.08	0.08	0.14
Norm. Refl.	1.00	1.19	1.39	1.52

background by computerized clustering.

2.3.5.7 CLASSIFICATION TECHNIQUE

The classification procedure utilized to demonstrate the uniqueness of the soils spectra studied is an interactive program package called STANSORT, developed at the Stanford Remote Sensing Laboratories (Honey et al, 1974). This system provides an extremely rapid, flexible and low cost tool for scene classifcationn. It is a non-statistical, unsupervised classification technique in which the data is split into its distinguishable groups with no prior knowledge of the groups. The primary classification procedure, utilizes a search, with variable gate widths, for similarities in the normalized or un-normalized digitized spectra. Results obtained from the application of STANSORT are presented in Fig. 2.3.5.9 and 2.3.5.10, the Farm Hill Road and Midway test sites respectively. Training was accomplished on the serpentine soil spectra of Farm Hill Road which is indicated by the clustering in Figure 2.3.5.9. Continued search for the serpentine spectra at Midway (the sedimentary test site)using identical classifiers, as expected, reveals its complete absence except for the single pixel indicated in Figure 2.3.5.10.

```
un-normalized cluster results for
FH1
erts tape 1075-1817330 2 4
area begins at row 1598,pixel 845 from edge of frame
tolerance level was 13
upper value of range for channel 4=30
lower value of range for channel 4=27
upper value of range for channel 5=26
lower value of range for channel 5=24
upper value of range for channel 6=29
lower value of range for channel 6=26
upper value of range for channel 7=14
lower value of range for channel 7=12
```

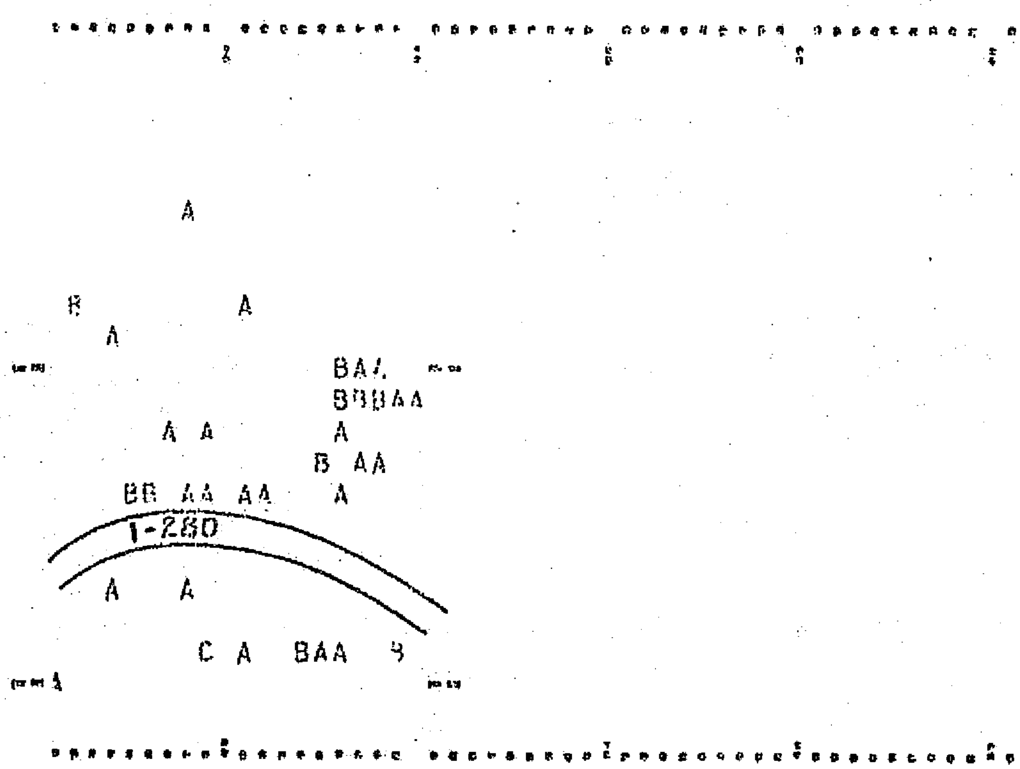

Fig. 2.3.5.8 Farm Hill Road - Results of Classification Program

```
un-normalized cluster results for
MD1
erts tape 1075-1817300 3 4
area begins at row 870,pixel 1799 from edge of frame
tolerance level was 13
upper value of range for channel 4=30
lower value of range for channel 4=27
upper value of range for channel 5=26
lower value of range for channel 5=24
upper value of range for channel 6=22
lower value of range for channel 6=24
upper value of range for channel 7=13
lower value of range for channel 7=12
```

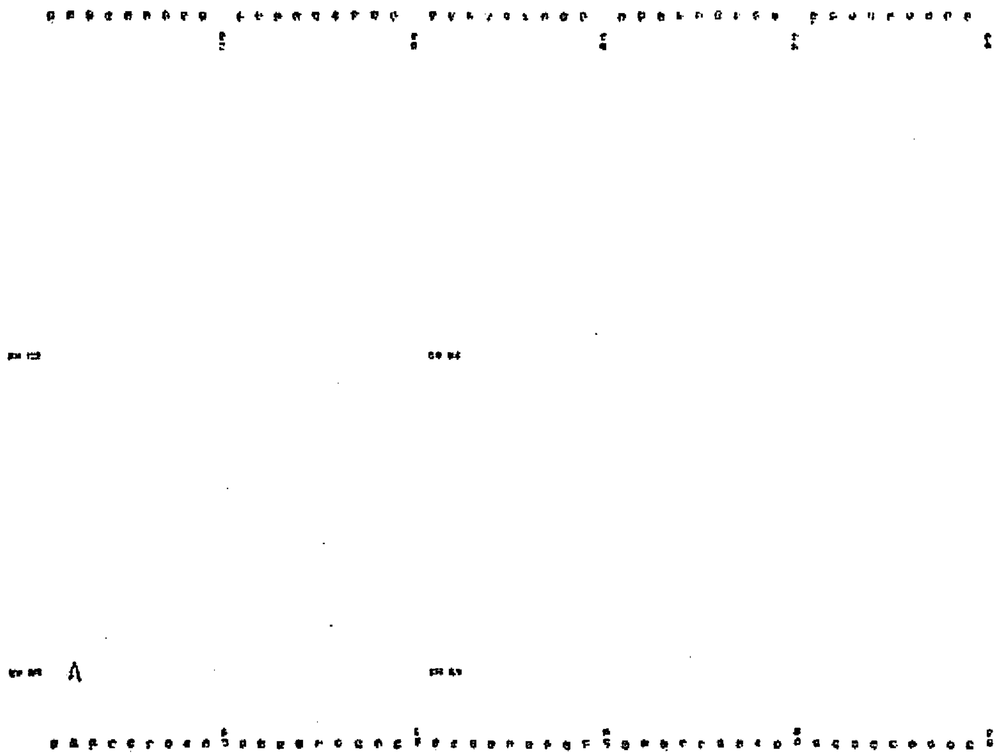

Fig. 2.3.5.9 Midway - Results of Classification Program

2.3.5.8 CONCLUSIONS

As a result of the foregoing study in the San Francisco Bay and adjacent Coast Range grassland areas the following may be concluded:

2.3.5.8.1 ERTS soil/grass four band spectra are in fact essentially soil spectra at the end of the dry or grass dieback season.

2.3.5.8.2 The ERTS four band spectra obtained is a function of the interaction of the soil and degree and type of grass cover which in turn is a function of the season.

2.3.5.8.3 A strong correlation exists between ground measured reflectance spectra and ERTS four band spectra for both serpentine and sedimentary deriven soils.

2.3.5.8.4 The ERTS four band spectra for serpentine and sedimentary deriven soils are sufficiently different from each other and their background to be classified by application of Stansort the SRSL interactive, unsupervised classification program.

2.3.6 CORRELATION BETWEEN GROUND METAL ANALYSIS, VEGETATION REFLECTANCE, AND ERTS BRIGHTNESS OVER A MOLYBDENUM SKARN DEPOSIT, PINE NUT MOUNTAINS, WESTERN NEVADA

2.3.6.1 ABSTRACT

In a cooperative study with USGS personnel, it has been possible to detect a 1.5 by 1 mile anomaly on ERTS CCT data directly, in the pine-covered mountains of western Nevada. This anomalous area is about 3-5 times larger than that of the known geobotanical anomaly which lies centrally within the area. The site has been studied on the ground and bi-directional reflectances (relative to $BASO_4$ obtained for 40 trees, using both in-vivo techniques (similar to cherry picker operations) and field determinations of cut branches. The anomaly can be seen best by color transparencies made from 5/4, 6/4, 7/4 ratioed digital data, the 3 ratios each being coded by one of 3 colors (blue, green, and red).

Field reflectance measurements of three modes were made, using EXOTECH ERTS-type radiometers -- cut branches, and viewing the trees both from vertically above, and horizontally. Each tree, either a Pinon pine or Juniper, was one previously marked by the USGS, who provided the molybdenum analyses of stems, twigs and needles (leaves). In addition sagebrush and bitterbrush shrubs were measured together with their background soils and rocks.

The correlation between Mo and Juniper leaf reflectance was positive, and significant at the 99% level (Channel 7 brightness) agreeing with the visual observation that even at values in excess of 500 ppm Mo in leaf ash, the junipers were healthy. With Pinon Pine however the correlation with leaf (needle) reflectance was negative but significant at the 97% level. The pines showed significant morphological change (needle loss, profusion of twiggy stems, and brittleness of branches) correlateable with mineral uptake of Mo.

Collectively all 62 tree samples showed a negative correlation with molybdenum significant at the 97% level.

Using unsupervised clustering techniques on CCT taped data (STANSORT program) ERTS spectra could be extracted for the total anomaly area, which were used to locate similar areas to the south, near Double Springs Flat. Field checking located weak gossan mineralization in the bleached andesites there.

Continuing field studies are aimed at specifically identifying the cause of the ERTS anomaly -- is it tree vigor, tree species, tree spacing, or sagebrush/soil ratio which can be observed from space over this skarn zone.

2.3.6.2 Table 2.3.6.1 which follows summarizes the results we obtained from several sets of field measurements in the Alpine-Cherokee Mines area, Pine Nuts Mountains, Nevada

The detailed descriptions are reproduced in Appendix D.

2.3.6.1 CORRELATION BETWEEN LOG Mo (ppm), Mo (ppm) WITH VARIOUS REFLECTANCE PARAMETERS

	Log Mo (ppm) (#3)			Mo (ppm) (#4)		
	All Branches N=62	Pine N=29	Juniper N=33	All Branches N=62	Pine N=29	Juniper N=33
RASNX	-.24	-.34	-.06	-.20	-.13	-.16
RASNY	-.21	-.08	-.22	-.16	-.20	-.01
BP4	-.06	-.28	-.22	.04	-.16	.28
BP5	-.04	-.05	.07	.04	-.20	.31
BP6	.17	-.03	.29	.13	.07	.13
BP7	(.30) *	.19	.33	(.35)**	.07	(.42)**
R4	.13	(-.40) *	.23	-.07	-.24	.19
R5	.11	-.18	.07	-.02	-.26	.25
R6	.08	-.15	.27	.00	-.02	.01
R7	(.25) *	.11	.32	(.26) *	.00	.32
R76	.11	.17	.06	.18	.00	.24
R75	.20	.21	.12	.09	.16	-.05
R74	.22	.28	.10	.19	.11	.13
R65	.10	.08	.06	-.04	.14	-.22
R64	.13	.19	.02	.03	.15	-.16
R54	-.04	.06	-.13	.02	-.09	.12
Significant						
(**) at 1%	.325	.47	.45	.33	.47	.45
(*) at 5%	.25	.37	.35	.25	.37	.35

SUMMARY

Pines: Negative, Juniper: Positive Reflectance Correlation with Mo.

Significant at

1% level	Juniper BP7 vs. Mo (ppm) 0.42
	All Branches BP7 vs. Mo (ppm) 0.35
3% level	Pine R4 vs. Log Mo (ppm) -0.40
5% level	All Branches BP7 vs. Log Mo (ppm) .30
	All Branches R7 vs. Log Mo .25
	All Branches R7 vs. Mo .26

2.3.7 APPLICATION OF DIGITAL SNOW MAPPING WITH ERTS-1 DATA, USING THE STANSORT, IMAGE PROCESSING SYSTEM

2.3.7.1 ABSTRACT

The STANSORT image processing system (Honey, et. al. 1974) was used in a digital snow mapping experiment with test sites in the Windriver Mountains (Wyoming). Using specific density slicing and cluster techniques it was possible to separate the following ground cover classes: dry snow,"metamorphic"-(partly-melted) snow, snow covered forest, snow/non-snow transition zone,and bare forest/other vegetation.Especially in heavily forested areas, where problems in manual image interpretation arise, the "snowline" - or better "transition" zone - could clearly be detected. The STANSORT system proved to be a very useful, easy to operate, lowcost interactive tool.

2.3.7.2 INTRODUCTION

With the first images from TIROS the potential for large-area snow mapping was recognized. With the ESSA-APT System many nations had the possibility of instantaneous satellite data for meteorlogical purposes, and in some of the countries these images (with resolutions in the order of kilometers) led to interesting snow mapping studies.

Basically the following main techniques were developed and applied: For flatlands - the US/NOAA method of computing 5-day composite minimum brightness charts were very successful. In mountainous terrain however up to now, digital methods were of less success. Therefore manual photointerpretation techniques were used. In the United States, snowline drawings were transferred onto topographic maps to locate the altitude of snowline. The technique known as SWISS uses transparent isolevel contour maps. By overlaying those onto the satellite imagery, a best fit method was used to estimate the snowline altitude. Very encouraging results have been achieved using this method.

With the advent of ERTS we were able to work with high resolution multiband imagery. The same image interpretation techniques were applied, but soon two main problems showed,

2.3.7.2.1) It is very easy to map the snowline as long as it is above the treeline. Detecting the limit of snow cover in forested areas however is very difficult.

2.3.7.2.2) Secondly, the improved resolution resulted in much more detail in the images - details no one had to deal with in satellite imagery previously - making the job of snowmapping very time consuming, almost impossible for larger areas.

In the Runoff Prediction model being developed at the Hydrology Branch of Goddard Space Flight Center, precise input data concerning the areal extent of the snow cover is essential. Therefore the question arose, whether existing digital image processing techniques can be applied to an automatic detection and classification of snow covered area.

In coordination with the above mentioned branch, the Windriver Mountains in Wyoming were selected as testsites. Image interpretation studies are conducted in the same area, and good "ground truth" in the form of high altitude U-2 photography is available (RC-8).

2.3.7.3 THE STANSORT SYSTEM

The STANSORT system allows to read directly the standard NDPF ERTS 9-track computer compatible tapes, and to apply the following functional handling procedures to the pixel data: Smoothing, ratioing, edge detection, normalized (as well as unnormalized) clustering, removing of atmospheric effects, calibration, shadeprinting, extraction of data values, histogramming* etc. (see Figure 1). The interactive access to the PDP-10 computer is achieved through a keyboard and instant control over the extremely fast operating process is possible via a black and white CRT display. A very fast primary evaluation of test results is thereby possible, and parameter changes may be applied very quickly. The system operation can be learned very quickly (1-3 hours) making it a very valuable tool for the discipline-oriented user-investigator who often is not a specialist in digital image processing.

*Since the time of writing this report (November 1974) "smoothing" has been taken out of STANSORT and replaced by "debanding" (6-line repeat bands) and "deconvolution" added. R.L.

2.3.7.3.1 The Procedure for the Snow Mapping Job

Step 1: Test area coordinates are calculated from the 1:1,000,000 scale image and directly introduced in the system, the region was controlled by viewing the shadeprint on the CRT display,and histograms were produced.

Step 2: Optimal shadeprints of the 68X60 pixel area (roughly 26 square km. or 10 square miles) were created in all bands. Careful comparison of the shadeprints and the histograms led to the conclusion to drop Channel 6 from further investigations due to the high level of banding and noise. This option is available in the "un-normalized" clustering" step.

Step 3: Establishment of test sites for each expected ground-cover class, e.g., dry snow/ metamorphic snow/forest with snow/bare forest + other vegetation.

Step 4: Special shadeprints of ERTS band 7 were made with density slicing of the saturation level 63, by which the dry snow areas could be obtained.

Step 5: Un-normalized cluster with Bands 4, 5, and 7. For bands 4 and 5 the upper values of ranges were set to 126 to exclude all snow from the clustering. With this step, and combining with the special shadeprint, the metamorphic snow area could be determined.
By changing the tolerance levels (gates) in the STANSORT clustering algorithm, different printouts were obtained. Careful comparison of these with the test field ground data led to the final application of the appropriate tolerance level for this specific application.

Step 6: Application of the same density slicing and clustering parameters to neighboring 68X60 pixel areas until the project area was covered.

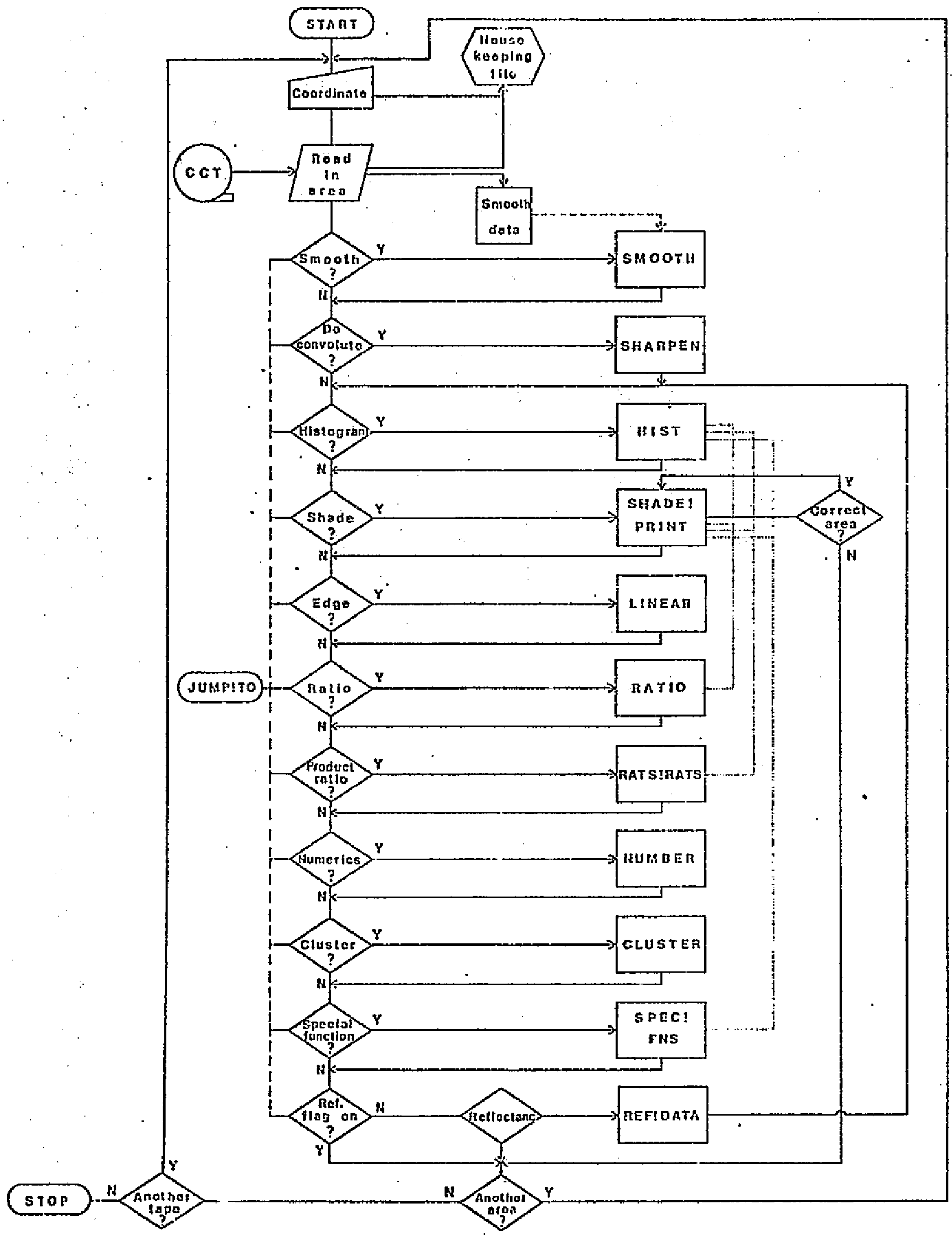

2.3.7.1 Flow diagram of STANSORT logic (including recent additions of "deconvolute" and product ratio, special function, etc.)

Discussion of the Procedure

2.3.7.3.2 Steps 1-3 do not offer problems, when either the coordinates (ERTS image coordinates) are known of the project area, or enough detail in the shadeprinted scene allows for easy location.

The density slicing in Step 4 requires an experience factor knowing that melting snow has a lower brightness in Band 7 than the dry snow which reaches saturation. Previous work with other image enhancing- and slicing-equipment showed the usefulness of this step.

In Step 5 the un-normalized cluster proved to be advantageous relative to the normalized cluster* approach because of too much loss of data variability in normalizing.

---

*All channels are normalized to Channel 4, which tends to remove sunlit-versus sun-shaded-slope problem.

The setting of the tolerance gate was the most difficult step in the whole procedure. Each intermediate result with a specific tolerance/gate setting, had to be carefully compared with a big number of testsites before rejecting it, or finally approving and apply it to the full project area. Good ground data is very essential in this evaluation step. Once the parameters were known, they could be saved in the computer memory and used for adjacent 68X60 pixel areas.

2.3.7.3.3 Evaluation of the STANSORT System relative to others.

In the comparison with results obtained by the LARSYS Ver.3 classification, the STANSORT cluster/slicing showed almost identical distribution of classes. The amount of time and effort however was considerably smaller than with LARSYS. On the other hand, the control and final accuracy achieved with LARSYS'supervised technique cannot be reached. There is a tradeoff between how fast and how accurate your final result should be. Figure 2 shows a direct comparison of hand colored samples of the results obtained with LARSYS and with STANSORT output.

2.3.7.3.3.1 Positive Points:

- easy to learn operation of the system
- very fast cluster algorithm, makes the system comparatively inexpensive.
- B/W CRT display for fast interaction by visual checkout of results.
- easy to operate special features, like edge detection, simple ratioing, removing of atmospheric effects etc.

2.3.7.3.3.2 Negative Points:

- 68X60 pixel area limitations on one run
- limited statistics
- no training/classify functions, except by using a selected tolerance set to classify adjoining areas.

2.3.7.3.4 Suggestions for Further Developments

2.3.7.3.4.1 Increment feature: The location of a feature in a scene is sometimes difficult when looking at single pixel resolution for a 68X60 area. In a first step, to get a better overview, every 2nd or even 10th or higher number of pixel sample interval could be used, thereby producing a smaller scale. Secondly, the 1X1 pixel resolution is not needed in some cases, esp. in large area mapping studies, thus computer time could be saved.

2.3.7.3.4.2 Group cluster feature: To be asked by the computer/system when all cluster parameters are established, and an interpretation of the different clusters is achieved. In the following example 14 clusters had been built up, and now we wish to merge several into three groups.

CRT Question	Answer
- "do you want to group clusters?"	*Y "
- "how many groups (classes) do you wish to create?".	*3"
- "assign symbol to group 1".	*W"
- "assign clusters to be grouped in group 1	*A,B,E,K"
- "assign symbol to group 2"	*$
- "assign clusters to be grouped in group 2".	*C,H,I
- "assign symbol to group 3".	*-
- "assign clusters to be grouped in group 3".	*D,F,G,J,L,M,N,
- "do you wish to shadeprint grouped cluster result?".	*Y

and so on.......

This feature would allow one to make a sort of a classification, and would be a great help in simplifying the display and in the final evaluation of the result.

2.3.7.2.4.3 Statistics feature: A coincident spectral plot showing the location (spectrally) of the clusters in the different wavelength bands, would help the interpretation and grouping steps considerably. Furthermore some statistics would be desirable on number of pixels grouped in group 1, group 2 etc.....as well as a table showing the distribution of the clusters within the groups (percentage of pixels of original cluster A in group 1, cluster B in group 1 etc..). The tabulated output of the spectral values (digital counts) assigned to each symbol is useful but additional statistics would be welcome.

2.3.7.2.4.4 Large area feature: In addition to the increment feature (par. 1), sometimes big areas have to be looked at or searched for a specific signature, and the stepwise procedure by adding 68X60 pixel areas until the whole area is covered is too time consuming. Therefore a special shadeprint feature - be it for raw ERTS data, for cluster/grouping results, for edge detection or anything else - could be desirable (see example).

CRT Question	Answer
- "do you wish to apply the same parameters to another area?.	*Y
- "type in title for output"	*Stanford Land Use Map
- "after next type in you may have to wait a while how many scanlines down to your area?".	*1000
- "how many lines are in your area?"	*1300
- "what line increment do you want?"	*5
- "how many pixels in to your area from tape edge?" . . .	*200
- "how many pixels wide is your area""	*1500
- "what column increment do you want?"	*5
and so on	

......followed by;

A confirmation of area coordinates, and a calculation of the time involved in waiting for a larger output result, which will for the lineprinter be divided in stripes, 68 columns wide, as long as stated. Mounting of those stripes would be considerably faster than mosaicing the 68X60 rectangles.

2.3.7.2.4.5 Special histogram approach for shadeprinting: In some cases an optimal shadeprint is wanted with a non linear scale according to the distribution in probability space. As the histogram feature is already implemented in the system, the histogram-controlled scaling of the shadeprint steps would be easy.

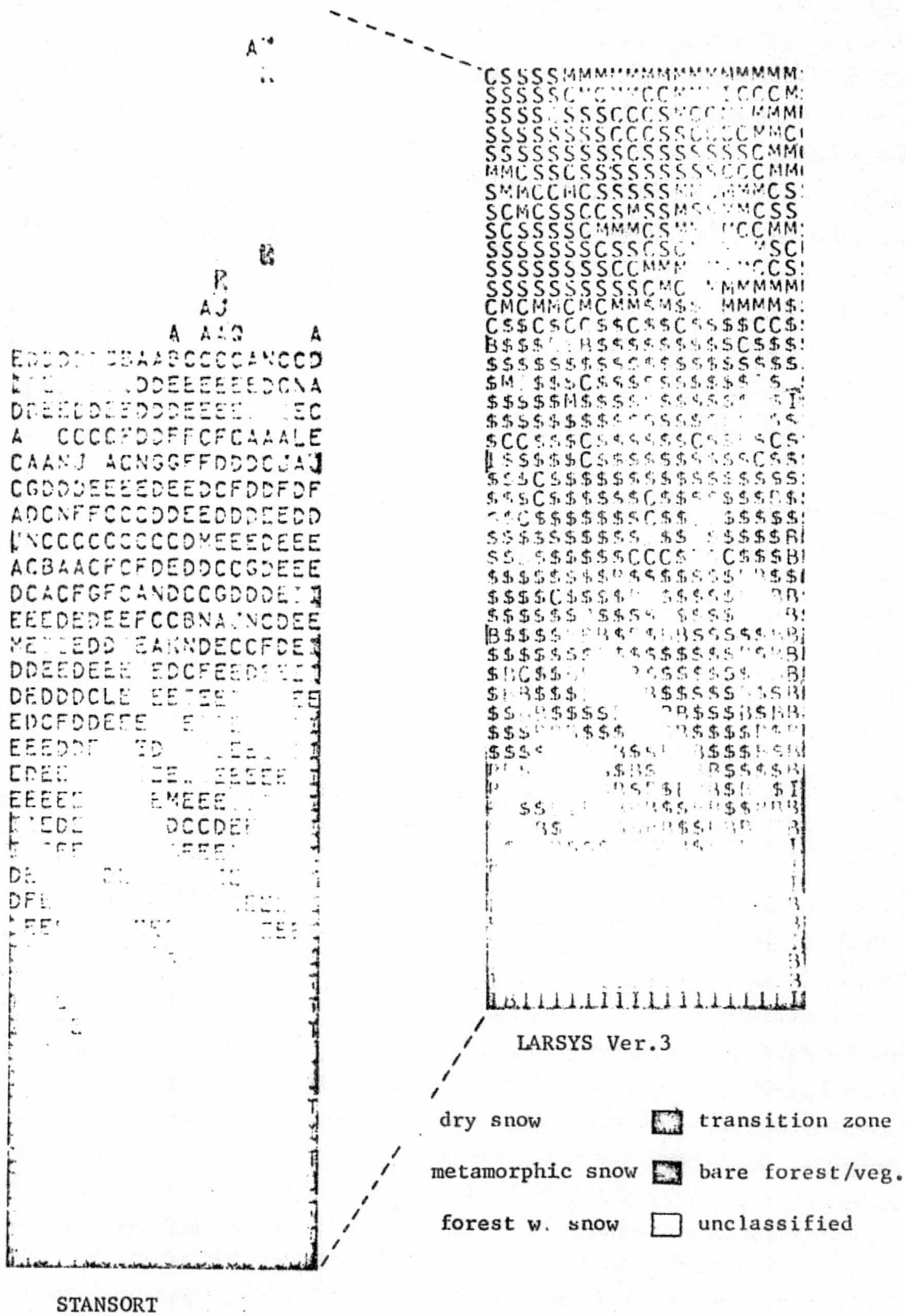

Figure 2.3.7.2 Comparison of interpretation samples made by using STANSORT (left) and LARSYS Ver. 3 (right), strip size roughly 4 km X 1.14 km.

2.3.7.3.5 Further Studies Using Different Processing Systems

As mentioned in the title, the use of the STANSORT system in the application of ERTS data to digital snow mapping is a part of a larger project, involving the use of also LARSYS Ver. 3 and the General Electric Image-100. The results achieved and the efforts that had to be made when using these different kinds of systems will be compared and carefully investigated in a forthcoming report issued from the Department of Geography, University of Zurich.

2.3.7.4 ACKNOWLEDGMENTS

The work described herein was co-sponsored by ESRO/ESA under their Fellowship Program, and Stanford University providing the facilities and the computer time. I wish to thank both institutions for their support. I am very grateful to Prof. Dr. R. J. P. Lyon of the Remote Sensing Laboratory, School of Earth Sciences, Stanford University for providing me with advice, instruction and systems-theory as my visit there also included theoretical and practical work with the Stanford Ground Spectra Measuring System, which serves as their basis to the ERTS image interpretation approach. Thanks are extended also to Dr. F. R. Honey, who helped me in the practical use of the processing system, and who went out of his way to implement special features needed in my specific application.

This paper is part of a larger project on "Comparative Application of Digital Snow Mapping" where the experiences and the results gained by using LARSYS Ver. 3, Image-100 and STANSORT are discussed

The work described herein was co-sponsored by ESRO/ESA (European Space Agency) under their Fellowship Program, and by Stanford University providing the facilities and the computer time needed in the project, under Contract NAS 5-21884.

2.4.1 NEW TECHNOLOGY

2.4.1.1 Hardware

2.4.1.1.1 Development of a projection-type densitometer for radiance measurements from ERTS MSS 70 mm transparencies (see Project A1).

2.4.1.2 Software

2.4.1.2.1 STANSORT, a fully interactive program for a PDP-10 computer with CRT displays, for processing ERTS CCT Tapes (see Project B3).

2.4.1.2.2 IMAGE, a program for a PDP-10 computer, to produce tapes of 250 x 300 pixel areas for use on a DICOMED imaging system, with geometric corrections of ERTS distortions (see Project B4).

2.4.2 SIGNIFICANT RESULTS

2.4.2.1 SCIENTIFIC

2.4.2.1.1 A far greater appreciation of the seasonal variability of vegetation, together with the technological abilities to measure these effects either stationary (on the ground) or mobile with a truck mounted bi-directional reflectance system (see Projects C2.1, C2.2, C2.3, C2.4 reports).

2.4.2.1.2 Correlation of leaf reflectances for Juniper and Pine, growing in Mo-bearing mineralized soils, with ground ERTS-type spectral data, significant at the 1% and 3% levels, respectively. (See Project C2.4, report section.)

2.4.2.1.3 ERTS image 1397-18051 (Aug. 24, 1973) covering W. Nevada and the copper mines of Yerington was made 13 days after a SKYLAB RB57 underflight obtained high-altitude photography (at 20 km) of the same area. A color IR (false color) image of 400 km^2 made by our IMAGE program (Ch. 5 and 6 and 7) shows a very high degree of <u>spatial</u> agreement with the airphoto. Both the airphoto (made at 0830 local time) and the ERTS image (made at 0905 local time) show the same topographic relief effects due to the sun angle. Significantly, a <u>color-ratio-composite image</u> made from h 5/4 + (Blue) + Ch 6/4 (Red) + Ch 7/4 (Green) shows greatly lessened topographic effects (from ratioing), but the tone patterns now closely resemble the published geological maps, specifically, precisely localizing three rock types, and differentiating "alteration zones" within three others. The best single ratio for

this purpose if Ch 6/4 (see Project B4; and C1.2). This high correlation of ERTS, RB57 air photograph and geological mapping is most important and is being further studied with the geological personnel of the copper mine.

2.4.3 TECHNOLOGY TRANSFER

2.4.3.1 EDUCATIONAL — STANFORD UNDERGRADUATE AND GRADUATE CLASSES USING ERTS

Successful transfer of the technology of using ERTS tapes, to the classroom, with both undergraduate and graduate geology students using the STANSORT interactive program in their regular studies of environmental geoscience monitoring the San Francisco Baylands (AES 133). The program has now been used also for two successive years in the Remote Sensing and Exploration classes in the Department of Applied Earth Sciences at Stanford (AES 294, 295). In all cases the geographic, map-like data displays proved very easy for students to comprehend and use. The interactive mode of data processing, based upon their matching the computed output (cluster classifications), with their maps as photos and field data, has shown itself to be very simple for them to operate.

2.4.3.2 INTERNATIONAL

Following visits to Stanford of several foreign geographers and geologists (students and professionals), the STANSORT programs have now been installed (with transliterations to other styles of computer) in Zurich (Switzerland),Trondheim (Norway), Hanover (W. Germany), Madrid (Spain), Sydney (NSW, Australia), and Perth (W.A., Australia). Continuing research programs (of varying extents) exist with all of the above groups, further showing the technological transfer. (See Projects A2, B3, C1.0, C2.2, C3.0 Summaries.)

2.5 REFERENCES

Section 2.2.1

Algazi, V.R. (1973), "Non Linear equalization and calibration of MSS scene response", in "An integrated study of Earth resources in the state of California using ERTS-1 data", 1973, Chapter 8, Appendix I.

Andenburg, W. (1971) "Cluster analysis for applications", Ph.D. Thesis, University of Texas an Austin (1971).

Andrews, H. C. (1972), "Introduction to mathematical technique in pattern recognition", Wiley Interscience, N.Y., 1972.

Effler, W.G., (1974), "An infrared version of the table look up algorithm for pattern recognition", Proc. IXth International Symposium on Remote Sensing of Environment, Willow Run Laboratories, 1974.

Rowan, L.C., Wetlaufe, P.H., Goetz, A.F.H., Billingsley, F.C. and Stewart, J.H. (1974), "Discrimination of Rock Types and Detection of Hydrothermally Altered Areas in South-Central Nevada by the use of Computer-Enhanced ERTS Images," U.S. Geol. Surv., Prof. Paper 883, 35 pp.

Honey, F.R. (1974), "IMAGE: An interactive program for producing computer-enhanced ERTS images, Part I, software development", Stanford Remote Sensing Laboratory Technical Report 74-12.

Itten, K. I., (1975), "Application of Digital Snoco Mapping with ERTS-1 Data, using the STANSORT Image Processing system", Stanford (AES) Remote Sensing Laboratory Technical Report 75-1, 11 pp.

Lizaur, P. (1975), "Study of the Alteration Zone around Goldfield Mining District by means of ERTS satellite multispectral scanner data", Stanford (AES) Remote Sensing Laboratory Technical Report 75-3, 57 pp.

Prelat, A. (1974), "Statistical correlation of biomass data versus bidirectional reflectances (Raw and normalized to Channel 4)", Stanford (AES) Remote Sensing Laboratory Technical Report 74-7, 75 pp.

Sebestyen, G.S. (1962), "Decision making processes in pattern recognition", MacMillan, London 1962.

Thomas, L.T. (173), "Generation and physical characteristics of the ERTS MSS system corrected computer compatible tapes", NASA x563-73-206.

Section 2.2.2

Honey, F. R., Prelat, A., and Lyon, R.J.P., (1974) STANSORT: Stanford Remote Sensing Laboratory Pattern Recognition and Classification System, Tech. Rept. 74-4, Stanford Remote Sensing Lab., also Proc. Ninth Int. Sym. Rem. Sens. Environ., Ann Arbor, Mich., pp. 897-905/

Section 2.3.1

F. R. Honey, and R.J.P. Lyon, 1974, A Comparison of Observed and Model-Predicted Atmospheric Perturbations on Target Radiances Measured by ERTS, Stanford Remote Sensing Laboratory, Stanford University.

Section 2.3.2

Anttonem, Gary, 1966, A Mechanical Analysis of Miocene Sandstone from the SLAC Site, Stanford Cal., Unpublished Student Report, Stanford University.

Atchley, F.W. and Grose, L.T., Feb., 1954, Geology of the Page Mill Quarry Area, Stanford, California, Unpublished student report for Utah Construction Company, Stanford University.

Atchley, Frank W., Jan., 1960, Preliminary Geologic Investigation of the Sand Hill and Felt Lake Linear Accelerator Sites, Stanford University, 12 p., maps (1:6000).

Cummings, J.C., 1956, Reconnaissance Geology of the Miningo Hill Area, California: Thesis, Stanford University.

Edwards, K.L., 1961, The Upper Eocene Fauna of the Stanford Foothills, California, Unpublished student report, Stanford University.

Hogg, S.L., 1963, The Geology of the Stanford Foothill, Santa Clara County, California, Unpublished student report, Stanford University.

Poland, Joseph F., 1939, The Page Mill Road Basalt Quarry, Unpublished student Report, Stanford University.

Section 2.3.3

Abrams, Leroy, 1940, Illustrated Flora of the Pacific States, Vol. I, Ophioglossaceae to Aristolochiaceae, Stanford University Press, Stanford, California.

Crampton, B., 1974, Grasses of California, University of California Press, Berkeley and Los Angeles, California.

Munz, P.A. and D.D. Keck, 1965, A California Flora, University of California Press, Berkeley and Los Angeles, California.

Thomas, J.H., 1961, Flora of the Santa Cruz Mountains of California, Stanford University Press, Stanford, California.

McNaughton, S.J., 1968, Ecology 49: 962-972, Structure and function of California grasslands.

APPENDIX A

TA1-2

A COMPARISON OF OBSERVED AND MODEL-PREDICTED ATMOSPHERIC PERTURBATIONS ON TARGET RADIANCES MEASURED BY ERTS: PART I - OBSERVED DATA AND ANALYSIS

R.J.P. Lyon
Professor of Mineral Exploration
Dept. of Applied Earth Sciences
Stanford University
Stanford, California 94305

F.R. Honey*
Post Doctoral Fellow
Remote Sensing Laboratory
Stanford University
Stanford, California 94305

G.I. Ballew
Graduate Student
Dept. Applied Earth Sciences
Stanford University
Stanford, California 94305

*now with CSIRO, Land Research Division
Private Bag, Wembley, West Australia 6013

Abstract

Two targets of measured, constant reflectivity in the area of San Francisco, California are studied. The first standard, a waste (carbon black)treatment pond at an oil refinery near Suisan Bay, having an area of approximately 0.3 square miles, (or 215 pixels), and bandpass reflectances of <0.5% in all four bands, is assumed to have a zero contribution to the radiance recorded by ERTS. The radiance observed then arises entirely from atmospheric scattering. The variation in these radiance values as a function of solar zenith angle has been analyzed.

A second target, a concrete parking apron for aircraft at Moffett Field, California, assuming that it remains dry during the period of study has constant reflectances of 27.8, 31.0, 30.0, and 32.3 percent bandpass reflectances in four MSS equivalent channels. Using these values, the radiance observed by ERTS may be corrected for the atmospheric contribution, and thus values for the radiance from the target may be calculated. These values were studied as a function of solar zenith angle.

1. Introduction

In order to be able to compare results from ERTS MSS data over a series of tapes, the perturbing effects of a variable contribution due to radiation scattered by the atmosphere into the detector field of view, and of the variation in the irradiance on a target with solar zenith angle, must be eliminated. These two effects may be compensated for, or entirely removed, by studying selected targets in a scene, one (or more of low (zero) reflectance, one (or more) of high, known reflectance. In some scenes, however, suitable reflectance targets may not be obtained. When this occurs, atmospheric modelling must be employed to arrive at some values for the atmospheric scattering contribution, and for the irradiance on the scene.

The technique of using standard targets within a scene was applied to a specific scene which contains an area of measured reflectivity.- the Stanford Grassland testsite.

To increase the contrast between targets and background in a LANDSAT-1 image scene it is necessary to attempt to remove the effects of atmospheric scattering. Several methods have been used generally based upon the scheme of "dark-area subtraction"-some area of very low brightness is observed on the LANDSAT image. It should be black but it is not and has finite values of brightness. These resulting radiance values are presumed to have arisen solely from the atmospheric column. Cloud shadows were used by Goetz(2) and by Vincent(4), but cloud shadows do not necessarily represent the darkest areas in any frame, particularly in MSS Channel 7.

We searched for suitable dark areas near Stanford in the San Francisco frames,specifically using Channel 5 for our search. We selected Ch 5 because all water over 3 cm depth is black in Ch 7, but in the same locality may have values as high as 30 in Ch 5, if the water is shallow with a sandy bottom, or is muddy. A spectrally black target should appear dark grey in all channels.

The area we located, which was black on all channels, occurred on the south shore of the Sacramento River just east of the Carquinez Straight Bridge about 47 km (25 miles) NNE of San Francisco. Inspection of the local topographic maps (Port Chicago, sheet) indicated that it was a part of an oil refinery complex (Phillips Petroleum-Port Chicago/Avon Plant) and with a telephone call we ascertained that the 0.8 km^2 area (0.3 sq. mi.) was a dam filled with carbon black waste product. Figures 1a and 1b are 1:250,000 scale enlargements of this area and Figure 2 is the maximum possible enlargement of Channel 5 (about 1:52,000 scale).

Bi-directional reflectance measurements made on February 1, 1974 using two EXOTECH-100 ERTS radiometers (15° FOV, relative to $BaSO_4$ powder) showed that the reflectance of the carbon product was below 0.5% in all four LANDSAT channel bandpasses.

We then proceeded to find a high reflectance target, so that we could calculate reflectance of terrain directly from LANDSAT data, using a zero reflectance (carbon black dump) and the high reflectance targets, and linearly interpolating between them.

Initially we tried to use the large dumps of salt harvested by evaporation on the shoreline of San Francisco Bay, near Redwood City. These dumps are several pixels in extent, but their brightness exceeds the 127 count number (7-bit) allowed in the dynamic range of the LANDSAT scanner telemetry. Often in the summer periods all four MSS

data channels were saturated making a target as bright as salt of little use. (Similarly many cloud-tops and snow saturate the system making their mutual discrimination very difficult).

ig. 1. Enlargements at 1:250,000 scale of LANDSAT images for 1075-18173. Fig. 1a is Channel 5; 1b is Channel 7. White arrows point at the Carbon Black dump at the Phillips Petroleum Avon Plant (Refinery) here used by us as a "zero-reflectance" standard. Letters, B=Benecia Bridge; C=Carquinez Bridge; S=mothballed ships in Suisan Bay; and V=Vallejo City.

We decided to use the large expanse of concrete used as a parking apron for U.S. Navy aircraft at Moffett Field, Mountain View, only 10 km (6 miles) ESE of Stanford. Similar bi-directional reflectance measurements with the same units gave the following reflectance values, relative to $BaSO_4$.

Concrete Apron, Moffett Field (N=15 measurements)

Channel	4	5	6	7
Ave.Refl.($\bar{x}$)	27.88	31.0	30.0	32.1
1 σ	2.71	3.42	3.53	3.14
Cov ($\sigma/\bar{x}$)	(0.10)	(0.11)	(0.12)	(0.10)

Both the carbon black and concrete target are at sea level.

Using the 14 LANDSAT CCT tapes of the Stanford area (San Francisco Bay) we extracted the average brightness (at the satellite) for each of the two standard localities - carbon black and concrete. Great care was taken not to use edge pixels, and just to take the central portion within each area to avoid effects of terrain contamination, and also forward scattering by other adjacent terrain. Table I lists the tapes used, together with their dates, solar elevation and zenith angles for the 24-month period of this study.

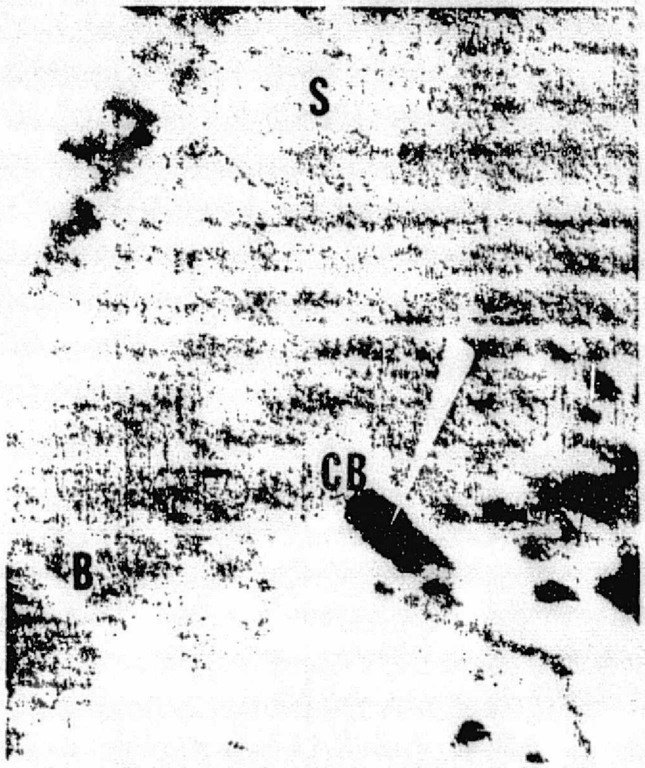

Fig. 2. Maximum enlargements (scale = 1:52,000) of the same Carbon Black area on Channel 5 image, as in Fig. 1a, showing the large area contained in an earthen dam near a small river.

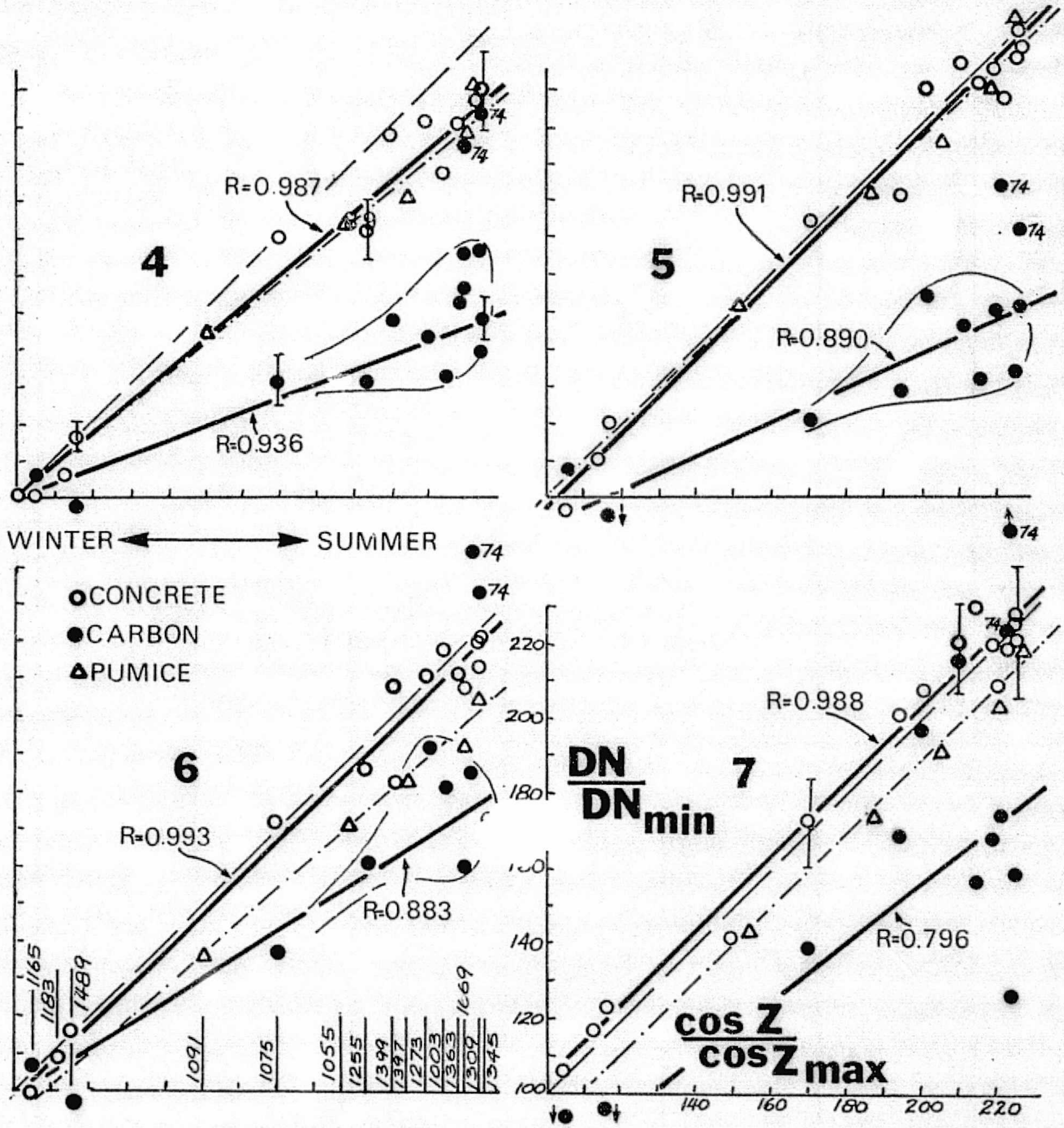

Figs. 3-6. Four plots of normalized LANDSAT (Channels 4,5,6 and 7) bandpass data for 17 overpasses. For each plot the ordinate is brightness (in DN), over brightness for the Winter scene (DN,min); the abscissa is cosine zenith angle of each pass, divided by the cosine of the maximum zenith angle (winter). For full adherence to the cosine-law all points should lie on the thin dashed line (1:1). Open circles are for the concrete at Moffett Field; solid circles for the Carbon Black; triangles for the Mono Lake pumice sand. Thick solid lines are least-squares fitted to the carbon and concrete data, dash-dot for the Mono sand. Error bars denote the 1-sigma limits, where N=50 (carbon) and N=15 (concrete). Channel 4 and 7 plots show departures from the 1:1 relationship.

Table II contains all the measured LANDSAT data, arranged in increasing zenith angle (roughly Winter to Summer). Mean brightnesses and standard deviations are calculated for each channel and date. Values are given in digital numbers (DN) directly off the bulk CCT tapes. This table also contains data for two sites at Mono Lake, California where one of us (Gary Ballew) has similarly measured a dark and a light target on the ground, and extracted their digital values from the 5 Mono Lake tapes (referred to in Table I).

Study of the Table II listings suggest a pattern of relationship with zenith angle, so we calculated their cosine Z values. To make the plots more clear we normalized the brightness data to that of the maximum zenith angle (winter data) and compared these ratioed values with a similar ratio of cosine zenith angle/cosine zenith angle maximum. From these normalizations Table III was produced, and the values were also graphed at Figures 3,4,5, and 6 for Channel 4 5 6 and 7 data respectively, as seen above.

2. Analysis

From the Tables and the graphs it is quite clear that for the bright target-concrete (open circle), in all channels, there is a high correlation between cosine zenith angle function and that of their LANDSAT brightnesses, indicating that the change in brightness is directly related to the elevation of the sun. For carbon black there is a different relationship (with much more spread) although some cosine-law aspects are preserved. One-sigma bars are shown on some of the points.

LEAST-SQUARES FIT WITH CORRELATION AND SLOPE

	Ch 4	Ch 5	Ch 6	Ch 7
Concrete				
R	0.987	0.991	0.993	0.988
Slope	.86	.99	.98	1.00
Mono Pumice				
R	0.981	0.980	0.992	0.986
Slope	.85	.96	.87	.99
Carbon Black				
R	0.936	0.890	0.883	0.796
Slope	.39	.45	.64	.82

In detail, the 1:1 straight line relationship for the bright target is most clear in Channels 5,6 and 7 data, but with almost all Channel 7 values lying slightly above the 1:1 line, whereas Channel 6 closely approximates the cosine zenith angle line. Channel 5 data lie slightly below the line.

Channel 4 data are much more spread, particularly with the higher sun (summertime) dates which all lie below the line. The concrete is less bright than one would expect directly from the sun elevation. This lowering (and probably also the spread) of Channel 4 data no doubt are related to the increased smog and air-pollution over the San Francisco Bay in the summer months. Air pollution levels are quite low in the winter (when also a much greater horizontal visability can be documented).

The carbon black target (solid circles) shows far less relation with the 1:1 cosine-law line, particularly with Channel 4 data, which are somewhat constant regardless of the zenith angle. There are higher values in the other channels (particularly Channel 6) but the data points are much more spread. In Channel 7 the basic DN values are so low that a change of ± 1 in the A-D decision (at the spacecraft) creates a high standard deviation (up to 40% cov., $\sigma/\bar{x}$). Errors are high.

Some yearly variation in the values can be noted, particularly in the 1974 tapes (ID:1687 and 1669) which show wildly high values for Channels 5,6 and 7. This may be drift in the satellite system, or a calibration change in ground data-processing. It may also be a change in the surface conditions of the dump itself (albedo change, etc.), although the reflectance measurements we made at the refinery were made on February 1, 1974.

3. Mono Lake Standard Terrains

Ballew[1] has measured two natural soil materials at Mono Lake, California, about 290 km (180 miles) due east of San Francisco, and calculated their bi-directional reflectances for a wide series of sun elevations. His data for a dark target (basalt lapilli) and a light target (pumice sand) have the following values, relative to Fiberfrax;

Average Bi-directional Reflectance ( )

	Ch 4	Ch 5	Ch 6	Ch 7
Dark Target (N=7)	7.6	8.4	8.4	8.0
Light Target (N=6)	21.6	23.1	24.0	23.5

From five LANDSAT tapes over Mono Lake (Table I), similar brightness ratios were prepared for the light target to compare with the concrete (Moffett Field), with allowance made for their different reflectance values. These are tabulated in Table IIIC and plotted on the graphs of Figures 3, 4, 5 and 6 as open triangles connected by a dash-dot line. These lines are sub-parallel to the 1:1 cosine-law line, but are lower in all channels, probably due to slight differences in the absolute values of the reflectance of the pumice and the concrete, the ratio of which was used to relate the two data sets. (1% error in either curve would change the Mono Lake data by 006 units at 180, Figs. 3-6).

4. Application

Our main research task was relating the LANDSAT data to ground measured reflectances of vegetated (grass) targets--four main rock types--on the 1850 hectare (5000 acres) of the Stanford Grassland Site (145 meters (475 feet) above sea level). We used the two calibration targets (carbon black and concrete) to reduce all our LANDSAT tape coverages over the site, to reflectance, and then compared them (whenever tapes and field data coincided!) with ground bidirectional reflectances. A reasonable agreement was found

and three of the areas have been selected from the 44 studied, and listed in Table IV. Channel 7 invariably shows a calculated reflectance much higher (5-15%) than the values for the ground measurement, a feature also noted by Levine[3] in other similar measurements elsewhere in the Bay Area.

Apart from this un-explained increase, the data in this calibrated "reflectance" form are quite useful for evaluation in clustering and other decision-making algorithms.

5. Conclusions

a. A very-low reflectance target has been located near Port Chicago, California and used for dark-area subtraction for atmospheric corrections. Ground measurements confirm the carbon-black material has a low reflectance (<0.5%). LANDSAT brightnesses have been extracted for 14 overpasses in 2 years. Some cosine-law effects appear.

b. A light-target (concrete, with about 30% reflectance has been used to extract similar brightnesses, which obey the cosine-law closely.

c. Use of both targets (which occur on the same tape and scene) enable one to calculate "reflectances" from LANDSAT tapes for any other set of pixels.

d. These reflectances compare favorably with ground-measured data, despite the many locational and sampling problems. A positive bias in reflectance for LANDSAT Channel 7 data gives high reflectance values. This may be due to problems with the low values of all Channel 7 data, to look-up table biases in decompressing the Channel 7 data, or problems with our basic concrete standard.

Table I

Dates and Sun Angles LANDSAT Tapes Used

LANDSAT ID	Date	Sun elevation	Zenith angle	Locality
1003-18175	07/26/72	58.7°	31.3°	Stanford
1055-18055	09/16/72	47	43	Mono Lake
1091-18062	10/22/72	36	54	Mono Lake
1165-18175	01/04/73	24.2	65.8	Stanford
1183-18175	01/22/73	26.3	63.7	Stanford
1255-18183	04/04/73	49.4	40.6	Stanford
1273-18183	04/22/73	55.2	34.8	Stanford
1307-18064	05/26/73	61	29	Mono Lake
1309-18181	05/28/73	61.0	29.0	Stanford
1345-18174	07/03/73	61.6	28.4	Stanford
1361-18060	07/19/73	59	31	Mono Lake
1363-18173	07/21/73	59.0	31.0	Stanford
1397-18053	08/24/73	53	37	Mono Lake
1399-18170	08/26/73	52.0	38.0	Stanford
1489-18157	11/24/73	27.0	63.0	Stanford
1525-18145	12/30/73	23.0	67.0	Stanford
1669-18111	05/23/74	60.0	30.0	Stanford
1687-18104	06/10/74	61.0	29.0	Stanford

Table II

LANDSAT Radiances from Standard Targets

LANDSAT ID	Z°	Mean digital no. (DN) CH4	CH5	CH6	CH7	Standard deviation σ4	σ5	σ6	σ7
A. Moffett Field--light target (concrete) N = 14									
1345	28.4	75.9	79.4	67.9	26.4	3.97	5.78	5.16	2.15
1309	29.0	75.2	77.4	65.5	26.8	1.42	2.81	2.79	1.09
1687	29.0	74.5	77.7	67.9	26.1	2.51	[illegible]	4.40	[illegible]
1669	30.0	70.1	73.6	63.7	24.5	2.82	3.55	2.55	1.93
1363	31.0	72.9	75.9	64.6	26.0	2.50	3.32	3.66	1.36
1003	31.3	67.7	74.7	66.9	27.3	1.19	2.72	3.78	1.19
1273	34.8	73.2	76.8	64.6	26.0	2.50	3.32	3.86	1.36
1399	38.0	71.7	73.8	65.7	25.6	2.83	4.56	3.09	1.69
1255	40.6	62.4	63.8	56.7	23.7	2.66	3.67	3.26	1.57
1075	48.4	61.6	61.6	52.7	20.4	1.29	2.46	2.06	1.31
1489	63.0	42.9	47.2	35.8	14.5	1.71	2.31	2.65	1.39
1183	63.7	38.3	38.7	33.2	13.8	1.64	1.94	1.40	0.72
1165	65.8	35.9	34.1	30.3	12.4	1.31	1.57	1.18	0.73
1525	67.0	36.2	35.3	30.6	11.8	1.30	2.35	1.59	0.82
B. Benecia Refinery--dark target (carbon black) N = 50									
1345	28.4	21.0	12.3	10.0	1.9	0.96	0.76	0.79	0.50
1309	29.0	19.7	11.0	8.1	1.5	0.72	0.63	0.62	0.61
1687	29.0	23.5	13.9	13.5	2.6	0.99	0.68	0.97	0.50
1669	30.0	23.4	15.0	14.0	3.7	1.12	0.82	1.32	0.53
1291	30.4	22.1	12.9	10.7	2.1	1.48	0.88	1.16	0.59
1363	31.0	21.5	12.8	9.2	2.0	1.13	0.77	0.54	0.73
1003	31.3	18.8	10.9	10.5	1.9	0.91	0.50	0.71	0.56
1273	34.8	20.3	11.9	11.0	2.6	0.84	0.84	0.85	0.62
1399	38.0	21.1	12.6	10.5	2.3	0.89	0.86	0.96	0.75
1255	40.6	18.6	10.5	9.3	2.0	0.78	0.83	0.82	0.57
1075	48.4	18.6	9.8	7.9	1.6	0.96	0.40	0.85	0.95
1489	63.0	13.6	6.8	5.3	0.5	0.80	0.97	0.81	0.61
1183	63.7		area clouded over						
1165	65.8	15.0	8.7	6.1	0.9	0.94	0.53	0.89	0.64
1525	67.0	14.2	8.2	5.8	1.2	0.79	0.44	0.82	0.68
C. Mono Lake--light target (pumice sand) N = 6 (after Bullew, 1975)									
1307	29	59.0	60.0	50.2	19.0				
1361	31	55.2	55.3	47.0	17.5				
1397	37	50.5	51.3	44.7	16.5				
1055	43	48.3	47.8	41.8	15.0				
1091	54	40.0	39.7	33.2	12.2				

D. Mono Lake--dark target (basalt lapilli) N = 7 (after Ballew, 1975)

1307	29	27.6	24.0	17.7	4.6
1361	31	27.0	22.9	19.6	6.1
1397	37	23.6	19.7	18.1	5.0
1055	43	24.1	20.7	15.6	4.9
1091	54	20.3	16.3	12.3	3.1

Table III

Ratios as a Function of Cosine Zenith Angle

LANDSAT ID	cos Z x 100 / cos Z at max (A+B)	channel brightness x 100 / channel brightness at max Z (A+B) CH4	CH5	CH6	CH7
A. Concrete (light target)					
1345	225	210	225	222	224
1309	224	208	219	214	227
1687	224 (1974)	206	220	232	232
1669	221	194	208	208	208
1363	219	201	215	212	221
1003	215	187	217	219	231
1273	210	202	217	212	221
1399	201	198	209	209	218
1255	194	172	181	186	201
1075	170	170	174	172	173
1489	116	116	120	117	123
1183	111	106	110	109	117
1165	105	99	96	99	106
1525	100	100	100	100	100
B. Carbon black (dark target)					
1345	225	148	151	173	160
1309	224	138	134	141	175
1687	224 (1974)	165	171	234	223
1669	221 (1974)	164	134	244	316
1291	221	155	158	186	175
1363	219	151	156	160	169
1003	215	132	134	182	157
1273	210	143	146	192	216
1399	201	148	155	183	197
1255	194	131	129	161	169
1075	170	130	120	137	139
1489	116	96	83	93	46
1165	105	105	107	106	75
1525	100	100	100	100	100
C. Mono Lake pumice sand (light target)					
1307	224*	210**	228	205	221
1361	219	196	210	192	203
1397	204	180	195	183	192
1055	187	173	182	171	174
1091	150	142	151	136	142

*Value calculated relative to Z max in A+B.
**Values calculated allowing for reflectances of target A relative to C.

LANDSAT	Field Data	
1687	June 19, 1974	June 22, 1974
1669	May 21, 1974	May 21, 1974
1399	Aug. 26, 1973	Aug. 26, 1974
1075	Oct. 6, 1972	Oct. 22, 1974
1489	Nov. 24, 1973	Nov. 23, 1974

6. References

1. Ballew, G.I., "A Method for Converting LANDSAT-1 MSS Data to Reflectance by Means of Ground Calibration Sites: S.R.S.L.*, Technical Report 75-5, pp. 90, 1975.

2. Goetz, A.F.H., F.C. Billingsley, A.R. Gillespie, R.L. Squires, E.M. Shoemaker, I. Lucchitta and D.P. Elston, "Application of ERTS Images and Image Processing to Regional Geologic Problems and Geologic Mapping in Northern Arizona": Tech. Report 32-1597, May 15, 1975. Jet Propulsion Lab., Cal. Tech. Pasadena, Calif., pp. 1-188, esp. p. 7-12.

3. Levine, S., "Correlation of ERTS Spectra with Rock/Soil Types in California Grassland Areas: Proc. Tenth Int. Symp. Remote Sens. of Environ. Ann Arbor, Mich., Oct. 1975, (in press); also S.R.S.L. Technical Report 74-10, pp. 33, 1975.

4. Vincent, R.K., "Mapping Iron Compounds: Task X: Second Type II Progress Report, MMC 075 ERIM, Univ. of Mich., Ann Arbor, Mich., 1974, pp. 32.

RSL Publication #75-15

*Stanford Remote Sensing Laboratory

Table IV

LANDSAT Brightness, and Calculated Reflectance Compared with Ground-Measured Bi-Directional Reflectance

LANDSAT ID	Z	LANDSAT brightness 4	5	6	7	LANDSAT calc. reflectance R4	R5	R6	R7	Ground* measured bidirectional ref. GR4	GR5	GR6	GR7
A. Site 082: Stanford; grassland on unnamed sandstone (Tus)													
1309	29.0	36	41	51	29	8	14	22	34				
1697	29.0	38	46	64	31	8	15	27	38	9	14	18	25
1669	30.0	36	37	59	33	8	12	27	43	9	13	31	44
1399	38.0	34	43	45	25	7	15	19	30	16	20	25	32
1075	48.4	32	31	29	14	9	12	14	22	10	13	16	22
1489	63.0	18	14	23	13	5	6	17	25	7	9	16	22
1165	65.8	15	10	28	16	2	2	27	42				
1525	67.0	16	10	19	10	2	3	16	26				
B. Site 013: Stanford, grassland on Santa Clara gravels (Qsc)													
1309G/D	29.0	33	37	51	28	7	12	22	33				
1687D	29.0	39	51	63	34	8	18	27	42	17	19	25	35
1669G	30.0	36	35	61	36	8	11	29	40	7	12	27	43
1399D	38.0	38	48	57	30	10	18	26	37	13	18	24	32
1075D	48.4	35	34	34	18	11	14	17	28	10	14	19	26
1489G/D	63.0	19	10	31	18	5	4	25	41	10	11	24	31
1165G	65.8	17	10	27	16	4	2	26	42				
1525G	67.0	17	10	28	16	4	3	[illegible]	42				
C. Site 047: Stanford, grassland on basalt (Tpb)													
1309	29.0	[illegible]	37	51	[illegible]	9	16	22	32				
1687	29.0	65	52	60	34	12	18	25	37	11	19	24	32
1669	30.0	39	44	59	30	10	16	27	39	9	16	29	34
1399	38.0	29	59	55	44	13	21	27	35	14	17	23	29
1075	48.4	32	31	32	14	9	12	16	22	14	17	22	20
1489	63.0	33	27	14	19	6	6	24	36	10	12	21	25
1165	65.8	18	12	28	17	6	4	27	45				
1525	67.0	16	10	29	18	6	3	27	42				

*Field data taken on different days from that of the LANDSAT overflight because of tape delays.

STANFORD SRSL TECHNICAL REPORT #74-4

STANSORT: STANFORD REMOTE SENSING LABORATORY PATTERN RECOGNITION AND CLASSIFICATION SYSTEM

F.R. Honey, Research Associate
A. Prelat , Research Associate
R.J.P. Lyon, Principal Investigator

School of Earth Sciences
Stanford University
Stanford, California 94305

ABSTRACT

The principal barrier to routine use of the ERTS multispectral scanner computer compatible tapes, rather than photointerpretation examination of the images, has been the high computing costs involved due to the large quantity of information (4×10^6 bytes) contained in a scene. STANSORT, the interactive program package developed at Stanford Remote Sensing Laboratories alleviates this problem, providing an extremely rapid, flexible and low cost tool for data reduction, scene classification, species searches and edge detection. The primary classification procedure, utilizing a search, with variable gate widths, for similarities in the normalized, digitized spectra is described in section 2, with associated procedures for data refinement and extraction of information. The more rigorous statistical classification procedures are described in section 3. The programs have been developed on an interactive computer (PDP-10) with the non-specialist operator in mind, requiring very little computing experience for their operation.

1. INTRODUCTION

When confronted with the overwhelming quantity of data available on magnetic tapes from the ERTS-1 multispectral scanner system, it may appear to an investigator that reduction, analysis and presentation of significant interpretations of the taped data using a digital computer would be an expensive and time consuming approach. In comparison, visual examination of the standard imagery product generated by NASA from the original data (or color-combinations of the data) is less expensive, though probably more time consuming. However, this photo-geologic approach can not be correlated readily with field-or laboratory-measured data (here referred to as "ground data").

Grouping data for a scene into distinguishable classes, for comparison with known (or suspected) geologic, geobotanical, crop or urban features, may be accomplished with either a statistical or a non-statistical classification procedure. These procedures may be divided further into supervised procedures (requiring training groups consisting of either areas which are known to be uniform, or of digitized "ground data"), and unsupervised (self-training) procedures in which the data is split into its distinguishable groups with no prior knowledge of the number, or species, of these groups. The statistical classification procedures are reviewed and evaluated in section 3.

*This research report is based upon work performed under NASA Contract NAS 5-21884, the receipt of which is gratefully acknowledged.

2. NON-STATISTICAL PATTERN RECOGNITION, CLUSTERING PROCEDURE

2.1 UNSUPERVISED CLUSTERING PROCEDURE

The non-statistical gating procedure described below developed as a result of manual examination of digitized spectra plotted for a area using the four MSS bands. It was realized that, for an area of reasonable size (e.g. 30 X 30 pixels, where a pixel, 57 meters X 79 meters, covers approximately 1 acre) only a finite number of patterns appeared. Figure 1a illustrates the patterns appearing when traversing across a row of pixels for a scene in Mono Lake, California (Figure 2). Although overall levels vary it may be observed that similar patterns appear across this traverse. This variation in level is due mainly to a topographic effect: slopes facing the sun appear brighter than slopes facing away from the sun; and partially due to the texture of the surface within the pixel: smoother surfaces (generally composed of smaller, closely-packed particles) appear brighter than coarser,rough surfaces of the same material. This change in brightness level may be reduced considerably by normalizing to one of the channels. The effect of normalizing to channel 4 the patterns plotted in Figure 1a is illustrated in Figure 1b.

These normalized patterns could be grouped into classes now, just by their shape. This is a tedious approach when performed manually, yet the concept provides a very simple, rapid and economical technique when performed by computer. The computer is required to perform the minimum of operations, all arithmetical, merely comparing values within some preset range, to discriminate different classes.

2.1.1 CONVERSION OF ERTS DIGITAL VOLTAGES TO REFLECTANCE VALUES

To compare the satellite results with ground data it is necessary to convert the ERTS digital values for each channel to some more absolute measurement which will be virtually independent of sun elevation and atmospheric effects. For this conversion, two (or more) "standard" targets are required in any ERTS scene. One of these should have as low a reflectance as possible (preferrably zero percent), so that it may be assumed that energy impinging on the de tor from the direction of the low reflectance target arises only from the radiation back scattered i to the sensor field of view from the atmosphere. The four ERTS channel values for this low reflectance target may then be subtracted from the corresponding values for all other pixels within the scene to give a measure of the radiation impinging on the detectors which arises specifically from the radiation reflected from each pixel. Obviously, not all scenes have zero-reflectance targets within them-in this case several targets having low reflectances must be chosen, and a linear extrapolation performed to give reasonable values for a zero-reflectance target.

To convert these corrected ERTS voltages to reflectance, a standard high reflectance target (or targets) within a scene must be chosen. By ratioing the corrected channel voltages for an unknown pixel to the corresponding corrected channel voltage for the high reflectance target, and then multiplying by the respective band pass reflectance (known from ground data) of the standard target(s) yields the band pass reflectance of the unknown pixels within the scene. This procedure may be represented explicitly by

$$\rho_{u,i} = \frac{Vu,i - Vz,i}{Vx,i - Vz,i} \times \rho_{s,i} \qquad (1)$$

where i is the channel number. $\rho_{u,i}$ is the bandpass reflectance of the pixel being examined. $\rho_{s,i}$ is the band pass reflectance of the standard target(s). Vu,i is the voltage in the ith channel of the unknown pixel. Vz,i is the voltage of the zero reflectance target Vs,i is the voltage of the high reflectance standard target.

The low and high reflectance standard targets must be chosen to cover an area at least three pixels square, preferrably larger, so that the center pixel (or pixels) of the standard target give voltages arising entirely from the standard targets, not affected by bordering species, particularly if the area is to be repetitively sampled by other ERTS overpasses.

Again, as would be expected, only a small, finite number of patterns appear when these reflectances are plotted. Levels of the reflectance patterns vary, due to the topographic and texture effects, but these variations may be removed by normalizing to one of the four channels (c.f. the ratio technique described by Vincent (1972)).

The technique described above has been developed into a rapid, inexpensive clustering program for an interactive computer system. With the man-machine interaction the investigator can rapidly choose his scene, display shadeprints as maps (for location) and optimize the gate used in the clustering to suit his particular requirement and the size or complexity of the area being examined.

The classification procedure searches through the array for the first unclassified pixel and a descriptor (alphabetic) assigned for this pattern. The remainder of the unclassified pixels are then compared with this "standard" pattern. If the pattern of an unclassified pixel agrees with

the current "standard" pattern within the gate width, it is given the same descriptor as the current "standard". The program recycles until all pixels have been classified, or until the number of classes exceeds twenty six (arbitrary). The set of "standard" patterns generated during the search are stored in an array to be u ed, if required, to classify another scene in the same area. In this manner very large areas may have a cluster analysis performed on them.

2.2 SUPERVISED CLASSIFICATION PROCEDURE

Whilst the unsupervised clustering technique described above is useful for examination of unknown scenes, separating them into their spectrally distinguishable species, a similar but more powerful technique may be used to search the band pass reflectance patterns for known types, using the ground spectral data. The gate generally employed in this method is two or three times the largest standard deviation of the normalized bandpass reflectances of the measured ground target. Obviously for this approach the standard targets in a scene must be chosen carefully, according to statistical sampling technique, and their reflectances measured.

2.3 NOISE AND SMOOTHING

When radiance data for a large, uniform scene (eg. water) is examined, noise with a six row periodicity may be observed, resulting from the basic detector design in the MSS. This noise is in phase for channels 4,5 and 7, but out of phase by two scan lines for channel 6. The origin of this noise is not clear-it may be due to slight differences in detector responses or to a misalignment of the detector array. This noise must be removed as completely as possible for a reliable cluster analysis to be performed, not to do so makes each sixth line a separate class. Since it is in the form of one or two unit spikes every sixth line, it is ideally suited to treatment by a digital smoothing technique described by Savitsky and Golay (1964). As the convolution blurs the image slightly, it must be performed in two dimensions in order that the change in contrast will be uniform.

The result of this smoothing is evident in Figures 3a and 3b. Figure 3a is the result of a cluster analysis without smoothing on an island in Mono Lake. Figure 3b shows the analysis of the same scene (with the same tolerance) after smoothing of the data. The water surrounding the island appears non-uniform in the unsmoothed cluster analysis result, but becomes uniform after smoothing.

2.4 BOUNDARY SEARCHES-EDGE DETECTION

After smoothing it is possible to search for abrupt changes in contrast, such as occur at sharp boundaries, deep valleys or borders between materials with large differences in reflectivity. In this manner, a search for linear, curvilinear or elliptical features may be pursued and, hopefully, some correlation between the presence of these features, their intersections and changes in classification using the clustering algorithm may be observed. Figure 4 illustrates the result of "edge detection" for the same scene clustered in Figure 3b.

2.5 COST IN COMPUTATION

The clustering technique as outlined above has proven to be very rapid. No direct comparison with a statistical clustering program is available yet, although the BMD07M stepwise discriminant program has been employed and found to require approximately ten times the computing time, even when using training groups initially generated by our unsupervised clustering program. Obviously the time required for classification is a function of the number of pixels in the scene, and also the width of the gate. Figure 5 illustrated the times required as a function of the area of the scene in the vicinity of the island in Mono Lake for different gate widths.

At present the program is being extended to "defocus" the scene, so that large areas may be examined by averaging four, nine or sixteen pixels (in a square), clustering them to look for broad patterns, then examining sub-scenes of the large scene in 1 X 1 pixel detail. Statistical procedures are being inserted to provide means, standard deviations and histograms of areas classified by the clustering algorithm, or of areas selected by the operator.

The program has been developed with the non-specialist in mind. It is completely interactive and self explanatory so that a person with no computing experience is able to examine ERTS tapes. It is designed specifically for use with a limited budget, with fast turn around time.

3. SRSL NUMERICAL CLASSIFICATION TECHNIQUES

This section outlines the theoretical basis of numerical classification technqiues used in conjunction with the procedure described above. Together they constitute the software system for analysis of ERTS multispectral data in operation at the Stanford Remote Sensing Laboratory. Four numerical classification procedures are discussed, two of which are supervised and two of which are unsupervised.

3.1 SUPERVISED CLASSIFICATIONS

A classification is supervised when data points of unknown origin are assigned into a priori defined classes.

3.1.1 NEAREST NEIGHBOR

Most of the classification techniques depend upon the assumption that samples have been drawn from a normal population. The Nearest Neighbor method makes inferences without any assumptions as to the form of distribution in the population. Such procedures are said to be non-parametric or distribution-free. The technique consists of classifying unknown data points into known categories through comparison with known data. Each unknown sample is allocated to that group to which it is nearest in terms of the D^2 generalized-distance statistic. Thus, the degree of similarity between two samples is provided by the distance that separates them; the shorter the distance the greater the degree of similarity, and vice-versa.

The nature of non-parametric statistical inferences usually requires testing with large amounts of data to achieve a respectable degree of accuracy (Swtizer el.al.,1968).

3.1.2 MULTIVARIATE DISCRIMINANT ANALYSIS

Multiple discriminant analysis is a statistical method of assigning samples in a probabilistic manner to previously defined populations on the basis of a number of variables considered simultaneously.

The use of the discriminant function may be considered in terms of a population consisting of X variables, which forms a cluster of points in X-dimensional space. A second population, described by the same X variables, consists of a second cluster of points. The linear combination of variables, that defined a multi-dimensional plane efficiently separating the two clusters of points is the discriminant function. The degree of distinctness of the two clusters can be analyzed by measuring the "distance" between their multivariate means. Once this distinctness has been established and the separating plane computed, additional unknown samples can be assigned in one or the other of the groups depending on which side of the discriminant plane they fall.

The basic assumptions about the data are: (i) the observations in each group are randomly chosen; (ii) the probability of an unknown observation belonging to either group is equal; (iii) the frequency distributions of the groups are each multivariate Gaussian distributions with a common covariance matrix. This means that the distributions have identical bell-shapes and differ only in that they are centered at different points.

The BMD07M is a stepwise discriminant analysis program, and is part of a series of bio-medical statistical analysis programs compiled by the UCLA Health Services Computing Facility. The stepwise discriminant analysis indicates that the computation of discriminant functions is not simply based on the original variables considered as a whole, but rather that the variables are entered separately and consecutively by order of discriminatory power. The advantage of this procedure is to recognize the relative importance of each variable in classifying the samples into the different groups. Ranking the variables by predictive power permits a concentration of efforts on those factors which are important for classifying groups, and this can represent a highly effective means of reducing costs of data collection and processing.

The computational procedure of the stepwise discriminant technique is described in the user's guide of the BMD07M program (Dixon, W.J.,ed.,1972).

3.2 UNSUPERVISED CLASSIFICATIONS

Classification is unsupervised when similar data points are placed into an unknown number of distinct classes in which the data points of each class have a closer similarity to each other than to the data points in all other classes.

3.2.1 CLUSTER ANALYSIS BASED ON DISTANCE-SIMILARITY MATRIX

A distance-similarity matrix is obtained to determine the relationship of the data. The use of distance is based on the concept that a quantitative measure of the degree of similarity between two variables or two samples is provided by the distance that separates them in a rectangular coordinate system. As the distance becomes shorter the degree of similarity increases and vice versa. The sample points are grouped or clustered in a hierarchical dendritic network (dendogram) in which their interrelationships, as contained in the distance-similarity matrix, are shown with greatest simplicity.

In a two-dimensional case, two samples are plotted according to the values of the two variables, X and Y. The distance between these two points is, by simple geometry, the square root of the sum of the squared differences between X and Y values of the two points; as in a right triangle the square of the hypotenuse is equal to the sum of the squares of the two sides of the triangle.

This calculation of the distance assumes that the input variables (or the axes from which they are measured) are uncorrelated, that is, orthogonal or at right angles to each other. However, most raw variables are correlated to different degrees so that the coordinate axes would not be at right

angles and the simple Euclidean distance formula would be inaccurate. To overcome this difficulty, the raw variables are transformed to a new set of uncorrelated orthogonal variables by a series of linear transformations (for details see Sebestyen, 1962). In calculating the distance coefficients for the similarity matrix it is convenient to limit its value to the range 0.0 to 1.0. To satisfy this requirement, the original data is transformed, so that all the measurements are positive and range from zero to one.

Finally, a cluster analysis is performed to measure the degree of similarity between samples on the basis of the distance-similarity matrix. Distances close to 0.0 represent maximum similarity, distances close to 1.0 represent minimum similarity. A cluster diagram is printed out with the value of the distance coefficients. Groups of similar samples can be selected at any desired level of similarity, and each group can be plotted on a geometric matrix or map.

The present procedure accomplishes clustering by computing a matrix to measure all pairwise similarities between data points on the basis of the measurements corresponding to the channels of the scanner. The procedures cannot be used when large data sets are to be analyzed because the size of the distance-similarity matrix becomes too large for the core storage requirement of the computing equipment.

4.1.2 ISOMIX: AN ITERATIVE CLUSTERING PROGRAM

Similar cluster programs have been developed by Stanford Research Institute (Ball and Hall, "ISODATA", 1965), Purdue University (Wacker and Landgrebe, 1971) and Lockheed Electronic Company (Kan, Holley and Parker, "ISOCLS", 1973). ISOMIX (Stanford) essentially follows the iterative clustering procedure of ISOCLS; however, new statistical techniques have been added to help the analyst in the interpretation and evaluation of the final data points grouped into clusters. The following is an outline of the main steps: The program first computes the initial cluster centers and assigns them to regions of high sample-point density. Then the samples are sorted, one by one, on the basis of their distance from a set of initial cluster centers which create a cluster of data points or vectors X and Y is defined as

$$d(X,Y) = \sum_{i=1}^{n} |X_i - Y_i| \qquad (2)$$

After the samples have been sorted the mean and standard deviation for each subset in each dimension (variable) is computed.

Those clusters which contain only a few sample points are discarded. Splitting of the clusters takes place if the standard deviation in any dimension is greater than a suitable threshold specified by the analyst. When the cluster is divided two new centers are formed. These centers are $(\mu_1, \mu_2, \ldots, \mu_k + \sigma_k, \ldots \mu_n)$ and $(\mu_1, \mu_2, \ldots, \mu_k - \sigma_k, \ldots \mu_n)$ where $(\mu_1, \mu_2, \ldots, \mu_n)$ and $(\sigma_1, \sigma_2, \ldots, \sigma_n)$ are the mean and standard deviation for the dimensions in the original cluster, and in the Kth dimension the original cluster contains the largest standard deviation.

The degree of distinctness of the clusters is measured by the similarity of "cluster centers" attached to regions of high density of data points. The distance or measure of similarity between two clusters C_1 and C_2, where C_1 is characterized by $\mu^{(1)} + (\mu_1^{(1)}, \ldots \mu_n^{(1)})$ and standard deviation $\sigma^{(1)} = (\sigma^{(1)}, \ldots \sigma_n^{(1)})$ and C_2 by $\mu^{(2)}$ and $\sigma^{(2)}$ (Kan, Holley and Parker, 1973), is defined as

$$D(C_1, C_2) = \left[\sum_{i=1}^{n} \frac{\left(\mu_i^{(1)} - \mu_i^{(2)} \right)^2}{\sigma_i^{(1)} \cdot \sigma_i^{(2)}} \right]^{1/2} \qquad (3)$$

If the distance D(.,.) between two clusters is less than a specified threshold, the two cluster centers are merged into one at a weighted mean of the two original clusters.

The progress is cycled repeatedly until the standard deviation in every channel of the generated clusters is less than the specified threshold, or the maximum number of clusters desired by the analyst is reached.

ISOCLS's chaining algorithm is used to link those subclusters which are close to at least one other subcluster. This linking process determines the subpopulations, the union of which constitutes the parent population.

In the last step the overall areal proportions of various clusters are obtained. For example, if p_j is the areal proportion of a specified cluster j, n_j is the number of sample points counted of the specified cluster j, and N the total number of sample points, then the usual estimator of

the areal proportion p_j is $\hat{p}_j = n_j/N$. Finally in the last step, the pattern complexity which gives the spatial scale of variation is also obtained. A pattern that has a cluster A with its samples in a contiguous body is less complex than another with the same proportion of cluster A distributed in many scattered smaller units. One index to express the pattern complexity (Switzer, 1973) is

$$X = \frac{\text{total length of boundaries between different sample points}}{(\text{area of region})^{1/2}} \qquad (4)$$

The value of X is invariant to the choice of the measurement unit. As the X value increases the pattern grows in complexity.

The output gives the statistics for each cluster and includes a map showing the final cluster assignments of all the points in the area analyzed. These maps are geographic matrices preserving the original position of the data points.

4. REFERENCES

Ball, G.H. and Hall, D.J.,1965, "ISODATA, a Novel Method of Data Analysis and Pattern Classification". Stanford Research Institute 1-16, Menlo Park, California.

BMD-Biomedical Computer Programs. Edited by W.J. Dixon, University of California, 1970, Publications in Automatic Computation, no.2, University of California Press.

Kan, E.P., Holley, W.A., and Parker, Jr.,H.D.,1973, "The JSC Clustering Program ISOCLS and its Applications", Proceedings of the IEEE on Machine Processing of Remotely Sensed Data, Catalog no.73 CHO 834 - 2IEE.,pp.4b36-4b50.

Savitsky,A. and Golay, M.J.E.,1964, "Analytical Chemistry", v.36, p.1627.

Sebestyen, George, 1962, Decision-Making Processes in Pattern Recognition. New York; The Macmillan Company.

Switzer, P.,et.al,1968, "Nearest Neighbor-A New Non-Parametric Test Used for Classifying Spectral Data". Stanford RSL Technical Report #68-3.

Switzer, P.,1972, "Applications of Random Process Models to Descriptions of Spatial Distributions of Qualitative Geologic Variables". 24th International Geological Congress. Montreal, Canada.

Vincent, R.K., 1972, "An ERTS Multispectral Scanner Experiment for Mapping Iron Compounds", Proc. 8th International Symposium on Remote Sensing of Environment, p.1239.

Wacker, A.G. and Landgrebe, D.A.,1970 "Boundaries in Multispectral Imagery by Clustering". IEEE Symposium on Adaptive Processes (9th) Decision and Control, pp.X14.1-X14.8

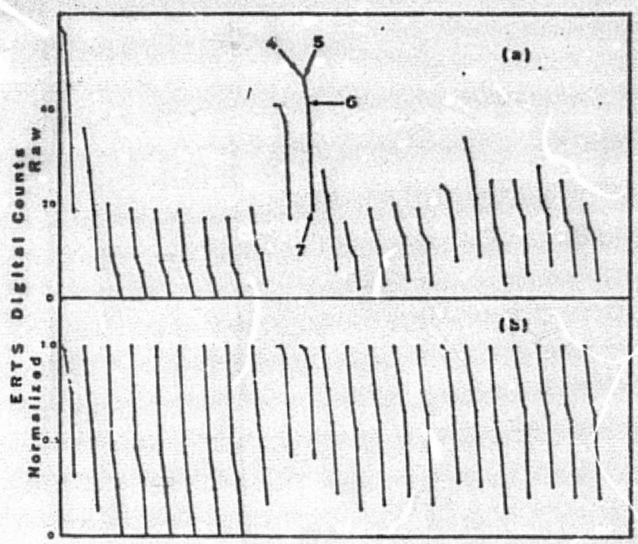

Figure 1. Digitized spectra resulting from plots of

(a) Raw ERTS digital voltages plotted against channel number.

(b) ERTS digital voltages normalized to channel 4, plotted against channel number,

for section of a scan line across Negit Island and portion of Mono Lake, California.

Figure 2. Negit Island, Mono Lake, California. Dark areas of island are basaltic lava flows and cones of varying texture, white "beaches" composed of calcareous tuffs.

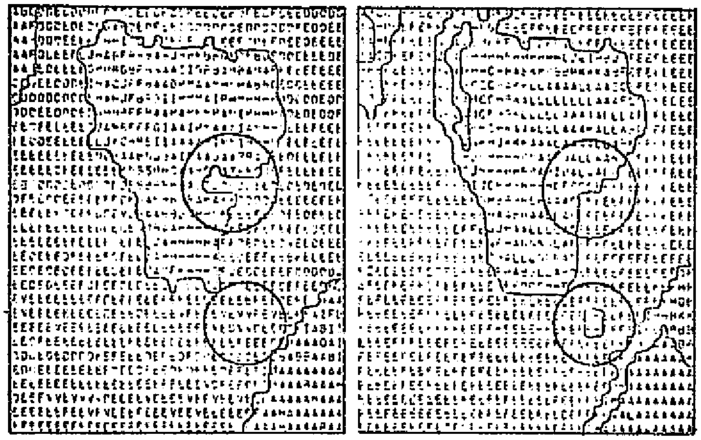

Figure 3. Cluster analysis result of the Mono Lake scene for

(a) unsmoothed data
(b) smoothed data

The water surrounding the island appears more uniform for the smoothed data . However, some structural detail of the island is removed due to the "defocusing" effect of the convolution.

Figure 4. Result of "edge detection" on Negit Island scene. Only those borders with a large change in contrast are emphasized. Lower steps in the scanning technique would result in more detail.

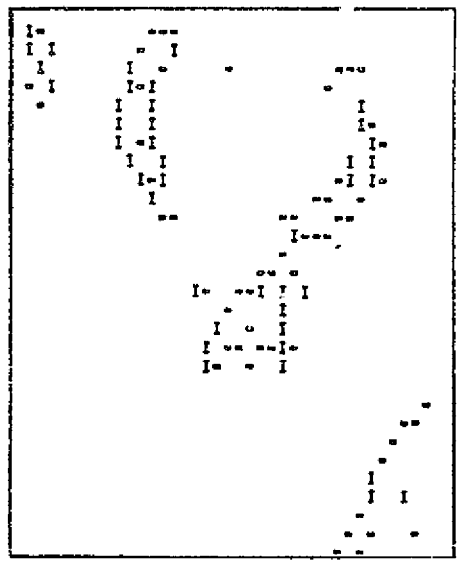

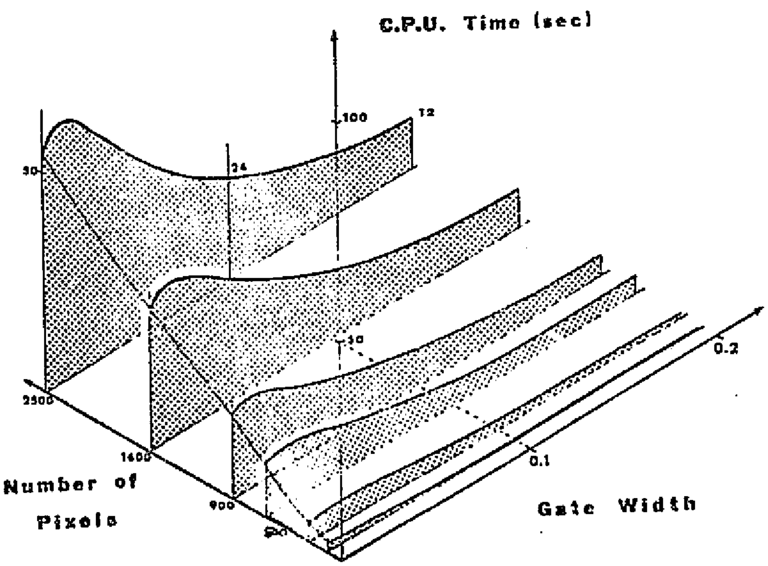

Figure 5. Computation times for unsupervised classification as a function of the number of pixels in the scene and of the gate width. In a first approach, gatewidths of approximately 0.1 normalized units are used.

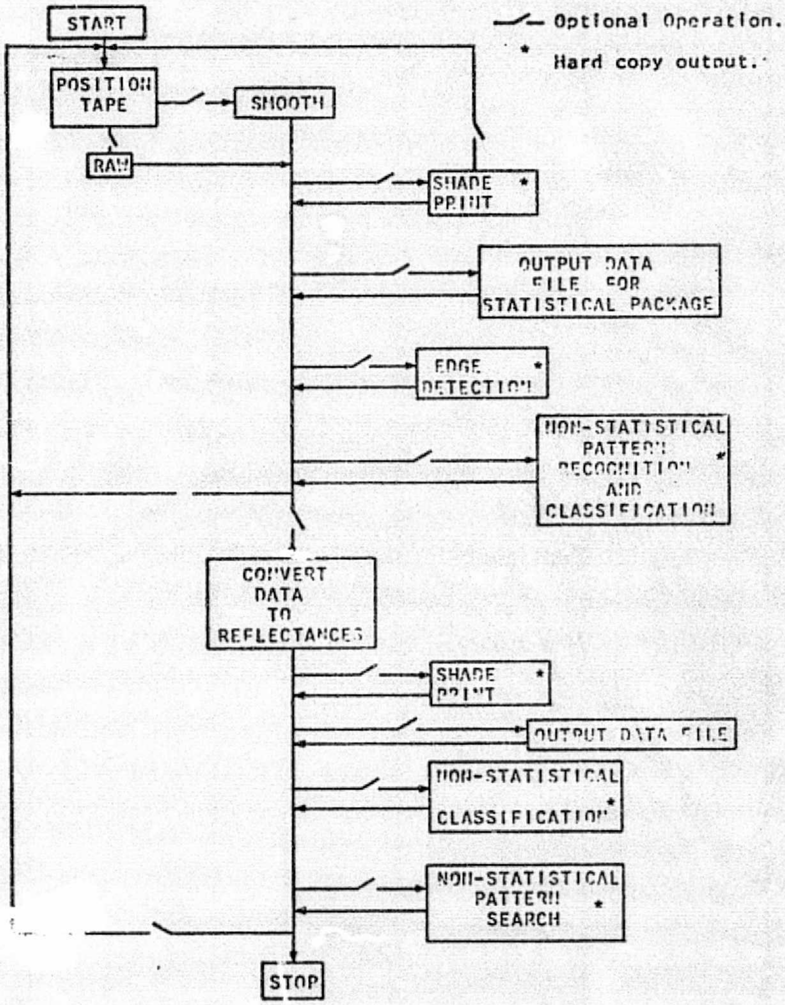

Outline of program described in section 2. Most steps are optional, the operator being asked which procedures he wishes as the program proceeds. Results of each step may be displayed on the screen for examination.

APPENDIX C

CORRELATION OF ERTS SPECTRA WITH ROCK/SOIL TYPES IN CALIFORNIAN GRASSLAND AREAS

Saul Levine

(Tech Report 74-10)
Stanford Remote Sensing Laboratory
Department of Applied Earth Sciences
Stanford University
Stanford, California 94305

SUMMARY

A seasonal study of ERTS-CCT data, accomplished by means of four band spectra plots of normalized reflectance, indicates that in the San Francisco Bay and adjacent Coast Range grassland areas, soils mapping or classification by computer techniques is possible at the end of the dry or grass dieback season. Excellent correlation is shown between ground reflectance measurements and CCT data at three test sites and two different soil types: serpentine and sedimentary. The uniqueness of their spectra is then demonstrated by the successful application of STANSORT, a computerized classification technique developed by the Stanford Remote Sensing Laboratory.

I. INTRODUCTION

The primary purpose of this investigation was to determine if the serpentine exposures and soils on the San Francisco Peninsula could be detected uniquely by means of ERTS imagery and/or the related CCT data. In doing so it was also hoped to evolve a methodology which would be useful in conducting similar studies in the future. As envisioned, the imagery (individual bands and color composites) were to be studied first to determine if these serpentine areas could be detected visually and then a study made to determine if any uniqueness existed in their four band spectra. This property, if existent, could then be utilized as a basis for the development of a computerized classification program to automize the detection and mapping procedure.

In the course of this investigation, it became evident that the seasonal response of the vegetative cover could be most important in obliterating or enhancing the information relating to the serpentine soil. Therefore, a careful systematic, spectral study of the CCT data for the yearly cycle was undertaken by means of four band radiance and reflectance plots of the test areas. Off season correlations of serpentine soil spectra vs. serpentine soil/grass spectra were also made possible by means of a fortuitous grass fire in the study area which had exposed a large area of bare soil. These correlations ultimately led to the conclusion that the soil/grass spectra were in fact essentially soil spectra at the end of the dry or dieback season.

After an extensive ground measurement program had substantiated the unique character of the serpentine soil spectra the study was expanded to include a sedimentary area on the east side of the Coast Range upon which a yearly controlled burn occurred. The same seasonal trends were evident and a strong correlation between ERTS reflectance spectra and ground measured spectra was again found. In addition, the spectra of the sedimentary soil was found to be distinguishable from the background as well as the serpentine soils studied on the San Francisco

Peninsula. (See Figure 1 for general location of the test sites.) The clustering program STANSORT developed by the Stanford Remote Sensing Laboratory was then applied to the study areas with significant success.

II. AREAS STUDIED

Two major exposures of serpentine rocks and soils mapped by the USGS, on the San Francisco Peninsula, were selected for study. The first, Area I, consists of exposures of highly weathered blue-gray serpentine, only a small percentage of which is outcrop, the remainder decomposed fragments, grading to a serpentine soil. These exposures are to the east of, and adjacent to, the Crystal Springs Reservoir segment of the San Andreas Fault Zone. They are surrounded by and occasionally penetrate the various rocks of the Franciscan assemblage. To a large degree the northern section of Area I is obliterated by housing developments and roads. Therefore, the study was focused on the southern section which is largely within the Crystal Springs watershed and is public land. The vegetation of this site, composed of annual broad leaved herbs and annual grasses, is readily distinguishable from the surrounding grassland on nonserpentine soil. It is marked by a different species composition, smaller size (height less than one foot), sparser cover and earlier onset of senescence and drying. The dominant broad leaved herbs are <u>Layia platyglossa</u> (tidy tips), <u>Orthocarpus sp</u>. (owl's clover) and <u>Plantago erecta</u> (California plantain) and the dominant grasses are <u>Bromus mollis</u> (soft chess) and <u>Lolium multiflorum</u> (ryegrass).

Area II is approximately 4 miles south of the Crystal Springs Reservoir, again on the east side and adjacent to the San Andreas Fault Zone. Because of the housing developments and roads an open field area of roughly 60 acres at the south end was selected for study. The serpentine is heavily weathered and blue gray in color with only a small percentage of outcrop; the remainder decomposed fragments and serpentine soil. Interstate 280 transverses the south end of the area exposing large amounts of fresh serpentine in the roadcuts. The serpentine vegetation of the Farm Hill Road site is clearly differentiated from the surrounding nonserpentine vegetation by the same features that distinguish the Crystal Springs Road serpentine vegetation, i.e., a different species composition, smaller size, sparser cover and earlier onset of senescence. It is made up of annual broad leaved herbs and grasses and shares several species in common with the Crystal Springs site. The dominant plants are a grass, <u>Festuca sp</u>. (fescue), and the broad leaved herbs, <u>Layia platyglossa</u> (tidy tips) and <u>Hemizonia sp</u>. (tarweed).

The third area studied consists of a sedimentary area located in San Joaquin County, California, at the base of the eastern foothills of the Coast Range. This area lies within the Lawrence/Livermore Radiation Laboratories Field Test Site 300 and is largely a yearly controlled burn area. The study site is typical of the rolling grassy eastern foothills of the Coast Range. It is roughly 600 acres in extent, crossing elevations varying from 250 to 400 meters. The sediments are semi-consolidated sandstones with the outcrops again a minor percentage compared to the soils deriven from the sandstone. The vegetation is that typically described as a California valley grassland community, dominated by annual species of the grasses <u>Bromus</u> (bromegrass), <u>Festuca</u> (fescue), <u>Avena</u> (cat) and others.

III. VISUAL STUDY

A visual study of available ERTS imagery, both the individual bands and color composites covering the San Francisco Peninsula was accomplished. Also included was U-2 imagery taken during the ERTS Simulation Program. It was noted, in the ERTS frame date 6 October 1972, that a distinct dark gray pattern existed which seemed to coincide generally with the Area I serpentine east of Crystal Springs Reservoir. Study of the imagery before and after this date indicated that the pattern persisted with diminishing intensity back to 26 July 1972 after which it could not be seen. The pattern was not evident again until 26 August 1973, at which time it was faintly discernible. The appearance and disappearance of the observed pattern correlated with the dieback and growth cycle of the grass in this area.

Review of the ERTS color composites substantiated the above, with the pattern readily discernible at the dates noted, as a dark purplish tone. In addition,

similar tones were also evident within Area II, south of Farm Hill Road, coinciding with the open field mentioned previously.

IV. RADIANCE SPECTRA

To study the possible uniqueness of the tones associated with the serpentine areas, the radiance values of ERTS-CCT pixels traversing these and adjacent areas were obtained and their spectra plotted. These pixel spectra traverses, across the Crystal Springs Reservoir and Farm Hill Road areas, are shown in Figure 2. The mean radiance values, standard deviations and coefficients of variation of the various terrain types, across these traverses were then computed. Radiance throughout this report is presented as digital or word count levels. Should absolute value of radiance be desired conversion factors must be applied. At this point no atmospheric corrections were made. The location of specific features was accomplished by means of a skewed pixel overlay of the proper scale and an ortho-photomap (1:24000), as well as aerial photographs of the areas.

It can be seen from examination of the spectra plots that the serpentine and grass areas as well as Interstate 280, water and the forested areas appear to have distinctive spectra. It is interesting to note that while the pixel spectra across the forested area in traverse AA are generally the same shape, peak values are evident at four points. The aerial photographs indicate that these coincide with the hilly terrain across which the traverse was made. Apparently, this effect is caused by the variation in sun angle due to hill slope. The repetitiveness of the individual water spectra is also very striking.

In traverse BB, the constancy of the pixel spectra of the serpentine soil/grass area on the east side of Interstate 280 as contrasted to the west can be correlated to the tones evident in the ERTS imagery. The slight variability evident on the west side is attributed to variability in the soil, grass cover or both. It seems apparent that the spectra obtained is a function of the interaction of the soil and degree and type of grass cover which in turn is a function of the season of the year.

V. SEASONAL REFLECTANCE SPECTRAL STUDY

Based on the results of the visual and radiance spectra study, it was evident that the serpentine soil/grass signature was unique at the 6 October 1972 date. It also seemed possible that because the grass dieback in this part of California, was complete by this date, that the recorded spectra was essentially that of the soil. To substantiate the above, a systematic study of the soil plus grass interaction at the Crystal Springs area through the yearly cycle was instituted. Due to a fortuitous 15 acre grass fire, within Area I which occurred 1 July 1973 and easily seen in the ERTS imagery, it was also possible to include spectra of the devegetated burn area in the study for comparative purposes. This study was accomplished by means of normalized four band spectra plots of the mean ground radiance values of the selected test areas. In so far as was possible, identical ten pixel areas within the ERTS frames covering an 11 month time interval were utilized.

In order to compare results from the ERTS multispectral scanner data over this time period, corrections were made for the perturbing effects of radiation scattered by the atmosphere and the variation in irradiance on the scene with solar zenith angle. These effects were removed by studying selected targets of low (zero) reflectance and high known reflectance (Honey and Lyon, 1974). In the scene studied, a waste products treatment pond at an oil refinery near Suisun Bay, with bandpass reflectance of <0.5% in all four bands was utilized as the zero reflectance standard. A concrete parking apron for aircraft at Moffet Field NAS California with reflectances of 27.8, 31.0, 30.0 and 32.3 percent bandpass in the four ERTS channels was used for the high reflectance standard. The factors derived were applied as follows:

$$\text{Target Reflectance} = \frac{\text{Target Radiance-Dump Reflectance (Meas)}}{\text{Concrete Radiance-Dump Reflectance (Meas)}} \times \text{Concrete Reflectance (Meas)}$$

Radiance plots as well as normalized reflectance are presented in Figure 3. Study of this data revealed the following:

a. Interpretability of the four band spectra is greatly improved by the application of the atmospheric corrections and normalization of the data to band 4.

b. The normalized reflectance of the soil/grass is at a maximum (particularly channels 6 and 7) at the height of the rainy season, 22 January 1973; roughly twice as high as that during 6 October 1972, near the end of the dry season.

c. The normalized reflectance of the soil/grass gradually diminishes with the end of the rainy season and the entry into the summer dry-out period.

d. In the burn area, on 3 July 1973, the normalized reflectance spectra drops to a minimum value, possibly as a result of both the devegetation and the residue of the carbonized-grass remains.

e. By 21 July 1973, the normalized reflectance spectra values in the area have increased, probably as a result of the dispersion of the carbonized ash by the wind. They now approximate the values at 6 October.

f. A slight increase in the normalized reflectance is noted at 26 August 1973, probably due to some revitalization of the grass in the burn area.

g. The 6 October 1972 reflectances are very close to those of the burn area at 3 July and 26 August 1973.

Based on the above, a strong likelihood exists that the reflectance spectra of 6 October is that of the serpentine soil with little or no reflectance introduced by the dead grass.

A 10 pixel block within the Farm Hill Road test site, (6 October 1972, serpentine soil/grass) was also selected and the normalized reflectance spectra plotted in Figure 4. A strong correlation was found with the reflectance spectra at Area I at the same time of year. Based on these results, it was decided to broaden the scope of the study somewhat to see if the same trends were obtained at a third site in which the terrain soil was of a different type and at which a similar burn situation existed. This test site (Area III) was located at the Lawrence/Livermore Radiation Laboratories Field Test Site 300 at which controlled burns were used to reduce the likelihood of uncontrolled fires as a result of explosives testing. It is on the east side of the Coast Range, approximately 15 miles east of Livermore. The terrain type had been mapped as marine sediments. In addition to the study of another soil type, a comprehensive verification program of ground reflectance measurements of bare soil was to be accomplished at all three test sites. Because of the size of the Midway site, approximately 960 acres, a grid pattern, at intervals of 10 pixels, was utilized across the burn area to obtain the reflectance spectra data. Study of this data again indicated that:

a. The normalized reflectance is at a maximum in the winter and gradually diminishes with the end of the rainy season and entry into the summer dry-out period.

b. The 6 October 1972 reflectance spectra and that of the burn area are comparable.

A comparison of the reflectance spectra for Area III (marine sediments) and Areas I and II (serpentine soils) (see Figure 4) indicates that they are considerably different, particularly in bands 6 and 7, thus leading to the conclusion that computerized classification could be applied.

Data relative to the ground reflectance measurements taken at the test sites are plotted in Figure 4. An Exotech ERTS Radiometer and scaled down satellite geometry were utilized to obtain this data. Figure 4 compares the ERTS-CCT deriven spectra with that obtained above. Study of this data reveals the following:

a. The ERTS-CCT normalized reflectance spectra for serpentine soils, at 6 October 1972 are almost identical at Crystal Springs and Farm Hill Road.

b. The ground reflectance spectra obtained at Midway correlate very well with that derived from the 6 October 1972 ERTS-CCT data.

c. The ground reflectance spectra for serpentine soil at Farm Hill Road compare very favorably with the CCT data. The ground spectra for the roadcut- and outcrop-serpentines, while comparable to each other are substantially different than that of the soil. It is believed that because of the small areal extent of the outcrops as compared to the soil and the limiting resolution of the ERTS system, the outcrops have little integrated effect and essentially only the serpentine soil is detectable on the CCT data.

d. The correlation of the ground spectra obtained at Crystal Springs with the ERTS-CCT data is not quite as good. It is believed that this is due to the infiltration of materials from adjacent soils derived from nearby Franciscan sandstone exposures.

e. A significant difference is seen in both the ERTS-CCT spectra and the ground spectra for the serpentine soils at Crystal Springs and Farm Hill Road and the sediments at Midway.

In general, from the seasonal spectral study made and the ground measurements obtained, it can be concluded that the four band ERTS spectra for serpentine soils and sedimentary soils are sufficiently different from each other at the end of the dry or dieback season, to be distinguished from each other and the background by computerized clustering.

VI. CLASSIFICATION TECHNIQUE

The classification procedure utilized to investigate the uniqueness of the soils spectra studied is an interactive program package called STANSORT, developed at the Stanford Remote Sensing Laboratories (Honey et al., 1974). This system provides an extremely rapid, flexible and low cost tool for scene classification. It is a non-statistical, unsupervised classification technique in which the data are split into distinguishable groups with no prior knowledge of the groups. The primary classification procedure utilizes a search, with variable gate widths, for similarities in the normalized or un-normalized digitized spectra. Training was accomplished on the serpentine soil spectra of Farm Hill Road and the clustering resulted in coverage approximating the serpentine soils mapped. Continued search for the serpentine spectra at Midway (the sedimentary test site) using identical classifiers revealed virtually complete absence of serpentine spectra.

VII. CONCLUSIONS

As a result of the foregoing study in the San Francisco Bay and adjacent Coast Range grassland areas the following may be concluded:

1. ERTS soil/grass four band spectra are in fact essentially soil spectra at the end of the dry or grass dieback season.

2. The ERTS four band spectra obtained is a function of the interaction of the soil and degree and type of grass cover which in turn is a function of the season.

3. A strong correlation exists between ground measured reflectance spectra and ERTS four band spectra for both serpentine and sedimentary deriven soils.

4. The ERTS four band spectra for serpentine and sedimentary deriven soils are sufficiently different from each other and their background to be classified by application of STANSORT the SRSL interactive, unsupervised classification program.

REFERENCES

F. R. Honey, and R. J. P. Lyon, 1974, A Comparison of Observed and Model-Predicted Atmospheric Perturbations on Target Radiances Measured by ERTS, Stanford Remote Sensing Laboratory, Stanford University.

F. R. Honey, A. Prelat, and R. J. P. Lyon, 1974, STANSORT: Stanford Remote Sensing Laboratory Pattern Recognition and Classification System, Stanford Remote Sensing Laboratory, Stanford University.

FIGURE 1. GENERAL LOCATION OF TEST SITES

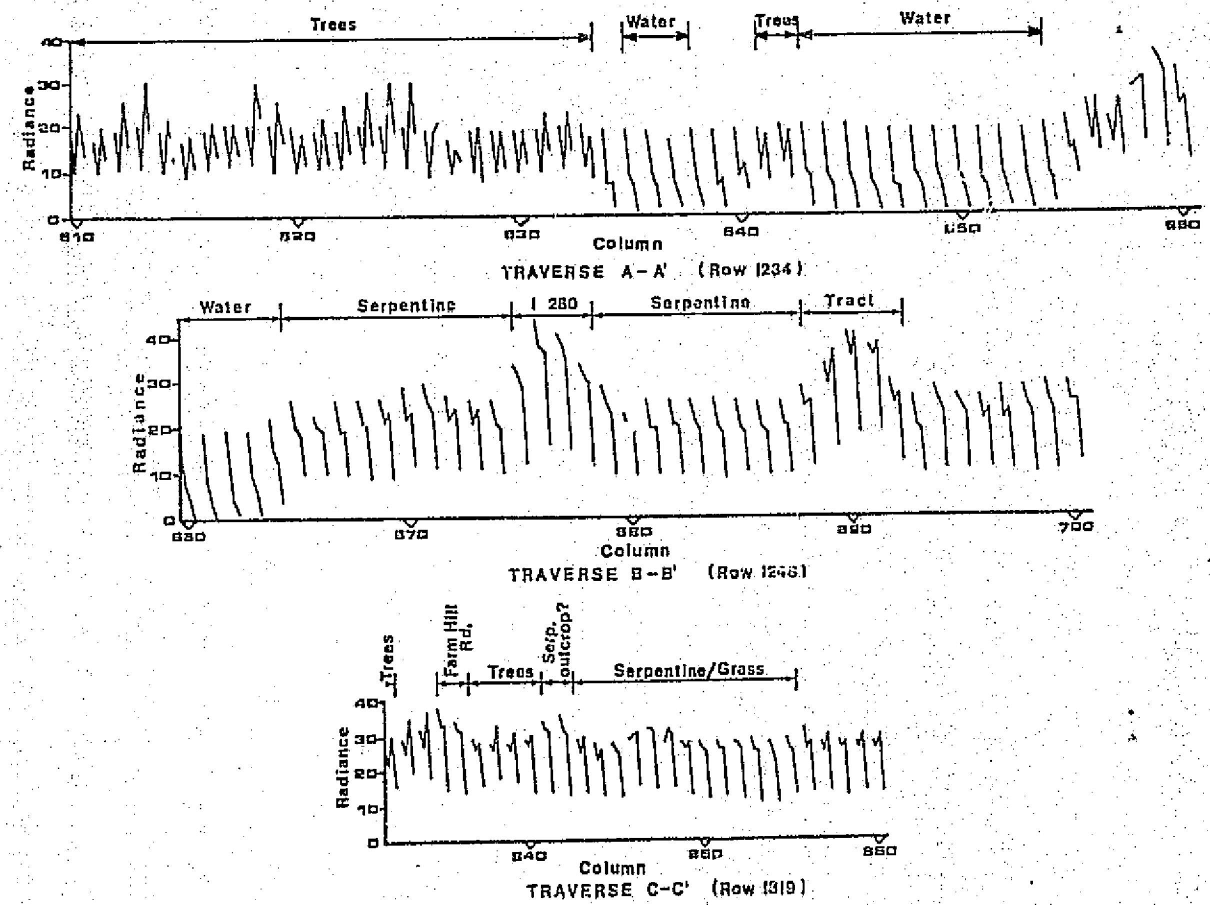

FIGURE 2. RADIANCE SPECTRA TRAVERSES (BY PIXEL)
ERTS FRAME ID 1075-18173

253

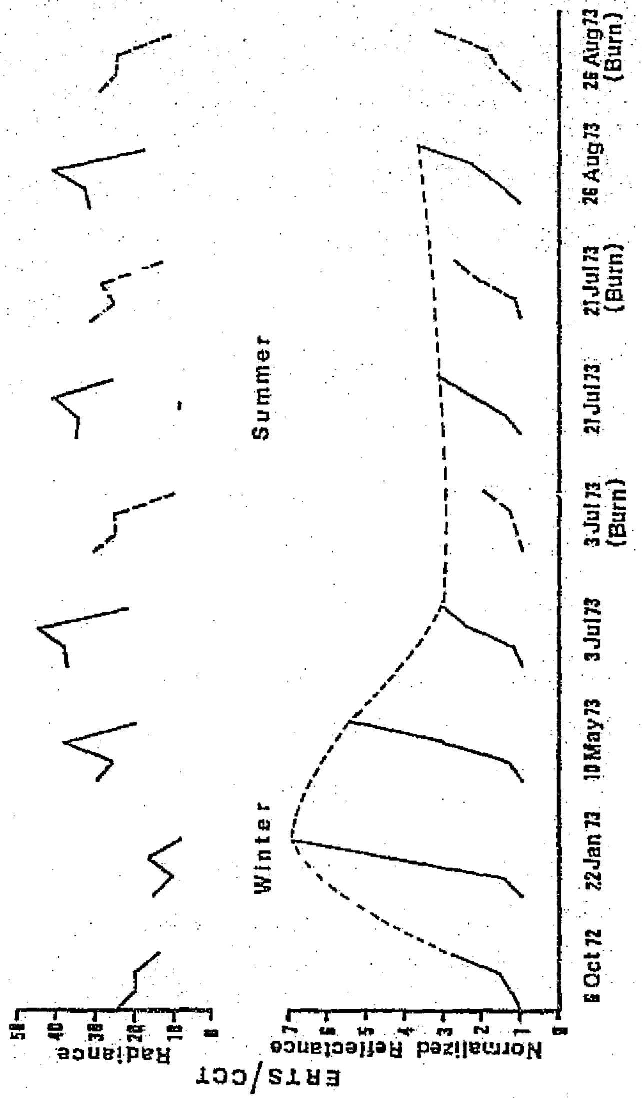

FIGURE 3. RADIANCE AND NORMALIZED REFLECTANCE SPECTRA SOIL/GRASS (CRYSTAL SPRINGS)

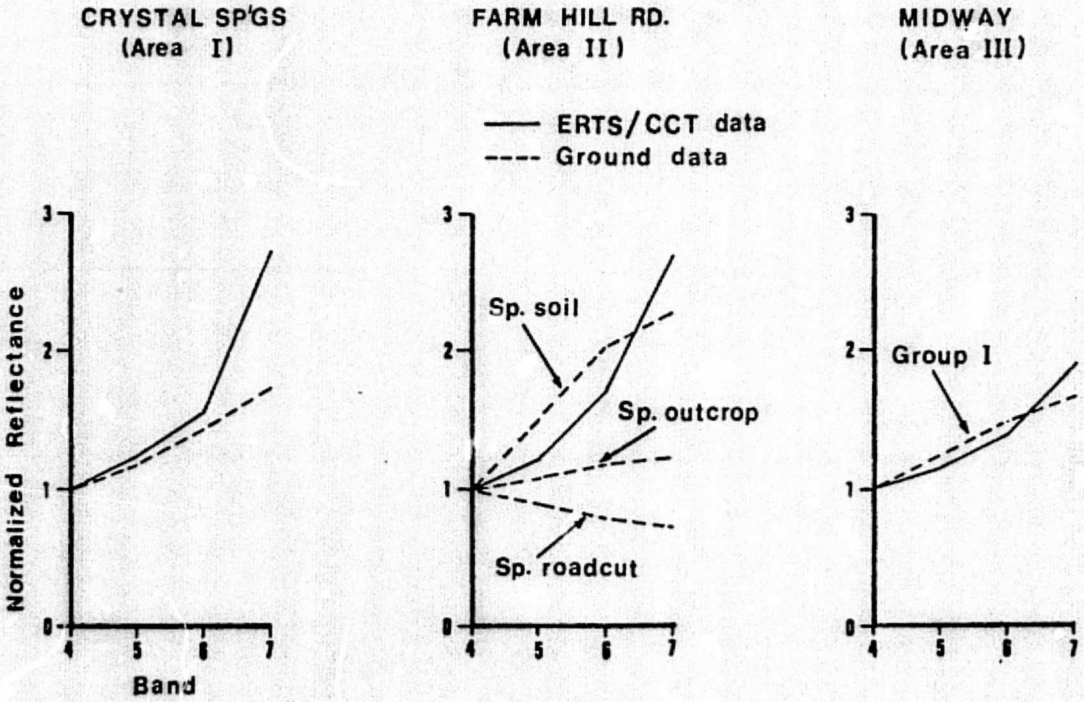

COMPARISON OF NORMALIZED ERTS/CCT AND GROUND MEASURED REFLECTANCE

FIGURE 4. COMPARISON OF NORMALIZED ERTS/CCT AND GROUND MEASURED REFLECTANCE

APPENDIX D

CORRELATION BETWEEN GROUND METAL ANALYSIS, VEGETATION REFLECTANCE, AND ERTS BRIGHTNESS OVER A MOLYBDENUM SKARN DEPOSIT, PINE NUT MOUNTAINS, WESTERN NEVADA

R. J. P. Lyon

Stanford Remote Sensing Lab.Tech. Publ. 75-16
Stanford Remote Sensing Laboratory
Stanford, California

1. ABSTRACT

In a cooperative study with U.S.G.S. and American Metals Climax (AMAX) personnel, it has been possible to detect a 2.0 by 1 mile anomaly on ERTS CCT data directly, in the pine- and juniper-covered mountains of western Nevada. This anomalous area is about 3-5 times larger than that of the known geobotanical anomaly which lies centrally within the area. The site has been studied on the ground and bi-directional reflectances (relative to $BaSO_4$) obtained for 40 trees, using both in-vivo techniques (similar to cherry picker operations) and field determinations of cut branches. The anomaly can be seen best by color transparencies made from 5/4, 6/4, 7/4 ratioed ERTS data, the 3 ratios each being coded by one of 3 colors (blue, green, and red) (Figure 3B). Ratio-image 7/4 is the best single view of these three ratios (Figure 2B).

2. BACKGROUND

Molybdenum mineralization is present as a skarn deposit in Upper Triassic limestones and mafic volcanics in Sections 23, 25 and 26; T 12 N; R 21 E, approximately 20 mils SE of Carson City, Nevada. DeLong (1971), of AMAX, in a paper presented orally at an AIME meeting at Vail, Colorado,described the deposits as tactized limestones from which there has been sporadic tungsten production principally during World War II from the Alpine (Mill), Divide and Cherokee mines. Work by AMAX resulted in defining a "sizeable molybdenum deposit" related to a quartz monzonite (Alpine Mill stock) in Section 25, although no grade or tonnage figures have been released. Geochemical sampling of the soils was hampered by the lack of mobility of Mo in calcareous environments. Vegetation sampling of the deeper-rooted pines and junipers was used to define the distribution of the heavy metal by analyzing leaf-ash (needles, and second-year twigs). Junipers were more useful than the pines because of their higher metal contents (DeLong, 1971). Subsequent work by the U.S.G.S. has further documented this pattern (Watson, 1974).

Molybdenum tends to be mobile, however, in the volcanic soils and moves down the hydraulic grade out into the recent gravels and alluvials of Pine Nut Creek, to the northeast. In this area pines and junipers also show high Mo contents.

Thus the mineralized area has a well-documented geobotanical anomaly with Mo appearing in the juniper needles up to >500 ppm and in the pine needles to >200 ppm. Unfortunately for our purposes no analyses of the ubiquitous sagebrush shrubs were made.

R. Watson and F. Canney of the U.S.G.S. discussed this botanical anomaly with the author in April 1974, but at the time were not specific as to the location in the Pine Nut Mountains, to maintain company confidentiality. We suggested using our set of ERTS CCT tapes and the STANSORT interactive program (Honey, et. al., 1974) to conduct a search for the section locations based upon ERTS reflectance data alone. This proved successful in indicating an N-S elongated

elliptical area of about 2 square miles, 3-5 times larger than the known vegetation anomaly, and centered on the western edge of Section 25 (Lyon and Honey, 1974). Our results were sent to Watson in May and field checked July 24-26, 1974 with him.

This paper deals with our subsequent attempt to document by field reflectance measurements that we had defined from ERTS altitudes.

3. VEGETATIVE COVER

The central area (Alpine Mill, Divide and Cherokee Mines) is on the east facing slope at an average altitude of 6500-7000 feet with about 1500 feet of relief. The hill is bounded on the west by Buffalo Canyon. To the east across Pine Nut creek the main range of the Pine Nut rises to 9000 feet with Mt. Siegel at 9450 feet. The principal source of moisture are the winter snows which dust the lower slopes but leave Mt. Siegel snow-covered for several months a year. The area lies in the "precipitation shadow" of the Sierra Nevadas. Minden, Nevada, 11 miles to the northwest and at 4800 feet averages 22 cm (8.5 inches) per year, water equivalent.

The vegetation is mainly pinon pine (Pinus monophylla) and juniper (Juniperus utahensis) (Billings, 1950). The trees average 3-4 meters in height and are moderately bushy in shape. A morphological change of the pine to a excessively-twiggy, sparsely-needled, brittle form was noted as the molybdenum content increased. The junipers appeared more healthy with metal contents.

Significantly for remote sensing, these trees (at 40 per acre in unaltered volcanics) covered only about 10-15% of the ground surface, when viewed from above using air photos at a scale 1:40,000. The tree-frequency-count varied somewhat in the immediate Alpine Mill area, showing about 30-35 per acre, but they are more closely bunched, leaving more open space, which appeared white on the airphotos. In the unaltered areas the space between the trees is a light gray on the photo indicating a more-even cover of smaller shrubs like sagebrush. Elsewhere in the carbonates about 0.5 mile to the west of the Mill, the tree count was as high as 50 per acre, still on the E-facing slope. No bare patches could be seen.

By far the greatest cover is from sagebrush (Artemesia tridentata), but because of its pale color it is difficult to estimate a percentage from the available black and white photography. Visual estimation would range from 10-40%. but as the shrub has an open, sparsely-leafed form, mostly soil and plant debris would be seen from above. This becomes important as it appears that a greater tree spacing, with an increased bleaching of the soil, determines the "ERTS-average spectrum" of the anomaly.

4. PREVIOUS WORK

At the central area the earliest efforts in World War II were mainly connected with tungsten mineralization. American Metals Climax (AMAX) spent considerable time mapping in 1967/68 and in studying the Mo geobotanical anomaly, culminating in drilling the prospect (DeLong, 1971). No logs were made available.

R. D. Watson and T. Hessin of the U.S.G.S. conducted measurements of the anomaly with the Fraunhoffer Line Discriminator (FLD), a device to measure secondary fluorescence from chlorophyll in leaves as seen in a black solar line (Fraunhoffer Line). They were in the field with us July 24-25, 1974 and used the identical branches cut from the marked (analyzed) trees as we did for our EXOTECH measurements. Watson (1975 a.b.) has indicated a high degree of correlation with FLD-fluorescence anomalies and Mo content of leaves, and significantly, was able to repeat the pattern of anomalies in a second program of helicopter-FLD measurements in 1975 (Watson, 1975, pers. comm.)

5. ERTS DIGITAL TAPE ANALYSES

ERTS CCT digital tapes, for scenes 1289-18063 (5/8/73) and 1397-18051 (8/24/73) were already available to us at Stanford and these we processed to enhanced-images using our STANSORT program (Honey, et.al., 1974). We quickly found that all four bands gave somewhat similar images, principally showing the topography of the central ridges (Alpine-Divide and Mt. Siegel). By dividing any of the three bands by the fourth (usually Channel 4) this "sunlit- and shadowed-enhancement" of topography

could be removed from the digital imagery giving a "flat'earth" presentation, the ratio-imagery retaining essentially only the spectral (colored) components. If one then combined any three of these black and white ratio images, using colored filters (red, green and blue) onto color film, a "color-ratio" image, enhancing all the spectral information may be prepared (Levine, 1975). These color-ratio images hold the key to the information content of the ERTS system, the image form being very significant to the geologist for photointerpretation, and anomaly location in the field.

Figure 1 shows enhanced ERTS images for Ch 4, Ch 6 and Ch 7.

Figure 2 A-C show B/W ratio-images (Ch 1/Ch 4) and Figure 3B, a B/W copy of an originally-colored ratio image (Ch 5/4 - R; Ch 6/4 - G; Ch 7/4 - B). Figure 3A is a B/W copy of a false color image (Ch 4 + Ch 6 + Ch 7).

The important anomaly covers about 2 square miles and is centrally located in these figures, forming an elliptical to pear-shaped mass elongated in a NNE direction across the NW trending Alpine-Divide ridge. The eastern edge is formed along Pine Nut Creek, the southern edge by the low pass between Pine Nut and Buffalo Creeks. The northeastern limb is parallel with a strong jointing pattern across the NW strike of the limestones, and may be also the location of two NNE faults.

The feature is subtle and varies in strength with differing combinations of ratios although remaining fixed in geographical position, centered just north of the mutual junction of sections 25, 26, 35 and 36.

These images cover about 300 square miles at an original scale of 1:210,000. An important feature of their areal coverage is that other anomalous areas may be identified simultaneously , either with similar or differing "color-tones". Another large anomaly, centered on Double Springs Flat along Highway 395 is also enhanced on the same color-ratio image. This has a circular shape with a central, alluvial-filled depression and several radial and concentraic drainage anomalies. We propose this as a caldera (andesitic) centered in section 23, T 11 N, R 21 E, and is particularly well shown on the Ch 6/Ch 4 image (Figure 2B), and on Ch 7 image (Figure 1C, arrow points outlining the shape).

Within a circular anomaly to the south a smaller one was located on Section 2/11 by using our search pattern in STANSORT/CLUSTER, trained on the Alpine-Divide area. A field traverse in this area located a new patch of weak gossan with many of the general appearances of the Alpine area.

6. FIELD MEASUREMENTS

We have taken extensive sets of ERTS-band reflectance measurement, using a pair of EXOTECH-100 ground radiometers on 5 field days in the area. These were concentrated mainly on the 60 analyzed (and tagged) juniper and pine trees along a drilling-road down the N-S axis of our color anomaly. A map of the Mo analysis results was provided by R. Watson with data on Mo contents of needles, twigs and stems of these marked trees.

Our joint field measurements with Watson on July 24, 1975, ensured that the same trees were used for both sets of experiments.

The reflectance measurements have been made with several sets of geometries

1) Cut branches, observed vertically (front and back) at about 1 m with an EXOTECH 15° FOV unit, giving concurrent bi-directional reflectance relative to $BaSO_4$ powder.

2) Living (in-place) trees, observed vertically down with a boom-mounted radiometer 5 m above the ground (concurrent bi-directional reflectance relative to $BaSO_4$ powder.

3) Living (in-place) trees, observed horizontally from 3-30 m distance, with a 15° FOV unit. Bi-directional reflectance, with intermittent (10-20 minutes) observation of a $BaSO_4$ standard.

4) Traverses, with measurements every 30 m, vertically viewing soils, rocks, sage-brush and trees (horizontally), with a 15° FOV unit, intermittently viewing a $BaSO_4$ standard. Traverse A; Alpine Mill ridge, to E to W, over 0.6 miles length. Traverse B; Double Springs anomaly (Sec. 11), with 0.5 miles in length. (Sept. 25, 1974).

7. DATA ANALYSIS

7.1 Correlation of Reflectance with Molybdenum Contents

The four ERTS bandpass brightness values for each pass target and $BaSO_4$ standard views were reduced using our ERTSRATS program (Salem, 1975). This yields several types of output:

7.1.1 Target and Reference Standard separately

a. Bandpass radiant emittance (w/cm^2)

b. Spectral radiant emittance ($w/cm^2/\mu m$)

c. Bandpass ratios (7/6, 7/5, 7/4, 6/5, 6/4, 5/4) (Vincent, 1973)

d. Spectral ratios (7/6, 7/5, 7/4, 6/5, 6/4, 5/4) (Vincent, 1973)

e. Pseudo-C.I.E. coordinates (using Ch. 4, 5 and 7, instead of visible-region data) - this is a running check on the sky-color for error detection).

7.1.2 Using both Target and Reference Data

a. Bidirectional reflectance (if both have same FOV and geometry, or else directional reflectance if hemispherical irradiance, 2Π, is used instead of a reference standard.

b. Reflectance ratios ($Ch_i/4$; $CH_i/5$; $CH_i/6$ $CH_i/7$; i = 4 ....7). Six non-redundant ratios may be prepared from four-channel data.

Using the "cut-branch" set of data the following analyses have been completed, to date (Table I).

A cross-correlation (BMDO2D) analysis of Mo (ppm) and log Mo (ppm) versus

a. Pseudo CIE coordinates RASNX and RASNY (target).

b. Bandpass brightness BP4, BP5, BP6, BP7 (target).

c. Bi-directional reflectance R4, R5, R6, R7.

d. Reflectance ratios R76, R75, R74, R65, R64, R54.

The results, tabulated in Table I show that the correlations are significantly positive with Mo content for Juniper and negative with log Mo content for pines.

Significant at	with	Parameters	"r"
1% level	Juniper	BP7 vs. Mo	+0.42
	All branches	BP7 vs. Mo	+0.35
3% level	Pine	R4 vs. log Mo	-0.40
5% level	All branches	BP7 vs. log Mo	+0.30
	"	R7 vs. log Mo	+0.25
	"	R7 vs. Mo	+0.26

7.2 Correlation of Reflectance Ratios with Anomalous Molybdenum Content in Leaves

Six Ratios of the four reflectance values (R76, R75, R74, R65, R64 and R54) were calculated for position of the tree samples relative to the Mo anomaly boundaries. (i.e. inside or outside the anomaly). For pines, needle assay values above 50 ppm and for juniper values above 75 ppm were considered anomalous. The three different viewing geometries (days 1, 2, and 3) were kept separate to avoid obscuring special aspect-dependant effects. Table II lists the data for the cut-branches, Table III for the vertical data and Table IV for the horizontally-viewed data. Ratio means (x 1000) and coefficient of variability (COV), where COV = $\sigma/\bar{x}$ are shown.

The following points may be made:

a. All three aspects have very similar ratios, with R75, R74, R65 showing the highest values.

b. Variability within a group ratio (COV) is above 15 to 25%, higher in the R75 and R65 ratios. Greatest variability occurs in the vertically -viewed trees where location of the radiometers relative to the needle masses is most difficult. Conversely, lowest COV values appear in the horizontally-viewed data where location in the field of view of an instrument is most easy.

c. The coefficient of variability of the means of each group may be used as a "criterion of separability" for each ratio (Goetz, et al 1975) i.e. in Table 4, which contains some 18% soils and 16% sagebrush in addition to the pines and Junipers, a COV value of 0.39 for R75 makes it the most-useable ratio (0.07 for R54 indicates the least use-able one).

d. The three most-usable ratios (R75, R74 and R65) show higher mean values inside the anomaly for all the pine spectra, and also for the cut-branch and horizontally-viewed juniper. Again variability exists for the vertically-viewed data, especially for the juniper. The horizontally-viewed set (Table 4) shows drops in mean ratio values of 20 to 37% outside the anomaly, for both pine and juniper.

e. As R75, R74 and R65 are correlated above 80% with each other, any one may be used, in preferance ratio R75 because of its consistantly higher COV. Color ratios should be made with R75 or R74, R64 and R54 to maximise their information content, R54 being in some ways a negative of R64.

8. SUMMARY

Field reflectance measurements of three modes were made, using EXOTECH ERTS-type radiometers -- cut branches, and viewing the trees both from vertically above, and horizontally. Each tree, either a pinon pine or juniper, was one previously marked by the U.S.G.S., who provided the molybdenum analyses of stems, twigs and needles (leaves). In addition sagebrush and bitterbrush shrubs were measured together with their background soils and rocks.

The correlation between Mo and juniper cut-branch reflectance was positive, and significant at the 99% level (Channel 7 brightness) agreeing with the visual observation that even at values in excess of 500 ppm Mo in leaf ash, the junipers were healthy. With pinon pine however, the correlation with cut-branch (needle) reflectance was negative but significant at the 97% level. The pines showed significant morphological change (needle loss, profusion of twiggy stems, and brittleness of branches) correlateable with mineral uptake of Mo. Within each set the location of the anomaly can be found statistically by the R75, R65 or R64 ratio levels, being higher within the Mo-rich areas.

Using unsupervised clustering techniques on CCT taped data (STANSORT program) ERTS spectra could be extracted for the total anomaly area, which were used to locate similar areas to the south, near Double Springs Flat. Field checking located weak gossan mineralization in the bleached andesites there.

Continuing field studies are aimed at specifically identifying the cause of the ERTS anomaly -- is it tree vigor, tree species, tree spacing, or sagebrush/soil ratio which can be observed from space over this skarn zone.

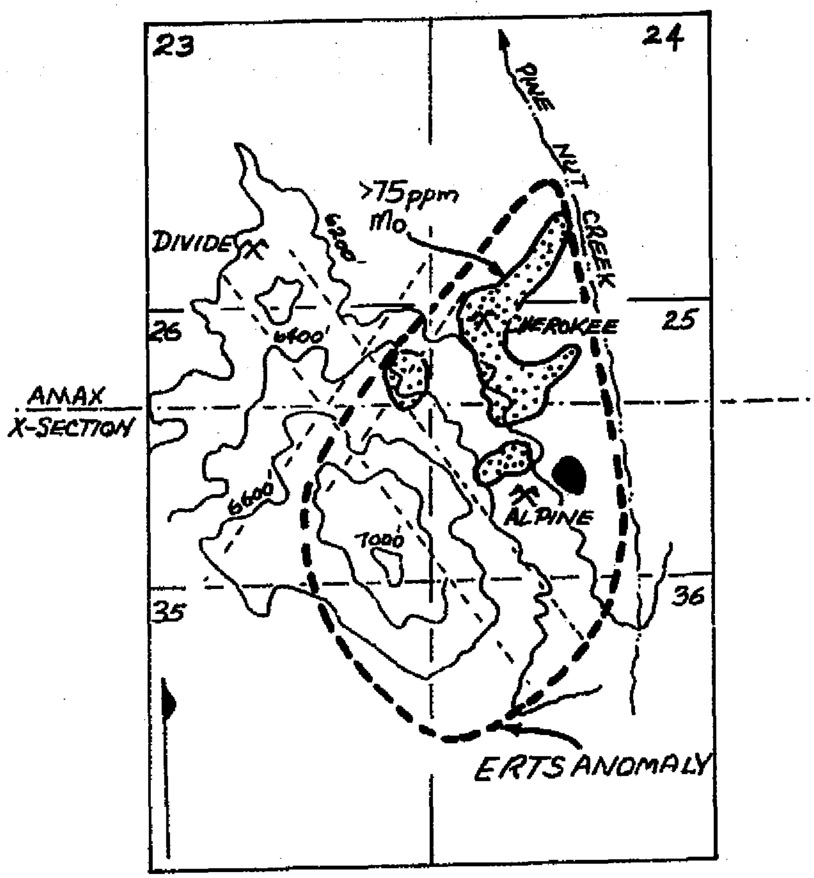

LOCALITY MAP of ERTS-detected anomaly (heavy dashed lines) and molybdenum anomaly (heavy stippled area above 75 ppm Mo in juniper needle ash). Sections given are in T12N; R21E, Mt. Siegel quad, Douglas Co., Calif. NW-trending linears are trends of limestone beds; NE-trends are strongly developed joints (faults?). Quartz monzonite outcrop is solid black. Scale about 1:30,200

REFERENCES

Billings, W.D. (1950) Vegetation and Plant Growth as Affected by Chemically Altered Rocks in the Western Great Basin: Ecology, 31, (1), 62-74.

DeLong, J.E., Jr. (1971) Molybdenum in Tree Ash as an Exploration Guide; paper presented at AIME meeting, Vail, Colo., July 29, 1971, 5 pp.

Goetz, A.F.H., Billingsley, F.C., Gillespie, A.R., Squires, R.L., Shoemaker, E.M., Lucchitta, I. and Elston, D.P. (1975) Application of ERTS Images and Image Processing to Regional Geologic Problems and Geologic Mapping in Northern Arizona: Tech. Report 32-1597, May 15, 1975. Jet Propulsion Lab., Cal. Tech. Pasadena, Calif., pp. 1-188, esp. p. 7-12.

Honey, F.R., Prelat, A., and Lyon, R.J.P. (1974) STANSORT: Stanford Remote Sensing Laboratory Pattern Recognition and Classification System: Proc. Tenth Int. Symp. Remote Sens. Environ., Ann Arbor, Michigan, 897-905.

Levine, S. (1975) An Interactive Program for Producing Computer-Enhanced ERTS Images (IMAGE) Part II - Methodology Development: Stanford Remote Sensing Lab. Tech. Rept. 75-4, 38 pp.

Lyon, R.J.P. and Honey, F.R. (1974) Multispectral Signatures in Relation to Ground Control Signature Using a Nested Sampling Approach: Abstr. in Nat. Tech. Info. Serv. (NTIS), NASA Earth Resources Survey Program, Weekly Government Abstracts. 93-74-41 Code E74-10690, p. 132 October 14, 1974.

Noble, D.C. (1962) Mesozoic Geology of the Southern Pine Nut Range, Douglas Co., Nevada: Unpubl. Ph.D. thesis, Stanford University, 200 pp. + maps.

Salem, B. (1975) ERTS Tapereading and Ground Data Processing Software for an IBM 360/67 at Stanford Center for Information Processing (SCIP): Stanford Remote Sensing Lab. Tech. Rept. 74-11, pp. 60.

Snedecor, G.W. (1946) Statistical Methods, Ames, Iowa, Iowa State College Press, p. 351.

Vincent, R.K. (1973) Spectral Ratio Imaging Methods for Geological Remote Sensing from Aircraft and Satellites: Proc. Symp. Man. & Utiliz. of Rem. Sens. Data, Sioux Falls, Oct. 29-Nov. 1, 1973, p. 377-397.

Watson, R.D. (1975) Luminescence as an Indicator of Geochemical Anomalies: Proc. First Annual W.T. Pecora Memorial Symp. Oct. 28-31, 1975, Sioux Falls, S.D. (Abstr.)

TABLE 1

CORRELATION BETWEEN LOG Mo (ppm), Mo (ppm) WITH VARIOUS REFLECTANCE PARAMETERS

	Log Mo (ppm) (#3)			Mo (ppm) (#4)		
	All Branches	Pine	Juniper	All Branches	Pine	Juniper
	N=62	N=29	N=33	N=62	N=29	N=33
RASNX	-.24	-.34	-.06	-.20	-.13	-.16
RASNY	-.21	-.08	-.22	-.16	-.20	-.01
BP4	-.06	-.28	-.22	.04	-.16	.28
BP5	-.04	-.05	.07	.04	-.20	.31
BP6	.17	-.03	.29	.13	.07	.13
BP7	(.30)*	.19	.33	(.35)**	.07	(.42)**
R4	.13	(-.40)*	.23	-.07	-.24	.19
R5	.11	-.18	.07	-.02	-.26	.25
R6	.08	-.15	.27	.00	-.02	.01
R7	(.25)*	.11	.32	(.26)*	.00	.32
R76	.11	.17	.06	.18	.00	.24
R75	.20	.21	.12	.09	.16	-.05
R74	.22	.28	.10	.19	.11	.13
R65	.10	.08	.06	-.04	.14	-.22
R64	.13	.19	.02	.03	.15	-.16
R54	-.04	.06	-.13	.02	-.09	.12
Significant						
(**) at 1%	.325	.47	.45	.33	.47	.45
(*) at 5%	.25	.37	.35	.25	.37	.35

(Snedecor, 1946, p. 351)

TABLE 2

VARIATION IN RATIOS OF GROUND SPECTRA-CUT BRANCHES

All Vegetation (cov = $\sigma/\bar{x}$, in parenthesis July 24, 1974)

CUT BRANCHES	N	$\overline{R76}$	$\overline{R75}$	$\overline{R74}$	$\overline{R65}$	$\overline{R64}$	$\overline{R54}$
Pines:							
Inside anomaly >50ppm	18	1400 (.13)	4500 (.19)	[illegible] (.14)	3252 (.23)	2800 (.13)	587 (.19)
Outside anomaly	12	1489 (.23)	4207 (.11)	3650 (.17)	2966 (.25)	2562 (.18)	883 (.18)
Juniper:							
Inside anomaly >75 ppm	18	1446 (.19)	5618 (.19)	4624 [illegible]	4017 [illegible]	3242 (.15)	836 (.19)
Outside anomaly	12	1421 (.10)	4416 (.14)	4039 (.15)	3131 (.16)	2863 (.16)	919 (.13)
TOTAL SET	60	1439 (.03)	4685 (.14)	4052 (.10)	3341 (.14)	2867 (.10)	882 (.04)

TABLE 3

VARIATIONS IN RATIOS OF GROUND SPECTRA-VERTICAL VIEWING

DAY 2 DATA, July 25, 1974 (IN-VIVO)

47% spectra of vegetation; 3% soils (cov = $\sigma/\bar{x}$, in parenthesis)

VERTICAL VIEWING	N	$\overline{R76}$	$\overline{R75}$	$\overline{R74}$	$\overline{R65}$	$\overline{R64}$	$\overline{R54}$
Pines:							
Inside anomaly >50 ppm Mo	22	1572 (.13)	4803 (.26)	5630 (.28)	3056 (.24)	3541 (.20)	1172 (.12)
Outside anomaly	30	1645 (.13)	4310 (.26)	5236 (.22)	2615 (.22)	3173 (.16)	1235 (.12)
Juniper:							
Inside anomaly >50 ppm Mo	31	1597 (.11)	4849 (.18)	5530 (.21)	3048 (.18)	3447 (.15)	1139 (.09)
Outside anomaly	34	1528 (.11)	5140 (.30)	5582 (23)	3387 (.30)	3638 (.17)	1119 (.12)
Sagebrush	6	1377 (.13)	1812 (.11)	2357 (.09)	1385 (.14)	1796 (.11)	1286 (.08)
Soils and Rocks	4	1174 (.04)	1599 (.17)	1936 (.11)	1360 (.14)	1649 (.12)	1216 (.07)
TOTAL DATA SET	127	1482 (.12)	3752 (.42)	4370 (.40)	2475 (.36)	2874 (.31)	1195 (.05)

TABLE 4

VARIATIONS IN RATIOS OF GROUND SPECTRA - HORIZONTAL VIEWING

Pine Nut Mountains, Nevada, Day 3, August 15, 1974
82% spectra of vegetation; 18% of soils
(cov = $\sigma/\bar{x}$, in parenthesis)

Horizontal View	N	$\overline{R76}$	$\overline{R75}$	$\overline{R74}$	$\overline{R65}$	$\overline{R64}$	$\overline{R54}$
Pines:							
Inside anomaly	15	1467(.26)	5211(.26)	5518(.23)	3524(.23)	3735(.20)	1067(.04)
Inside anomaly	23	1479(.05)	5019(.15)	5395 (.14)	3414 (.14)	3660 (.12)	1076 (.06)
Outside	18	1399(.05)	3793(.08)	4209 (.11)	2708 (.06)	3000 (.08)	1109 (.08)
Juniper:							
Inside anomaly (analyzed)	25	1493 (.04)	5031 (.15)	5627 (.12)	3368 (.14)	3762 (.11)	1123 (.10)
Outside	20	1421 (.05)	4046 (.21)	4396 (.19)	2815 (.18)	3061 (.15)	1095 (.05)
Sagebrush	15	1192 (.27)	2040 (.18)	2290 (20)	1616 (.12)	1807 (12)	1122 (.08)
Soils and Rocks	25	1077 (.07)	1153 (.12)	1505 (.09)	1069 (.09)	1396 (.06)	1307 (.05)
Total Data Set	141	1369 (.1)	3826 (.39)	4217 (.36)	2699 (.32)	2969 (.30)	1123 (.07)

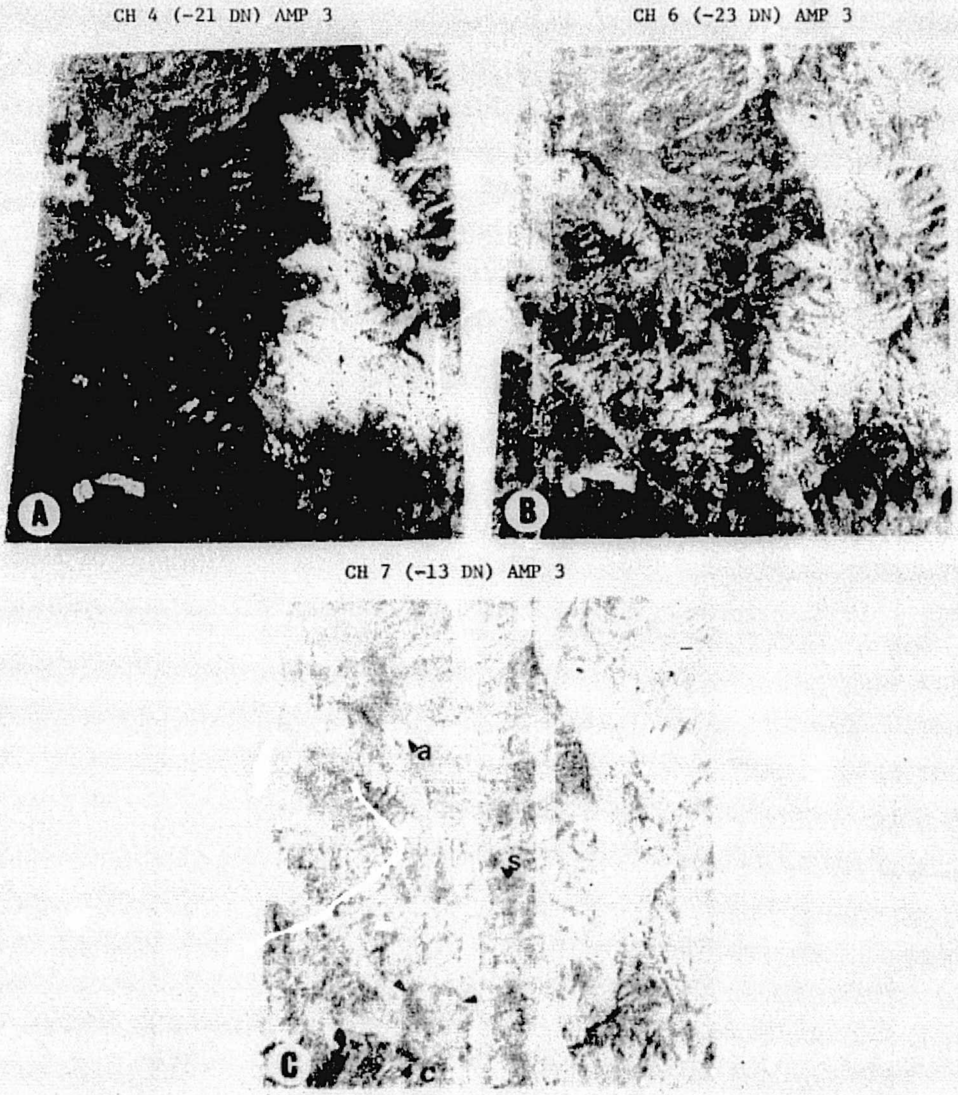

1289-18063 May 8, 1973

PINE NUT MTNS, NEVADA

Figure 1. Computer-enhanced images of ERTS data for 300 square miles surrounding the Alpine-Divide-Cherokee Mines, Pine Nuts Mtns., Nevada.
S= Sugarloaf Mtn; A= dry farming area, C= caldera. White line in lower left is Highway 395.

RATIO 5/4 (-41 DN) AMP 2

RATIO 6/4 (-63 DN) AMP 2

RATIO 7/4 (-28 DN) AMP 1

1289-18063 May 8, 1973

PINE NUT MTNS, NEVADA

Figure 2. Ratio-images for Ch 5/4 (A), CH 6/4 (B), and CH 7/4 (C)
B= fire scar, A= dry farming area, C= Caldera anomaly.

2608

CH 7 (-13 DN) AMP 2 (RED)
CH 6 (-23 DN) AMP 3 (GREEN)
CH 4 (-21 DN) AMP 3 (BLUE)

RATIO 7/4 (-28 DN) AMP 3 (RED)
RATIO 6/4 (-63 DN) AMP 3 (GREEN)
RATIO 5/4 (-41 DN) AMP 3 (BLUE)

A 1289-18063 May 8, 1973 B

PINE NUT MTNS, NEVADA

Figure 3. LEFT(A): False Color Image, prepared directly from ERTS tapes, adding CH4+CH6+CH7, closely resembling a normal air photo. White is snow, lake in lower left is Double Springs Flat, white line is Highway 395.

RIGHT(B): Color-Ratio Image, prepared from ratioing ERTS brightness values. Snow area appears unusual due to saturation on the original data tapes. Anomaly is indicated by arrow points.